



Manoharan, Indrani (2014) *Identification and characterization of novel histone modifications during cellular senescence*. PhD thesis.

<http://theses.gla.ac.uk/5553/>

Copyright and moral rights for this work are retained by the author

A copy can be downloaded for personal non-commercial research or study, without prior permission or charge

This work cannot be reproduced or quoted extensively from without first obtaining permission in writing from the author

The content must not be changed in any way or sold commercially in any format or medium without the formal permission of the author

When referring to this work, full bibliographic details including the author, title, awarding institution and date of the thesis must be given

Enlighten:Theses  
<http://theses.gla.ac.uk/>  
theses@gla.ac.uk

# **Identification and Characterization of Novel Histone Modifications during Cellular Senescence**

Indrani Manoharan

Submitted in fulfillment of the requirements for the Degree of Doctor of  
Philosophy

Institute for Cancer Sciences

CRUK Beatson Labs

University of Glasgow

February 2014

## **Abstract**

Cellular senescence is a stable cell cycle arrest and can be triggered by various signals including telomere shortening, oncogenic activation and other stress activators. Senescence is accompanied by changes in the cellular organization, gene expression and induction of the secretome. It is established and maintained by at least two major tumor suppressor pathways, the p53-p21 and p16-pRB pathways. Senescence is now recognized as a potent barrier to tumor progression and is directly and indirectly linked to a large array of age-related pathologies. However the precise molecular mechanisms of senescence, particularly how cells are driven into irreversible proliferation arrest, is not fully understood. It is well known that widespread changes in the chromatin structure of senescence contribute to the senescent phenotype.

In line with this, the primary objective of this project is to understand how senescence is regulated by its chromatin structure. I have focussed on the identification and characterization of novel histone modifications that occur during senescence. Large-scale profiling of histone modifications was performed in replicatively senescent cells in comparison to proliferating cells. Candidate histone modifications were identified that alter during senescence from the screen, of which, H3CS.1 and H4R3me2a were chosen for subsequent study. To our knowledge, this is the first study to have implied a novel role for these two modifications during senescence. Also a third histone modification, H4K16ac, was chosen for study based on ChIP-seq observations made in the lab. The mark has also been extensively linked to cancer and aging.

All together, work from this project imparts new knowledge on how H3CS.1, H4R3me2a and H4K16ac might regulate senescence via critical modulation of its chromatin structure and how they may impinge on senescence-associated effects such as ageing and cancer.

## Table of contents

Abstract.....	2
Table of contents.....	3
List of tables.....	9
List of figures.....	10
Acknowledgements.....	13
Publications arising from this work and other collaborations.....	14
Declaration.....	15
Abbreviations.....	16
1. Introduction.....	20
1.1 Senescence as a cellular stress response.....	21
1.2 Signals initiating senescence.....	21
1.2.1 Telomere dysfunction.....	21
1.2.2 Oxidative Stress.....	22
1.2.3 Oncogene activation.....	22
1.2.4 Other inducers.....	23
1.3 Effectors of the senescence programme.....	25
1.3.1 Control by p53-pRB pathways.....	25
1.3.1.1 The p53 pathway.....	25
1.3.1.2 The pRB pathway.....	26
1.3.2 DNA damage signalling.....	27
1.3.3 Effect of autophagy.....	29
1.4 Senescent phenotype.....	30
1.4.1 Stable proliferation arrest.....	30
1.4.2 Senescence Associated Secretory Phenotype.....	30
1.4.3 Apoptosis Resistance.....	32
1.4.4 Markers of senescence.....	33
1.5 Functions and pathologies of senescence.....	34
1.5.1 Functional consequences of senescence.....	35

1.5.1.1	Role in tumor suppression .....	35
1.5.1.2	Role in wound healing.....	37
1.5.1.3	Role in embryogenesis .....	39
1.5.2	Aspects of senescence in pathologies .....	40
1.5.2.1	Role in ageing .....	40
1.5.2.2	Role in tumor promotion.....	41
1.6	Chromatin.....	43
1.6.1	Chromatin structure .....	43
1.6.2	Histone variants.....	44
1.6.3	Histone modifications .....	47
1.6.4	Histone modification binding proteins.....	49
1.6.5	Nucleosome positioning .....	51
1.6.6	Role of non-coding RNAs .....	51
1.7	Epigenetics of cellular senescence .....	52
1.7.1	Chromatin reorganization in senescence .....	52
1.7.2	Loss of histones in senescence.....	55
1.7.3	Histone modifications in senescence .....	56
1.8	Aims of the project.....	58
2.	Materials and Methods.....	61
2.1	Materials.....	62
2.1.1	General Reagents .....	62
2.1.2	Antibodies and Dyes.....	65
2.2	Methods.....	67
2.2.1	Cells.....	67
2.2.2	DNA Preparation .....	67
2.2.3	DNA Quantification .....	68
2.2.4	Plasmids .....	69
2.2.5	Site Directed Mutagenesis.....	70
2.2.6	DNA Sequencing .....	71
2.2.7	DNA Analysis.....	71
2.2.7.1	Diagnostic Restriction Digest.....	71

2.2.7.2	Preparative Restriction Digest .....	72
2.2.7.3	Agarose Gel Electrophoresis .....	72
2.2.8	Non-Viral Transfections .....	72
2.2.9	Viral Transfections .....	73
2.2.10	Protein Extraction .....	75
2.2.11	Protein Quantification .....	75
2.2.12	Protein Analysis .....	75
2.2.12.1	SDS-PAGE Electrophoresis .....	75
2.2.12.2	Western Blotting .....	77
2.2.13	Slot blotting .....	77
2.2.14	Immunofluorescence .....	78
2.2.15	Cellular Fractionation .....	78
2.2.16	Chromatin Immunoprecipitation (ChIP) .....	79
2.2.17	ChIP-sequencing .....	84
2.2.18	ChIP-seq Analysis .....	84
2.2.19	Quantitative ChIP-PCR .....	84
2.2.20	Histone Peptide Array .....	86
2.2.21	Models of Senescence .....	87
2.2.22	Markers of Senescence .....	87
2.2.22.1	Senescence Associated $\beta$ -Galactosidase Assay .....	87
2.2.22.2	EdU Proliferation Assay .....	88
3.	Profiling of histone modifications in senescent cells in comparison to proliferating cells .....	90
3.1	Introduction .....	91
3.2	Results .....	91
3.2.1	Establishment of replicative senescent cells in vitro .....	91
3.2.2	Loss of histones observed in senescent cells in vitro .....	95
3.2.3	Profiling of various modifications in senescent cells compared to proliferative cells .....	95
3.2.4	Changes in histone modifications observed in two different models of senescence .....	100
3.2.5	Other stress factors do not facilitate increase of histone marks in IMR90 .....	103

3.2.6	Changes in histone marks occur specifically in senescence and not simply cell cycle arrest.....	104
3.3	Discussion .....	105
4.	H3CS.1 in cellular senescence.....	109
4.1	Introduction.....	110
4.2	Results .....	111
4.2.1	Validation of H3CS.1 antibody specificity .....	111
4.2.2	Establishment of an inducible-model system of senescence to follow kinetics of H3CS.1 .....	113
4.2.3	H3CS.1 abundance gradually increases with the induction of RAS .....	116
4.2.4	Cathepsin L cleaves histone H3 to produce histone H3CS.1 and is increased in senescent cells .....	118
4.2.5	Cytoplasmic localization of nuclear histone H3CS.1 observed in RAS-induced senescent cells. ....	118
4.3	Discussion .....	122
5.	H4R3me2a in cellular senescence.....	124
5.1	Introduction.....	125
5.2	Results .....	125
5.2.1	Validation of H4R3me2a antibody specificity .....	125
5.2.2	Increase in H4R3me2a in senescence confirmed by a second antibody ..	127
5.2.3	H4R3me2a abundance gradually increases after induction of RAS.....	129
5.2.4	Regulation of H4R3me2a in cellular senescence.....	129
5.2.4.1	Increase in H4R3me2a in OIS is not inhibited by expression of SV40 LT Antigen.....	129
5.2.4.2	Expression of PRMT1 is elevated in senescent cells .....	135
5.2.4.3	Generating IMR90 cells with constitutive KD of PRMT1 .....	137
5.2.4.4	PRMT1 is a pre-requisite for increased H4R3me2a in senescent cells	140
5.2.5	Global distribution of H4R3me2a in senescence.....	143
5.2.5.1	Optimization of ChIP-seq conditions.....	143
5.2.5.2	ChIP-seq of H4R3me2a in proliferating and senescent cells.....	148

5.2.5.3 H4R3me2a ChIP in proliferating and senescent cells presents technical issues.....	151
5.3 Discussion .....	153
6. H4K16ac in cellular senescence.....	158
6.1 Introduction.....	159
6.2 Genomic distribution of H4K16ac in senescence.....	160
6.2.1 H4K16ac is enriched at gene-rich regions and co-relates to gene expression. ....	160
6.3 Results .....	163
6.3.1 Validation of antibody specificity.....	163
6.3.2 Independent confirmation of H4K16ac enrichment in senescence by real time quantitative PCR.....	163
6.3.3 Using IR-induced senescence to study specific enrichment of H4K16ac..	166
6.3.3.1 Real-time quantitative PCR confirms relative enrichment of H4K16ac IR-induced model of senescence.....	166
6.3.4 In vitro approaches to deplete H4K16ac in senescent cells .....	169
6.3.5 Knocking down the acetyl transferase hMOF .....	169
6.3.5.1 Validation of hMOF antibodies using siRNA approaches .....	170
6.3.5.2 shRNA KD of hMOF.....	170
6.3.6 Overexpression of the deacetylase, SIRT1 .....	173
6.3.6.1 Confirmation of impaired deacetylase activity in SIRT1-H363Y cells using Etoposide.....	173
6.3.6.2 Generating IR-induced senescent SIRT1 cells .....	175
6.3.7 Establishment of H4K16R and H4K16Q mutant cells .....	178
6.3.7.1 Site-specific mutagenesis to create H4K16R and H4K16Q retroviral constructs.....	178
6.3.7.2 Overexpression of H4K16 mutants in proliferating cells .....	178
6.3.7.3 Induction of senescence in H4WT and H4K16R cells using IR .....	181
6.3.7.4 Loss of H4K16ac enrichment observed in H4K16R mutants.....	181
6.3.8 KD of HIRA .....	184
6.3.8.1 KD of HIRA in pre-senescent cells.....	184
6.3.8.2 Establishing senescent cells lacking HIRA via long-term passaging ...	184

6.3.8.3	Decreased H4K16ac in senescent cells lacking HIRA.....	186
6.3.8.4	HIRA maybe required for enrichment of H4K16ac at gene promoters in senescent cells .....	186
6.4	Discussion .....	191
7.	Discussion and future perspectives.....	196
7.1	H3CS.1 and senescence.....	197
7.2	H4R3me2a and senescence .....	200
7.3	H4K16ac and senescence .....	203
8.	References.....	206

## List of tables

Table 1.1 Outline of distinct types of modifications occurring on histones.....	46
Table 2.1 Reagents and solutions.....	65
Table 2.2 Antibodies and dyes.....	67
Table 2.3 Plasmids.....	70
Table 2.4 Primers.....	71
Table 2.5 DNA sequencing primers .....	71
Table 2.6 Percentage of agarose gel .....	72
Table 2.7 Resolving gel.....	76
Table 2.8 Stacking gel.....	76
Table 2.9 Percentage of polyacrylamide gel .....	76
Table 2.10 Reagent volumes for different packed cell volumes.....	79
Table 2.11 ChIP buffers .....	80
Table 2.12 PCR conditions .....	83
Table 2.13 Quantitative ChIP-PCR conditions .....	85
Table 2.14 Quantitative ChIP PCR primers .....	86
Table 2.15 Reaction components in EdU proliferation assay .....	89
Table 3.1 List of antibodies used in the histone modification screen.....	99
Table 3.2 Candidate histone modifications that increase in replicative senescence as identified from the screen in Figure 3.5.....	101
Table 5.1 The plasmids used in the study along with the given virus name. ....	132
Table 5.2 Statistical summary of H4R3me2a ChIP-sequencing. ....	150

## List of figures

Figure 1.1 Various triggers for cellular senescence.....	24
Figure 1.2 Senescence signaling pathways.....	28
Figure 1.3 The senescence secretome and its associated effects. ....	31
Figure 1.4 Senescence, a double-edged sword.....	38
Figure 1.5 Structure of chromatin.....	42
Figure 1.6 Histone modifications.....	48
Figure 3.1 Establishment of replicative senescence in human diploid fibroblasts IMR90. ....	93
Figure 3.2 Western blot analysis of proteins in proliferating and senescent IMR90 cells.....	94
Figure 3.3 Loss of histones observed in senescent cells <i>in vitro</i> . ....	96
Figure 3.4 Titration of histone H3 in senescent cells compared to proliferative cells. ....	97
Figure 3.5 Profiling of various histone modifications in senescent cells in comparison to proliferating cells. ....	98
Figure 3.6 Levels of candidate histone marks in two different models of senescence, RS and OIS.....	102
Figure 3.7 Increased levels of histone marks in IMR90 is exclusive to senescence.....	106
Figure 3.8 Changes in histone marks observed specifically in senescence and not simply cell cycle arrest. ....	107
Figure 4.1 Confirmation of cleaved H3 in senescent cells. ....	112
Figure 4.2 Establishment of inducible model of senescence in IMR90.....	114
Figure 4.3 Western blot analysis of proteins in control (uninduced) and 4OHT-induced senescent cells.....	115
Figure 4.4 H3CS.1 abundance gradually increases after induction of RAS.....	117
Figure 4.5 Cathepsin L, the enzyme responsible for H3 cleavage is upregulated in OIS.....	119
Figure 4.6 Cytoplasmic localization of histone H3CS.1 in OIS visualized by immunofluorescence.....	120
Figure 4.7 Cytoplasmic localization of histone H3CS.1 in OIS. ....	121
Figure 5.1 Specificity of H4R3me2a antibody assessed using MODified Peptide Array Analysis.....	126

Figure 5.2 Increase in H4R3me2a as confirmed by a second antibody to H4R3me2a. .....	128
Figure 5.3 Gradual increase in H4R3me2a abundance after induction of RAS.....	130
Figure 5.4 Overexpression of SV40LTA <sub>g</sub> in IMR90.....	131
Figure 5.5 Control and SV40LTA <sub>g</sub> transduced cells co-infected with RAS virus. ....	133
Figure 5.6 Increase in H4R3me2a in OIS is not inhibited by expression of SV40LTA <sub>g</sub> . .....	134
Figure 5.7 Expression of PRMT1 is elevated in senescent cells. ....	136
Figure 5.8 Generating IMR90 cells with constitutive KD of the enzyme PRMT1. ....	138
Figure 5.9 Confirmation of PRMT1 KD in biological replicates with new antibodies.	139
Figure 5.10 Generation of PRMT1 KD cells with activated RAS.....	141
Figure 5.11 PRMT1 is required for induction of H4R3me2a in senescence. ....	142
Figure 5.12 Optimization of sonication conditions in proliferating and senescent cells. .....	144
Figure 5.13 Optimization of H4R3me2a ChIP conditions.....	146
Figure 5.14 H4R3me2a ChIP in proliferating and senescent cells.....	147
Figure 5.15 Quality control analysis of ChIP libraries using Agilent 2100 Bioanalyzer. .....	149
Figure 5.16 Distribution of H4R3me2a on a region of Chr22 as viewed on UCSC genome browser.....	152
Figure 6.1 Aligned reads from histone H4 and H4K16ac ChIP of proliferating and senescent cells visualized on the UCSC Genome Browser. ....	161
Figure 6.2 H4K16ac distribution relates to gene expression in senescence.....	162
Figure 6.3 Specificity of H4K16ac antibody confirmed using MODified Peptide Array Analysis.....	165
Figure 6.5 Establishment of IR-Induced Senescent cells.....	167
Figure 6.6 ChIP PCR confirms relative enrichment of H4K16ac in the IR-induced model of senescence. ....	168
Figure 6.7 Characterization of hMOF antibodies using siRNAs.....	171
Figure 6.8 Establishment of stable hMOF KD in IMR90s resulting in loss of H4K16a. .....	172
Figure 6.9 Etoposide treatment of SIRT1 WT and SIRT1-H363Y mutant cells demonstrating impaired deacetylase activity of mutant cells.....	174

Figure 6.10 Induction of senescence in SIRT1 WT cells. ....	176
Figure 6.11 SIRT1 overexpression in proliferating cells.....	177
Figure 6.12 DNA sequencing confirms creation of histone H4K16 mutants. ....	179
Figure 6.13 Establishment of histone mutant cells.....	180
Figure 6.14 Induction of senescence in histone mutant cells.....	182
Figure 6.15 Depletion in H4K16ac levels observed in HA-H4K16R-expressing senescent cells.....	183
Figure 6.16 KD of HIRA in pre-senescent cells.....	185
Figure 6.17 Senescent cells lacking HIRA exhibit SA $\beta$ -Gal staining. ....	187
Figure 6.18 Confirmation of growth arrest in senescent cells lacking HIRA. ....	188
Figure 6.19 Senescent cells lacking HIRA show decreased total H4K16ac. ....	189
Figure 6.20 Depletion of H4K16ac at regions of the genome observed in senescent cells lacking HIRA. ....	190

## **Acknowledgements**

First and foremost, I would like to thank my mentor, Prof. Peter Adams, for providing me with an opportunity to work in his lab. He is, without a doubt, one of the best teachers I have had in my life. I thank him for believing in me, especially during the difficult times and supporting me through his patient guidance. I have also had the opportunity to meet and work alongside amazing people through this project. I would like to thank my lab mates for always being there and for all the support they have provided me. Not to forget, all the support staff of Beatson, Central services, Molecular Technology services and the Animal house facility for their excellent support. A special acknowledgement to Prof. Kevin Ryan, who has been my advisor and a great source of encouragement. Thank you to the funding bodies - University of Glasgow, CRUK and NIH for supporting this project.

I have made amazing friends in Glasgow and they too have had a part in this project unknowingly. For that I would like to thank them. I would like to dedicate this work to my dad, mum and my entire family, for they have been relentless in their support. They now know (atleast I think) what senescence is ! Of special note, I would like to mention Nila for helping me with the illustrations in this project.

Lastly I would like to mention Pravin for being with me through this journey. I couldn't have possibly made it without his love and support.

I have learnt a lot by being part of the Adams family and I hope this helps me to go places in the future.

## **Publications arising from this work and other collaborations**

A. L. Kennedy, J. P. Morton, I. Manoharan, D. M. Nelson, N. B. Jamieson, J. S. Pawlikowski, T. McBryan, B. Doyle, C. McKay, and K. A. Oien, G. H. Enders, R. Zhang, O. J. Sansom, and P. D. Adams, "Activation of the PIK3CA/AKT pathway suppresses senescence induced by an activated RAS oncogene to promote tumorigenesis," *Molecular cell*, vol. 42, pp. 36-49, 2011.

A. Ivanov, J. Pawlikowski, I. Manoharan, J. van Tuyn, D. M. Nelson, T. S. Rai, P. P. Shah, G. Hewitt, V. I. Korolchuk, J. F. Passos, H. Wu, S. L. Berger, and P. D. Adams, "Lysosome-mediated processing of chromatin in senescence," *J Cell Biol*, vol. 202, pp. 129-43, Jul 8 2013.

T. S. Rai, J. Cole, D. M. Nelson, D. Dikovskaya, T. McBryan, J. V. Tuyn, N. Morrice, I. Manoharan, N. Pchelintsev, W. Faller, A. Ivanov, C. Brock, M. Drotar, C. Nixon, W. Clark, A. King, O. Sansom, K. Blyth, P. D. Adams, "Histone chaperone HIRA orchestrates dynamic chromatin in senescent cells and is required for suppression of oncogene-induced neoplasia," *In preparation*.

## **Declaration**

I declare that all of the work in this thesis was performed personally. No part of this work has been submitted for consideration as part of any other degree or award.

## Abbreviations

53BP1	p53 binding protein 1
ARF	alternate reading frame
ASF1	anti-silencing function 1 homolog
ATG	autophagy-related genes
ATM	ataxia telangiectasia mutated
ATR	ataxia telangiectasia and Rad3 related
ATRX	alpha thalassemia/mental retardation syndrome X-linked
B-RAF	V-raf murine sarcoma viral oncogene homolog B1
BAX	BCL2-associated X protein
BCL-xL	B-cell lymphoma-extra large
BCL2	B-cell lymphoma 2
BMI1	B lymphoma Mo-MLV insertion region 1 homolog
BNIP3	BCL2/adenovirus E1B 19kDa interacting protein 3
BNIP3L	BCL2/adenovirus E1B 19kDa interacting protein 3-like
BPTF	bromodomain PHD finger transcription factor
BRCA1	breast cancer 1, early onset
BSA	bovine serum albumin
BubR1	budding uninhibited by benzimidazoles 1 homolog (yeast)
C/EBP- $\beta$	CCAAT-enhancer-binding proteins beta
CAF1	chromatin assembly factor 1
CDK	cyclin dependent kinase
CENP-A	centromere protein A
ChIP	chromatin immunoprecipitation
ChIP-Seq	chromatin immunoprecipitation sequencing
CXCL1	chemokine (C-X-C motif) ligand 1
CXCR2	chemokine (C-X-C motif) receptor 2
DAPI	4'6-diamidino-2-phenylindole
DAXX	death-domain associated protein
DDR	DNA damage response
DMEM	Dubelcco's modified eagle medium

DMSO	dimethyl sulfoxide
DNA	deoxyribonucleic acid
DNA-Scars	DNA segments with chromatin alterations reinforcing senescence
DNA-PK	DNA-dependent protein kinase
DTT	dithiothreitol
ECL	enhanced chemiluminescence
ECM	extra-cellular matrix
EDTA	ethylenediaminetetraacetic acid
EdU	5 ethynyl-2ÅL-deoxyuridine
EZH2	enhancer of zeste homolog
FOXO	forkhead box O
GAllx	genome analyzer IIx
GROα	melanoma growth stimulating activity alpha
HAT	histone acetyl transferase
HDAC	histone deacetylase
HDF	human diploid fibroblast
HIRA	HIR histone cell cycle regulation defective homolog A
HP1	heterochromatin protein 1
HRAS	harvey rat sarcoma viral oncogene homolog
hTERT	human telomerase reverse transcriptase
IF	immunofluorescence
IgG	immunoglobulin G
IL	interleukin
IMR90	human fetal lung fibroblast
IP	immunoprecipitation
IPDB	immunoprecipitation dilution buffer
IR	ionizing radiation
LC3B	light chain 3 beta
lncRNA	long non-coding ribonucleic acid
MAPK	mitogen-activated protein kinases
MBT	malignant brain tumor domain
MDC1	mediator of DNA-damage checkpoint 1

MEF	mouse embryonic fibroblast
mM	millimolar
MMP	matrix metalloproteinase
mNLB	modified nuclear lysis buffer
mRNA	messenger ribonucleic acid
mTOR	mammalian target of rapamycin
MYC	myelocytomatosis viral oncogene homolog (avian)
NBS1	nijmegen breakage syndrome gene
ncRNA	non-coding ribonucleic acid
NF- $\kappa$ B	nuclear factor kappa-light-chain-enhancer of activated B cells
nM	nanomolar
NURF	nucleosome remodelling factor
OIS	oncogene-induced senescence
p53	cellular tumor antigen p53 or tumor suppressor p53
PAGE	polyacrylamide gel electrophoresis
PAI1	plasminogen activator inhibitor-1
PanIN	pancreatic intraductal neoplasia
PBS	phosphate buffered saline
PcG	polycomb group
PCNA	proliferating cell nuclear antigen
PCR	polymerase chain reaction
PD	passage doubling
PEI	polyethylenimine
PHD	plant homeo domain
PI3K	phosphoinositide-3-kinase, regulatory subunit
PML	promyelocytic leukemia
PMSF	phenylmethylsulfonyl fluoride
PRC	polycomb repressive complex
PTM	post-translational modification
PVDF	polyvinylidene fluoride
RB	retinoblastoma protein
REL	v-rel avian reticuloendotheliosis viral oncogene homolog
RNA	ribonucleic acid

ROS	reactive oxygen species
RPA	replication protein A
RS	replicative senescence
SA $\beta$ -gal	senescence-associated beta-galactosidase
SAHF	senescence-associated heterochromatin foci
SASP	senescence-associated secretory phenotype
SDF	senescence damage foci
SDS	sodium dodecyl sulfate
shRNA	short hairpin ribonucleic acid
SMAD	human orthologue of, <i>Drosophila melanogaster</i> mothers against decapentaplegic homolog
SUZ12	suppressor of zeste homolog
SWI/SNF	switch/sucrose nonfermentable complex
TBS	tris-buffered saline
TGF- $\beta$	transforming growth factor beta
TIF	telomere dysfunction-induced foci
TSS	transcription start site
ULK3	unc-51 like kinase 3
VEGF	vascular endothelial growth factor
WB	western blot
WNT	wingless-type MMTV integration site family
WT	wild type
X-gal	5-bromo-4-chloro-3-indolyl- $\beta$ -d-galactopyranoside
Zmpste24	zinc metallopeptidase (STE24 homolog, <i>S. cerevisiae</i> )
$\mu$ M	micromolar

## **1. INTRODUCTION**

# 1 INTRODUCTION

---

## 1.1 Senescence as a cellular stress response

More than half a century ago, Leonard Hayflick and colleagues first coined the term 'cellular senescence' [1, 2]. The 'Hayflick limit' was defined as the limit in proliferative capacity of cultured primary human cells. Although this finding was strongly challenged then, senescence as a cellular phenomenon is now appreciated and accepted more widely. Hence the term cellular senescence simply denotes stable and long term loss of proliferative capacity. This work has had an enduring impact over the years and cited about 3000 times between 1961 to 1999 [3].

Senescence is a complex response depending on the context and can have both beneficial and detrimental effects, like a double-edged sword [4-6]. Senescence is a potent tumor suppressive mechanism [7-11]. While there is considerable debate as to whether cellular senescence contributes to ageing, accumulating evidence suggests a plausible relationship between the two [9, 12-14]. The senescence response may be antagonistically pleiotropic by suppressing tumourigenesis early in life and limiting organismal longevity later in life [15]. Understanding senescence in the context of normal cell physiology and its effects on disease states is extremely important.

## 1.2 Signals initiating senescence

Senescence can be initiated by an array of different triggers (Figure 1.1) and some of them are detailed in the following sections.

### *1.2.1 Telomere dysfunction*

Normal diploid vertebrate cells with a limited capacity to proliferate [1] is in part due to telomere shortening [16-18]. Cells, with each round of replicative division, undergo progressive shortening of the ends of their chromosomes called telomeres, resulting in "critically short" or "uncapped" telomeres, at which point the cells lose their capacity to divide [19]. Telomeres present at the ends of the chromosomes are simple G-rich sequence repeats containing TTAGGG [20, 21]. Telomeric repeats protect the ends

of eukaryotic chromosomes from degradation or end to end fusion [22]. Loss of telomeres in the absence of telomerase triggers cell senescence [23]. The role of telomeres in replicative senescence was further supported by work demonstrating that mutations in the RNA component of telomerase (the enzyme responsible for adding DNA repeats at telomeric regions) leads to telomere attrition and senescence in *Tetrahymena* [24]. Wright and Shay initially described how telomere attrition lead to programmed changes in cell behaviour and regulated the senescence programme [25]. Activation of DNA damage checkpoints occurs at shortened or uncapped telomeres, following which cells undergo growth arrest [26]. This and other reports confirmed the establishment of replicative senescence (RS), at least in part, as a consequence of dysfunctional telomeres [27, 28].

### *1.2.2 Oxidative Stress*

Replicative senescence is just one part of a more widespread response called cellular senescence. Another potent inducer of senescence is DNA damage caused by oxidative stress. Treatment with low doses of hydrogen peroxide leads to irreversible senescence in human diploid fibroblasts. [29, 30]. Experiments suggest that senescence could be delayed by culturing under low oxygen conditions and accelerated under high oxygen conditions [31, 32]. Also, metabolism within the cell produces ROS (Reactive Oxygen Species), which are chemically reactive molecules containing oxygen [33]. ROS can also be produced as a result of external stress, such as hydrogen peroxide, UV (Ultra Violet) rays or IR (ionizing radiation) [34]. ROS can function as an important signalling factor to trigger senescence [35, 36]. Hence it is clear that telomere attrition is not the only stimulus for senescence and other triggers such as oxidative stress can function to initiate senescence.

### *1.2.3 Oncogene activation*

Oncogene-induced senescence (OIS) was first reported in primary human fibroblasts following overexpression of an oncogenic form of RAS (Rat Sarcoma) [37]. Although activation of RAS in fibroblasts initially induces a mitotic burst, the cells eventually progress to senescence. RAS provoked permanent arrest in G1 phase of the cell cycle is accompanied by increased expression of p53, p21 and p16. Inactivation of

p53 or p16/pRB pathway by overexpression of E1A bypasses senescence [37]. E1A is a viral oncoprotein known to perturb pRB and p53-mediated growth arrest [38]. This shows that OIS depends on intact pRB and p53 pathways and that an oncogenic trigger is a potent inducer of senescence.

Indeed several lines of evidence now show induction of senescence following activation of a variety of oncogenes such as B-RAF (V-raf murine sarcoma viral oncogene homolog B1) [39], MEK (MAPK/Erk kinase), MYC (Myelocytomatosis viral oncogene homolog) along with tumor suppressors such as PTEN (Phosphatase and tensin homolog) or NF1 (neurofibromin 1) in a wide-variety of cell lines [40-43]. Based on the above, significant differences are apparent between telomere-dependent replicative senescence and oncogene-induced senescence.

#### 1.2.4 Other inducers

Induction of senescence also occurs due to other factors. For example, DNA Damage Response (DDR) activation due to DNA damage is a potent inducer of senescence and DDR activation contributes to OIS [44]. This and other studies involving both OIS and replicative senescence have indicated that activation of DDR may be inherently characteristic to cellular senescence [26, 27]. DNA-damage inducing senescence under *in vitro* and *in vivo* conditions was demonstrated in a study involving a human carcinoma cell line expressing wild-type p53 [45]. Also stress signals from the environment are shown to result in rapid G1 growth arrest different to the progression of replicative senescence via telomere shortening [46-49]. Nevertheless the resultant growth arrest is similar to that of replicative senescence, failing to show a response to mitogenic stimulus and characteristic changes to the cellular morphology [37, 49, 50]. Such growth arrest or senescence induced due to upregulation of growth inhibitory genes and repression of cell cycle genes following culture shock or environmental stress factors can be called as Stress-induced senescence or STASIS (STress or Aberrant Signaling-Induced Senescence) [49, 51].

Another instance of the induction of senescence is reported through the effects of various agents used in clinical applications such as chemotherapeutic agents and ionizing radiation [11, 45, 52-58]. Drug-treated cells specifically acquire a senescent phenotype following treatment [59]. Some of the most potent inducers of senescence

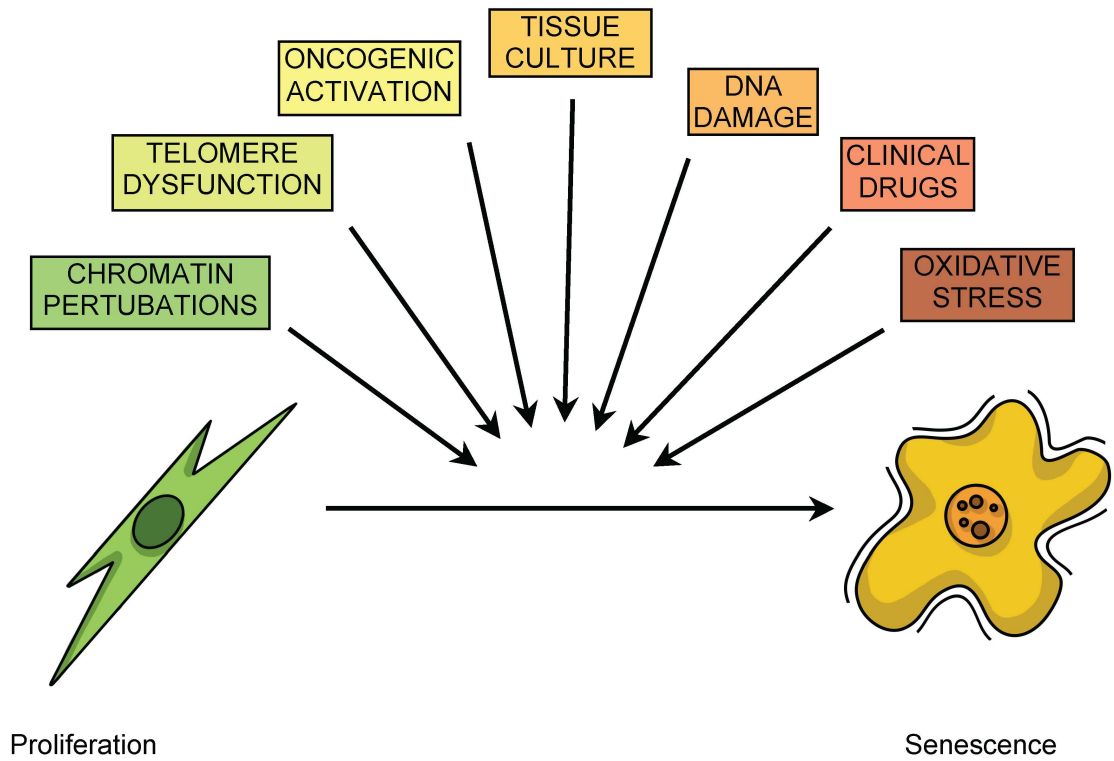


Figure 1.1 Various triggers for cellular senescence.

Senescence can be triggered by various external factors or stress signals such as telomere dysfunction, oncogenic activation resulting in the conversion of a proliferating cell to a senescent cell.

are etoposide, cytarabine, cisplatin, aphidicolin, doxorubicin and ionizing radiation [53]. These agents strongly affect the DNA structure. Tumor cell senescence is reported to be induced by a host of other agents, such as TGF- $\beta$  [60], retinoids [61, 62], differentiating agents such as sodium butyrate [63] and antiestrogens [61]. Hence DNA-damaging agents such as anti-cancer drugs and chemotherapeutic treatments contribute towards irreversible growth arrest.

In addition, it is noted that senescence can also be caused by chromatin perturbations [64, 65] and this will be discussed in detail in subsequent sections. To summarize, the above-mentioned studies clearly demonstrate various cellular stresses can act as a molecular trigger for cellular senescence.

### 1.3 Effectors of the senescence programme

Senescence as a cellular stress response involves multiple effector mechanisms (Figure 1.2), which contribute differently depending on the trigger and cell type. In order to understand the senescence programme it is essential to understand the effector mechanisms. These are discussed as follows:

#### *1.3.1 Control by p53-pRB pathways*

Two of the most important master regulators of senescence are the p53-p21 and p16-pRB pathways. Although these two pathways interact with one another, they establish growth arrest independently [66]. I will discuss these independently.

##### *1.3.1.1 The p53 pathway*

p53 is a tumor suppressor and establishment of senescence is primarily facilitated through activation of the p53 pathway following activation of DDR, for example by telomere shortening or ionizing radiation [26, 67]. To activate the pathway, HDM2 stabilizes p53 by targeted degradation, following which activation of p53's transcriptional targets, such as p21, occurs [68]. p21, which inhibits cyclin/cdk2 complexes, is an essential mediator of p53-dependent cell cycle arrest [69-73]. Mouse embryonic fibroblasts lacking p21 are impaired in their ability undergo senescence [74]. In fact, lack of p21 is shown to abrogate senescence in several

studies [69, 75, 76]. Also reports from mice and human studies show that reduction of p53 or DDR proteins, such as ATM or CHK2, prevents or even reverses senescence in some cases [26, 44, 69, 77-79]. Although p21 is a key player in the establishment of p53-mediated senescence, it is to be emphasized that a plethora of other players are also involved in the same pathway [80-83]. p53, apart from heavily contributing to the establishment of senescence, is also a key regulator of metabolic and physiological pathways with various known targets [84]. In summary, p53 is a potent effector of the senescence programme.

### 1.3.1.2 *The pRB pathway*

pRB is a tumor suppressor and activation of pRB tumor suppressor pathway occurs to induce senescence, in part, as a secondary effect after activation of the p53 pathway following a DDR trigger [85, 86]. Nevertheless, establishment of senescence via the p16-pRB pathway also occurs independently without p53, in a cell-type dependent and context-specific manner. Inactivation of pRB and p53 results in bypass of senescence in human and mouse cells, despite the initial trigger [66, 87-89]. Some species-specific differences lie in the fact that mouse cells engage only p53 pathway upon telomere disruption, whereas human cells employ both p53 and p16-pRB pathways [90].

Several key players regulate activation of the pRB-p16 pathway. Upon inhibition of cyclin/cdk2 complexes by p21, downstream of p53, activation of the pRB pathway occurs. p16, another well-known CDK inhibitor, orchestrates the maintenance of pRB in its activated hypophosphorylated form, thereby resulting in the inhibition of E2F target genes responsible for normal cell proliferation and control [68]. During oncogenic activation of RAS, p16 expression increases as a result of activation of ETS (E26 transformation-specific) transcription factors, which are negatively regulated by the ID family of helix-loop-helix (HLH) proteins [91]. Another class of proteins known as the Polycomb group (PcG) also regulate p16-mediated senescence [92]. PcG proteins including BMI1 (B lymphoma Mo-MLV insertion region 1 homolog), CBX7 (chromobox homolog 7) and CBX8 (chromobox homolog 8) are involved in the regulation of growth arrest through INK4A-ARF locus encoding p16 and p14 upstream of pRB and p53 pathways, respectively [92, 93]. The PcGs

comprises of two main complexes PRC1 (Polycomb Repressive Complex 1) and PRC2, which consists of various subunits such as EZH2 (Enhancer Of Zeste Homolog 2), EED (Embryonic Ectoderm Development), SUZ12 (Suppressor Of Zeste 12 Homolog) and RbAp48 (Retinoblastoma-Binding Protein P48). EZH2 is a known di/tri-methyl transferase for K27 on H3 [94]. EZH2-dependent H3K27me3 represses INK4A-ARF locus together with other PcGs such as BMI1 and SUZ12-containing PRC2 complex to mediate cell cycle arrest and senescence [92]. Also emerging roles of coordination between p38MAPkinase and PcG proteins suggest contribution towards p16-mediated senescence [95]. Hence a plethora of players take part in the complex regulation of pRB-p16 pathway, a key effector of senescence.

### *1.3.2 DNA damage signalling*

DNA damage signalling is a major effector of senescence [96]. DDR is an evolutionary conserved pathway sensing damage in the cell's DNA [97]. A signalling cascade is then activated to facilitate repair of the damage. Either the damage is repaired promptly in proliferating cells and the cells resume normal proliferation, or they may undergo programmed cell death if the damage is particularly severe [98]. A third possibility is that cells attain senescence.

During replicative senescence, critical shortening of telomeres induces senescence via activation of ATM/ATR signalling, leading to p53-and p16-mediated senescence in humans [90, 99, 100]. Also, uncapped telomeres are potent inducers of DDR [26]. The DNA damage pathway is activated via recruitment of signalling kinases, such as ATM, ATR and possibly DNA-PK, to the site of damage resulting in phosphorylation of Ser-139 of histone H2A.X molecules ( $\gamma$ -H2A.X) [26, 27]. The phosphorylation event facilitates the assembly of DNA checkpoint and repair factors, such as 53BP1 (P53 Binding Protein 1), NBS1 (Nijmegen breakage syndrome 1) and MDC1/NFBD1 (Mediator of DNA damage checkpoint protein 1/ nuclear factor with BRCT domains protein 1). Following this, activation of the transducer kinases CHK1 and CHK2 occurs via phosphorylation, which then relays information to p53 [26, 27]. Inactivation of ATM/ATR and CHK1/CHK2 in cells lead to bypass of senescence and re-entry into the S phase of the cell cycle [26, 27]. To summarize, dysfunctional telomeres are recognized as DNA breaks at the chromosome ends leading to activation of DDR signalling, thereby resulting in senescence.

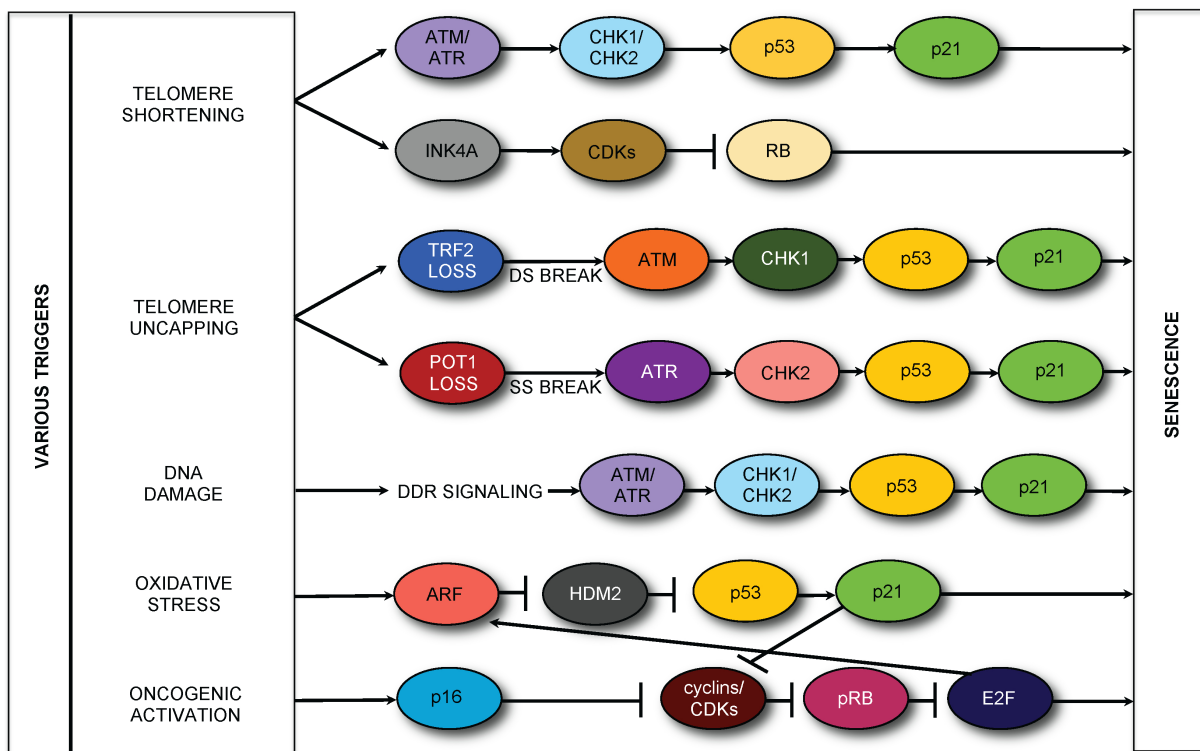


Figure 1.2 Senescence signaling pathways.

The two major effectors of senescence are the p53 and pRB pathways. Recent evidence show that multiple types of cellular stresses can activate these two pathways by common or overlapping mechanisms. Telomere dysfunction leads to DDR signaling via ATM/ATR activation and engaging downstream kinases CHK1/CHK2 resulting in p53 phosphorylation which regulates genes essential for senescence establishment. p53 imparts its effects by engaging p21, which is a well-known cyclin/CDK inhibitor. Telomere shortening could also engage the INK4A-pRB pathway and PcG proteins to induce senescence, although this remains poorly understood. Alternatively, telomere uncapping can result in activation of senescence via TRF2/ATM activation or POT1/ATR activation. In response to other stresses, such as cytotoxic drugs, culture stress including telomere shortening and oncogenic insult, the DNA damage response results in ATM/ATR check point activation leading to increased p53. ARF negatively regulates HDM2 and HDM2 in turn has a negative impact on p53 thereby facilitating its degradation. Another key pathway that regulates senescence is the p16-pRB pathway, resulting in downstream repression of E2F target genes, enabling cell cycle arrest. E2F can also activate ARF expression to enable growth arrest. Adapted from [66, 101].

OIS is also reported to activate DDR signalling [44, 102-108]. Oncogenic RAS activation leads to a biphasic response with robust activation of DDR at the time of transition from initial hyperproliferation phase to growth arrest [109]. Activated RAS induces senescence-associated DNA-damage foci (SDF), harboring activated ATM, ATR and RPA, along with other key mediators of DDR such as histone  $\gamma$ -H2A.X, 53BP1, MDC1 [44]. These data imply that senescence, both OIS and RS, is accompanied and actively maintained by DNA damage signalling [29, 96, 110].

### 1.3.3 Effect of autophagy

Autophagy was recently identified as a modulator of senescence [111]. Autophagy is a catabolic process involving degradation of unwanted materials from cells, using lysosomal machinery [112]. Although both senescence and autophagy can be considered a cellular response to stress [113], it was not until recently that the link between the two was established. Young et al., found that following RAS activation, the autophagic response peaked at the transition phase, where cells enter growth arrest following hyperproliferation. The authors describe an initial 'mitotic phase' followed by the 'senescence phase' with a transition phase between the two. Activation of autophagy is associated with inhibition of mTOR, an inhibitor of autophagy [111]. Autophagy-related genes (ATG) were increased during OIS, along with ULK3 (unc-51 like kinase 3), LC3B (light chain 3 beta), BNIP3 (BCL2/adenovirus E1B 19kDa interacting protein 3), and BNIP3L (BCL2/adenovirus E1B 19kDa interacting protein 3-like) [111, 114]. This observation was not only restricted to *in vitro* models of senescence, but also extended to *in vivo* settings where chemically induced skin papillomas (with RAS mutations containing senescent cells [115]) also exhibited autophagic activity [111]. Although inhibition of autophagy did not result in abrogation of senescence, it delayed senescence response and also accumulation of senescence-associated secreted proteins [111, 114]. The role of SASP will be discussed later (Section 1.4.2). Direct evidence of activated autophagic flux was also reported in replicative senescence [116]. Following this original observation, a number of studies reported induction of autophagy and senescence within the same setting [117-122]. In contrast to this, an inverse relationship between autophagy and senescence is also reported where inhibition of autophagy promotes senescence [123, 124]. This can be explained in part with levels of autophagic activity as high

levels bypass senescence whereas low levels promote senescence [124]. Nevertheless, autophagy is an important effector of the senescence program facilitating efficient establishment and quality of the senescent phenotype [125].

#### 1.4 Senescent phenotype

Although some of the phenotypes acquired by senescent cells are not exclusive to the programme, senescent cells display several characteristic features, which together define the senescent state and these will be discussed below.

##### *1.4.1 Stable proliferation arrest*

First and foremost, the most striking feature of cellular senescence is the stable proliferation arrest caused by various stresses. The growth arrest observed essentially cannot be reversed by any known physiological stimuli. In some cases, it has been demonstrated that p16 forms a formidable second barrier to growth arrest as inactivation of p53 in the absence of p16 lead to resumed robust growth [126]. Despite having other characteristic features, growth arrest remains the most fundamental feature of senescence.

##### *1.4.2 Senescence Associated Secretory Phenotype*

Another distinct feature of senescence is the SASP (Senescence Associated Secretory Phenotype). Despite exit from the cell cycle, senescent cells are very much metabolically active and are noted to develop a characteristic secretory phenotype [127]. The SASP encompasses a plethora of secreted factors, typically comprised of pro-inflammatory cytokines and chemokines and matrix remodelling enzymes (Figure 1.3) that can have an effect on its surrounding cells and tissue microenvironment [13]. The SASP components include MMP3, IL-6, IL-8, PAI1, VEGF and GRO $\alpha$ . IL-6 and IL-8 also act to reinforce the senescence-associated proliferation arrest [128]. Induction of varying degrees of SASP is reported in those cells undergoing senescence as a result of DNA damage, oxidative stress, telomere shortening, chromatin alterations and other stress factors [128-138].

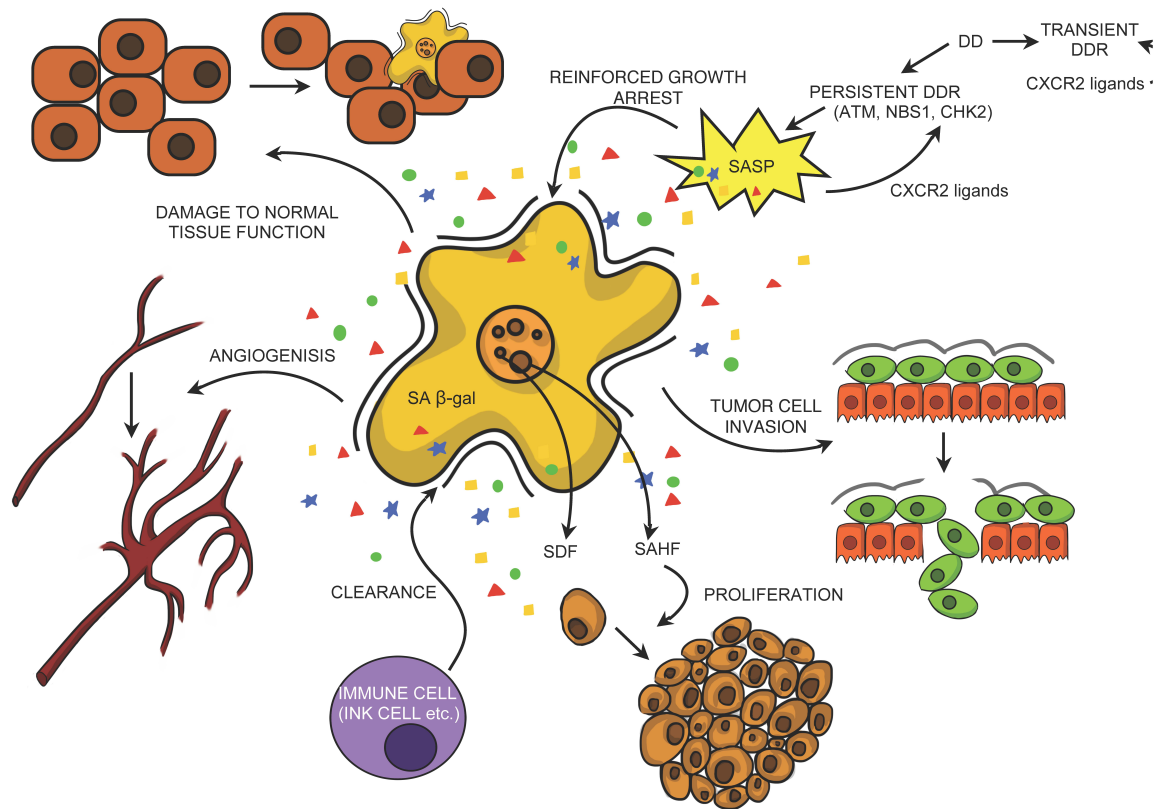


Figure 1.3 The senescence secretome and its associated effects.

A key feature of senescence is the secretion of a myriad of cytokines, growth factors. These are collectively known as SASP. A DDR trigger activates ATM, NBS1 and CHK2 to induce senescence via p53/pRB pathways. The secretory factors in turn act in a feedback loop to ensure sustained DNA damage, which in re-enforces senescence. Chemokines, such as CXCR2 ligands, take part in this activity. The SASP can have various effects on cells. It can contribute to immune clearance of senescent tumor cells, proliferation of neighboring tumor cells, tumor cell invasion, impairment of normal tissue function and angiogenesis. The functions of SAHF are discussed in section 1.7.1. Adapted from [13, 139].

The SASP can be regulated by various factors. The SASP is essentially a response to DDR signalling [129, 131]. Hence, cells undergoing senescence without genomic damage or chromatin perturbations, for example, via overexpression of p21 or p16 do not secrete SASP factors despite showing features characteristic to senescence [140]. SASP factors are regulated by components of persistent DNA damage signalling, such as ATM, NSB1 and CHK2 [131, 132]. TIFs (Telomere dysfunction foci) at telomeres [141] and DNA-Scars (DNA Segments with Chromatin Alterations Reinforcing Senescence), containing DNA damage proteins such as 53BP1, are thought to be required for SASP establishment [129, 131, 142]. The SASP can also be regulated positively by NF- $\kappa$ B [132, 135, 143] and C/EBP- $\beta$  [128], and negatively by p53 [129, 131]. In the case of p53, KD studies using RNA interference or dominant negative proteins to disrupt p53 has resulted in increased SASP secretion [129]. Thus, complex networks of proteins cooperate to regulate the SASP during senescence.

#### *1.4.3 Apoptosis Resistance*

Replicative senescence is associated with resistance to apoptosis [144-146]. Many genes associated with apoptosis are associated with senescence. As an example, p53 plays a crucial role in senescence and is also required for certain types of apoptosis following DNA damage. Nevertheless, senescent cells undergo p53-dependent necrosis rather than apoptosis [146]. Necrosis is a form of cell death accompanied by swelling of the cells, loss of membrane integrity resulting in the release of cell contents leading to inflammation [147]. Reports suggest that stabilization of p53 is impaired in senescent fibroblasts resulting in the switch in death pathways from apoptosis to necrosis [146]. However, p53-related apoptosis resistance is reported only in certain cells [148]. The precise mechanism by which senescent cells are resistant to apoptosis is incompletely understood.

A proposed mechanism for senescent cells acquiring apoptosis resistance is the associated increase of BCL-2, an anti-apoptotic gene, during senescence [144]. BCL-2 negatively impacts apoptosis by cooperation with other BCL-2 family members such as BAX (reviewed [149]). Also another anti-apoptotic gene, BCL-xL, is implicated in the regulation of apoptosis resistance in senescence [150]. Using RNA interference, an increase in apoptosis was reported in senescent cells following

reduction in basal levels of BCL-xL. Hence, regulatory roles for the BCL-2 family of proteins are revealed during senescence.

A dual role for p21 in senescence and apoptosis was reported where increased p21 levels in senescence evidently protected cells from apoptosis [151]. It appeared that lowering levels of p21 reverses this phenomenon by making senescent cells more susceptible to cell death.

Although apoptosis resistance is clearly demonstrated in senescent cells, its precise regulation and functionality remains to be well studied.

#### 1.4.4 Markers of senescence

Although no single marker exists for senescence, combinations of biomarkers are currently employed to assay establishment of senescence both under *in vitro* and *in vivo* conditions. Nevertheless, the most striking feature of senescence is an irreversible growth arrest [9]. Some senescent cells appear to have a distinctive phenotype by acquiring enlarged flattened morphology [2]. This type of flattened cell morphology was noted in cells undergoing RAS-induced senescence [37, 152] due to DNA damage [153, 154] or other stress. However, this is not universal as B-RAF induced senescence or senescence due to p400 silencing have resulted in spindle-shaped morphology [39, 155]. Also, senescent melanocytes following RAS activation but not its downstream target B-RAF, showed massive vacuolization and expansion of the endoplasmic reticulum as a result of unfolded proteins [152]. Hence, various features are manifested in a senescent cell in a cell type and context dependent manner.

A key feature of senescence is the presence of Senescence-Associated  $\beta$ -galactosidase (SA  $\beta$ -gal) activity detectable at pH 6.0 [50]. Dimri et al. first reported this when cultured cells undergoing induced or replicative senescence showed enhanced  $\beta$ -galactosidase activity [50]. This is essentially a readout for increased lysosomal content [156] in senescent cells which is detected *in-situ* in mammalian cells with the use of X-Gal (5-bromo-4-chloro-3-indolyl  $\beta$ -D-galactopyranoside), a chromogenic substrate. SA  $\beta$ -gal activity is found specifically in cells undergoing senescence and not quiescence or terminal differentiation. Senescence accumulates in aged tissues and concordant to this SA  $\beta$ -gal activity has been detected in organs from aged animals and individuals [157-160]. Despite using enhanced SA  $\beta$ -gal

activity as a gold standard marker of senescence, its origin and exact role in senescence still remains elusive and somewhat obscure. Although controversial [158, 161-164], using SA  $\beta$ -gal activity as readout for senescence has remained as a valid marker of senescence along with other characteristic markers.

Also, senescent cells show an increase in intrinsic fluorescence, in other words, enhanced autofluorescence, which is thought to occur as a result of oxidatively, damaged lipids called lipofuscin [165, 166].

As discussed previously, the p53-pRB pathways are major effectors regulating the establishment of senescence. Notably, senescent cells have altered gene expression with increase in levels of p53, p16 and/or p21 [167-170]. Some other commonly used markers for assaying senescence are loss of cyclin A, PCNA, phosphorylation of RB at serines 807/811 [71, 86, 171] and, more recently, loss of lamin B1 and histones [172-175]. The latter will be discussed in subsequent sections (Section 1.7.3). Thus, a lot of the markers used for identifying senescent cells are players in the p53/pRB pathways.

Another biomarker for senescence is the formation of distinct punctate foci called Senescence Associated Heterochromatic Foci (SAHF) [176]. These foci are considered to help facilitate silencing of cell cycle associated genes and are found in some cells, if not all [177]. The exact role of chromatin and SAHF in senescence will be discussed in further section (Section 1.7.1) [178]. Also, as cells approach senescence, the chromatin regulator HIRA exhibits colocalization with PML bodies [178]. This phenomenon will be discussed subsequently (Section 1.7.1). In summary, various markers are used for determining successful establishment of senescence.

## 1.5 Functions and pathologies of senescence

Over 50 years of research into senescence has made it clear that it has various functions and consequences, not just in diseases states or age-related pathologies, such as Alzheimer's, but also in the normal physiology of a cell. Senescence impacts a wide range of processes, such as tumor suppression, wound healing, tissue degeneration and tumor promotion (Figure 1.4).

## 1.5.1 Functional consequences of senescence

### 1.5.1.1 Role in tumor suppression

Substantial research provides evidence for senescence to act as a tumor suppressive mechanism. Although the potential functionality of OIS as a tumor suppressive mechanism *in vivo* was questioned, it was logical owing to its dependence on tumor suppressive pathways involving p53 and pRB.

Firstly, any mutations in the p53 and pRB pathways, two major regulators of senescence, have resulted in high susceptibility to develop cancer, apparent from studies in both humans and mice [66, 168, 179]. Disruption to the senescence programme, for example via inactivation of p53, has resulted in driving premalignant lesions to form potent tumors [180].

Unambiguous evidence has demonstrated the establishment of senescence *in vivo* as a potent barrier to tumor progression [9, 181-183]. Studies from both mice and men have demonstrated the presence of senescence in precancerous neoplasms as a result of an oncogenic insult or loss of tumor suppressor [39, 115, 180, 184, 185]. Also, human nevi are excellent examples of senescence acting as a tumor suppressive mechanism. Nevi are benign tumors of melanocytes, which rarely progress to malignant melanoma and remain growth arrested over long-term due to sustained signalling from B-RAF (V600E) [39]. Acquired nevi often harbour B-RAF mutations, whilst congenital nevi are shown to possess N-RAS mutations, and Spitz nevi have H-RAS mutations [186-188]. These mutations are not only reported in the benign nevi but also malignant melanoma, suggesting that some melanocytic nevi bypass OIS to become aggressive melanoma [43, 189, 190]. Senescence as an effective cancer block is demonstrated in various mouse models of cancer [180, 184, 191-194]. In a mosaic model of mouse liver carcinoma, tumor regression was shown upon reactivation of endogenous p53 [195]. Upon p53 induction, the primary response was that of senescence and not apoptosis resulting in reduced tumor growth. Similarly, another study with p53 restoration in sarcomas lead to suppression of tumor growth with features of cellular senescence [196]. The relative contribution of senescence was also determined in p53-mediated tumor suppression using mouse *knock-in* studies and proved that dysfunctional-telomere mediated senescence is an effective tumor suppressive mechanism [197]. This, along with other reports, provided

*in vivo* evidence for senescence in response to telomere shortening and OIS acting as an effective tumor suppressive mechanism [198, 199].

Another key feature supporting senescence as a tumor suppressor mechanism is in its given nature to stimulate immune clearance of oncogene-expressing cells, those that have succumbed to senescence and also those that have bypassed senescence to transform into aggressive cancer [200]. Senescent cells facilitate recruitment of cells such as destructive leukocytes along with a host of other innate and adaptive immune cells such as T cells, natural killer cells and macrophages [196, 201]. These in turn promote immune clearance of not only cancer cells but also senescent cells [201, 202]. The SASP plays a key role in establishing senescence-mediated immune surveillance for disposal of cancer cells [203, 204].

The SASP also plays an important role in aiding senescence suppress cancer development in other ways. RAS and B-RAF are frequently mutated in human cancers [186, 205]. Following RAS or B-RAF oncogenic insult, secreted factors such as IL-6, IL-8 and IGFBP7 participate in reinforcement of senescence [128, 135, 138]. Similarly, secreted factors such as PAI-1 [206] and GRO $\alpha$  [207] contribute to growth arrest during RS and OIS, respectively. GRO $\alpha$  is a targeted ligand of the enzyme CXCR2. An important role for CXCR2 chemokine signalling in reinforcing growth arrest in a p53-dependent manner was established in fibroblasts undergoing OIS [135]. During senescence increase in CXCR2 was detected and modulating levels of the chemokine enzyme modulated promotion or delay of senescence [135]. Also WNT16B, a SASP factor, was shown to be an enforcer of growth arrest during stress-induced senescence or OIS in fibroblasts under culture conditions, and also *in vivo* in a mouse murine model of K-RAS induced senescence [208]. Collectively, this suggests that SASP components play an important role in the establishment and reinforcement of senescence as a tumor suppressive mechanism.

Also, reports have suggested that induction of senescence as a result of genotoxic chemotherapy evidently resulted in a degree of tumor regression in some cancers [209, 210].

In summary, senescence acts as an effective tumor suppressor largely due to its two main features, growth arrest [66, 168, 179, 211] and the SASP [128, 135, 138, 206].

### *1.5.1.2 Role in wound healing*

Senescence has also been reported to contribute to wound healing. Wound healing proceeds in a sequential/timely manner and can be broken down into the following stages: inflammation, re-epithelialization, and tissue remodelling [212, 213]. Any abnormal interruption to this process would result in the development of a wound and can become chronic over time. Also, younger skin is likely to be less susceptible to chronic wounds due to absence of senescent cells, unlike aged skin.

Senescence mediates its effect on wound healing in various ways. An increase in senescence occurs in pressure and venous ulcers during wound healing [214-216]. Also, growth arrest and features of senescence are reported in fibroblasts following exposure to chronic wound fluid, which increases p21 and decreases phosphorylated RB [214, 217]. Senescence is also attributed to other cell types such as keratinocytes, which are activated at the site of wound healing, and brings about changes in protein expression [218]. Hence senescent cells can induce a by-stander effect by spreading senescence to neighboring cells. This event occurs along with the induction of cRel, a transcription factor in the Rel/NF- $\kappa$ B family [218, 219]. Another crucial event that is part of normal development and wound healing is the growth and turnover of new blood vessels. Decreased proliferative capacity and activation of senescence occur in EC (endothelial cell) during angiogenesis [220]. Phenotypic alterations as a result of senescence in ECs were associated with increased uPA (urokinase-type plasminogen activator) and PAI-1 [221]. Hence, various factors help mediate senescence-associated wound healing.

SASP MMPs play a role during senescence-mediated tissue repair [129, 133]. Dermal fibroblasts, in which senescence is reported, play two key roles within cells: deposit ECM (Extra Cellular Matrix) and facilitate intercellular signalling and repair via growth factor secretion [222]. During acute liver damage, fibrotic scar rich in ECM is produced. Evidently, stellate cells develop senescence with induction of MMPs resulting in dissolution of fibrotic scar [202]. Stellate cells were incapable of healing the wound when senescence was impaired following inactivation of p53/pRB pathways emphasizing the importance of senescence in wound healing during severe fibrosis [202]. Also, in myofibroblasts and fibroblasts, dynamic expression of the ECM protein CCN1 (also known as CYR61; cysteine-rich protein 61) was noted at the site of wound healing-induced senescence [223]. This response was lost in CCN1 mutant

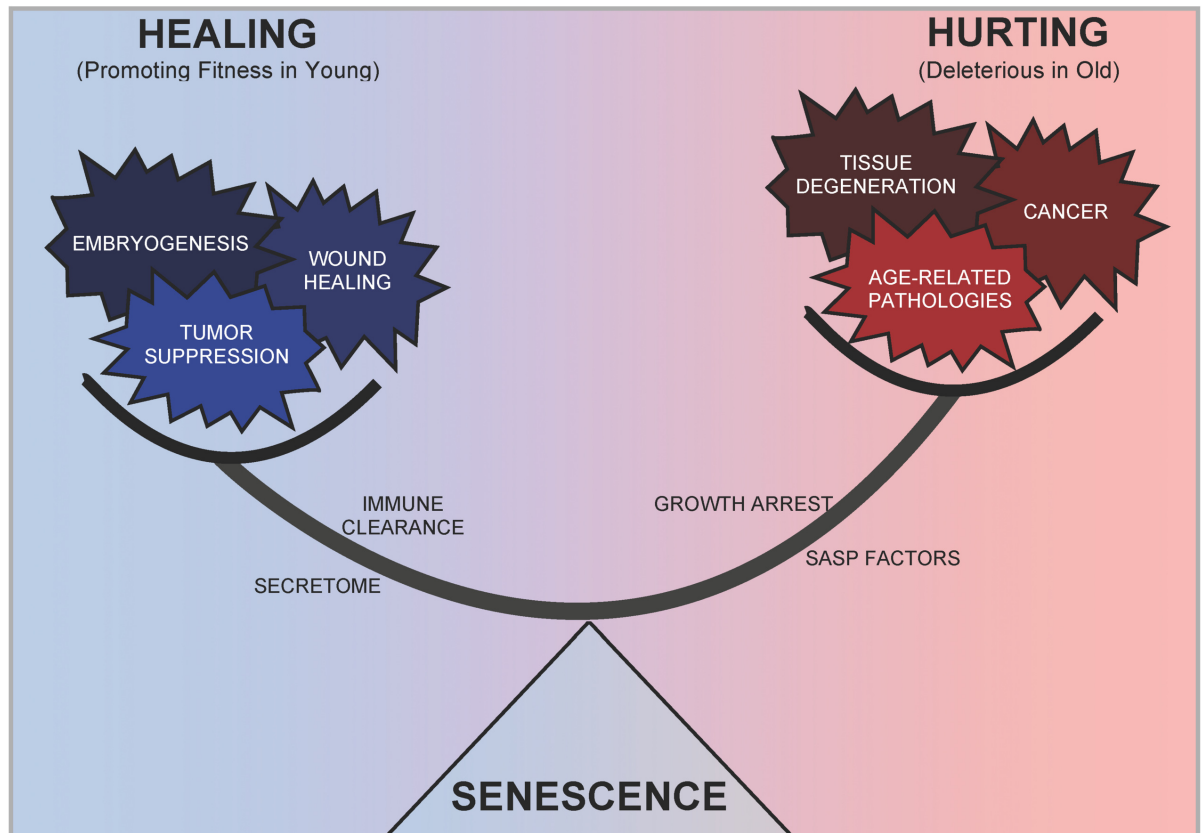


Figure 1.4 Senescence, a double-edged sword.

Senescence has both beneficial and detrimental effects on cells by promoting tumor suppression and wound healing in the young, and tissue degeneration and cancer in the old. Remarkably, evidence now supports a role for senescence during embryogenesis and although paradoxical, senescence is a known contributor of biological ageing. Adapted from [224].

mice that are senescence-defective resulting in exacerbated fibrosis. The importance of senescence is hence emphasized to curb fibrosis during tissue repair.

Therefore, senescence, along with its secretome including MMPs and chemokines, plays a crucial role in coordinating events during wound healing of the liver and other tissues.

### *1.5.1.3 Role in embryogenesis*

Senescence is implicated in various pathological responses in humans as discussed above and surprisingly recent studies shed a new light on the potential role of senescence during embryogenesis.

Studies from Manuel Serrano's [225] and William Keyes' labs [226] provided evidence for the origin of damage-induced senescence during development. A potential role for senescence during early embryonic development was proposed after a study reported the presence of SA  $\beta$ -gal activity in regressing mesonephros in birds [227]. Curiously enough, developmentally programmed senescence was detected by the presence of SA  $\beta$ -gal activity in the mesonephric tubules (present as part of the transitory embryonic kidney) and endolymphatic sac (present in the ear) [225]. Apart from this, the presence of other senescence markers such as H3K9me<sub>3</sub>, HP1 $\gamma$  and absence of Ki67, a proliferation marker, was reported in the above-mentioned structures along with expression of key effectors, namely p53, p21, p15 and p27. Extensive analysis showed that senescence detected was mediated via p21 independently of p53 without DDR. Conceptually the report indicated involvement of TGF- $\beta$ /SMAD and PI3K/FOXO pathways and p21 during developmental senescence [225].

Storer et al., reported detection of senescence in the AER (Apical Ectodermal Ridge) during limb formation [226]. Overlapping factors such as secretion of certain SASP factors including p15 and p21 expression was noted between developmental senescence and oncogene-induced senescence. Notably, disruption of p21 in mice impaired senescence response and alterations to developmental patterns [226]. Also, it was shown that senescent cells undergo immune mediated clearance and cell death suggesting that senescence may in part contribute to the maintenance of

different cell populations by halting growth. Hence, these two hallmark papers implicate senescence in the control of the developmental programme.

## 1.5.2 *Aspects of senescence in pathologies*

### 1.5.2.1 *Role in ageing*

The contribution of senescence towards ageing is a complex phenomenon. The first evidence of senescence associated with ageing was discovered when senescent cells were found to accumulate with age in various species such as rodents, primates including humans [50, 228-230]. Interestingly, senescence is also associated with age-related degenerative pathologies such as osteoarthritis, atherosclerosis, degenerating intervertebral discs, renal tubulointerstitial fibrosis, glomerulosclerosis and slow healing venous ulcers [229, 231-234]. Also, the GWAS (Genome-Wide Association Studies) provided a striking association between senescence and age-associated diseases, such as cancer [235]. This study identified several SNPs (Single Nucleotide Polymorphisms) linked to important human diseases and particularly genetic susceptibility to age-related diseases was associated with senescence.

The contribution of senescence during ageing was demonstrated *in vivo*, as depletion of p63 (a p53 related gene) resulted in senescence and accelerated ageing in mice [236]. Baker et al., showed that inactivation of p16 promoted a delay in senescence and ageing in BubR1-insufficient mice, whereas the opposite effect was shown with inactivation of p19 acting as an attenuator of senescence and ageing [237]. Senescence was also demonstrated at the cellular level in *Zmpste24*-deficient mice, a progeroid mice model [238]. The progeroid phenotype in the mice could be partially rescued or elevated by reducing DDR signalling and the p53-mediated senescence response. Also, CHIP (carboxy terminus of Hsp70-interacting protein)-deficient mice with compromised elimination of damaged proteins showed an increased senescence and ageing phenotype characterized by decrease in bone density, loss of adiposity and thin skin [239]. Senescence is implicated in yet another mammalian model of accelerated ageing, the Klotho-deficient mouse [240] via modulation of Wnt signaling [241]. Hence, different studies reiterate the importance of senescence during ageing.

SASP factors secreted during senescence are multifaceted in their contribution and evidently have detrimental effects on tissue structure and integrity including stem cell niches [9, 242]. Not surprisingly, inflammation caused by the SASP is a potent contributor to age associated hyperproliferative diseases such as cancer and other degenerative diseases [204, 243]. Since reports demonstrate accumulation of senescent cells with age, it is possible that the inflammation caused by the SASP is a continuous driver of multiple age-related pathologies [244, 245].

Hence, the above mentioned reports support how senescence might drive ageing in various ways.

#### *1.5.2.2 Role in tumor promotion*

Although senescence was originally described as a tumor suppressive mechanism, senescence also has a dark side in promoting tumor formation. Inflammatory responses play decisive roles in the initiation, establishment, maintenance and spreading of cancer [246]. Similarly they are known to play a key role in senescence. Hence, in principle, senescence could promote tumor promotion via the SASP [129, 247]. Individual SASP factors (VEGF, GRO $\alpha$ , IL-6, IL-8) have been shown to stimulate cancer and promote aggressive phenotypes. Apparent evidence arise from mouse xenograft studies where senescent cells coinjected with premalignant or malignant epithelial cells were prone to promote tumor burden solely due to the effect of senescent cells and not the non-senescent counterparts [12, 133, 248]. Evidently, this was in part due to the SASP MMPs secreted during senescence [133, 248, 249]. Another *in vivo* setting where senescence plays a critical role is the human nevi. Despite being able to facilitate maintenance of nevi in a long-term benign state, B-RAF induced senescent cells escape senescence due to insufficient growth arrest and/or additional genetic alterations, to support the development of melanoma [26, 39, 102, 126]. Although there is no direct evidence to support senescence promotes cancer in nevi, possibly, failure or bypass of senescence leads to melanoma. Also, it is essential to emphasize that age is one of the biggest risk factors for senescence in tumor promotion. The incidence of cancer increases exponentially with age [250, 251]. In summary, senescence is implicated as an important contributor to cancer.

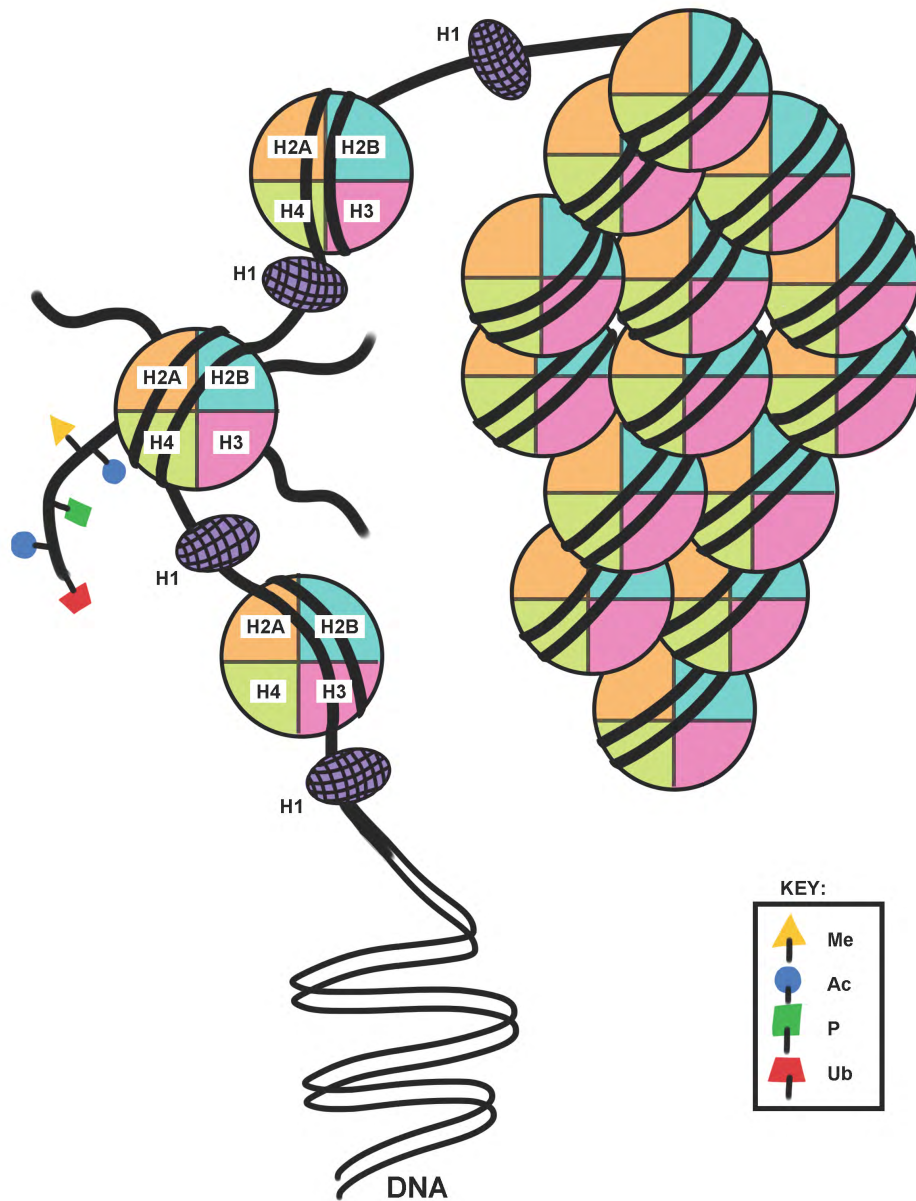


Figure 1.5 Structure of chromatin.

In higher eukaryotes, DNA undergoes several fold compactations and together with proteins forms a complex called chromatin. The basic repeating unit of chromatin is termed the nucleosome consisting of four core histones H2A, H2B, H3 and H4 wrapped around by 146 bp of DNA. This typical beads-on-a-string structure is connected together with linker histone H1. Each nucleosome contains a structured globular domain and an unstructured N-terminal tail that can be subjected to various modifications such as methylation (Me), acetylation (Ac), phosphorylation (P), ubiquitination (Ub). Adapted from [252].

Functional consequences and pathological aspects of senescence can be summarized as follows: senescence can be described as antagonistically pleiotropic (Figure 1.4) by supporting fitness earlier on in life by promoting tumor suppression, wound healing and embryogenesis and causing detrimental effects later on in life by promoting cancer, age-related pathologies and tissue degeneration.

## 1.6 Chromatin

### 1.6.1 *Chromatin structure*

Within higher order organisms such as eukaryotes, DNA is folded into a highly compact and organized structure called chromatin. Chromatin (Figure 1.5) is the basic component of the chromosome containing DNA and histones folded into a specific structure. The fundamental repeating unit of chromatin is the nucleosome consisting of four 'core' histones wrapped around by 146 bp of DNA double helix to form a typical 'bead on a string' structure which then gets folded multiple times to form higher order structure termed chromatin [253-255]. Each globular nucleosome contains an octamer of four histones, H2A, H2B, H3 and H4 [254, 256]. In the physiological state, H3/H4 forms a stable tetrameric unit, whilst H2A/H2B form a dimeric unit [257, 258]. A tripartite protein helix is formed within the nucleosome in an end to end fashion as (H2A/H2B)–(H4/H3)–(H3/H4)–(H2B/H2A) around which the DNA is wrapped [258]. These nucleosomes are connected by short strips of DNA containing the linker histone H1 to form a nucleosomal filament that is part of the higher order structure of chromatin fibre [259]. New histones are deposited in complex with CAF1 (Chromatin Assembly Factor 1), which is recruited to the replication fork site by PCNA (Proliferating Cell Nuclear Antigen) [260]. The core histones are conserved in their amino acid sequence through evolution. All four histones contain a (C)-terminal domain where histone-histone and histone-DNA interactions occur, and a protruding (N)-terminal tail at the other end [261].

The distribution of chromatin is variable through the genome with regions structured into organized domains termed euchromatin and heterochromatin [262]. Two forms of staining distinguish them cytologically. Whilst heterochromatin stains

intensely with methyl blue, euchromatin stains lightly indicating loose packing. Heterochromatin [263], located normally at the periphery of the nucleus, can be further sub-divided into two classes - constitutive and facultative heterochromatin. Constitutive heterochromatin possess a localized gene effect (position-effect variegation) whilst facultative heterochromatin generally exerts its effect on genes through mechanisms such as RNAi (RNA interference) or DNA methylation. Heterochromatin is comprised of repetitive regions such as satellite DNA and its primary function is to repress genes. Regions of the chromosome that are generally heterochromatic are the centromeres and telomeres and another example is the Barr body of the inactivated second X chromosome in females [263]. Given the nature of dense DNA packing, some of its critical functions within the cell can range from protecting the integrity of the chromosome to controlling gene regulation. Euchromatin presents an opposite scenario with less condensed and more accessible DNA to facilitate transcription and are normally gene-rich regions of the chromosome [264]. Thus, chromatin is a highly dynamic structure and undergoes constant changes along with the various proteins necessary for controlling processes within a cell such as DNA replication, transcription, repair and recombination [264].

### *1.6.2 Histone variants*

Apart from the four core histones (H2A, H2B, H3 and H4) deposited during replication, variants of histones also occur, which are deposited outside of replication (reviewed [265]). These variants are generally slight modifications of the canonical histones, although some variants are profoundly different from canonical forms in terms of deposition and functionality [266, 267]. Decades of research now highlight the importance of these histone variants in epigenetic maintenance and shed information on the special machineries that deposit them.

Different isoforms of H3 have been identified: CENP-A, H3.1, H3.1t (testis-specific), H3.2 and H3.3 [265]. CENP-A and H3.3 are the two most extensively studied variants, each with distinct functions. At mitosis, chromosomal segregation is facilitated by the presence of a centromere and a centromere-specific protein identified is termed CENP-A [268, 269]. CENP-A along with its counterparts in mammalian eukaryotes is generically referred to as CenH3. Its importance during kinetochore assembly and spindle microtubules attachment at mitosis and meiosis is

implicated in several studies [270-273]. Faithful maintenance of CenH3-containing chromatin is a key feature in the maintenance of centromeres through evolution. Another universal variant of H3 is H3.3 that shares extreme similarities [274-276] to the core histone H3. H3.3 occurs throughout the cell cycle and is commonly detected at sites that are transcriptionally active [277, 278]. Deposition of H3.3 is now known to occur outside of the S phase and both replication independent and replication coupled deposition of H3.3 was discovered. Whereas deposition of the H3.1 variant is tightly linked to DNA replication [279]. Also the difference between H3.1 and H3.3 deposition lies in the fact that the former is carried out by CAF-1 and latter by the histone chaperones HIRA, ATRX and DAXX [278, 280]. Interestingly, both H3.1 and H3.3-containing complexes contain HAT1 (Histone Acetyltransferase), possibly meaning that histones are acetylated prior to deposition [265].

For H2A, several variants have been reported, some of which include:  $\gamma$ -H2A.X, H2A.Z, macroH2A, H2ABBD (H2A-bar-body-deficient) and H2AvD, of which H2A.Z is the most widely studied [281-283]. Knocking out H2A.Z resulted in embryonic lethality with embryos failing to develop beyond the gastrulation stage [284]. Also RNAi mediated KD (Knock Down) of H2A.Z in mammalian cell lines lead to various abnormalities, such as chromosomal mis-segregation and disruption of the normal distribution of the heterochromatin-specific protein HP1 $\alpha$ , suggesting a putative role for H2A.Z in the maintenance of heterochromatin [285]. Unlike H2A.Z, deletion of  $\gamma$ -H2A.X in mice is not lethal but leads to various defects such as male infertility, genomic instability [286-288]. In yeast and humans, the C-terminal of H2A.X is phosphorylated at residue Ser139 (Serine139) in response to DS breaks [289]. Another variant, macroH2A is a hallmark for X-inactivation in females [290-292]. Presence of macroH2A is associated with gene silencing as the C-terminal and N-terminal domain of the protein inhibit transcription factor binding and activity of nucleosome-remodeling factors respectively [293]. Lastly, very little is known about the variant H2ABBD. It is excluded from inactive X-chromosome and is associated with euchromatic function [294, 295].

H2B variant, termed TH2B, is found in the testis [296]. This testis-specific variant encodes specific sites for phosphorylation. TH2B is targeted by protein kinases like Aurora-C and protein kinase C [297].

Chromatin Modifications	Functions Regulated	Residues Modified
Acetylation	Transcription, Repair, Replication, Condensation	<b>K-ac</b>
Methylation (lysines)	Transcription, Repair	<b>K-me1 K-me2 K-me3</b>
Methylation (arginines)	Transcription	<b>R-me1 R-me2a R-me2s</b>
Phosphorylation	Transcription, Repair, Condensation	<b>S-ph T-ph</b>
Ubiquitylation	Transcription, Repair	<b>K-ub</b>
Sumoylation	Transcription	<b>K-su</b>
ADP ribosylation	Transcription	<b>E-ar</b>
Deimination	Transcription	<b>R &gt; Cit</b>
Proline Isomerization	Transcription	<b>P-cis &gt; P-trans</b>

Table 1.1 Outline of distinct types of modifications occurring on histones.

Residue(s) at which the particular modification occurs are outlined along with general functions regulated by the modification (Adapted from [298]).

Linker histone H1 also has known variants such as H1t, H1t2, HILS1 (testis-specific), H1A and H1B [299, 300]. They have highly specialized roles in establishing cell polarity and regulatory role within germ cells [301]. H1 linker histones most notably play a role in chromatin folding and reconstitution [302].

Lastly, there are no known variants of histone H4. Genes encoding H4 are constitutively expressed through cell cycle and the reason behind lack of variants is not clear [303].

In summary, in addition to the core histones, histone variants have also been shown to play key roles in epigenetic regulation of the cell.

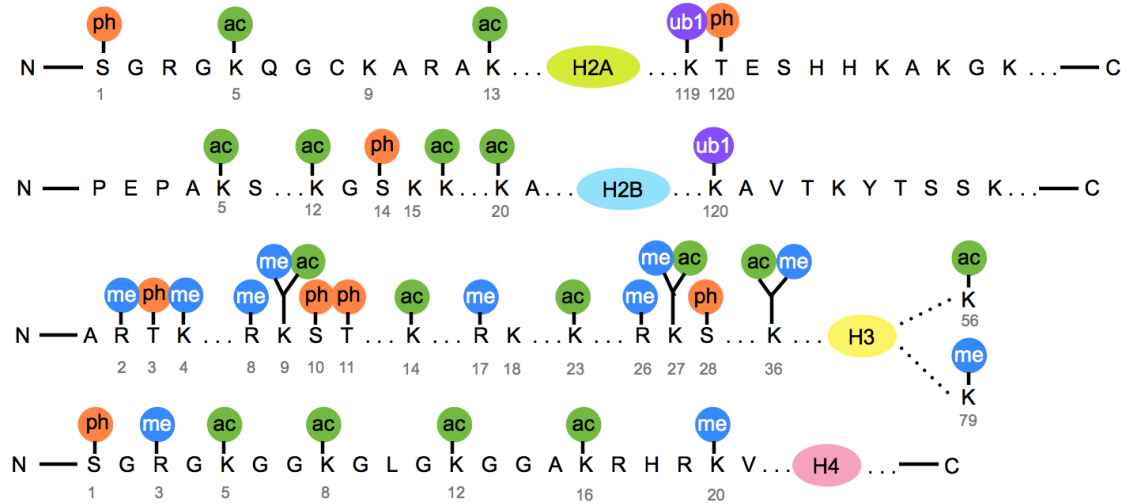
### *1.6.3 Histone modifications*

The unstructured N-terminal tails of core histones are subjected to a myriad of various post-translational modifications (Figure 1.6). The tails contain a high affinity to bind to DNA owing to the basic amino acid residues [255]. They facilitate inter-nucleosomal interactions with the tightly bound chromatin fibres. Various modifications (outlined in Table 1.1) occur on the tails, that exquisitely regulate gene expression and also their structure and function [298]. It is important to note that currently the known histone modifications maybe a gross underestimate of what may occur on histones. It is also essential to emphasize that not all modifications occur at any known singular time [298].

A range of histone modifying enzymes deposit specific histone modifications such as acetylation [304], methylation [305], ubiquitination [306], phosphorylation [307], deamination [308], ADP-ribosylation [309], sumoylation [310] and proline isomerization [311]. Evidence suggests that histone modifications play a critical role in several functions including DNA repair, DNA replication, gene expression and chromosome dynamics [312]. How the different histone modifications are maintained by the enzymatic system and their function as a major genome integrator of different signalling pathways are reviewed extensively in literature [313-315]. Chromatin modifications are shown to either act in concert with each other or individually to modify chromatin-mediated outcomes in a context-specific style [316].

Some well-studied modifications include arginine methylation, lysine acetylation, lysine methylation. Arginine methylation can act both as an activating or

(A)



(B)

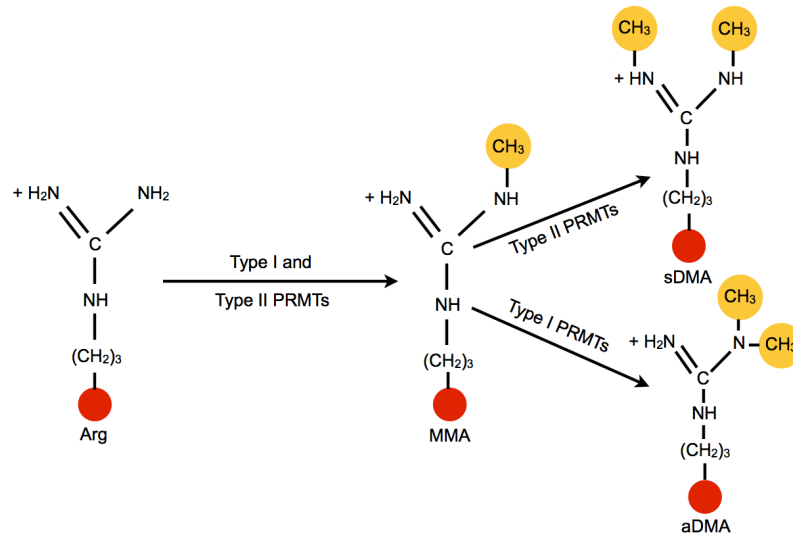


Figure 1.6 Histone modifications.

(A) Mostly along the N-terminal but also at the C-terminal regions, histones H2A, H2B, H3 and H4 undergo diverse post-translational modifications (ph-phosphorylation, ac-acetylation, ub-ubiquitination, me-methylation). The residue number at which the modification is present is also depicted. (B) One type of modification is arginine methylation (Arg) catalyzed by Type I or II PRMT family. Arginine methylation can occur as monomethylation (MMA) occurring by addition of one methyl group to one terminal guanidino nitrogen of arginine, symmetrical dimethylation (sDMA) and asymmetrical dimethylation (aDMA) occurring by addition of two methyl groups to either one guanidino nitrogen or two different guanidino nitrogen atoms, respectively. Adapted from [317, 318].

repressive mark in terms of facilitating transcription [298]. Enzymes termed PRMTs (Protein Arginine Methyl Transferase) are recruited to promoters by TFs (transcription factors) and a frequently studied promoter in this regard is the pS2 promoter where arginine methylation is cycling during activation [319, 320]. Although there are no clear evidence of a specific demethylase for this modification, the process of deimination by PADI4 (Protein Arginine Deiminase-4) has been shown to convert mono-methylated arginine to citrulline [321]. Citrulline conversion acts as an antagonist of arginine methylation [322].

Another well-known modification is acetylation, which is generally associated with active transcription. The three main families of acetyltransferases are GNAT (Gcn5-related N-acetyltransferase), MYST (named after members MOZ, Ybf2/Sas3, Sas2, and Tip60) and CBP/p300 (cAMP response element binding (CREB)-binding protein/E1A-associated protein 300 kDa) [304]. Generally N-terminal tails are most likely to get acetylated, however, lysine present in the H3 core domain (K56) is also acetylated [323]. Acetylation is a reversible mark and this reaction is facilitated by HDACs (Histone deacetylases). It is a key mark in regulating gene expression and most crucially chromatin structure [324, 325].

In summary, emerging studies now point to key DNA functions regulated by various histone modifications and associated proteins.

#### *1.6.4 Histone modification binding proteins*

As part of the epigenetic code, proteins that bind to chromatin in a specific modification-dependent manner recognize histone modifications to mediate important cellular outcomes. Some of the recognition motifs and their corresponding binding proteins are outlined as follows, methyl cytosine/methyl-CpG-binding domain proteins [326], acetyl lysines/bromo-domain proteins [327-329], methyl lysines/chromo, tudor, MBT domain proteins and PHD (Plant Homeo Domain) fingers [330-333], and phospho-serine and phospho-threonine/14-3-3 binding proteins [334].

Two key histone binding proteins will be discussed further. Although the first PHD finger was identified over 20 years ago [335], it was not until recently that its role in binding lysine methylation was identified. Several PHD fingers such as ING(1,3-5), JARID1A, KDM7A, KIAA1718, MLL1, PHF(2,8), PHO23, PYGO(1,2), RAG2, TAF3 and YNG(1,2) recognize and interact with H3K4me3 [332]. PHD fingers that bind to

H3 modifications play a key role in cellular processes such as gene regulation, recombination and nucleosome remodeling [332]. PHD fingers occurring in macromolecules possess enzymatic properties such as methyltransferase activity and histone demethylase activity. They also act as scaffolding proteins to facilitate recruitment of multimeric protein complexes to specific genomic locations [332]. Such characteristics reiterate the importance of histone-PHD binding fingers in the modulation of deposition and removal of PTMs, thereby modulating chromatin dynamics. Apart from binding histone proteins, PHD fingers also bind non-histone proteins, hence proving themselves to be versatile components in the epigenetic machinery [332].

Another characteristic histone binding protein is the bromo-domain protein (BRD) known to recognize acetyl-lysine residues on proteins. So far over 100 acetylated lysine binding proteins are identified in humans and yeast [336, 337]. Apart from regulating gene transcription, BRD proteins are also implicated in several disease processes such as cancer, viral infection, inflammation [336]. They are often found in combination with other histone binding proteins such as PHD fingers, MBT domain and/or WD40 domain [338]. As an example, H4K16ac and H3K4me is bound simultaneously by the NURF chromatin remodeling complex subunit BPTF, which contains both PHD finger and a bromo-domain within the same nucleosome [339]. Alternatively, some other BRD proteins can bind two acetylated lysine residues at the same time [340]. Most of the protein belonging to this class can be categorized into three main types: components of chromatin remodeling complexes; histone acetyl transferase complexes; and bromodomain-extraterminal (BET) proteins [338]. Also emerging studies now show that specific inhibition of BRD-proteins themselves pose as potent drug targets during infectious diseases such as malaria and cancer [338, 341]. Hence, histone binding proteins play exceptional roles in regulating basic functions of cell by regulating chromatin dynamics.

In summary, the above findings imply that, the level of complexity within chromatin network arising from modular organization of the chromatin itself along with other interacting partners highlighting the challenges involved in understanding histone cross talk.

### 1.6.5 Nucleosome positioning

The term nucleosome positioning simply refers to the position of the nucleosome in relation to specific genomic sequence. Nucleosome occupancy refers to regions occupied by the nucleosome such as promoters, enhancers and terminators [342-344]. These factors have been shown to be extremely critical in mediating cellular outcomes mainly because nucleosome occupancy negatively impacts on the interaction of DNA-binding proteins [345-347]. Reports suggest a large-scale loss of nucleosomes around the TSS (Transcription Start Sites), both in human and yeast, is linked with gene activation [348-351]. For example, following viral infection, activation of interferon- $\beta$  promoter is facilitated as a result of nucleosome sliding to mediate nucleosome eviction [352]. Likewise ATP-dependent chromatin remodeling enzymes, SWI/SNF complex [353-355], histone modifications (hyperacetylation) [350, 351] and histone variants such as H2A.Z and H3.3 are associated with nucleosome eviction and/or repositioning [356, 357]. Collectively, these reports suggest the importance of nucleosome positioning on DNA accessibility and chromatin-higher order structures.

### 1.6.6 Role of non-coding RNAs

Non-coding RNAs are functional RNAs that are not translated into any specific protein. The human genome project revealed that only 2% of the genome accounts for protein coding regions and the activity of those genes are in part being maintained by chromatin [358, 359]. Although most of the cell's DNA is transcribed to RNA, not all of it goes on to produce protein. In fact only 75% of the genome is being transcribed into RNA and only a small percentage of this transcribed RNA codes for protein, meaning that a large proportion remain as 'non-coding' RNAs [360]. Non-coding RNAs largely fall under two categories, long ( $\geq 200$  nucleotides) and short ( $< 200$  nucleotides). Long non-coding RNAs (lncRNA) are comprised of intergenic, intronic, antisense and overlapping bidirectional transcripts. Short non-coding RNAs include short-interfering RNAs (siRNA), microRNAs (miRNAs) and PIWI-interacting RNAs (piRNAs) [360].

The importance of miRNAs (approximately 22 nucleotides long) have emerged recently in processes such as proliferation, inflammation, fibrosis, differentiation [361]. The report of the first miRNA, *lin-4*, in *C.elegans* [362] has since lead to the identification of thousands of miRNAs. As an example, miR-34a is implicated in

cellular senescence in various cell types [363, 364]. miR-34a accumulates during biological ageing [365, 366]. Recent work from Overhoff et al., report accumulation of 22 different senescence-associated microRNAs (SA-miRNAs) belonging to mir-34 and let-7 families during epithelial cell senescence [367]. Interestingly, they showed that increased expression of some of these SA-miRNAs initiates a positive feedback regulatory loop acting in concert with PcG (Polycomb group) proteins to activate other members of SA-miRNAs resulting in enforcement of senescence. Most notably this was regulated by the p16 pathway. Also, senescence has posed as an endogenous trigger for miRNA/AGO-2 (Argonaute-2) mediated transcriptional gene silencing in human cells [368]. miRNAs are also involved in the regulation of DDR signaling, DNA methylation and chromatin structure [369].

lncRNAs are shown to act as recruiters for chromatin remodelling enzymes to specific loci to alter chromatin structure and gene expression [361]. As an example, expressions of several hundred lncRNAs at the human HOX loci regulate chromatin structure and accessibility involving differential histone methylation and RNA polymerase [370]. Also, the non-coding RNA HOTAIR is involved in PRC2-mediated silencing of chromatin at the HOX loci [370].

Collectively, this along with other studies, demonstrate the emerging importance on non-coding RNAs in the maintenance of chromatin structure, genomic stability, senescence, ageing and also various diseases including cancer, neurological disorders, and cardiovascular diseases [361, 369, 371, 372].

## 1.7 Epigenetics of cellular senescence

### 1.7.1 *Chromatin reorganization in senescence*

Chromatin regulation is thought to be important for the onset and maintenance of senescence and senescent cells are characterized by extensive remodeling of chromatin structure. One of the key features of chromatin reorganization in senescence is visualized by the formation of SAHF (Senescence Associated Heterochromatic Foci) [373-375]. Although restricted to certain cell-types, SAHF can be visualized using DAPI (4,6-diamidino-2-phenylindole) staining and strikingly

appear to be small punctate foci. Narita et al., described these punctate foci as heterochromatic based on the accumulation of HP1 (Heterochromatin Protein 1), H3K9me3, a repressive histone mark, and macroH2A, a variant associated with gene silencing [374]. Changes in chromatin structure are also reported for senescent cells occurring in premalignant tumors [184, 376-378]. In humans, histone chaperones HIRA (Histone Repressor A) and ASF1a (Anti-Silencing Function 1a) as part of the HUCA complex, function to mediate formation of SAHF [178]. Importantly, the HUCA complex is also implicated in the deposition of variant H3.3 into chromatin, suggesting a possible involvement of H3.3 during SAHF formation [379-381]. Histone chaperone DAXX, in cooperation with ATRX, can also perform H3.3 deposition at heterochromatic loci [280, 382, 383]. In line with this, a recent paper reported that H3.3 is excluded from SAHF in senescent cells and included in PML bodies in a DAXX-dependent manner [384]. SAHF are reported to originate from individual chromosomes, i.e., each chromosome condenses to form a single DAPI focus and show increased HMGA2 (High Mobility Group A2) and decreased linker histone H1 [373, 385, 386]. Therefore, various reports inexplicably link SAHF and senescence.

SAHF formation leads to specific consequences during senescence. The p53 and pRB pathways, the two major effectors of senescence, regulate the formation of SAHF, although the effect of p53 is marginal during OIS [155, 176, 387]. Following RAS induction, KD of p16 or pRB dampened SAHF formation despite the establishment of senescence. Nevertheless, these SAHF-negative cells revealed some deregulated cell cycle genes, suggesting an inexplicable link between p16/pRB-mediated SAHF formation and repression of cell cycle associated genes [176]. Also, HMGA2 protein cooperates with p16 to promote SAHF formation and evidently contributes towards senescence stabilization via repression of proliferation-associated genes [373]. SAHF might therefore contribute towards the tumor suppressive nature of senescence as intervention in genes associated with SAHF formation leads to senescence perturbation.

It is also true that during the establishment of senescence, the DDR pathway plays a significant role in regulating chromatin structure. BRAC1, a pre-disposition gene to breast and ovarian cancer in women, plays an important role in DDR [388, 389]. RAS-induced senescence resulted in disassociation of BRAC1 from chromatin and promoted induction of SAHF formation [390]. This was further supported when

removal of BRAC1 resulted in triggering the DDR pathway, SAHF induction and senescence. Further, association between BRAC1 and BRG1 subunit of the ATP-dependent SWI/SNF remodeling complex was established [391]. As pointed out before, pRB, a key regulator of SAHF formation, also interacts with BRG1 and the role of BRG1 during cell cycle arrest has been previously implied [392, 393]. Interestingly, the interaction between BRAC1 and BRG1 was disrupted at the onset of senescence owing to BRG1's chromatin remodeling activity and this correlated to SAHF formation accompanied with increased p21 and p16 levels [394]. Hence, downstream signaling of DDR has significant implications in regulating senescence.

A novel interplay between DNA damage and heterochromatin formation was described during OIS by di Fagagna's lab. As noted earlier, SAHF could promote the silencing of genes associated with the cell cycle, such as cyclin A and therefore promote growth arrest via heterochromatinization. An interesting twist to the tale was brought about by observations from Fabrizio d'Adda di Fagagna and colleagues who suggested that SAHF are not required for gene silencing and proposed a new relationship between DDR and SAHF [395]. BJ cells (newborn foreskin fibroblasts) used for the study show resistance to premature p16 induction and these cells showed induction of SAHF only following OIS and not replicative senescence or stress-induced senescence from ionizing radiation or etoposide. Inactivation of p53 or ATM resulted in the reversal of senescence through induction of proliferation and remarkably this was accompanied with SAHF retainment. This suggested that SAHF and its associated repression of cell cycle genes are not essential for growth arrest. In fact, SAHF was reported to have beneficial effects on senescence by reducing apoptosis induced by high DNA damage signaling, thereby maintaining viability of senescent cells [395]. Although DDR and SAHF are two key components of senescence, a causal relationship between the two was implied through this study.

Though a number of studies have demonstrated a connection between the induction of SAHF and senescence, SAHF formation appears dispensable in some scenarios. For example, AKT activation and KD of PTEN does not result in SAHF formation [390, 396] apart from the fact that SAHF induction is also cell-line dependent [397]. As noted earlier, BJ cells are not associated with SAHF formation, whereas other primary cells, such as IMR90 and WI38, are marked with SAHF formation upon senescence [176]. Notably, mouse cells also do not show formation of

punctate foci although they possess certain components of SAHF such as macroH2A [398]. Nevertheless, SAHF differs from other heterochromatic regions such as inactivated X-chromosome (Xi) in female [399]. In summary, extensive molecular changes along with chromatin restructuring occurs during senescence and emerging evidence now shows how they could be the driving force behind the senescent phenotype.

### *1.7.2 Loss of histones in senescence*

Histone biogenesis and its role in biological outcomes have recently acquired significant interest. O'Sullivan et al., provided evidence for reduced histone biosynthesis during replicative senescence as a result of DNA damage from shortened telomeres [400]. Western blotting assays showed reduction in H3 and H4 between early and late-passaged cells. Along with this, SLBP (Stem Loop Binding Protein), a protein involved in histone pre-mRNA processing and translation, also showed decreased levels. This may potentially mean that less efficient translation of histone messages occurs during senescence. However, not all histone levels were affected, as H1 levels were not reduced in RS. But, some well-known chromatin players such as ASF1a/b, CAF1-p150/p60 were also significantly reduced in senescent cells. It was believed that this cascade of localized changes starting with the regulation of H3 and H4 synthesis translates into a genome-wide state of persistent DNA damage effectively acting as a feedback loop mechanism to enable establishment of senescence and its subsequent maintenance [400].

Around the same time, Jessica Tyler and colleagues reported profound loss of histones during biological ageing [173]. Prior to this report, an important study from Shelley Berger's lab showed that in yeast Sir2 deacetylase decreased with ageing along with an increase in its substrate H4K16ac [401]. This was accompanied by concomitant loss of histones at specific sub telomeric regions of the genome. However the mechanistic relevance of loss of histone in ageing was unclear at this point. Tyler and colleague demonstrated that interventions to increase levels of histones in yeast cells remarkably promoted life span extension. Although decrease in histones was reported, there was an increase in histone transcript levels during ageing [173, 401]. It is conceivable that aged cells are perhaps trying to compensate for loss of histones in attempt to replace them via increased transcript levels. In

addition to this, decrease in histone occupancy across various genomic regions such as rDNA, mating-type loci, silent regions adjacent to telomeres was demonstrated with ChIP and chromatin fractionation experiments. Also, lack of histones is likely not a reflection of increased dead cell population as reports suggest that aged yeast cells in senescent-like state are very much metabolically active for a long time after the last population doubling [402].

Apart from evidence supporting loss of core histones during RS and replicative ageing, loss of histone variant H2A.Z was reported during RS in human diploid fibroblasts IMR90 [403]. Deposition of H2A.Z is mediated by two different classes of ATP-dependent SWI2/SNF-2 remodeling complex containing either SRCAP or p400 [404-406]. While SCRAP is involved in global deposition of H2A.Z, p400 is well-known for localized deposition of the variant [407]. Loss of function studies for H2A.Z and p400 has shown induction of a premature senescence phenotype in HDF (Human Diploid Fibroblast) in a p53-p21 dependent fashion [155, 408].

Clearly replicative ageing or senescence from yeast to humans is accompanied by loss of histones, thereby contributing to alterations in the chromatin structure along with altered histone modifications [174, 385, 401, 409, 410]. Evidently, this contributes to an open chromatin structure and increased genomic instability.

### *1.7.3 Histone modifications in senescence*

The onset of senescence is also accompanied by changes in histone modifications.

Two frequently associated histone modifications occurring with senescence are H3K9me3 and H3K27me3. HP1 and PcG proteins bind H3K9me3 and H3K27me3, respectively [411]. Once recruited to the site of histone mark, HP1 in turn recruits SUV39H1 (Suppressor of variegation 3-9 homolog 1), a histone-lysine N-methyltransferase, which then leads to spreading of H3K9me3 to form constitutive heterochromatin [330, 331, 412]. Chandra et al., reported that SAHF occur with H3K9me3 and H3K27me3 in discrete compartmentalized structures [413]. Although their data implied that these two repressive marks are not essential for the formation of SAHF, the authors speculate about the possibility of other repressive marks that could be involved in the process, but as yet these remain undetermined.

Work from other labs shows alterations of histone modifications upon senescence. Consistently, levels of the repressive marks H3K27me3, H3K9me3 and

H4K20me3 are increased upon induction of senescence [414]. Conversely, decrease in the active mark H3K4me3 was observed during senescence. H3K4me3 was found to have an effect on gene expression of a subset of E2F target genes in senescence [414]. Jarid1a/b mediated demethylation of H3K4 was promoted at E2F target regions via cooperation with pRB. Hence, the study establishes a causal relationship between epigenetic alterations and promotion of gene silencing in senescence.

To further substantiate a role for histone modifications and other chromatin players during senescence, localized loss of H3K27me3 was noted at the *INK4a-ARF* locus following RAS-induced senescence [415]. Along with this, loss of EZH2 was noticed coupled with increased binding of JMJD3 at the locus. EZH2 is the methyltransferase for H3K27me3, whilst JMJD3 is the demethylase. The changes were also noted along with decreased binding of PcG proteins such, as CBX7 and BMI1, and a reciprocal increase in activating mark H3K4me3 and association of RNA Pol II. In summary, this study demonstrated a dynamic relationship between epigenetic alterations and signal transduction pathways, in this case, RAS downstream signaling, to facilitate establishment of senescence.

Additionally, *in vivo* studies in mice revealed epigenetic regulation involving H3K9me3 following OIS and its effect on tumor suppression. Braig et al., showed that H3K9me3-mediated senescence as a novel SUV39H1-dependent tumor suppressive mechanism in Eμ-*N-RAS* transgenic mice [184]. *In vitro* demonstration supported that SUV39H1 knockout resulted in abrogation of senescent phenotype in lymphoid cells expressing RAS. These results have important ramifications for epigenetic control mediating senescence during tumorigenesis.

H3K9me3 is also associated with HGPS (Hutchinson–Gilford Progeria Syndrome) [416]. An effective *in vivo* mimetic model for the disease was created with mice lacking prelamin A-processing metalloprotease, *Zmpste24* [417]. The mice demonstrated increased truncated prelamin A, termed progerin, and sustained DNA damage foci that were associated with H3K9me3 [416]. As a consequence of H3K9me3-mediated heterochromatin remodeling, defective DNA repair mechanism were in place, which in return contributed to senescence in this laminopathy-based premature ageing syndrome [416].

Two other histone modifications of note in senescence are H3K27me3 and H3K4me4. Collaborative work between Shelly Berger's lab and Peter Adam's lab

focused on the distribution of these histone modifications between proliferating and senescent cells [418]. The authors uncovered large-scale changes in the epigenome of senescent cells with regions of gains and losses for these modifications referred to as 'mesas' and 'canyons'. Remarkably, some of these regions overlapped with LADs (Lamin-Associated Domains). Bivalent domains containing both H3K4me3 (active mark) and H3K27me3 (repressive mark) over LADS were found in senescence. Importantly, this was closely related to loss of Lamin B1, a nuclear laminar protein in senescence. Inherently decreased Lamin B1 lead to the induction of premature senescence along with acquisition of mesas and canyons resulting in chromatin instability. H3K4me3 mesas were also found in fibroblast cells derived from HGPS patients suggesting a link between accelerated senescence and premature ageing. Also, results obtained in senescence showed striking similarities to features of colorectal cancer epigenome. Thus, the work [418] highlights profound changes in chromatin structure of senescent cells and how they impinge upon ageing and cancer.

In summary, although studies demonstrate that histone modifications play a significant role during senescence, these observations are restricted to only a few known occurring modifications. Any potential effects or importance of other known modifications remain poorly characterized and understudied in the context of cellular senescence.

## 1.8 Aims of the project

Over the years, research has unravelled the importance of epigenetic programming of the human genome in influencing the basic building blocks in the developmental programme such as gametogenesis and early embryogenesis. And with the advent of revolutionizing technology, the recent recognition of various chromatin modifications and regulatory factors, such as DNA methylation, histone modifications, histone modifiers, chromatin-remodelling complexes are expected to increase our understanding of how epigenetic programming can control mammalian development. Cellular senescence, characterized by irreversible proliferation arrest, is also marked by extensive changes in the chromatin structure. Senescence effectors such as p53, pRB and ING, that were believed to exert their effect primarily as checkpoint

regulators are now implied in chromatin remodelling and act as epigenetic regulators of cellular senescence by their ability to direct activities of HATs, HDACs and HMTs, among others. Such epigenetic mechanisms that are important in senescence further suggest that epigenetic deregulation might play a key role in bypassing senescence and acquisition of tumourigenic phenotype.

Increasingly, chromatin modifications are shown to impart an additional layer of stability to the senescent phenotype. Evidence suggests that histone modifications play critical roles in various cell functions including DNA repair, DNA replication, gene expression and chromosome dynamics. Despite the established importance of this phenomenon, the contribution of individual histone modifications toward senescence and its associated effects on cancer and ageing remains poorly understood and largely uncharacterized.

Hence, with this project I aim to identify and characterize novel histone modifications that are important during the senescence programme.

Specific aims of the project were:

1. Profiling of various histone modifications in senescent cells in comparison to proliferative cells.
  - Perform histone modification slot blot screen.
2. Identification of novel histone modifications that are regulated at the onset of senescence.
  - Test if changes in histone modifications occur specifically in senescence or non-specifically to stress and/or cell cycle arrest.
  - Validate histone antibody specificity and establish appropriate *in vitro* model systems for study.
3. Study the functional significance and/or regulatory mechanism of candidate modifications in the context of senescence.
  - *In vitro* tools such as gene KD, ChIP-Seq was used to specifically assess the contribution of H3CS.1 and H4R3me2a during senescence.
4. Understand the contribution of these modifications to senescence-mediated tumor suppression and/or tissue ageing.
  - Characterize histone modifications using appropriate animal models.

Establishing the functional regulation and mechanistic characterization of these modifications may have significant implications for senescence-associated events, such as ageing, and potential clinical implications, as there is increasing interest in so-called pro-senescence cancer therapies.

## **2. MATERIALS AND METHODS**

## 2 MATERIALS AND METHODS

---

### 2.1 Materials

#### 2.1.1 *General Reagents*

Reagent	Details	Source
Acrylamide 29:1 (40%w/v)		National Diagnostics
Agar		Sigma-Aldrich
Agarose		Melford
Ampicillin		Sigma-Aldrich
APS		Sigma-Aldrich
Bromodeoxyuridine (BrdU)		Sigma-Aldrich
Bovine Serum Albumin (BSA)		Sigma-Aldrich
DAPI 4',6-diamidino-2-phenylindole		Sigma-Aldrich
DMEM (Dulbecco's modified eagle medium)		Life Technologies
DMSO (dimethyl sulfoxide)		Sigma-Aldrich
DNA ladders		New-England Biolabs
DNA loading dye		Invitrogen
DTT (dithiothreitol)		Sigma-Aldrich
ECL Western blotting substrate		Thermo Scientific
EDTA		Sigma-Aldrich
Ethanol		Thermo Fischer Scientific
Ethidium bromide		Sigma
Foetal Calf Serum		GE Healthcare
Formaldehyde, 16%		Electron-Microscopy Services

Glutaraldehyde		Sigma
Goat serum		Vector Labs
Immobilon-P PVDF Transfer Membrane		Millipore
L-Glutamine (200 mM)		Gibco
Laemmli Sample Buffer (SB)	63 mM TrisHCl, 10% Glycerol, 2% SDS, 0.0025% Bromophenol Blue, pH 6.8	
LB (Lysogeny Broth)	1% Bacto-Tryptone 86 mM NaCl 0.5% Yeast Extract	Beatson Institute Central Services
LB Agar	1% Bacto-Tryptone 86 mM NaCl 0.5% Yeast Extract 1.5% Agar	Beatson Institute Central Services
Magnesium chloride		Sigma-Aldrich
Methanol		Thermo Fischer Scientific
Non-fat dried milk powder		Marvel
Opti-MEM		Life Technologies
Paraformaldehyde		Sigma-Aldrich
PBS (Phosphate Buffered Saline)	170 mM NaCl, 3.3 mM KCL, 1.8 mM Na <sub>2</sub> HPO <sub>4</sub> , 10.6 mM H <sub>2</sub> PO <sub>4</sub>	Beatson Institute Central Services
PBST	PBS+0.5%Tween20	
PBT	PBS+1%BSA +0.5%Tween20	
PBS/EDTA (PE)	PBS+1 mM EDTA	Beatson Institute Central Services

Penicillin-Streptomycin		Life Technologies
PfuUltra II Fusion HS DNA Polymerase		Agilent Technologies
Phosphatase Inhibitor Cocktail		Sigma-Aldrich
PMSF (Phenylmethanesulfonyl fluoride) 1M	174.19 g, 1 L ddH <sub>2</sub> O	
Polybrene		Millipore
Protease Inhibitor Cocktail		Sigma-Aldrich
Proteinase K		Sigma-Aldrich
ProLong gold antifade Reagent with DAPI		Life Technologies
Puromycin		Millipore
Resolving gel	8-12% acrylamide, 375 mM Tris-HCl, pH 8.8, 0.1% SDS, 0.1% APS, 50 mM TEMED	
RNase A		Qiagen
SDS (Sodium Dodecyl Sulphate), 10%		Beatson Institute Central Services
SDS-PAGE running buffer (10X)	0.1% SDS, 192 mM Glycine, 25 mM Tris-HCl, pH 8.3	Beatson Institute Central Services
SDS-PAGE transfer buffer (10x)	288 g glycine, 60.4 g Tris base, 1.6 L ddH <sub>2</sub> O	Beatson Institute Central Services
Sodium Azide		Sigma- Aldrich
Stacking gel	5% acrylamide, 0.4% SDS, 500 mM Tris pH 6.8	
TAE (Tris-acetate EDTA)	40 mM Tris, 0.1% glacial acetic acid, 1 mM EDTA	

TBS (Tris Buffered Saline)	10 mM Tris-HCl, pH 7.4,150 mM NaCl	Beatson Institute Central Services
TBST	TBS + 0.1% Tween-20	Beatson Institute Central Services
TE (Tris-EDTA)	10 mM Tris-HCl, pH 8.0,1 mM EDTA	Beatson Institute Central Services
TEMED (Tetramethylethylenediamine)		Sigma-Aldrich
Triton X-100		Sigma-Aldrich
Trypsin 2.5%		Life Technologies
Tween-20		Sigma-Aldrich
Xylene		Fischer Scientific
$\beta$ -Mercaptoethanol		Sigma-Aldrich

Table 2.1 Reagents and solutions

### 2.1.2 Antibodies and Dyes

Antigen	Host/Application	Dilution	Source
Alexafluor 594 goat (secondary)	Rabbit/IF	1:500	Life Technologies A11012
Alexafluor 555 goat (secondary)	Rabbit/IF	1:500	Life Technologies A-21428
Alexafluor 488 goat (secondary)	Mouse/IF	1:500	Life Technologies A11001
Alexafluor 488 goat (secondary)	Rabbit/IF	1:500	Life Technologies A11008
Beta-actin	Mouse/WB	1:7000	Sigma A1978
Cathepsin L	Mouse/WB	1:1000	Abcam ab6314
Cathepsin L	Mouse/WB	1:500	R&D systems MAB9521
Cyclin A	Rabbit/WB	1:1000	Santa Cruz SC-751
ER- $\alpha$	Rabbit/WB	1:2000	Santa Cruz SC-543
H3CS.1	Rabbit/WB	1:1000	Active Motif 39573

HA tag	Mouse/WB	1:1000	Cell Signalling 9101
HIRA	Mouse/IF	1:125	WC cocktail (Adams Lab)
Histone H3, C-terminal	Rabbit/WB	1:1000	Active Motif 39163
Histone H3, N-terminal	Mouse	1:1000	Active Motif 39763
Histone H4	Mouse/WB	1:1000	Abcam ab31830
Histone H4	Rabbit/WB	1:1000	Millipore 05-858
Histone H4	Rabbit/WB	1:1000	Cell signalling 2592
Histone H4 acetyl	Rabbit/WB	1:1000	Millipore 06-866
Histone H4K16ac	Rabbit/WB	1:1000	Millipore 07-329 (ab1)
Histone H4K16ac	Rabbit/WB	1:1000	Abcam ab109463 (ab2)
Histone H4R3me2a	Rabbit/WB	1:1000	Active motif 39705
Histone H4R3me2a	Rabbit/WB	1:1000	Suming Huang Lab
hMOF	Mouse/WB	1:1000	Abcam ab54276
hMOF	Mouse/WB	1:1000	Abgent A01112a
hMOF	Rabbit/WB	1:1000	Bethyl Laboratories A300-992A
IgG control	Mouse/IP	Variable	Sigma-Aldrich M7023
IgG, HRP-linked (secondary)	Rabbit/WB	1:2000	GE Healthcare NA934
IgG, HRP-linked (secondary)	Mouse/WB	1:5000	DAKO P0447
p16 (G175-405)	Mouse/WB	1:1000	BD 51-1325GR
p21	Mouse/WB	1:1000	Santa Cruz SC-817
p53-acetyl (Lys382)	Rabbit/WB	1:1000	Cell Signalling 2525
PCNA	Mouse/WB	1:1000	Santa Cruz SC-56
Phospho-Histone H2A.X(ser139)	Mouse/WB	1:1000	Millipore 05-636
pRB (Ser807/811)	Rabbit/WB	1:1000	Cell Signalling 9308
PML	Rabbit/IF	1:500	Santa Cruz SC-5621

PRMT1	Rabbit/WB	1:1000	Cell Signalling 2449
PRMT1	Rabbit/WB	1:1000	Abcam ab73246
RAS	Mouse/WB	1:1000	BD 610001
RB	Mouse/WB	1:1000	Cell Signalling 9309
SIRT1	Rabbit/WB	1:2000	Millipore 07-131
SIRT1	Mouse/WB	1:1000	Millipore 05-1243

Table 2.2 Antibodies and dyes

## 2.2 Methods

### 2.2.1 *Cells*

HEK-293T cells originally derived from human embryonic kidney cells was obtained from ATCC (Cat No: CRL-11268) (<http://www.atcc.org/>). Phoenix-AMPHO cells expressing amphotropic envelope protein was obtained from ATCC (Cat No: CRL-3213). The above cell types were cultured in Dulbecco's modified Eagle's medium (DMEM) supplemented with 10% foetal calf serum, 2 mM L-glutamine, 10 units/ml penicillin and 10 ug/ml streptomycin at 37°C in a humidified atmosphere containing 5% CO<sub>2</sub>. IMR90 cell derived from the lung of 16-week female fetus was obtained from Coriell Cell Repositories (<http://ccr.coriell.org/>). They were cultured in DMEM supplemented with 20% foetal calf serum, 2 mM L-glutamine, 10 units/ml penicillin and 10 ug/ml streptomycin at 37°C in a humidified atmosphere containing 5% CO<sub>2</sub> and 3% O<sub>2</sub>.

### 2.2.2 *DNA Preparation*

Sub-cloning Efficiency™ DH5α™ Competent Cells from Life technologies (Cat No.18265-017) are a versatile strain of chemically competent cells that provide a transformation efficiency of  $> 1 \times 10^6$  cfu/μg plasmid DNA. These were used for routine DNA preparation and extraction by both long or short recovery methods. 50 μl competent cells and 0.5 μg DNA were mixed and incubated on ice for 30 minutes. Following incubation, the mixture was heat-shocked at 42°C for 45 seconds. Cells were allowed to recover on ice for 2-3 minutes. For the short recovery method, 100 μl

LB broth was added and the cells were plated onto LB agar plate containing 100 µg/ml ampicillin and incubated overnight at 37°C. For the long recovery method, 500 µl LB broth was added to cells and incubated at 37°C shaking at 180 rpm for an hour. The cell suspension was then re-suspended in a smaller volume by spinning and plated onto LB agar plates for overnight 37°C incubation. Single colonies were selected the next day and left shaking at 37°C in LB broth supplemented with 100 µg/ml ampicillin using 5ml for mini preparation and up to 500 ml<sup>-1</sup> L for maxi preparation. Mini-preps were performed by the Beatson Molecular Technology Services with the QIAGEN BioRobot 9600 following QIAprep 96 Plus Miniprep protocol. Maxi-preps were carried out by the Beatson Molecular Technology services using the PureLink® HiPure Plasmid Maxiprep Kit from Life technologies.

### 2.2.3 DNA Quantification

DNA was quantified using Qubit® dsDNA BR Assay Kit for samples ranging from 100 pg/µl-1,000 ng/µl and Qubit® dsDNA HS (High Sensitivity) Assay Kit for samples ranging from 10 pg/µl to 100 ng/µl. Thin-walled PCR tubes were used to quantify DNA preparations using Qubit® 2.0 Fluorometer from Life Technologies. Quant-iT™ Working solution was prepared by diluting the Quant-iT™ reagent 1:200 in Quant-iT™ buffer. 200 µl of working solution was used per sample along with two standards used for calibration. The two standards were prepared by aliquoting 10 µl of each standard solution and 190 µl of working solution. The samples were prepared by aliquoting 1 µl into 199 µl of working solution. All tubes were mixed vigorously by vortexing for 3 seconds and incubated for 2 minutes at RT. Calibration for the DNA assay was performed using the standards. Readings were obtained in µg/ml. This value corresponded to the concentration of sample after dilution into assay tube. To calculate the concentration of sample, the following equation was used:

$$\text{Concentration of your sample (}\mu\text{g/ml)} = \text{QF value} \times (200 / x)$$

where QF value = the value given by the Qubit® 2.0 Fluorometer; x = the number of microliters of sample added to the assay tube.

## 2.2.4 Plasmids

The following plasmids (Table 2.3) were used in this study:

Plasmid	Details	Source
pBabe-neo	Empty vector	Peter Adams Lab
pBabe-neo-H-RASG12V	Activated Ras	Peter Adams Lab
pBabe-neo-SV40LT	Activated SV40 Long terminal	From Bill Hahn
pBabe-puro	Empty vector	From Bill Hahn and Bob Weinberg
pBabe-puro-H-RASG12V	Activated Ras	From Bill Hahn and Bob Weinberg
pBabe-puro-HA-H4K16Q	Activated H4K16ac mutant	Site-directed mutagenesis
pBabe-puro-HA-H4K16R	Activated H4K16ac mutant	Site-directed mutagenesis
pBabe-puro-HA-H4WT	Activated H4 Wild type	Cloning
pBabe-puro-SIRT1	Activated SIRT1	Addgene
pBabe-puro-SIRT1-H363Y	Activated SIRT1 (dominant negative)	Addgene
pLenti6-puro	Empty vector	Peter Adams Lab
pLenti6-puro-H-RASG12V	Activated Ras	Peter Adams Lab
pLKO.1-hMOF(1)	hMOF KD	Open Biosystems TRCN0000034875
pLKO.1-hMOF(2)	hMOF KD	Open Biosystems TRCN0000034877
pLKO.1-hMOF(3)	hMOF KD	Open Biosystems TRCN0000034876
pLKO.1-hMOF(4)	hMOF KD	Open Biosystems TRCN0000034874
pLKO.1-Luciferase	Non-targeting control	Open Biosystems
pLKO.1-puro	Empty vector	Open Biosystems

pLKO.1-shPRMT1(1)	PRMT1 KD	Open Biosystems TRCN0000035929
pLKO.1-shPRMT1(2)	PRMT1 KD	Open Biosystems TRCN0000035930
pLKO.1-shPRMT1(3)	PRMT1 KD	Open Biosystems TRCN0000035931
pLKO.1-shPRMT1(4)	PRMT1 KD	Open Biosystems TRCN0000035932
pLKO.1-shPRMT1(5)	PRMT1 KD	Open Biosystems TRCN0000035933
pLMIP-shHIRA1	HIRA KD	Peter Adams Lab
pLMIP-shHIRA1	HIRA KD	Peter Adams Lab
pLNC-RAS:ER	Inducible Ras	From Jesus Gil
pLP-VSVG	Packaging plasmid	Invitrogen
pQCXIP/GFP	GFP control	Peter Adams Lab
ps-PAX2	Packaging plasmid	From Dave Schultz

Table 2.3 Plasmids

### 2.2.5 Site Directed Mutagenesis

To perform site directed mutagenesis, PfuUltra II Fusion HS DNA Polymerase from Agilent Technologies was used. The following components were added in order to a thin-walled PCR tube placed on ice; ddH<sub>2</sub>O, 5 µl PfuUltra II reaction buffer, 250 µM of each dNTP, 5-30 ng DNA, 0.2 µM of forward and reverse primer, 1 µl PfuUltra II fusion HS DNA polymerase in a 50µl reaction. The cycling parameters used were: 95°C for 2 minutes initial denaturation; 35 cycles of 95°C denaturation for 20 seconds, 55-58°C annealing for 20 seconds, 72°C extension for 30 seconds and 72°C for 10 minutes final extension. Mutagenic primers outlined in Table 2.4 were designed using DNASTAR- Lasergene SeqBuilder and synthesized using IDT, Integrated DNA Technologies (<http://www.idtdna.com/>).

Primer	Sequence 5'-3'
HA H4 fp	gcgcggatccaccatggcctaccctacgacgtgcccgactacgcctccctctctgggc gaggtaaaggtggcaag
HA H4 rp	gcgcgaattctcaaccgccgaaaccataaagg
H4K16R fp	ggaggcgcccggcgccaccggaaggtg
H4K16R rp	ccggtggcgccggcgccctcccttacc
H4K16Q fp	ggaggcgcccagcgccaccggaaggtg
H4K16Q rp	ccggtggcgctggcgccctcccttacc

Table 2.4 Primers

### 2.2.6 DNA Sequencing

DNA sequencing performed through the Beatson Molecular Technology Services on an Applied Biosystems 3130xl genetic analyser confirmed the right sequence of cloning products. The DNA sequence chromatogram data were analysed using FinchTV. The following sequencing primers outlined Table 2.5 was designed using SeqBuilder and synthesized using IDT.

Primer	Sequence 5'-3'
pBabe FP-MCS	tcaccaggttaagatcaagg
pBabe RP-MCS	cctcggcctctgcataaata
pLenti MCS	gctgcaataaacaagttcctctc

Table 2.5 DNA sequencing primers

### 2.2.7 DNA Analysis

#### 2.2.7.1 Diagnostic Restriction Digest

For diagnostic digests, 0.5 µg of purified plasmid DNA, 1 µl of 10x buffer, 0.5 µl of restriction enzyme prepared up to 10 µl volume using ddH<sub>2</sub>O was incubated at 37°C for at least 1 hour. After digestion, DNA was analysed on an agarose gel.

### 2.2.7.2 Preparative Restriction Digest

For preparative digest, 1-2 µg (if >4kb vector) or 2-5 µg (if <4kb vector) of purified DNA was mixed with 4 µl of 10x buffer, up to 4 µl of restriction enzyme and prepared up to 40 µl volume using ddH<sub>2</sub>O. This was incubated at 37°C for at least 3 hours or overnight. The digested DNA was run on an agarose gel and purified using Qiagen QIAquick gel extraction kit.

### 2.2.7.3 Agarose Gel Electrophoresis

50 ml of 0.5-3% agarose was prepared in 1x TAE buffer by microwaving until all the agarose was dissolved. It was allowed to cool until warm enough to hold with bare hands. 5 µl of 10 mg/ml Ethidium bromide (EtBr) was added. Gel was poured into a cast with comb and allowed to set. Once set, the gel was placed in the gel tank, covered with 1x TAE buffer and the comb removed. The samples were loaded with molecular weight standards. The gel was run at 50 V and 30 V for large and small gels, respectively. Table 2.6 was used to determine the percentage of agarose gel required for analysis.

Size of DNA Fragment	Percentage of Agarose
>5kb	0.5
3-5kb	0.6
1-3kb	0.7
0.5-1kb	0.8
0.3-0.5kb	1.0
0.2-0.3kb	1.2
0.1-0.2kb	1.5
<0.1kb	2

Table 2.6 Percentage of agarose gel

### 2.2.8 Non-Viral Transfections

Cells were transfected using The Nucleofector™ II Device and Amaxa® Cell Line Nucleofector® Kit R. For siRNA transfection, cells were seeded at  $6.5 \times 10^5$  cells/ml 24

hours prior to transfection. Cells were harvested by trypsinization and the cell pellet containing about  $1 \times 10^6$  cells was resuspended in 100  $\mu$ l RT (Room Temperature) Nucleofector® Solution. 30-300 nM siRNA was added to the cell suspension and transferred to supplied cuvette without air bubbles. The correct nucleofector programme was applied to the cuvette. 500  $\mu$ l of pre-equilibrated media was then added to the cuvette and suspension was gently transferred to a 6-well plate. Gene expression or down regulation was analyzed between 24-72 hours post transfection. A GFP positive control was added by using the plasmid (pmaxGFP® Vector) supplied in the kit.

### *2.2.9 Viral Transfections*

For retroviral transfections using the calcium phosphate method, Phoenix-AMPHO cells were used. 24 hours prior to transfection, cells were seeded at  $5 \times 10^6$  cells per 10 cm dish. 9ml of fresh media was replaced 4 hours prior to transfection. A 10x stock of 2.5 M  $\text{CaCl}_2$  was diluted to 1x using ddH<sub>2</sub>O. 27  $\mu$ g plasmid DNA was added to 0.5 ml of 1x  $\text{CaCl}_2$ . To this mixture, 0.5 ml 2x BBS (50 mM BES, 280 mM NaCl, 1.5 mM  $\text{Na}_2\text{HPO}_4$ , pH 6.95) was added gently drop-wise. After 15 minutes, the mixture was distributed drop-wise to the plate and incubated overnight at 37°C.

For retroviral infections, after 24 hours of transfection of Phoenix-AMPHO cells, old media was replaced with 6 ml fresh media and the cells were incubated overnight at 32°C, 5% CO<sub>2</sub>. Target cells, in this case, IMR90 were prepared for infection. 48 hours post transfection, the media-containing virus was spun at 1000 rpm for 5 minutes and the supernatant was passed through a 0.45  $\mu$ m filter. The plate was replaced with 6 ml fresh media for second virus harvest and incubated at 32°C overnight. On the day of infection, IMR90 cells were pre-incubated for 2 hours with 3 ml fresh media containing 8  $\mu$ g/ml of polybrene per 10 cm dish. Plates were infected with 3 ml virus and incubated at 37°C, 5% CO<sub>2</sub>, 3% O<sub>2</sub>. A second round of infection was performed on IMR90 as outlined. After two rounds of infections, IMR90 cells were selected with the appropriate drug, such as 1 mg/ml puromycin or 0.5 mg/ml neomycin, and took about 3 days and 5 days respectively to kill non-infected cells.

For lentiviral transfections, HEK-293T cells were seeded at  $12 \times 10^6$  cells per T175 flask in 25ml media 24 hours prior to transfection. 12.5 ml media was taken out of the flask on the day of transfection. The flask contained approximately 12 ml media. To 1.5 ml pre-warmed DMEM, 120  $\mu$ l Lipofectamine was added and incubated for 5 minutes at RT. To another 1.5 ml pre-warmed DMEM, 5  $\mu$ g pCMV-VSVG (packaging plasmid), 8  $\mu$ g psPAX (packaging plasmid), and 20  $\mu$ g vector genome were added and incubated for 5 minutes at RT. A GFP (TRC Lentiviral eGFP shRNA) positive control was also included along with sample transfection. Both mixes were combined together to get a total of 3 ml DMEM containing DNA and lipofectamine, and incubated for 20 minutes at RT. A 5 ml pipette was used to introduce bubbles into the solution to mix well and then added gently to the flask. After 5-6 hours, the media was replaced with 15 ml fresh media. After 24 hours, 15 ml media containing virus was harvested by spinning at 1000 rpm for 5 minutes, ran through a 0.45  $\mu$ M filter and stored at 4°C overnight. 15 ml fresh media was also added to the flask for a second harvest the next day. The next day, media was harvested as before and the cells discarded after appropriate disinfection. 30 ml filtered supernatant was transferred to a 25x89 mm polyallomer centrifuge tube. PBS was used to equalize tubes with a balance in the flow-hood. The supernatant was centrifuged at 47,000 x g for 2 hours at 10°C in a *SW-28 rotor, Beckman coulter ultracentrifuge*. Supernatant was discarded and 30  $\mu$ l PBS was added to pellet and left overnight at 4°C shaking gently to re-suspend. Concentrated virus was aliquoted in small volumes and stored at -80°C.

For lentivirus infections, a dose curve was determined for each individual batch of virus prepared. IMR90 cells were seeded 24 hours prior to infection in a 6-well plate. Cells were pre-incubated in fresh media and 8  $\mu$ g/ml polybrene for 2 hours. A viral dose titre ranging from 2  $\mu$ l to 32  $\mu$ l was performed. After adding virus, the plate was gently rocked and incubated overnight at 37°C, 5% CO<sub>2</sub>, 3% O<sub>2</sub>. 24 hours later, the virus was removed and replaced with fresh media containing drug, either 1 mg/ml puromycin or 0.5 mg/ml neomycin. The minimum viral dose required for efficient infection was determined after 3 and 5 days for puromycin and neomycin selected cells, respectively, along with uninfected cells as control.

### 2.2.10 *Protein Extraction*

Cells were washed in PBS at RT. 200  $\mu$ l-1 ml of hot freshly boiled SDS/Laemmli sample buffer with DTT was added per 10cm plate and the cells were scraped. The lysate was transferred to an Eppendorf and boiled for 5 minutes at 97°C. DNA was sheared by vortexing and any viscosity was treated by running the lysate in a 18-22 gauge needle repetitively. Protein lysate was stored at -80°C until analysis.

### 2.2.11 *Protein Quantification*

Thin-walled PCR tubes were used to quantify protein lysates using Qubit® 2.0 Fluorometer from Life Technologies. Quant-iT™ Working solution was prepared by diluting the Quant-iT™ reagent 1:200 in Quant-iT™ buffer. 200  $\mu$ l of working solution was used per sample along with three standards for calibration. The three standards were prepared by aliquoting 10  $\mu$ l of each standard solution and 190  $\mu$ l of working solution. The samples were prepared by aliquoting 1  $\mu$ l into 199  $\mu$ l of working solution. All tubes were mixed vigorously by vortexing for 3 seconds and incubated for 15 minutes at RT. Calibration for the protein assay was performed using the standards. Readings were obtained in  $\mu$ g/ml. This value corresponded to the concentration of sample after dilution into assay tube. To calculate the concentration of sample, the following equation was used:

$$\text{Concentration of your sample } (\mu\text{g/ml}) = \text{QF value} \times (200 / x)$$

where QF value = the value given by the Qubit® 2.0 Fluorometer; x = the number of microliters of sample added to the assay tube.

### 2.2.12 *Protein Analysis*

#### 2.2.12.1 *SDS-PAGE Electrophoresis*

The stacking gel and resolving gel were cast according to the weight of the protein for study. SDS-PAGE electrophoresis was performed as described originally [419]. Table 2.7 and 2.8 were used as a guide.

For 10 ml separating gel:

Acrylamide percentage	6%	8%	10%	12%	15%
H <sub>2</sub> O	5.2 ml	4.6 ml	3.8 ml	3.2 ml	2.2 ml
Acrylamide/Bis-acrylamide (30%/0.8% w/v)	2 ml	2.6 ml	3.4 ml	4 ml	5 ml
1.5M Tris (pH=8.8)	2.6 ml				
10% (w/v) SDS	100 µl				
10% (w/v) ammonium persulfate (AP)	100 µl				
TEMED	10 µl				

Table 2.7 Resolving gel

For 5 ml stacking gel:

H <sub>2</sub> O	2.975 ml
0.5 M Tris-HCl, pH 6.8	1.25 ml
10% (w/v) SDS	0.05 ml
Acrylamide/Bis-acrylamide (30%/0.8% w/v)	0.67 ml
10% (w/v) ammonium persulfate (AP)	0.05 ml
TEMED	0.005 ml

Table 2.8 Stacking gel

The acrylamide percentage used for the preparation of the SDS-PAGE gel depended on the size of the target protein as outline in Table 2.9.

Acrylamide %	M.W. Range
6-8%	50 kDa - 500 kDa
10%	20 kDa - 300 kDa
12%	10 kDa - 200 kDa
15%	3 kDa - 100 kDa

Table 2.9 Percentage of polyacrylamide gel

The gel tank was filled with 1X SDS-PAGE buffer (Refer Section 2.1) after placing the prepared gel. Protein samples were boiled in sample buffer (Refer Section 2.1) for 5 minutes at 97°C and then loaded on to the gels along with protein ladder.

Electrophoresis was performed at 90-120 V until fully resolved. Bio-Rad's Mini-Protean Tetra electrophoresis system or Thermo Scientific's Owls P10DS Dual Gel System was used.

#### *2.2.12.2 Western Blotting*

Prior to the transfer of proteins, PVDF membrane was activated using 100 % ethanol and washed in ddH<sub>2</sub>O until all the greasiness was removed. The membrane was equilibrated in 1X transfer buffer for 5 minutes (Refer Section 2.1). Proteins were transferred on to the membrane in 1X transfer buffer for 1 hour at 100 V. Following transfer, the membrane was allowed to dry for at least 15 minutes at RT. This allows proteins to bind well to the membrane. After re-activation of the membrane using ethanol, blocking was performed with gentle agitation for 1 hour at RT using TBS containing 5% non-fat dry milk. Primary antibody was diluted according to the recommended dilution in TBS containing 5% non-fat dry milk, 4% BSA and 0.02% NaAz and the membrane incubation was performed either for 1 hour at RT or overnight at 4°C with gentle agitation. Washing was performed 3 times, 5-15 minutes each with TBST. The secondary antibody incubation was performed after appropriate dilution in TBST containing 5% non-fat dry milk at RT with gentle agitation. Washing was performed 3 times, 5-15 minutes each with TBST. Proteins were detected using enhanced chemiluminescence (ECL).

#### *2.2.13 Slot blotting*

Protein lysates were separated using SDS-PAGE. For this purpose 15% polyacrylamide gels were prepared at 1.5 mm thickness with one large sample well and one reference well. Appropriate volumes of proliferating and senescent cell lysates were run in this manner and separated proteins were transferred onto a PVDF membrane. For detection of proteins, Mini-PROTEAN II multiscreen apparatus (Cat No: 170-4017) from Bio-Rad was used for slot blotting. Slot blotting is similar to Western blotting, but allows screening of multiple antibodies in individual "slots" without having to cut the PVDF transfer membrane. Assembly of the multiscreen apparatus, sample loading, washing and detection were performed according to manufacturer's instructions. All membranes were probed (Refer Chapter 3, Section

3.2.3) with total histone H3 antibody raised in rabbit as a positive control for loading (indicated as +ve), and an anti-mouse antibody raised in rabbit as negative control (indicated as -ve).

#### 2.2.14 *Immunofluorescence*

Cells were split on to coverslips and allowed to adhere for 24 hours. The coverslips were washed twice with PBS (pH 7.3) at RT. 2 ml fresh 4% paraformaldehyde in PBS (pH 7.3) was added for fixing the cells for 10 minutes at RT. Coverslips were then washed twice with PBS (pH 7.3) at RT. 2 ml PBS (pH 7.3) + 0.2% Triton X-100 was added to coverslips for permeabilization for 2 minutes at RT. Coverslips were washed twice with PBS (pH 7.3). For blocking buffer, PBS (pH 7.3) + 3% BSA + 1% goat serum was used. Cells were incubated for 1 hour at RT. Primary antibody was diluted appropriately in 200 µl blocking buffer and coverslips incubated for 1 hour at RT by inverting on to parafilm. Coverslips were transferred back to the 6-well plate facing up and washed thrice in PBS (pH 7.3) + 1% Triton X-100 at RT. Secondary antibody was diluted in PBS (pH 7.3) + 3% BSA + 1% goat serum and incubated in the dark for 1 hour at RT. Coverslips were washed thrice with PBS (pH 7.3). Pre-warmed mounting media with DAPI was added to the clean glass slide and the coverslips were inverted with cells facing down. The edges were sealed with nail varnish and allowed to dry at RT for 10 minutes. The slides were stored at -20°C for long-term storage.

#### 2.2.15 *Cellular Fractionation*

Cells were lysed and step-wise centrifugal isolation of nuclear and cytoplasmic protein fractions were performed using NE-PER™ Nuclear and Cytoplasmic Extraction Kit (Thermo Scientific) according to manufacturer's instructions.  $1-10 \times 10^6$  cells adherent cells were harvested using trypsin and transferred to an RE. The cell pellet was washed with ice cold PBS and spun at 500 g for 2-3 minutes. The supernatant was removed and ice cold Cytoplasmic Extraction Reagent I (CER I) was added according to the packed cell volume as indicated in Table 2.10.

Packed Cell Volume (μl)	CER I (μl)	CER II (μl)	NER (μl)
10	100	5.5	50
20	200	11	100
50	500	27.5	250
100	1000	55	500

Table 2.10 Reagent volumes for different packed cell volumes

The Eppendorf was vortexed at the highest setting for 15 seconds to fully resuspend the cell pellet. The mixture was incubated for 10 minutes on ice. Ice cold CER II was then added maintaining the ratio in accordance to Table 2.10. The tube was vortexed at the highest setting for 5 seconds and incubated on ice for 1 minutes. Again, the tube was vortexed at the highest setting for 5 seconds and centrifuged at max speed (~ 16,000 x g) for 5 min at 4°C. The supernatant (cytoplasmic fraction) was transferred to a pre-chilled tube. The insoluble pellet, which contains the nuclei, was suspended in ice-cold Nuclear Extraction Reagent (NER). The sample was vortexed at the highest setting for 15 seconds, placed on ice, and then subsequently vortexed every 10 minutes for a total of 40 minutes incubation on ice. The tube was spun at the max speed in a microcentrifuge for 10 minutes. The supernatant (nuclear fraction) was transferred to a pre-chilled tube. The extracted fraction was stored at -80°C until use.

### 2.2.16 Chromatin Immunoprecipitation (ChIP)

The buffers outlined in Table 2.11 were used in this protocol:

Buffers	Components
mNLB (modified Nuclear Lysis Buffer)	50 mM Tris pH 8.0; 10 mM EDTA pH 8.0; 5 mM EGTA pH 8.0; 1% SDS
IPDB (Immunoprecipitation Dilution Buffer)	20 mM Tris pH 8.0; 1 mM EDTA pH 8.0; 1 mM EGTA pH 8.0; 1% Triton X-100; 0.01% SDS; 150 mM NaCl
High Salt Wash	20 mM Tris pH 8.0; 1 mM EDTA pH 8.0; 1% Triton X-100; 0.01% SDS; 500 mM NaCl
IPWB	10 mM Tris pH 8.0; 1 mM EDTA pH 8.0; 1% NP-

(Immunoprecipitation Wash Buffer)	40; 1% deoxycholic acid; 250 mM LiCl
TE (Tris-EDTA)	10 mM Tris pH 8.0; 1 mM EDTA
IPEB (Immunoprecipitation Elution Buffer)	50 mM Tris pH 8.0; 10 mM EDTA pH 8.0; 1% SDS; 300 mM NaCl
Inhibitors	1X Protease inhibitor cocktail-Sigma + 1X Phosphatase inhibitor cocktail-Sigma + 50 µg/ml PMSF-Phenylmethanesulfonyl Fluoride

Table 2.11 ChIP buffers

#### Harvesting Cells:

IMR90 cells were cultured to almost 95% confluency in 10 cm petridishes containing 10 ml media. Cells were crosslinked for 15 minutes at RT with 1 % formaldehyde with gentle rocking. Crosslinking was quenched using 1.25 M glycine at 1/10<sup>th</sup> of volume per plate (e.g. 1 ml per 10 cm plate) to get 125 mM final concentration for 5 minutes at RT. Media was aspirated and plates were washed twice in ice-cold PBS. Cells were scraped into PBS containing inhibitors (Refer Table 2.11). Cells were spun at 200 x g for 5 minutes at 4°C. The supernatant was aspirated and cell pellets were either stored at -80°C for future use or used in the following steps.

#### Chromatin Preparation:

Cells pellets were re-suspended in mNLB:IPDB = 1:1 (+inhibitors) using 1 ml of buffer per 20-40X10<sup>6</sup> cells. The suspension was incubated on ice for 10 minutes and then spun at 200 x g in a microcentrifuge for 5 minutes. Supernatant was manually aspirated using pipette. Pellet was re-suspended in mNLB:IPDB = 1:1 (+inhibitors) using 0.5 ml of buffer per 20X10<sup>6</sup> cells. 0.5 ml cell suspension was transferred to 2 ml Eppendorf tubes. Cells were sonicated at the highest amplitude setting in a Bioruptor XL water bath sonicator (Diagenode) for 15-25 minutes using 24 seconds ON/OFF cycle. Un-sonicated and sonicated samples were visualized by agarose gel electrophoresis if needed. Cells were spun at max speed in a microcentrifuge for 5 minutes at 4°C. Supernatant containing sheared chromatin was transferred to a new tube and spun again. At this point identical chromatin samples were pooled together.

Using QUBIT, DNA was measured in the chromatin samples. IPDB (+inhibitors) was added to chromatin preps to get final composition of mNLB:IPDB = 1:4. Since chromatin prepared in the previous step was already at a 1:1 ratio of mNLB:IPBD, 1.5x volume of IPBD was added to obtain 1:4 ratio of mNLB:IPDB. Chromatin samples prepared were then used for immunoprecipitation.

Immunoiprecipitation:

Bead-antibody complexes were prepared using Dynabeads® M-280 Sheep anti-Rabbit IgG. 100 µl beads were used per IP reaction. Beads were washed thrice using recommended wash buffer (PBS + 0.1% BSA + 0.02% NaAz) with the help of the magnetic rack. Beads were re-suspended in 0.5 ml wash buffer and appropriate amount of antibody was aliquoted into the mixture. This was incubated for 30 minutes at RT with gentle rotation. After binding, beads were washed thrice with 0.5 ml IPDB each time. The bead-antibody complexes formed were now ready for immunoprecipitation with the chromatin samples prepared. Chromatin and bead-antibody mixtures were incubated overnight rotating at 4°C. A small volume of chromatin prior to incubation was saved as input sample for downstream analysis.

Washing and Elution:

The following day, beads were washed with buffers in the order mentioned: IPDB x2, High Salt Wash x1, IPWB x1 (contains LiCl), TE x2. Depending on the stringency conditions, washing with IPWB buffer (LiCl wash) was either included or excluded. After washing, the samples were used for different types of analysis as outlined:

ChIP-PCR quantification - ChIP DNA was extracted using Chelex-100. After aspirating TE from the beads, 50 µl of 10% Chelex-100 suspension (Bio-RAD) was aliquoted. The tube was vortexed at max speed for 20 seconds – 30 seconds and incubated for 15 minutes at 97°C. Samples were spun at max speed in a microcentrifuge at 4°C for 5 minutes. The first elution containing 25 µl of supernatant was carefully aliquoted into a new tube. 350 µl of ddH<sub>2</sub>O was added to the mixture and vortexed again. Tubes were spun as before at 4°C for 5 minutes. The second elution containing 325 µl of supernatant was aliquoted into the same tube giving a total of 350 µl of ChIP DNA for downstream analysis using quantitative PCR.

ChIP-sequencing - For Illumina sequencing, 250-300 µl of IPEB was added after aspirating TE along with 5-10 µg of RNaseA. The sample was incubated at 65°C for 30 minutes. The supernatant containing ChIP DNA was separated from the beads using magnetic rack. The DNA was reverse cross linked for 6 hours to overnight at 65°C. 100 µg of proteinase K was added and incubated for 2 hours at 55°C or overnight at 45°C. The next day, DNA was purified and eluted in 30 – 40 µl volume using QIAGEN PCR purification kit according to manufacturer's instructions.

Protein Analysis - For downstream analysis by SDS-PAGE electrophoresis and western blotting, beads were incubated in 40 µL of 1x SB for 30 minutes at 97°C after TE aspiration. The supernatant was separated from the beads and to this 1M DTT was added and incubated for 5 minutes at 97°C, and the sample was then loaded on to a SDS gel along with appropriate loading markers.

Preparation of ChIP-seq Libraries:

NEBNext® ChIP-seq Sample Prep Kit (Cat: E6240S) was used. All samples were kept on ice during library preparation.

For end repair reaction, 10 ng of ChIP DNA was used. The following components were added in a sterile microfuge tube: 1-40 µl ChIP DNA, 5 µl NEBNext End Repair Reaction Buffer, 1 µl NEBNext End Repair Enzyme Mix and prepared up to total volume of 50 µl. Tubes were mixed by flicking and spun briefly and incubated in a thermal cycler for 30 minutes at 20°C. DNA was purified using QIAquick PCR purification kit (Cat: 28104) and 45 µl water was added in the final elution step.

For dA-Tailing of End Repaired DNA the following components were mixed in a sterile microfuge tube: 44 µl End Repaired DNA, 5 µl NEBNext dA-Tailing Reaction Buffer (10X), 1 µl Klenow Fragment (3'→5' exo-) and prepared up to total volume of 50 µl with ddH<sub>2</sub>O. The tube was incubated at 37°C for 30 minutes in a thermal cycler. dA tailed DNA was purified using QIAGEN MinElute kit (Cat: 28004) and eluted in 20 µl ddH<sub>2</sub>O.

For Adaptor Ligation of dA-Tailed DNA the following components were mixed in a sterile microfuge tube: 19 µl End Repaired, dA-Tailed DNA, 6 µl Quick Ligation Reaction Buffer (5X), 1 µl 1.5 µM DNA Adaptors, 4 µl Quick T4 DNA Ligase and

prepared up to total volume of 30  $\mu\text{l}$  with ddH<sub>2</sub>O. Tubes were incubated at 20°C for 15 minutes in a thermal cycler. DNA was purified using QIAGEN MinElute kit and eluted in 10  $\mu\text{l}$  ddH<sub>2</sub>O.

Agarose gel size selection of adaptor ligated DNA was performed by loading samples on to the gel and applying 50V for separation of DNA based on size. Genecatcher (6.5 mm X 1 mm, Web Scientific, PKB6.5) or a sterile scalpel was used to cut in the range between 200-275 bp. The excised DNA was purified using QIAquick Gel Extraction Kit (Cat:28704) and eluted in 37  $\mu\text{l}$  ddH<sub>2</sub>O.

PCR Enrichment of Adaptor Ligated DNA was performed by mixing the following components in a sterile microfuge tube: 36  $\mu\text{l}$  Adaptor ligated DNA, 10  $\mu\text{l}$  Phusion® HF Buffer (5X) 1.5  $\mu\text{l}$  dNTP Mix, 0.9  $\mu\text{l}$  Primer 1 (25  $\mu\text{M}$  stock), 0.9  $\mu\text{l}$  Primer 2 (25  $\mu\text{M}$  stock), 0.5  $\mu\text{l}$  Phusion® High-Fidelity DNA Polymerase, 0.2  $\mu\text{l}$  DNase/RNase free water and the total volume was prepared up to 50  $\mu\text{l}$ . The PCR conditions are outlined in Table 2.12.

Cycle step	Temp	Time	Cycles
Initial Denaturation	98°C	30 seconds	1
Denaturation	98°C	10 seconds	18
Annealing	65°C	30 seconds	
Extension	72°C	30 seconds	
Final Extension	72°C 4°C	5 minutes hold	1

Table 2.12 PCR conditions

The DNA was purified using QIAGEN MinElute kit and eluted in 16  $\mu\text{l}$  ddH<sub>2</sub>O. The quality and the quantity of the DNA prepared were analysed using 2100 Agilent Bioanalyzer and QUBIT, respectively. The Bioanalyzer provided a platform to evaluate DNA samples qualitatively by using a fluorescent assay involving electrophoretic separation. The machine measured the amount of fluorescence as the DNA samples were pulsed through a microchannel over time. The Agilent Bioanalyzer software that diagrams fluorescence over time created a graph called an electropherogram. The software created a gel image to accompany the graph for each sample loaded.

### 2.2.17 *ChIP-sequencing*

Molecular Technology Services, Beatson Institute performed the sequencing using Illumina GAllx sequencer. Stock dilution of 2 nM ChIP DNA libraries were denatured with 0.1 N NaOH and then diluted to 5 pM stocks. For cluster generation, the libraries were hybridized to Illumina flow cells using TruSeq SR Cluster v2–cBot-GA kit on the Illumina cBot cluster generation instrument. The flow cells were inserted onto the sequencer and subjected to single-read sequencing using the TruSeq SBS Kit v5-GA kit.

### 2.2.18 *ChIP-seq Analysis*

Tony McBryan and John Cole in our laboratory performed bioinformatic analysis of the ChIP-seq data. The analysis involved the following steps;

- 1) Raw data was obtained from the sequencer.
- 2) Consensus Assessment of Sequence and Variation (CASAVA) software program from Illumina was used to convert raw image data into intensity scores, base calls, quality scored alignments etc.
- 3) Statistical analysis and quality control checks were performed using FastQC (Babraham Bioinformatics).
- 4) Peak calling was performed using SICER ([http://www.genomatix.de/online\\_help/help\\_regionminer/sicer.html](http://www.genomatix.de/online_help/help_regionminer/sicer.html)).
- 5) Reads were mapped to the human genome using BOWTIE (<http://bowtie-bio.sourceforge.net/index.shtml>).
- 6) Mapped reads were read on the UCSC (University of California Santa Cruz, <http://genome.ucsc.edu/>) genome browser.
- 7) Motif identification was performed, peaks were annotated with genes and functional enrichment analysis of the peaks was carried out.

### 2.2.19 *Quantitative ChIP-PCR*

ChIP DNA was obtained using the chelex DNA extraction method. Thermo Scientific DyNAmo HS SYBR Green qPCR Kit was used. The following components were added in a 20 µl reaction: 4.8 µl Nuclease-free water, 5 µl ChIP DNA, 0.1 µl Primer 1,

0.1  $\mu$ l Primer 2 and 10  $\mu$ l 2x master mix. Reaction conditions are outlined in Table 2.13.

Cycle step	Temp	Time	Cycles
Initial Denaturation	95°C	15 minutes	1
Denaturation	94°C	10 seconds	39
Annealing	58°C	20 seconds	
Extension	68°C	30 seconds	
Fluorescence data collection			
Final Extension	68°C	10 minutes	1
Melting Curve	55°C - 95°C	20 minutes ramp time	1
Incubate	4°C	Forever	

Table 2.13 Quantitative ChIP-PCR conditions

The following primer pairs (outlined in Table 2.14) were used for assaying regions of specific enrichment and non-enrichment of H4K16ac in the genome of senescent cells compared to proliferating cells. The PCR primers were chosen according to the DiffBind regions, which identified differential enrichment of H4K16ac in senescent cells compared to growing cells. The reaction was set up in a BioRad Chrome4 thermocycler. Following real-time SYBR green reaction, quantitative PCR was carried out using primers sets corresponding to different regions of the genome along with control IgG. The threshold cycle value for each sample was chosen from the linear range. The relative amount of DNA in the ChIP product was calculated with the use of the  $2^{-\Delta\Delta CT}$  method expressed relative to input DNA within the same reaction.

Primer	Sequence
chrX FP	TTGTCCGGGACGTACATTTT
chrX RP	CAGGACGTTTTCTGGCATT
chr1 FP	AGAAAACAAATGCCCATTC
chr1 RP	TCCCTTTGTTCCCATATCCA
chr5 FP	GATCAGTTTCCCATGTGCT

chr5 RP	GCTGGGACAAGCTGAAAGTC
chr6 FP	TGCTTCATCAAGCTGCCTAA
chr6 RP	CCTCCTCGAACATGAACTCG
chr13 FP	GTGACTGAGGAAGCCCAGTG
chr13 RP	GGGTCAGTTTGCTGCTCTTT
chr16 FP	CCTCCCCCAACACTACTG
chr16 RP	GGGAGGCCTGCTATGCTG
chr17 FP	CGGTCCGGGTATAAATAGCTC
chr17 RP	GGGAGGCCACCCATACAG
chr17 region2 FP	TTGGTGATTGGCAGGATCCT
chr17 region2 RP	ACCTTGACCTCACCCATTCC
chr19 FP	ACCCTCAGTCTGTCCGTTTG
chr19 RP	AGGGGGAAGCTGGTTTCTAA

Table 2.14 Quantitative ChIP PCR primers

### 2.2.20 *Histone Peptide Array*

The MODified Histone Peptide Array (Active Motif) containing 384 unique histone modification combinations in duplicate was used to screen specificity of histone antibodies. The array was blocked in TBST + 5% milk for 1 hour at RT. After blocking, the array was briefly rinsed with TBST and immersed in primary antibody solution prepared in TBST + 5% milk. Incubation was performed 1 hour at RT. The array was washed 3 times for 5 minutes in TBST and then incubated in secondary HRP antibody for 1 hour at RT. Washing was performed thrice in TBST for 5 minutes each time at RT. ECL detection reagent was used for detection of antibody interaction. Multiple exposure times were captured using films, scanned, and saved as a .tif file. The images were analysed using Active Motif's Array Analyse Software. A graphical analysis of the histone peptide modification interaction was generated using the software by analysing the intensity of spot interactions between the antibody of interest and peptides.

### 2.2.21 *Models of Senescence*

Replicative Senescence (RS) – IMR90 cells at population doubling (PD) 27.5 were passaged long-term under *in vitro* conditions to replicative senescence. Cells were cultured according to conditions mentioned previously (refer Section 2.21). The PDs were calculated according to the following formula:

$$\text{PDL} = 3.32 (\log X_e - \log X_b) + S$$

X<sub>b</sub> is the cell number at the beginning of the incubation time

X<sub>e</sub> is the cell number at the end of the incubation time

S is the starting PDL

The cells were split every 3 to 4 days at a 1:2 to 1:4 ratio. Cells attained replicative senescence after exhaustion of the exponential growth phase. Cells were harvested at least 15 days after the last split and assayed for routine senescence markers.

Oncogene-induced Senescence (OIS)- Proliferative IMR90 were infected with Control and H-RASG12V virus and drug selected with puromycin. Cells were harvested 12-15 days after drug selection and assayed for several senescence markers.

Ionizing Radiation Induced Senescence (IRS)- Proliferative IMR90 (<PD 30) were seeded at very low density, about 30% coverage in a 10 cm dish. Cells were given 20 Gy dose using Xstrahl RS225 X-Ray irradiator. After irradiation, the plate was replaced with 10 ml fresh media. Media was changed every 3 days after irradiation and cells were not split thereafter. 10 days after irradiation regular senescence assays were performed and cells were then harvested.

### 2.2.22 *Markers of Senescence*

#### 2.2.22.1 *Senescence Associated $\beta$ -Galactosidase Assay*

The Senescence  $\beta$ -Galactosidase Staining Kit from Cell Signaling was used to detect  $\beta$ -galactosidase activity at pH 6, a known characteristic of senescent cells. Cells were seeded on to glass coverslips placed in 6-well plate. After 24 hours, cells were rinsed with PBS. 1 ml fixative solution (2% formaldehyde, 0.2% glutaraldehyde in PBS) was

added to the cells and incubated for 10-15 minutes. Cells were rinsed twice in PBS. 1 ml  $\beta$ -Galactosidase Staining Solution (40 mM citric acid/sodium phosphate pH 6.0, 150 mM NaCl, 2 mM MgCl<sub>2</sub>, 5 mM potassium ferrocyanide, 5 mM potassium ferricyanide, 1 mg/ml X-gal in Dimethylformamide) was added and incubated at 37°C overnight in a dry incubator. 24 hours later, cells were monitored for development of blue colour. Coverslips were washed and mounted using ProLong® Gold Antifade Reagent (Life Technologies) on glass slides. These were stored at -20°C for long periods.

### 2.2.22.2 EdU Proliferation Assay

Cell proliferating assay was performed using Click-iT® EdU Alexa Fluor® 488 Imaging Kit from Life Technologies. This has proved to be a better alternative to traditional BrdU (Bromodeoxyuridine) cell proliferation assay [420, 421]. With the help of EdU (5-ethynyl-2'-deoxyuridine), which is a nucleoside analog of thymidine, cell proliferation could be measured owing to its incorporation into DNA during active DNA synthesis [422]. The reaction was based on click chemistry as explained here [423-426]. Cells were grown on glass coverslips for at least 24 hours to allow full adherence in presence of 10  $\mu$ M EdU. It is to be noted that pulse length of EdU can be varied 3-48 hours depending on preference. After which cells were washed twice with PBS and fixed with neutral buffered 4% formaldehyde for 3 minutes at room temperature. Cells were washed twice with PBS. 1X Click-iT® EdU buffer additive was prepared by diluting the 10X solution 1:10 in deionized water. This solution was prepared fresh and used on the same day. Click-iT® reaction cocktail was prepared according to table below. It was important to add the ingredients in the order listed in table 2.15, otherwise, the reaction does not proceed optimally. Click-iT® reaction cocktail was used within 15 minutes of preparation.

Reaction Components	Number of Coverslips						
	1	2	4	5	10	25	50
1X Click-iT® reaction buffer	430 $\mu$ l	860 $\mu$ l	1.8 ml	2.2 ml	4.3 ml	10.7 ml	21.4 ml
CuSO <sub>4</sub>	20 $\mu$ l	40 $\mu$ l	80 $\mu$ l	100 $\mu$ l	200 $\mu$ l	500 $\mu$ l	1 ml

Alexa Fluor® azide	1.2 µl	2.5 µl	5 µl	6 µl	12.5 µl	31 µl	62 µl
1x Reaction buffer additive	50 µl	100 µl	200 µl	250 µl	500 µl	1.25 ml	2.5 ml
Total volume	500 µl	1 ml	2 ml	2.5 ml	5 ml	12.5 ml	25 ml

Table 2.15 Reaction components in EdU proliferation assay

Cells were incubate for 30 minutes at RT with 100-500 µl/well of Click-iT ® reaction cocktail. Cells were then washed with PBS thrice and mounted with DAPI.

### **3. PROFILING OF HISTONE MODIFICATIONS IN SENESCENT CELLS IN COMPARISON TO PROLIFERATING CELLS**

### 3 PROFILING OF HISTONE MODIFICATIONS IN SENESCENT CELLS IN COMPARISON TO PROLIFERATING CELLS

---

#### 3.1 Introduction

Senescence can be largely considered as a cell's response to an external stress. Oxidative damage, activated oncogenes, telomere attrition, insufficient growth conditions, DNA damage and a host of other cellular stresses trigger senescence [9, 48, 51, 224, 427]. Given the enormous implications senescence has as a tumor suppressive mechanism and also its association with normal human ageing (review [428]), understanding its basic mechanism will enable us to better understand normal cell physiology and also its effect on age-related diseases such as cancer. It is reported that senescent cells undergo extensive nuclear changes in comparison to proliferating cells, including alterations to chromatin structure (review [429]). Epigenetic changes involving N-terminal histone tail modifications appear to regulate gene expression changes in senescence via chromatin remodelling [298, 430], suggesting an explicit link between senescence and chromatin modifications. Also, epigenetic deregulation plays an important role in contributing towards senescence-associated diseases such as cancer and Alzheimer's disease [431-434]. Hence, with the need to better understand how epigenetic mechanisms control senescence, I set out to better understand, how senescence is regulated by its own chromatin structure, specifically via histone modifications. The aim included large scale profiling of histone modifications in senescent cells in comparison to proliferating cells, to identify any novel histone modifications that may alter during senescence. The model system used during the course of this study was human Caucasian fetal lung (primary) fibroblasts, IMR90.

#### 3.2 Results

##### 3.2.1 *Establishment of replicative senescent cells in vitro*

IMR90 have been regularly used to study senescence under plastic culture conditions [1, 2]. IMR90 cells obtained from Coriell Cell Repositories were cultured in optimal

conditions at 37°C, in a humidified atmosphere containing 5% CO<sub>2</sub> and ambient (20%) O<sub>2</sub>. For the purpose of addressing experimental questions it was important to establish a well-defined model of senescence, which would give consistently reproducible results. In order to establish replicatively senescent cells in culture, cells were serially passaged in growth media containing nutrients by sub-culturing every 3-4 days to avoid confluence. Population doublings were routinely calculated as outlined in Chapter 2, section 2.2.20. After about 60 population doublings, cells stopped dividing. They were assayed for features of senescence 2 weeks after the last population doubling. Light microscopy images of proliferating (PD 26) and senescent (PD 62) cells were captured (Figure 3.1.A) to show contrasting morphological features between the two. Cells were assayed for presence of SA β-gal, a widely used marker of senescence [50]. Both proliferating and senescent cells were stained, and the appearance of intensely stained blue cells was more prominent in senescent cells as compared to its proliferative counterparts (Figure 3.1.B). More than 95% of the cell population stained positive in senescent cell sample as compared to less than 5% in proliferating cells. Also, cells were assayed by immunofluorescence to visualize two different proteins, HIRA and PML (Promyelocytic leukemia protein) along with visualization of the nuclei using DAPI staining. The difference in size and number of PML bodies was noted in senescent cells as compared to proliferative cells, with PML bodies appearing as intense punctate foci in the former (Figure 3.1.C). HIRA was also characteristically redistributed to PML bodies in senescent cells. The appearance of characteristic SAHF formation in senescent cells was visualized in the DAPI channel as described previously [176, 386, 435], hence confirming defined and controlled establishment of senescent cells.

In addition, whole cell lysates from proliferating and senescent cells were subjected to SDS-PAGE separation and Western blotting (Figure 3.2), which indicated loss of cyclin A, decreased phosphorylation of RB at serines 807/811 and a marked increase in p16, denoting absence of proliferation in senescent cells.

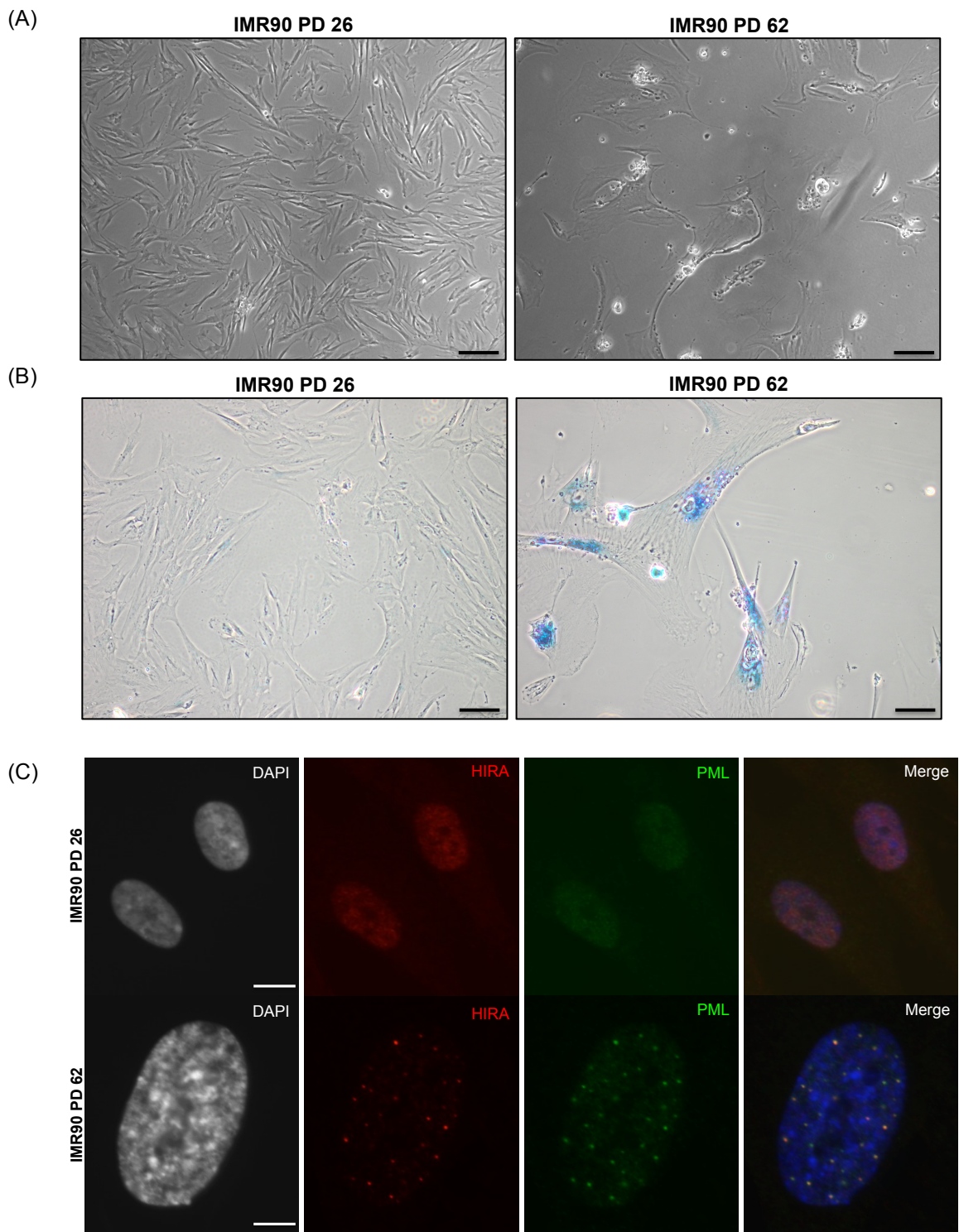


Figure 3.1 Establishment of replicative senescence in human diploid fibroblasts IMR90.

(A) Light microscopy images (under 20X objective) of IMR90 cells passaged to senescence (PD 62 - 97.6% SA  $\beta$ -Gal+) under *in vitro* conditions in the presence of ambient oxygen (20%) along with proliferating cells (PD 26 - 4% SA  $\beta$ -Gal+) as control. (B) Proliferating and senescent cells stained for SA  $\beta$ -Gal activity. (C) Immunofluorescence staining (under 100X objective) for HIRA localization (red) and PML bodies (green) along with DAPI staining (blue) for nuclear visualization, performed on proliferating (PD 26) and senescent cells (PD 62).

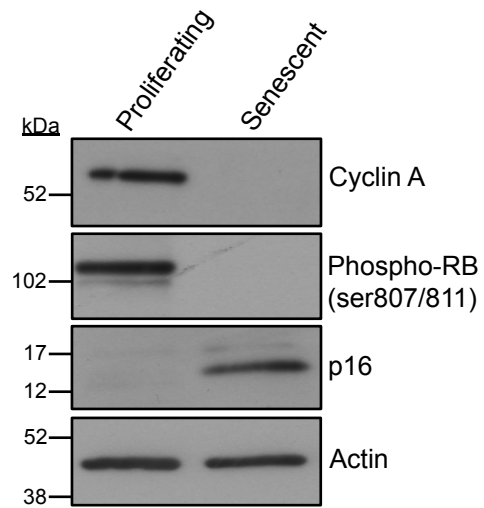


Figure 3.2 Western blot analysis of proteins in proliferating and senescent IMR90 cells. Whole cell lysates were harvested 2 weeks after onset of senescence and subjected to separation using SDS-PAGE containing 20  $\mu$ g protein each and Western blotted for cyclin A, Phospho-RB (ser807/811), p16. Actin was used as loading control.

### *3.2.2 Loss of histones observed in senescent cells in vitro*

Loss of core histones was observed in yeast that have undergone increasing number of cell divisions and this was linked to de-repression of genes which otherwise would have been silenced [173, 401]. This loss was also observed in human diploid fibroblasts that have undergone senescence [174]. Whole cell lysates from proliferating and senescent IMR90 were fractionated by SDS-PAGE and Western blotted for core histones H3, H4, H2A, H2B (Figure 3.3). Results indicated loss of these proteins when loaded according to equal cell number, as supported by Lamin A/C blotting.

In order to facilitate profiling of several different histone modifications in senescent cells as compared to proliferative cells, I was required to achieve equal histone loading between the two cell types. To achieve this, different volumes of whole cell lysates harvested from proliferating cells were compared to a fixed amount (20 µg protein) of whole cell lysate from senescent cells. These were subjected to SDS-PAGE separation and Western blotted using an anti-H3 antibody. In order to achieve equal histone loading between the two cell types, loading volumes were titrated for proliferating cells (Figure 3.4). Subsequently more gels were run to determine equal histone loading between proliferating and senescent cells. This enabled us to compensate for the reduced histone content in senescent cells, providing an unbiased approach to detect changes in post-translational modifications occurring on the core histone tails based on equal histone loading.

### *3.2.3 Profiling of various modifications in senescent cells compared to proliferative cells*

A panel of 83 different antibodies to various histone modifications was obtained from Active Motif. After establishing equal histone loading for proliferating and senescent cells, multiple antibodies to histone modifications were screened by slot blotting.

Although the majority of the histone modifications did not change between the two conditions, some histone modifications increased in abundance in senescence (bottom) in comparison to proliferation (top); for example, lanes 15, 38 and 51 corresponding to histone modifications H3K27me3, H3CS.1 and H4K20me3, respectively (Figure 3.5). Some histone modifications decreased in abundance in senescence in comparison to proliferating cells; for example, lanes 5 and 48

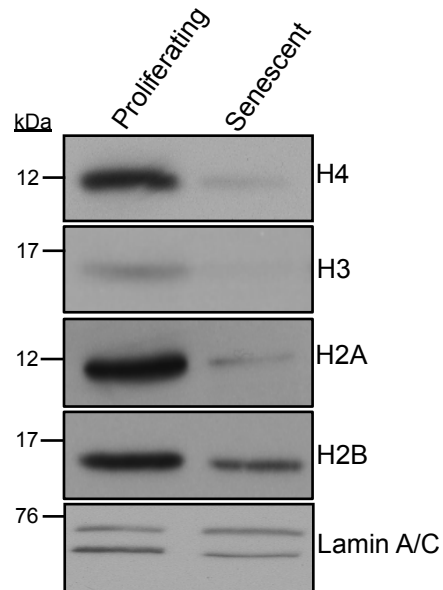


Figure 3.3 Loss of histones observed in senescent cells *in vitro*.

Western blot analysis of core histones in proliferating and senescent cells. Whole cells lysates were harvested (as per Figure 3.2) 2 weeks after onset of senescence and subjected to separation using SDS-PAGE by loading equal cell number and Western blotted for histone H4, H3, H2A, H2B. Lamin A/C was used as loading control.

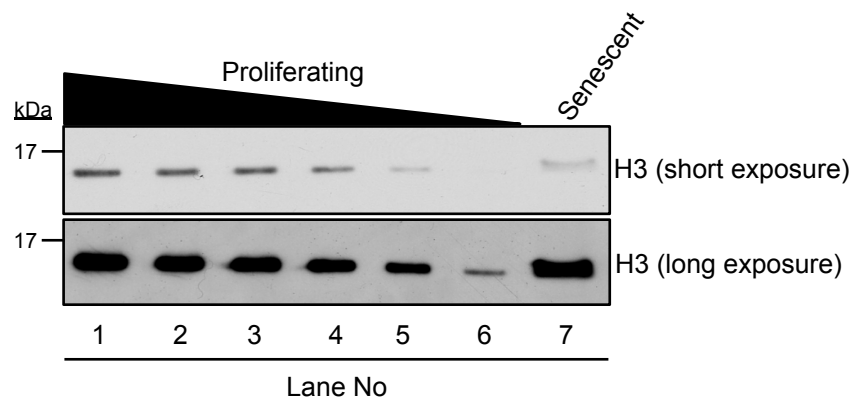


Figure 3.4 Titration of histone H3 in senescent cells compared to proliferative cells. Different volumes of whole cell lysates from proliferating cells were titrated against 20  $\mu\text{g}$  of protein lysate from senescent cells by SDS-PAGE and Western blotting.

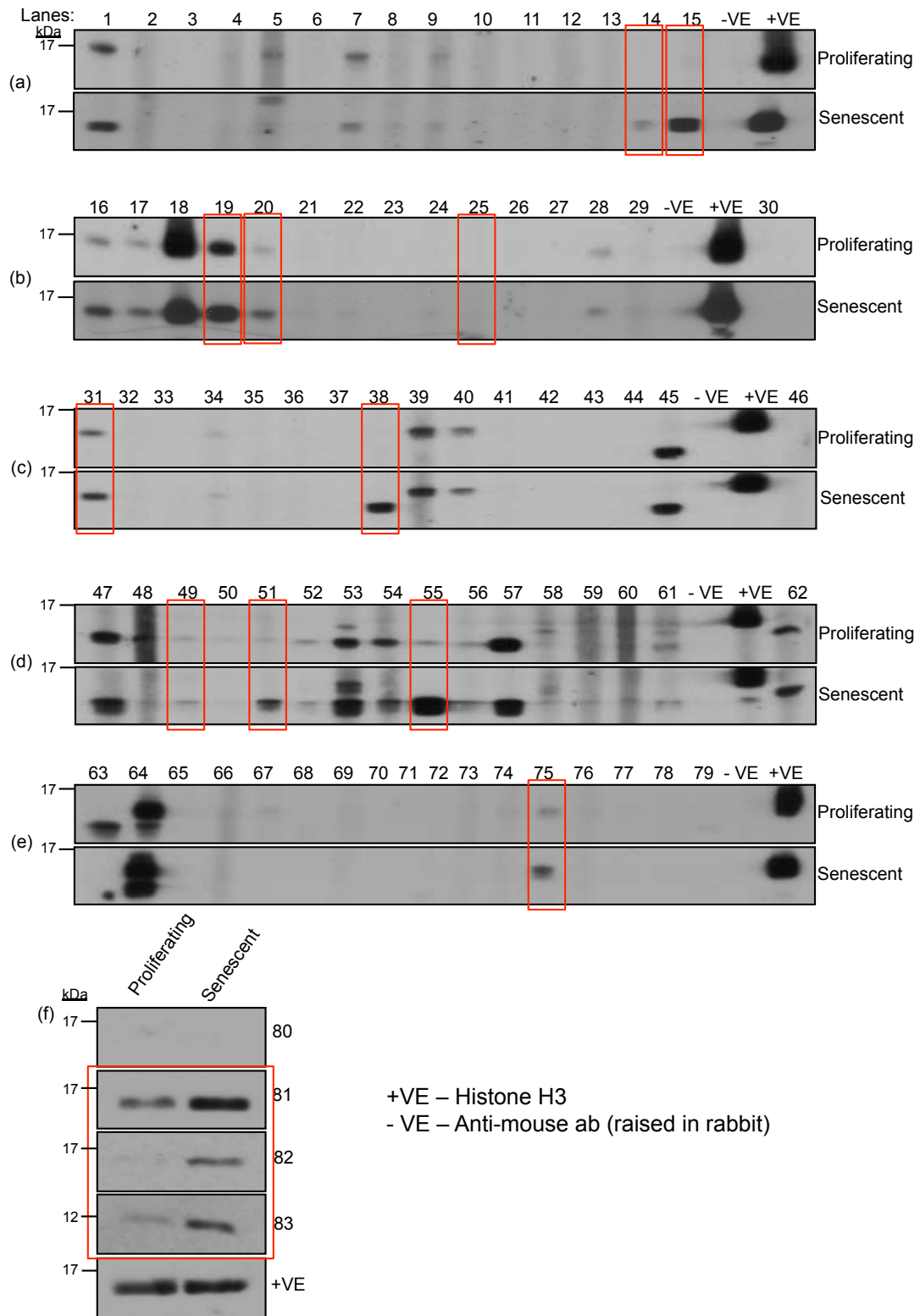


Figure 3.5 Profiling of various histone modifications in senescent cells in comparison to proliferating cells.

Whole cell lysates were assayed by slot blot format (a to e) similar to Western blotting (f) with antibodies to various histone modifications (1 to 83) as defined in Table 3.1. Electrophoresis was performed at 90-120V using 15% SDS gel. To ensure equal loading of total histones, lysates were subjected to blotting with total histone H3 antibody (+ve) and the appropriate negative control (-ve).

Lane	Antibodies	Lane	Antibodies
1	Histone H3 acetyl Lys18 pAb	43	Histone H3 dimethyl Arg8 asymmetric rabbit pAb
2	Histone H3 acetyl Lys23 pAb	44	Histone H3 dimethyl Lys23 rabbit pAb
3	Histone H3 acetyl Lys27 pAb	45	Histone H4 acetyl Lys12 pAb
4	Histone H3 acetyl Lys27 pAb	46	Histone H4 acetyl Lys16 pAb
5	Histone H3 acetyl Lys9 pAb	47	Histone H3 dimethyl Lys9 pAb
6	Histone H3 acetyl pAb	48	Histone H4 acetyl Lys8 pAb
7	Histone H3 dimethyl Lys4 pAb	49	Histone H4 dimethyl Lys20 pAb
8	Histone H3 dimethyl Lys79 pAb	50	Histone H4 monomethyl Lys20 pAb
9	Histone H3 monomethyl Lys79 pAb	51	Histone H4 trimethyl Lys20 pAb
10	Histone H3 phospho Ser10,28 pAb	52	Histone H4 tetra-acetyl pAb
11	Histone H3 phospho Ser28 pAb	53	Histone H4 tetra-acetyl pAb
12	Histone H3 phospho Thr11 pAb	54	Histone H4 pAb
13	Histone H3 phospho Thr3 pAb	55	Histone H4 dimethyl Arg3, symmetric pAb
14	Histone H3 trimethyl Lys27 pAb	56	Histone H4 monomethyl Lys31 pAb
15	Histone H3 trimethyl Lys27 pAb	57	Histone H4 acetyl Lys5 pAb
16	Histone H3 trimethyl Lys4 pAb	58	Histone H2A pAb
17	Histone H3 trimethyl Lys9 pAb	59	Histone H2A acetyl Lys5 pAb
18	Histone H3, C-terminal pAb	60	Histone H2A acetyl Lys9 pAb
19	Histone H3 dimethyl Lys9 pAb	61	Histone H2A, acidic patch pAb
20	Histone H3 pan-methyl Lys9 pAb	62	Histone H2A.Z pAb
21	Histone H3 dimethyl Lys27 pAb	63	Histone H4 pan-acetyl pAb
22	Histone H3 monomethyl Lys9 pAb	64	Histone H2A/H4 phospho Ser1 pAb
23	Histone H3 phospho Ser10 pAb	65	Histone H2AX phospho Ser139 pAb
24	Histone H3 dimethyl Lys36 pAb	66	Histone H2A phospho Ser129 pAb
25	Histone H3 monomethyl Lys56 pAb	67	Histone H2A phospho Thr120 pAb
26	Histone H3 dimethyl Lys56 pAb	68	Histone H2A, C-terminal pAb
27	Histone H3 acetyl Lys56 pAb	69	Histone macroH2A1 pAb
28	Histone H3 monomethyl Lys4 pAb	70	Pht1 / H2AZ pAb
29	Histone H3 dimethyl Lys14 pAb	71	Pht1 / H2AZ acetyl pAb
30	Histone H3 monomethyl Lys122 pAb	72	Histone H2B pAb
31	Histone H3 dimethyl Lys9 pAb	73	Histone H2B pAb
32	Histone H3 monomethyl Lys27 pAb	74	Histone H2B acetyl Lys120 pAb
33	Histone H3 acetyl Lys36 pAb	75	Histone H2B acetyl Lys16 pAb
34	Histone H3 acetyl Lys4 pAb	76	Histone H2B acetyl Lys5 pAb
35	Histone H3 monomethyl Lys23 pAb	77	Histone H2B dimethyl Lys46 pAb
36	Histone H3 acetyl Lys64 pAb	78	Histone H2B acetyl Lys46 pAb
37	Histone H3 acetyl Lys79 pAb	79	Htz1 pAb
38	Histone H3.cs1 pAb	80	Histone H3 trimethyl Lys9 mAb (Clone 2AG-6F12-H4)
39	Histone H3 acetyl Lys9 pAb	81	Histone H3 trimethyl Lys27 mAb
40	Histone H3 acetyl Lys18 pAb	82	Histone H3 trimethyl Lys27 mAb
41	Histone H3 acetyl Lys14 pAb	83	Histone H4 dimethyl Lys20 mAb
42	Histone H3.3 phospho Ser31 pAb	-VE	Anti-mouse IgG antibody
		+VE	Histone H3 C-terminal pAb

Table 3.1 List of antibodies used in the histone modification screen.

The lane numbers (1 to 83) correspond to those shown in Figure 3.5.

corresponding to H3K9ac and H4K8ac, respectively. The histone modifications corresponding to the different lane numbers (1 to 83) are outlined in Table 3.1. Although both increases and decreases in abundance may be important and novel in the context of senescence, for the purpose of simplification and also since modifications that increase are more likely to be drivers of senescence, I focussed only on those histone modifications that are elevated upon induction of senescence. The potential candidate histone modifications for further analysis as a result of the screen are listed in Table 3.2.

#### *3.2.4 Changes in histone modifications observed in two different models of senescence*

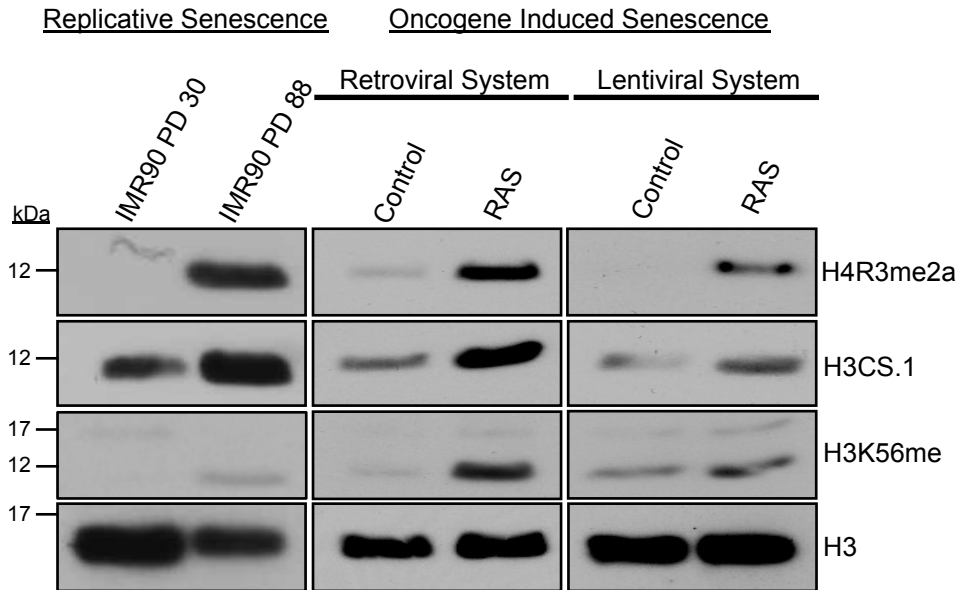
From the candidate altered histone modifications listed in Table 3.2, three histone modifications H4R3me2a, H3CS.1 and H3K56me, hereafter termed collectively as histone marks, which has not been previously demonstrated to change in senescence were chosen for further probing. Relatively little is known about these histone marks, especially in the context of senescence. As a first measure, changes in these histone marks were independently confirmed by SDS-PAGE and Western blotting with a second set of replicative senescent cell lysates (PD 88) grown under low oxygen conditions of 3% compared against proliferating cell lysate (PD 30). David M Nelson, a former graduate student from the lab, prepared these lysates. Figure 3.6.A indicates elevated levels of all three histone marks in the above lysates based on equal histone H3 loading. It is to be noted that H3K56me appeared as a doublet when resolved on a 15% polyacrylamide gel. Histone H3 typically migrates about 17 kDa; in this case, a faster migrating band at around 12 kDa was noted to increase in senescence (see Discussion). The lysates were also blotted for markers of proliferation arrest and the senescent cells were noted to have decreased cyclin A expression and reduction of phosphorylation of RB at serines 807/811 (Figure 3.6.B). These results clearly confirm the changes observed in the histone marks in replicative senescence with two independent experimental setups.

I set out then to ask if these changes were recapitulated in another model of senescence, specifically oncogene-induced senescence. In this case, H-RASG12V oncogenic insult was used to establish OIS cells as shown previously [37]. The approach was performed using two different modes of viral gene transfer, namely

No	Candidate histone modifications
1	H3K27me3
2	H3K9me2
3	H3K9 pan-me
4	H3K56me
5	H3CS.1
6	H4K20me2
7	H4K20me3
8	H4R3me2a
9	H2BK16ac

Table 3.2 Candidate histone modifications that increase in replicative senescence as identified from the screen in Figure 3.5

(A)



(B)

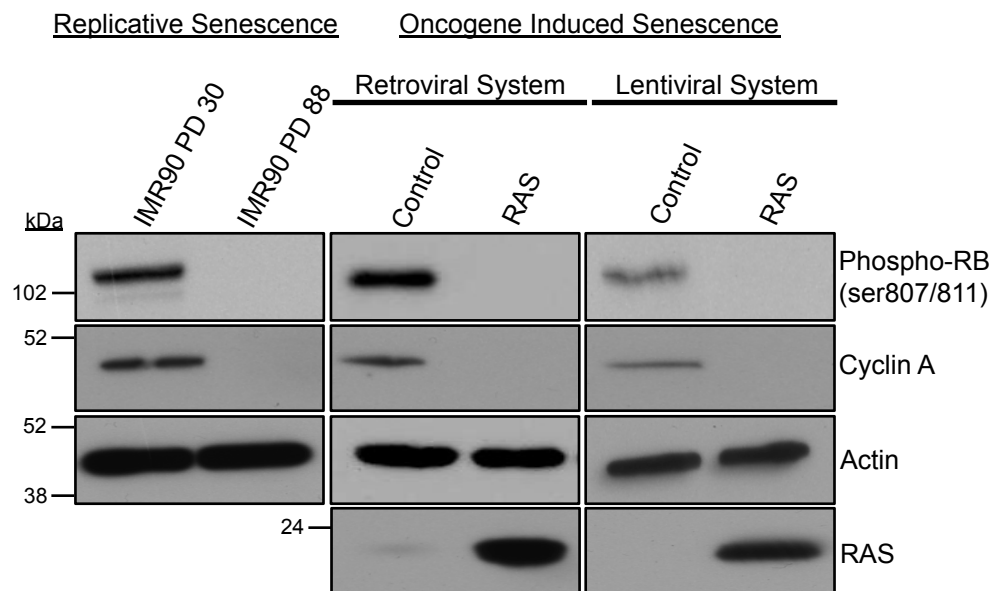


Figure 3.6 Levels of candidate histone marks in two different models of senescence, RS and OIS.

(A) IMR90 cells were grown to senescence (PD 88) under low oxygen (3%) and compared to proliferative IMR90 (PD 30). PD 88 cell lysates obtained from David M Nelson. OIS cells were established using IMR90 cells infected with control & RAS retrovirus and lentivirus, followed by puromycin selection. RAS-induced senescent cells were harvested 9 days post infection and drug selection. Whole cell lysates were assayed by SDS-PAGE by loading equal histone content and Western blotting with respective antibodies to different histone modifications. To ensure equal loading of nuclear protein, lysates were subjected to blotting with total histone H3 antibody. (B) Whole cell lysates for RS and OIS were assayed by loading 30  $\mu$ g protein, for markers of proliferation using appropriate antibodies. Actin was used as loading control.

retroviral and lentiviral gene transfer using vectors that confer puromycin resistance. Following transfer of oncogenic H-RASG12V (henceforth referred to as RAS) via retroviral system into IMR90 [169] along with control/empty vector virus, cells were subjected to puromycin selection. Whole cell lysates were harvested 9 days post drug selection and subjected to SDS-PAGE separation and Western blotting. The results in the RS model were reproduced in the OIS model with the histone marks showing elevated levels (Figure 3.6.A). Control and RAS lysates were also subjected to blotting and analysis of senescence markers such as cyclin A, phosphorylation of pRB at serines 807/811 with actin as loading control (Figure 3.6.B). Results confirmed that the cells were truly senescent along with confirmation of overexpression of RAS. I then set out to ask if this was reproducible in a biological replicate by using lentiviral mode of RAS transfer. Figure 3.6.A confirmed elevated levels of histone marks in lentiviral RAS-induced senescence. Figure 3.6.B confirmed absence of cell cycle marker cyclin A, loss of phosphorylation of RB at serines 807/811 and also RAS overexpression with actin as loading control.

### *3.2.5 Other stress factors do not facilitate increase of histone marks in IMR90*

In simple terms, cellular senescence can be considered to be a stress response. Observations of elevated levels of histone marks in senescent cells raised the question as to whether the changes are simply an acute response to stress, rather than part of the senescence programme itself. To address this, cells were treated with different stress inducers such as Trichostatin A (TSA), sodium butyrate (NaBu) and Hydroxyurea (HU). TSA is a potent and specific inhibitor of histone deacetylase [436, 437] and causes accumulation of acetylated forms of histone and non-histone proteins [438, 439]. IMR90 cells were treated with TSA for 24 hours at a previously tested concentration of 3.3  $\mu$ M in the lab. Whole cell lysates were harvested along with untreated parental cells and vehicle (DMSO) treated cells and subjected to SDS gel separation and Western blotted for histone marks. Figure 3.7.A demonstrates that an increase in the histone marks was not observed following TSA treatment. As a measure of control, TSA treated cells showed marked increase in acetylation of total H3 in comparison to control cells along with signs of DNA damage as noted by elevated expression level of  $\gamma$ H2A.X (H2A.X phosphorylated on serine 139). Similarly IMR90 cells were treated for 24 hours with NaBu at a pre-determined concentration of

15 mM. NaBu causes accumulation of acetylated histones in the nuclei of cells and the concerted effects are similar to TSA treatment [440-444]. Whole cell lysates harvested from NaBu-treated cells exhibited (Figure 3.7.A) no increase in the histone marks observed in senescence, in fact, a marginal decrease might be apparent. Cells also confirmed increase in total H3 acetylation as expected (Figure 3.7.B) thereby confirming effective NaBu treatment. Along with the above two treatments, HU, a potent DNA damage inducer, was also used to induce stress in IMR90. The inhibitory mechanism of HU on DNA synthesis has been tested in a wide range of organisms as outlined in [445]. IMR90 cells were treated with HU for 24 hours at a previously tested concentration of 1 mM in the lab. Following treatment, immunoblotting assays on whole cell lysates exhibited profound induction of DNA damage markers such as  $\gamma$ H2A.X and p53 as expected along with actin as loading control (Figure 3.7.B). Similarly to the previous two treatments involving TSA and NaBu, HU treatment did not induce elevated levels of the histone marks in comparison to parental cells and DMSO (vehicle) treated cells. These results suggest that the marked abundance of histone marks noted in IMR90 is specifically linked to senescence, and not to other acute stresses.

### *3.2.6 Changes in histone marks occur specifically in senescence and not simply cell cycle arrest*

Although one of the characteristic features of senescence is growth arrest, not all adult cells that have undergone growth arrest are senescent. A state of reversible growth arrest can be termed as quiescence [446, 447]. The difference between the two states can be simplified by terming senescence as an irreversible proliferation arrest and quiescence as a reversible state. Also it is to be noted that senescent cells are not terminally differentiated cells [448-450] even though they are both growth arrested. In order to validate if the results obtained with senescent cells were exclusive only to this state and not as a result of mere cell cycle arrest, quiescent cells were established in the lab. IMR90 cells were grown to confluence and serum starved for 3-4 days. Following this, cells were harvested for protein lysates and subjected to SDS-PAGE separation and Western blotting for phosphorylation of RB at serines 807/811 and cyclin A and histone H3 (Figure 3.8.A). Results indicated that loss of phospho-pRB and cyclin A was noted in both senescent and quiescent cells,

confirming proliferation arrest in both cases. However, quiescent cells did not show altered histone modifications. With Figure 3.8.B, it can be concluded that the increase in abundance of histone marks occurs only in the senescence programme.

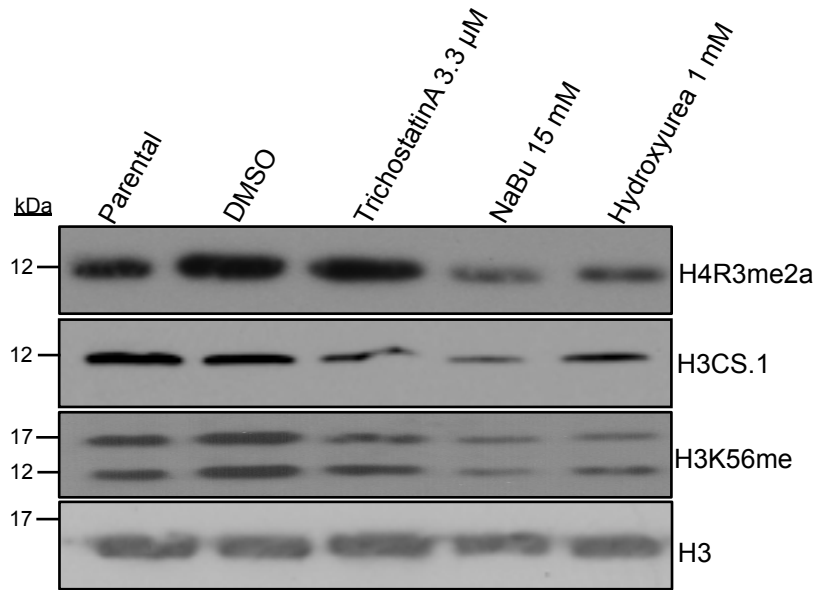
### 3.3 Discussion

Two different model systems of senescence, RS and OIS, were reliably established. These cells were rigorously tested for various markers of senescence such as absence of cyclin A and phospho-pRB [50]. Chromatin structure plays a crucial role in mediating key events reported in the senescence programme [176, 177, 451, 452]. In order to better understand how the senescence programme is regulated by its own chromatin structure, I set out to perform large-scale profiling of various histone modifications in senescent cells in comparison to proliferating cells to facilitate an unbiased approach of identifying potentially key changes.

A panel of 83 different antibodies to various histone modifications was tested using slot blotting technique. From the screen, it was interesting to note that whilst a lot of the modifications exhibit no change across the two cell states, some modifications exhibited elevated levels in senescent cells, whilst a few others exhibited decreased levels. Whilst either of the changes maybe unique and important to the mechanism of senescence, I focused only on those changes that were elevated with the induction of senescence, because modifications that increase may be more likely be drivers of senescence. From the screen, a list of potential candidates that were elevated in RS was chosen. In the interest of time, three different histone marks H4R3me2a, H3CS.1 and H3K56me were chosen for further probing. Relatively little is known about these histone marks and to my knowledge, this is the first time they are reported to be altered, i.e., increased in abundance during senescence. These changes were also common to the OIS model of senescence, but not acute stresses and reversible quiescence, suggesting that they may be exclusive to the process of cellular senescence.

With these observations in mind, H4R3me2a and H3CS.1 were chosen as histone marks of interest to study further. Characterization of these two histone modifications will be discussed in the following chapters. As for H3K56me, the

(A)



(B)

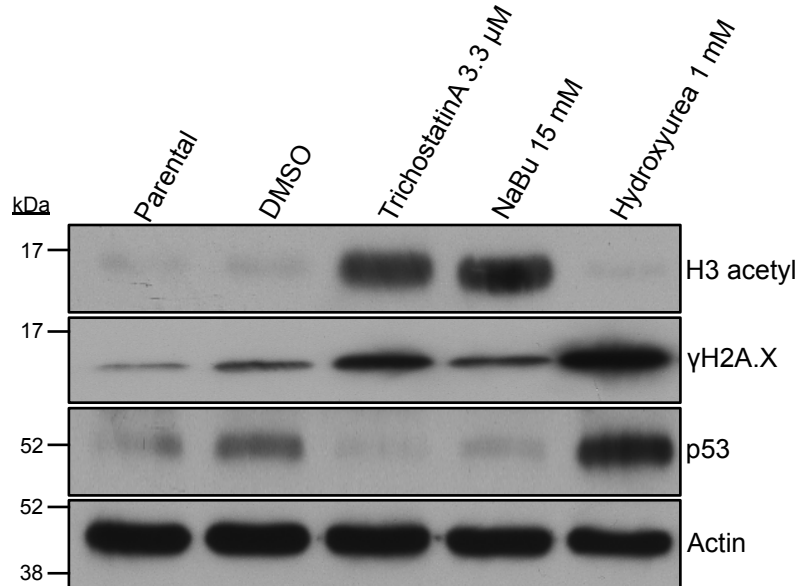
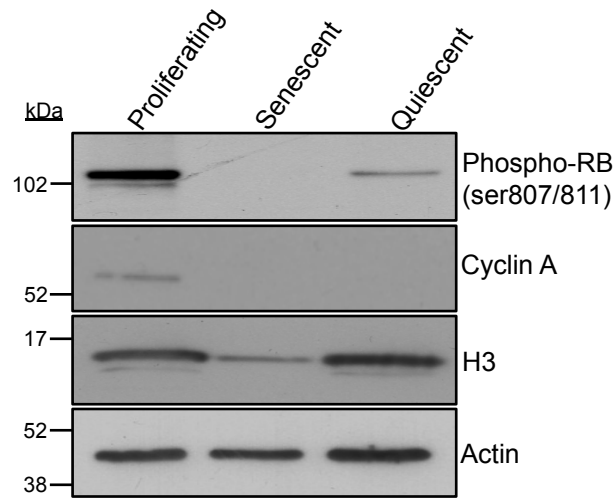


Figure 3.7 Increased levels of histone marks in IMR90 is exclusive to senescence.

IMR90 cells were treated with two classical HDAC inhibitors, Trichostatin A (TSA) and sodium butyrate (NaBu) along with DNA damaging agent, Hydroxyurea (HU) at indicated concentrations for 24 hours. Whole cell lysates were harvested after this time point and subjected to SDS-PAGE separation at 90-120V using 15% gel by loading 30  $\mu$ g protein each and Western blotted for (A) markers of DNA damage induction ( $\gamma$ H2A.X and p53) and HDACi treatment (H3 acetyl) where actin is used as loading control and (B) histone marks where H3 is used as loading control.

(A)



(B)

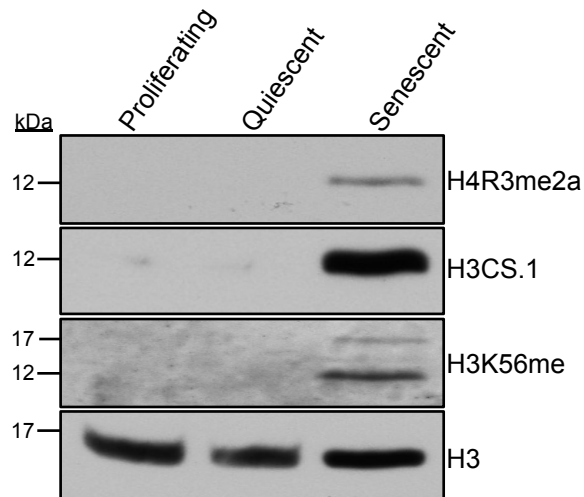


Figure 3.8 Changes in histone marks observed specifically in senescence and not simply cell cycle arrest.

Whole cell lysates from proliferating, senescent and quiescent cells were subjected to SDS-PAGE separation by loading 20  $\mu$ g protein each and Western blotted for (A) markers of cell cycle arrest and senescence with actin as loading control, and (B) histone marks of interest with histone H3 as loading control.

antibody remains to be tested for specificity and, at the time of study, this was the only known commercially available antibody. It is tempting to speculate that the faster migrating band may be another isoform of H3K56me or possibly the modification occurs on the cleaved version of histone H3 (H3CS.1) as described in Chapter 4. In general, histone lysine methylation is considered to be a relatively stable modification and is thought to play an important role in organizing chromatin domains and also in the epigenetic control of genes. H3K56me was discovered for the first time in 2003 by Peters and colleagues and only a very low methylation frequency ( $\leq 5\%$ ) was reported in comparison to previously described methylation at positions such as H3K9, H3K27 and H3K36 with high prevalence of methylation ( $\geq 50\%$ ), or H3K79 with a moderate prevalence of methylation at  $\sim 10\%$  [453]. A recent study demonstrated that H3K56me is deposited by histone lysine methyltransferase G9a/KMT1C in mammalian cells and also reported a potential role for H3K56me<sub>3</sub> as a chromatin docking site to facilitate binding of PCNA prior to its role in DNA replication during cell cycle [454]. H3K56me remains underexplored and my preliminary results demand an understanding of how this modification may regulate senescence, and perhaps ageing and cancer.

## **4. H3CS.1 IN CELLULAR SENESENCE**

## 4 H3CS.1 IN CELLULAR SENESCENCE

---

### 4.1 Introduction

In the previous Chapter, to gain insight into chromatin alterations that happen at the onset of senescence and how they may play an important role in regulating the process, I performed profiling of various histone modifications in senescent cells compared to proliferating cells.

Controlled and site-specific proteolysis is implicated as an important mechanism in controlling basic cell mechanisms such as differentiation, signal transduction, cell cycle progression, transcription, and cell death [455, 456]. Cathepsins are a large family of proteases implicated not only in the degradation of junk protein aggregates [457] but also in the control of cell death by caspases [458] and cancer metastasis [459]. In 2002 it was discovered that Cathepsin L is a pro-survival protease in *C.elegans*, since transient KD of this enzyme using siRNAs proved to be embryonically lethal [460]. Despite this, it was noted that in mice, knocking down Cathepsin L lead to several abnormalities in the skin, brain and heart but not embryonic lethality [461-464]. These findings suggest that Cathepsin L may be important in normal organ development and cell survival. Cathepsin L plays a major role in autophagy, involving degradation of the cell's own components primarily within the lysosomal compartments [465, 466]. Lysosomes are membrane-enclosed sacs containing hydrolytic enzymes located in the cytoplasm [467-469]. Localization of active Cathepsin L is both nuclear and cytoplasmic [455, 470-473].

In 2008, a specific endogenously regulated mechanism of proteolysis of histone H3 was documented in mammalian embryonic stems cells for the first time, thereby underscoring an importance for chromatin signature in development and differentiation that was previously not appreciated [474]. It was shown that the H3.2 variant of H3 may be preferentially cleaved over H3.3 and significantly less H3 cleavage was detected in H3.1 in ESCs. The cleavage was shown to occur at various sites between amino acids 21 and 28, with the primary cleavage site positioned between amino acid 21 and 22 [474]. The study also showed that Cathepsin L is the enzyme responsible for producing cleaved histone H3.

As a result of the histone modification screen performed at the start of this study, H3CS.1 was discovered to have elevated abundance in senescence for the first time. Perhaps this change has unsuspected functions as part of the senescence programme that are yet to be understood. In this chapter, I focused on characterizing and validating H3CS.1 in the context of senescence and also potentially the contribution of this particular histone mark to the senescence program.

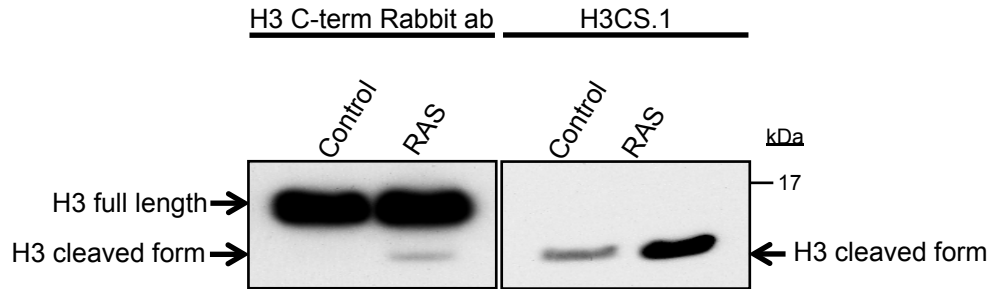
## 4.2 Results

### *4.2.1 Validation of H3CS.1 antibody specificity*

The validity and reproducibility of results using antibodies directed to histone modifications has been open to discussion in the past. In 2010, Egelhofer et al., demonstrated that 25% of 200 antibodies to several histone modifications failed assessments for specificity by Western blots or dot blots [475]. Therefore, in order to have reproducibility and biological relevance to any study pertaining to a histone modification, it is very important for the antibody to be specific and/or the result to be validated. In the previous Chapter, the antibody to H3CS.1 was purchased from Active Motif. The antibody was raised against a peptide containing the primary site of Cathepsin L cleavage between amino acids 21 and 22 at the N-terminus.

To confirm up regulation of H3CS.1 in another model of senescence and to validate antibody specificity, whole cell lysates from control and RAS-infected senescent cells were harvested 9 days after puromycin selection following infections, fractionated using SDS-PAGE and Western blotted for H3CS.1 along with total H3 antibody, using an antibody raised to the C-terminus of full length H3 (retained in H3CS.1) (Figure 4.1.A). H3CS.1 antibody specificity was evident based on its recognition of a shorter form of histone H3 running at 12 kDa that co-migrated with a 12kDa polypeptide detected by the H3 C-terminal antibody. An elevated level of cleaved H3 was consistently observed in two different model systems of senescence (RS and OIS) (Refer also to Figure 3.6.A).

A)



(B)

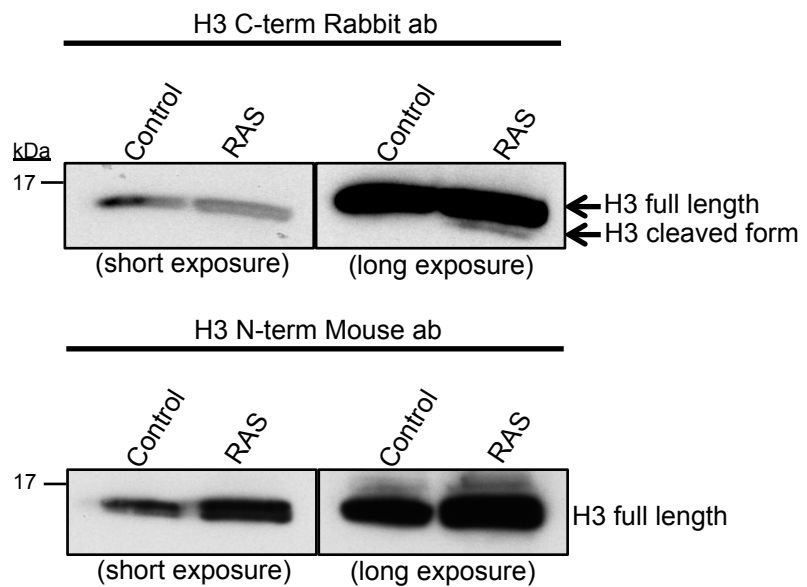


Figure 4.1 Confirmation of cleaved H3 in senescent cells.

Whole cell lysates from control and RAS-induced senescent cells were subjected to SDS-PAGE separation. Electrophoresis was performed at 90-120V using 15% SDS gel and Western blotted with antibodies against (A) C-terminus of histone H3 and H3CS.1 (B) histone H3 C-terminus and histone H3 N-terminus.

To further substantiate the specificity of the H3CS.1 antibody, protein lysates from the same control and RAS-induced senescent lysates were separated on a gel with equal histone loading and Western blotted with antibodies raised to both C- and N-termini of histone H3 (Figure 4.1.B). Whilst the H3 C-terminal antibody recognized the increase in the cleaved form of the histone in senescent cells, the H3 N-terminal antibody failed to do the same even at higher exposures using ECL, reflecting the fact that H3CS.1 lacks the N-terminus of full length H3. Based on these results, the validity of the antibody was confirmed for further use for Western blot. Any subsequent lots of the antibody purchased from Active Motif were rigorously tested applying the same criteria (data not shown) and found to perform consistently well.

#### *4.2.2 Establishment of an inducible-model system of senescence to follow kinetics of H3CS.1*

To better study H3CS.1, I set out to establish an inducible-model system of senescence that could be used to study the kinetics and regulation of H3CS.1. Here, I used an inducible RAS model system of senescence, in which activated RAS is fused to ER- $\alpha$  (Estrogen Receptor Alpha), first described by Littlewood et al., [476]. In this model, fusion protein (ER: RAS) is derived from mouse ER Hormone Binding Domain (HBD) as in-frame fusion with full length H-RASG12V [477], encoded in retrovirus pLNC-RAS:ER [415]. Owing to a mutation present within the ER at codon 525 (G525R), the system is largely insensitive to 17 $\beta$ -estradiol but is still responsive to its synthetic ligand 4-hydroxytamoxifen (4OHT) [477]. Binding of 4OHT to the ER domain of ER:RAS results in activation of RAS due to de-repression of the fusion protein by 'unfolding', i.e., in the absence of 4OHT, the fusion protein is complexed with hsp90 (heat shock protein) in the cytoplasm, preventing downstream H-RAS signaling.

ER:RAS cells were produced using the retroviral construct by following the standard protocol outlined in Materials and Methods section 2.2.9. Infected and drug selected cells were induced with 100 nM 4OHT for 9 days for induction of senescence. Light microscopy images showed typical morphological changes associated with senescence in 4OHT cells as they appear large, flattened, vacuolar and multi-nucleated in comparison to control (uninduced) cells (Figure 4.2.A). 4OHT-induced cells also exhibited enhanced SA  $\beta$ -Gal activity in comparison to control cells

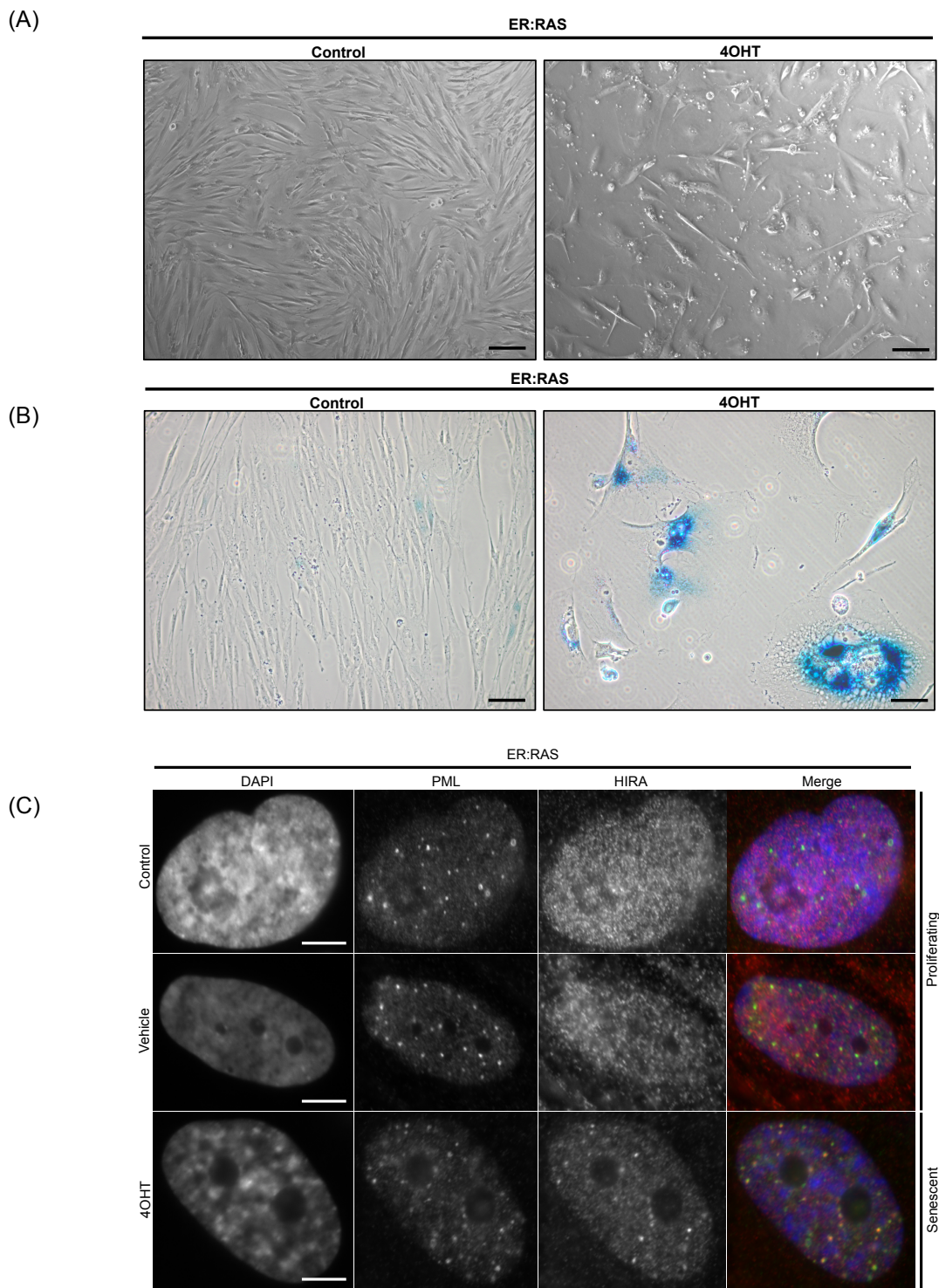


Figure 4.2 Establishment of inducible model of senescence in IMR90.

(A) Light microscopy images of control (uninduced) and 4OHT (induced) ER:RAS cells under 20X objective. (B) Control (uninduced) (5.7% SA  $\beta$ -Gal+) and 4OHT cells, i.e., 4OHT-induced ER:RAS senescent cells (98.4% SA  $\beta$ -Gal+) stained for SA  $\beta$ -Gal activity 9 days after 4OHT induction under 20X objective. (C) Immunofluorescence staining for HIRA localization, PML bodies along with DAPI staining for nuclear visualization performed on control (uninduced), vehicle (EtOH) treated and 4OHT-treated ER:RAS cells 9 days after induction under 100X objective. .

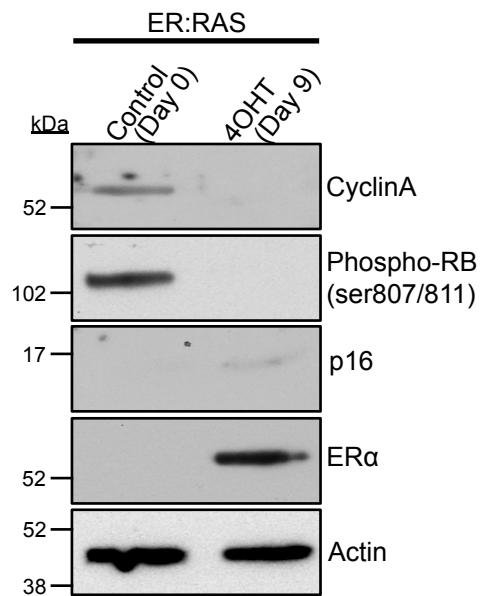


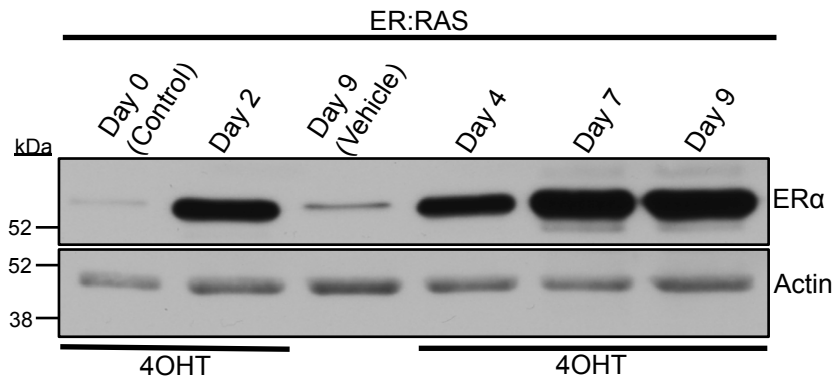
Figure 4.3 Western blot analysis of proteins in control (uninduced) and 4OHT-induced senescent cells. Whole cells lysates were harvested 9 days post 4OHT induction and subjected to separation using SDS-PAGE. Electrophoresis was performed at 90-120V using 4-12% gradient SDS gel and Western blotted for makers of proliferation arrest and ER $\alpha$ . Actin was used as loading control.

(Figure 4.2.B). Control (uninduced), vehicle (EtOH) treated and 4OHT-treated ER:RAS cells were also seeded onto coverslips for visualization of proteins using IF. HIRA co-localization along with PML bodies was observed in 4OHT-induced ER:RAS cells, in comparison to the controls (Figure 4.2.C), along with SAHF formation as visualized in the DAPI channel. Whole cell lysates were also harvested for further downstream analysis using SDS-PAGE and Western blotting. Control (uninduced) and 4OHT-induced senescent cells were blotted for markers of senescence and induced cells showed elevated levels of p16, decreased cyclin A and decreased phosphorylation of RB at serines 807/811 relative to actin as a loading control (Figure 4.3). Ectopically expressed RAS fused to the ER was also visualized only in the induced cells using an anti-ER antibody, whereas uninduced cells fail to express the fusion protein due to the absence of 4OHT. With the above-mentioned analysis, establishment of a 4OHT-inducible model system of senescence was utilised for further experiments.

#### *4.2.3 H3CS.1 abundance gradually increases with the induction of RAS*

In order to understand how H3CS.1 might be regulated in the senescence programme, the ER:RAS inducible system was used. A time course was performed by harvesting cells at the following time points post 100 nM 4OHT induction: control (day 0), day 2, day 4, day 7, day 9 and vehicle (EtOH) treated (day 9). Whole cell lysates were prepared and fractionated by SDS-PAGE. Western blotting was performed using antibodies to H3CS.1 (Figure 4.4.A). Total H3 was used as a loading control. It was found that H3CS.1 gradually increases after induction of RAS in IMR90, with the increase especially apparent from day 4 of induction. Induction of RAS en-route to senescence was also visualized using an anti-ER antibody with actin as a loading control (Figure 4.4.B). Also uninduced control cells and 4OHT-induced (day 9) cells were extensively tested for other senescence markers previously (Refer to Figure 4.2, 4.3). Hence, evidence suggests that H3CS.1 is essentially induced at the onset of senescence and gradually increases as the cells become more senescent. This potentially may suggest an important and yet unknown role of H3 proteolysis in onset of senescence in these cells.

(A)



(B)

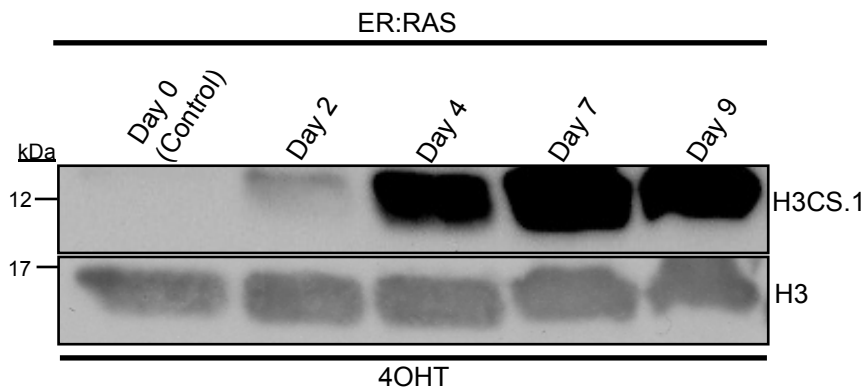


Figure 4.4 H3CS.1 abundance gradually increases after induction of RAS.

4OHT-induced ER:RAS cells were harvested at various time points from day 0 of induction (control) to day 9 of induction along with vehicle (EtOH) treated cells on day 9. Electrophoresis was performed at 90-120V using 4-12% gradient SDS gel. Whole cell lysates were subjected to immunoblotting technique for (A) expression of ectopically expressed RAS using anti-ER antibody with actin as loading control (B) levels of H3CS.1 along with total H3 as loading control.

As mentioned previously, Cathepsin L is the enzyme responsible for H3 cleavage in mammalian cells [474]. The enzyme was originally described as a lysosomal protease [466]. The functions of lysosomal proteases have been implicated in bulk protein degradation thereby maintaining cells' vital functions via recycling of junk material [478]. Perhaps trafficking of H3 through lysosomes/autophagosomes of senescent cells produces H3CS.1 and may have a potentially novel role in senescence. This will be investigated further in this chapter.

#### *4.2.4 Cathepsin L cleaves histone H3 to produce histone H3CS.1 and is increased in senescent cells*

Given the finding that the level of H3CS.1 is elevated in senescence, it was interesting to determine if levels of the enzyme responsible for generating H3CS.1 [474] also change in senescence. Whole cell lysates were prepared from control and senescent cells constitutively expressing RAS. These had previously been tested for induction of various senescence markers (Figure 3.6). Lysates were fractionated by SDS-PAGE for separation and Western blotted with a previously validated antibody [479] to enzyme Cathepsin L (Figure 4.5). Results from these analyses showed that Cathepsin L level is elevated in OIS in comparison to proliferating control cells, as noted by the increase in proteolytically cleaved active form of the protein (~25 kDa) and the inactive form termed Pro-Cathepsin L (~42 kDa). This is consistent with the idea that up regulation of Cathepsin L contributes to generation of H3CS.1 in senescent cells.

#### *4.2.5 Cytoplasmic localization of nuclear histone H3CS.1 observed in RAS-induced senescent cells.*

Given the involvement of Cathepsin L as a H3 protease [474], it was interesting to test the distribution of H3CS.1 in senescence. ER:RAS cells were treated with 4OHT for induction of senescence. On day 9 cells were harvested for assay by immunofluorescence. Cells were stained using antibodies to H3CS.1 and negative control antibody (Figure 4.6). DAPI staining of the nuclei were also performed. Results indicated an increased cytoplasmic localization for nuclear H3CS.1 in

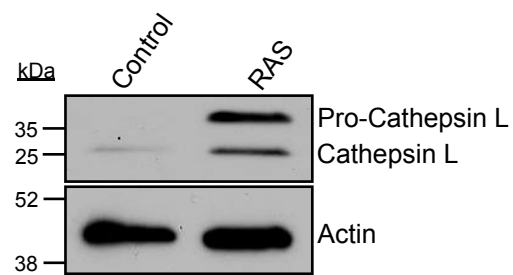
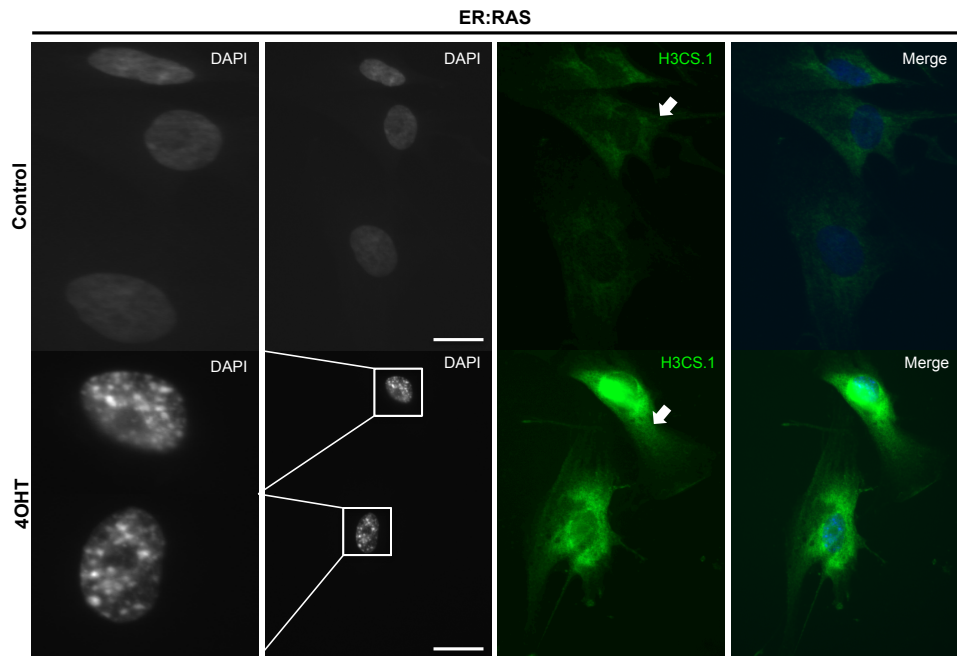


Figure 4.5 Cathepsin L, the enzyme responsible for H3 cleavage is upregulated in OIS. Whole cell lysates were harvested from control and RAS-induced senescent cells and analyzed by immunoblotting using anti-cathepsin L antibody. Electrophoresis was performed at 90-120V using 4-12% gradient SDS gel. Actin was used as loading control.

(A)



(B)

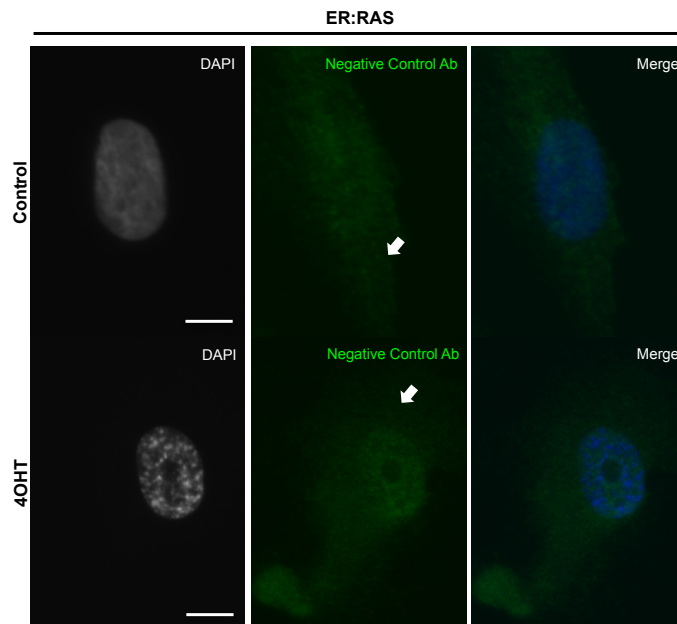


Figure 4.6 Cytoplasmic localization of histone H3CS.1 in OIS visualized by immunofluorescence. Control (uninduced) and 4OHT-induced senescent cells were stained using (A) anti-H3CS.1 antibody (raised in rabbit) along with (B) anti-Mouse IgG (raised in rabbit) as negative control. All images were taken at the same exposure under 60X objective.

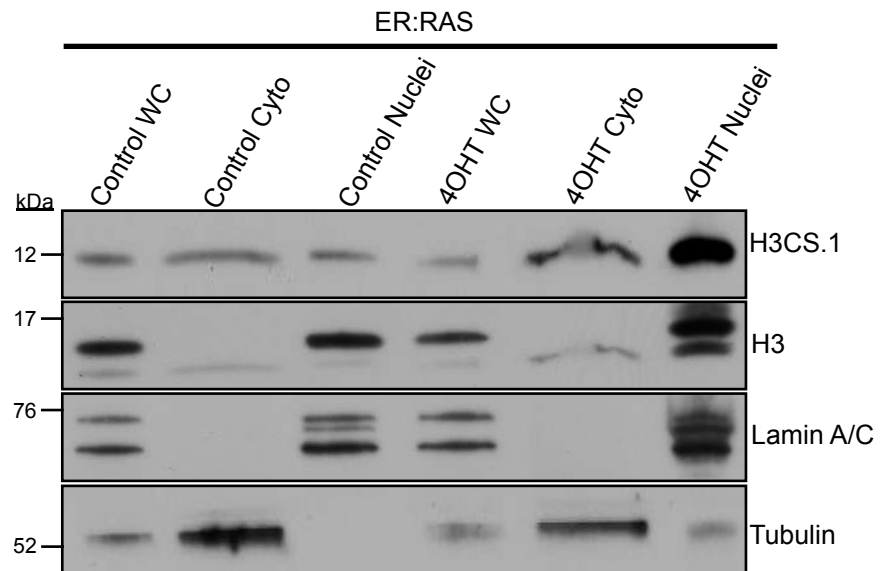


Figure 4.7 Cytoplasmic localization of histone H3CS.1 in OIS.

Cellular fractionation to separate nuclear and cytoplasmic fraction was performed according to the protocol in Materials and methods in section 2.2.14. Whole cell lysate (WC) was separated by SDS-PAGE electrophoresis at 90-120V using 4-12% gradient gel along with cytoplasmic (cyto) and nuclear (nuclei) fraction for control (uninduced) and 4OHT-induced ER:RAS senescent cells and blotted for H3CS.1 and H3, along with fractionation controls, lamin A/C for nuclear fraction and tubulin for cytoplasmic fraction.

senescent cells (4OHT-treated) in comparison to proliferating control (untreated) cells (Figure 4.6.A). Also DAPI staining depicted the formation of SAHF clearly in senescent cells. The negative control antibody detected marginal non-specific cytoplasmic staining but well below the signal observed using H3CS.1 antibody (Figure 4.6.B). This result shows not only the increase in H3CS.1 in senescent cells (as shown previously by Western blot), but also its cytoplasmic localization. The result was further validated by a subcellular fractionation experiment. Control (uninduced) and 4OHT-induced ER:RAS cells were harvested 9 days after 4OHT induction. Cells were subjected to subcellular fractionation to separate nuclear and cytoplasmic fractions. Three different types of cell fractions were analyzed by SDS-PAGE electrophoresis and Western blotting: whole cell lysate, cytoplasmic fraction, and nuclear fraction from both control and 4OHT-induced senescent cells. Membranes were probed using antibodies to H3CS.1 and H3 (Figure 4.7). Lamin A/C and tubulin blotting were also used as controls for nuclear and cytoplasmic fractions, respectively. Although histones are typically localized almost exclusively to the cell nucleus, these results indicated that H3CS.1 is remarkably localized to the cytoplasm of senescent cells.

### 4.3 Discussion

To dissect the potential role of H3CS.1 in the senescence programme, an inducible ER:RAS model system was established. Results indicated that the levels of H3CS.1 gradually increased with the induction of RAS leading to senescence.

Also the enzyme thought to be responsible for the mark, Cathepsin L, was elevated during senescence. Reports suggest that autophagy plays a key role during the induction of senescence [111, 116] and it was found that autophagy increases in senescent cells via negative feedback signalling and repression of the mTOR pathway [111]. Given the role of Cathepsin L in autophagy, it is tempting to speculate that elevated levels of the enzyme aid in trafficking of H3 through lysosomes/autophagosomes of senescent cells resulting in increased H3CS.1. A recent study has shown that Cathepsin L activity significantly increases with human ageing [480] and it is shown to be largely synthesized and secreted by various malignantly transformed cells [481]. Considering the implications senescence has as

a barrier to cancer and also a contributor to human ageing, the initial observations undoubtedly suggest that there may be an important role for Cathepsin L and its proteolytic cleavage of H3 in senescence.

Despite H3 being typically a nuclear protein, H3CS.1 was unusually found to have a cytoplasmic distribution in senescence. Part of this work contributed towards the paper published in the Journal of Cell Biology (Ivanov, Pawlikowski, Manoharan et al., 2013 [482]). This paper reported that senescent cells dissipate nuclear chromatin in the form of CCF (Cytoplasmic Chromatin Fragments) via a breakdown of nuclear envelope integrity and lysosomal/autophagic processing. This was supported by both *in vitro* & *in vivo* observations by demonstrating loss of total histone content in senescent cells [482]. Nuclear integrity is compromised in senescent cells leading to progressive loss of H3K27me3-enriched chromatin into the cytoplasm through a nuclear-cytoplasmic 'blebbing' process. This profound loss of histones is associated with decreased expression of nuclear membrane protein, lamin B1. Results suggest that histone loss in senescent cells is in part linked to lysosomal processing, perhaps via the action of Cathepsin L resulting in accumulation of H3CS.1 as an intermediate to histone degradation. Importantly, accumulation of H3CS.1 in senescent cells was suppressed by ATPase inhibitors, suggesting its possible dependence on lysosomal processing, although presence of this modified histone within lysosomes is as yet undetected.

Proteolytically cleaved H3 has been shown to contain a combination of both active and repressive chromatin marks [474, 483]. Using recombinant Cathepsin L that has comparable activity to its native protein it has been shown that methylation of H3 on K27 and acetylation of K18 increases cleavage, whereas K23 acetylation reduces it. Hence, it is plausible that Cathepsin L and its substrate H3CS.1 may play an important role in senescence by regulating the distribution of euchromatic and heterochromatic marks across the genome altering the gene expression pattern. Clearly this warrants additional studies to learn how this histone mark might be contributing towards regulation of senescence and perhaps its associated effects on tissue ageing and/or cancer.

## **5. H4R3<sub>ME2A</sub> IN CELLULAR SENESENCE**

## 5 H4R3ME2A IN CELLULAR SENEESCENCE

---

### 5.1 Introduction

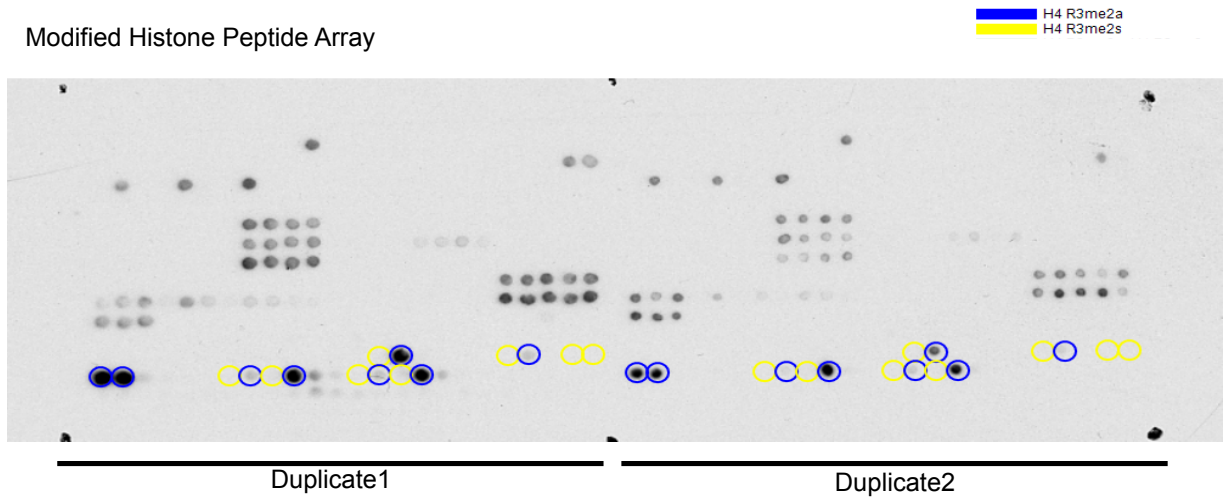
One of the most important post-translational modifications in eukaryotes is protein arginine methylation. However, this is an understudied modification in comparison to lysine methylation that has a well-documented role in epigenetic gene regulation [319, 484, 485]. Arginine can be methylated once (monomethylation) or twice (dimethylation), in the latter case with either one methyl group on each of the two nitrogen atoms (symmetric methylation) or both methyl groups on one terminal nitrogen (asymmetric methylation). Such histone marks can either be transcription activating or repressive depending on location and context [486]. From the histone modification screen, H4R3me2a (asymmetric modification) was found to be elevated in replicative senescence and later in oncogene-induced senescence. H4R3me2a is classically associated with facilitating a state of active chromatin [319, 487] and is also noted to play a critical role in the prevention of heterochromatic marks [488]. However, the physiological role of H4R3me2a in senescent cells and its involvement in human disease is not well understood. In this chapter, I will investigate the regulation and function of H4Rme2a in cell senescence, with a view to understanding its potential contribution to senescence-mediated tumor suppression and/or tissue ageing.

### 5.2 Results

#### *5.2.1 Validation of H4R3me2a antibody specificity*

Prior to further investigation of the role of H4R3m2a in senescence, it was important to validate specificity of the antibody used in the screen. The only commercially available antibody to this mark was from Active Motif. It was essential to test if the antibody has any cross reactivity to other histone modifications. The H4R3me2a antibody raised in rabbit was tested for specificity using a MODified histone peptide array from the same company. The array contains 59 acetylation, methylation, phosphorylation, and citrullination modifications on the N-terminal tails of histones H3,

(A)



(B)

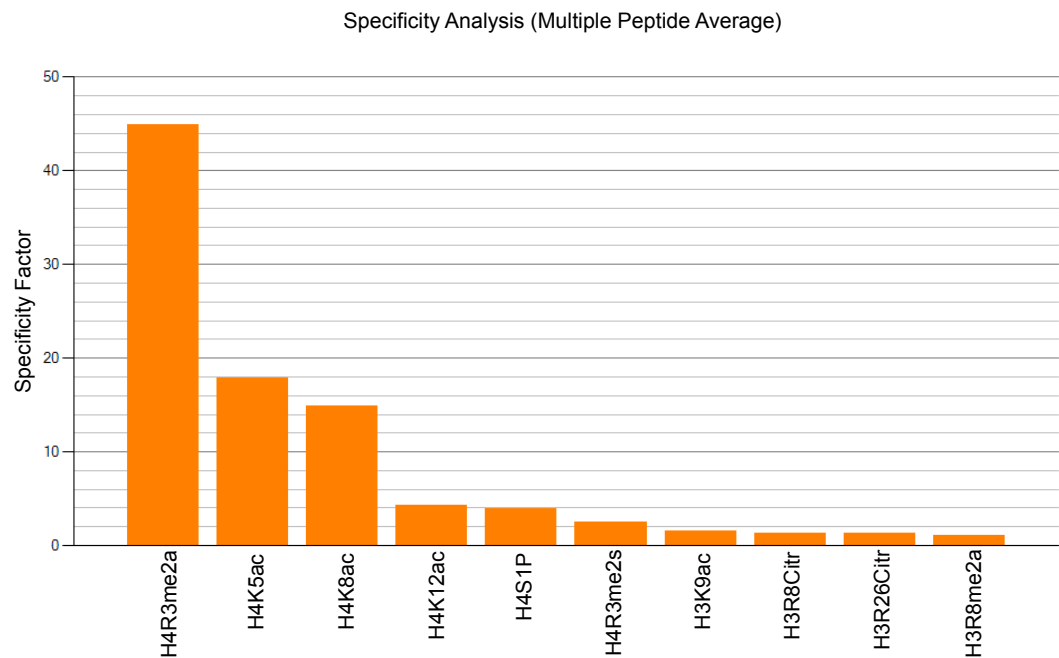


Figure 5.1 Specificity of H4R3me2a antibody assessed using MODified Peptide Array Analysis. H4R3me2a antibody was evaluated using Active Motif's Peptide Array. (A) ECL images of the array shown in duplicate. Blue circles represent antibody reactivity to H4R3me2a and yellow circles represent reactivity to symmetric version of the modification, H4R3me2s, observed along with other spot intensities corresponding to different histone modifications. (B) Based on the array, specificity factors were calculated for the antibody using the Array Analyse Software to check for any cross reactivity with other modifications. The specificity factor was calculated from the average intensity of all spots containing the mark divided by the average intensity of all spots not containing the mark.

H4, H2A and H2B. Each array holds 384 unique histone modification combinations (spotted in duplicates), hence offering extensive coverage. Figure 5.1.A shows spot intensities on the array after ECL detection. The antibody to H4R3me2a is largely specific for the intended modification, as denoted by the blue circles. Yellow circles denote some cross-reactivity to the symmetric version of the same modification (H4R3me2s). Other spot intensities observed denote cross reactivity to different histone modifications. Using Array Analyse Software, a spot densitometry programme was applied in order to measure relative intensity of each peptide quantitatively. Graphical analysis of the specificity was generated (Figure 5.1.B) by calculating average intensity of all spots containing the mark divided by the average intensity of all spots not containing the mark. Results indicated that although the H4R3me2a antibody showed substantial preference for the intended mark, some cross reactivity to histone modifications H4K5ac and H4K8ac was observed. Other potential cross-reactions as observed by the quantification were largely negligible, especially to H4R3me2s.

### *5.2.2 Increase in H4R3me2a in senescence confirmed by a second antibody*

Although the antibody tested to be quite specific, having a second antibody to the same modification would better confirm the increase in H4R3me2a in senescence and be an invaluable tool for downstream analysis. At the time of study there were published papers [489-491] using a different antibody to H4R3me2a (Millipore 07-213) that was commercially available, but the antibody was discontinued by the company. At this time, Dr. Suming Huang from University of Florida kindly agreed to donate a sample of their in-house antibody to H4R3me2a. I set out to test if the second antibody could detect the increase in H4R3me2a in senescence by harvesting whole cell lysates from control and RAS-expressing senescent cells. Lysates were subjected to fractionation using SDS-PAGE and blotted for H4R3me2a, using the antibody from Huang's lab and total histone H3 as a loading control (Figure 5.2). Results confirmed an increase of H4R3me2a in senescent cells, with the pre-immune bleed from the same rabbit serving as a negative control in Western blot. This, along with results from the peptide array, provided substantial evidence of a specific change in H4R3me2a in the senescence programme and provided strong rationale for further experiments to understand potential functional and regulatory role of H4R3me2a in

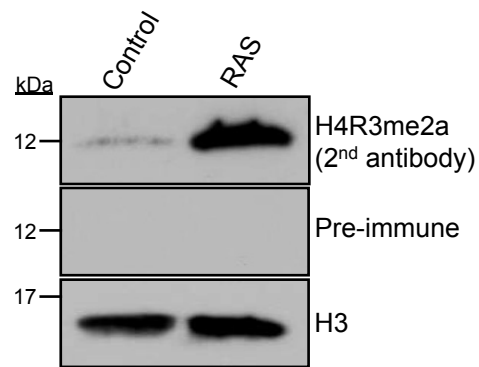


Figure 5.2 Increase in H4R3me2a as confirmed by a second antibody to H4R3me2a. Whole cell lysates were harvested from control and RAS-induced senescent cells and analyzed by SDS-PAGE electrophoresis at 90-120V using 15% gel. Immunoblotting was performed using a second antibody to H4R3me2a donated by Dr. Suming Huang. Pre-immune bleed was also tested as negative control along with H3 as a loading control.

senescence.

### *5.2.3 H4R3me2a abundance gradually increases after induction of RAS*

The establishment of an inducible system of senescence was explained in Chapter 4 Section 4.2.2. To understand how H4R3me2a might be regulated in senescence, whole cell lysates from ER:RAS cells were harvested from the following time points after induction with 100 nM 4OHT: day 0 (control), day 2, day 4, day 7, and day 9. Following fractionation by SDS-PAGE, lysates were blotted for H4R3me2a and total histone H3. Levels of H4R3me2a gradually increased after induction of RAS (Figure 5.3). A striking increase in H4R3me2a abundance was found, especially from day 4 of induction indicating increase in pre-senescent cells. It is therefore tempting to suggest that increase in the histone mark may promote senescence as increase occurs prior to onset of senescence.

### *5.2.4 Regulation of H4R3me2a in cellular senescence*

#### *5.2.4.1 Increase in H4R3me2a in OIS is not inhibited by expression of SV40 LT Antigen*

pRB and p53 tumor suppressive pathways are key players in the regulation of senescence. Senescence is abolished if these two pathways are inactivated in human or mouse cells [9, 51, 427]. In order to test if these two pathways are required for elevated levels of H4R3me2a in senescence, IMR90 cells were transduced with SV40-LTA<sub>g</sub> (Simian Virus 40 Large T Antigen). SV40LTA<sub>g</sub> is known to bind to p53 and pRB thereby inactivating them [492]. IMR90 cells were transduced using retrovirus encoding SV40LTA<sub>g</sub> in comparison to control cells (Ctrl1) (Figure 5.4). Plasmids used in this section and their given names are outlined in Table 5.1. SV40LTA<sub>g</sub>-expressing cells showed no phenotypic differences and remained long and spindly (Figure 5.5.A). Ctrl1 and SV40LTA<sub>g</sub> cells were then infected with RAS virus or the appropriate control virus (Ctrl2). Subsequently, bright field images of the cells were taken 9 days after infection and drug selection. As expected, RAS-infected cells acquired a typical enlarged, flattened senescent morphology both in parental and control cells (Figure 5.5.A,B). Unexpectedly, SV40LTA<sub>g</sub> cells transduced with RAS also acquired a phenotype similar to Ctrl1+RAS cells. This may mean that

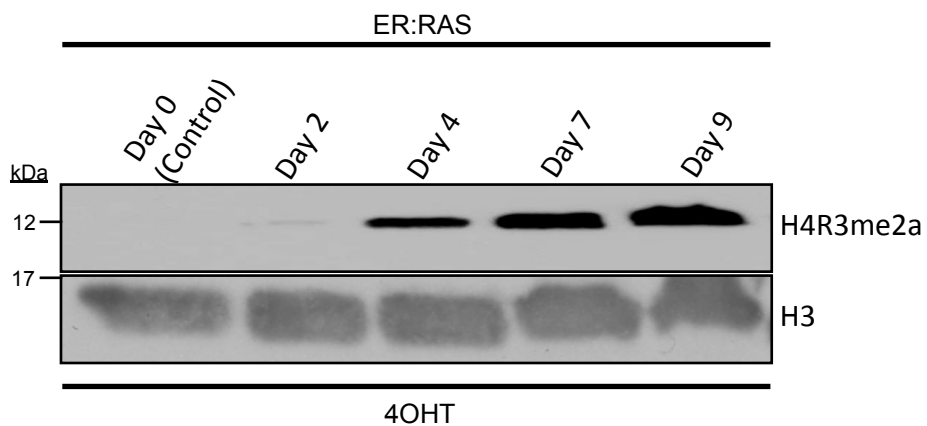


Figure 5.3 Gradual increase in H4R3me2a abundance after induction of RAS.

4OHT-activated ER:RAS cells were harvested at time points from day 0 of induction to day 9 of induction. Whole cell lysates were harvested from all time points and analyzed by Western blot for levels of H4R3me2a along with total H3 as loading control. SDS-PAGE electrophoresis was performed at 90-120V using 15% gel. It is to be noted that the same gel was used to assay H3CS.1 abundance in Chapter 4.

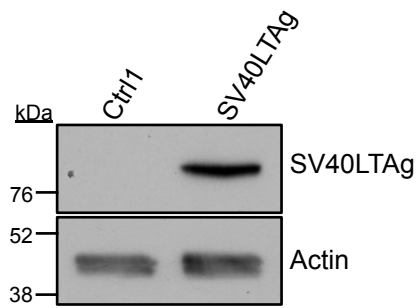


Figure 5.4 Overexpression of SV40LTA in IMR90.

Whole cell lysates were harvested from Ctrl1 and SV40LTA cells 5 days after drug selection of the infected cells. Lysates were fractionated using SDS-PAGE electrophoresis at 90-120V using 12% gel and Western blotted using an antibody to SV40LTA. Actin was used as loading control.

<b>Plasmids</b>	<b>Virus Name</b>
pBABE-neo	Ctrl1
pBABE-neo-SV40LTA <sub>g</sub>	SV40LTA <sub>g</sub>
pBABE-puro	Ctrl2
pBABE-puro-H-RASG12V	RAS

Table 5.1 The plasmids used in the study along with the given virus name.

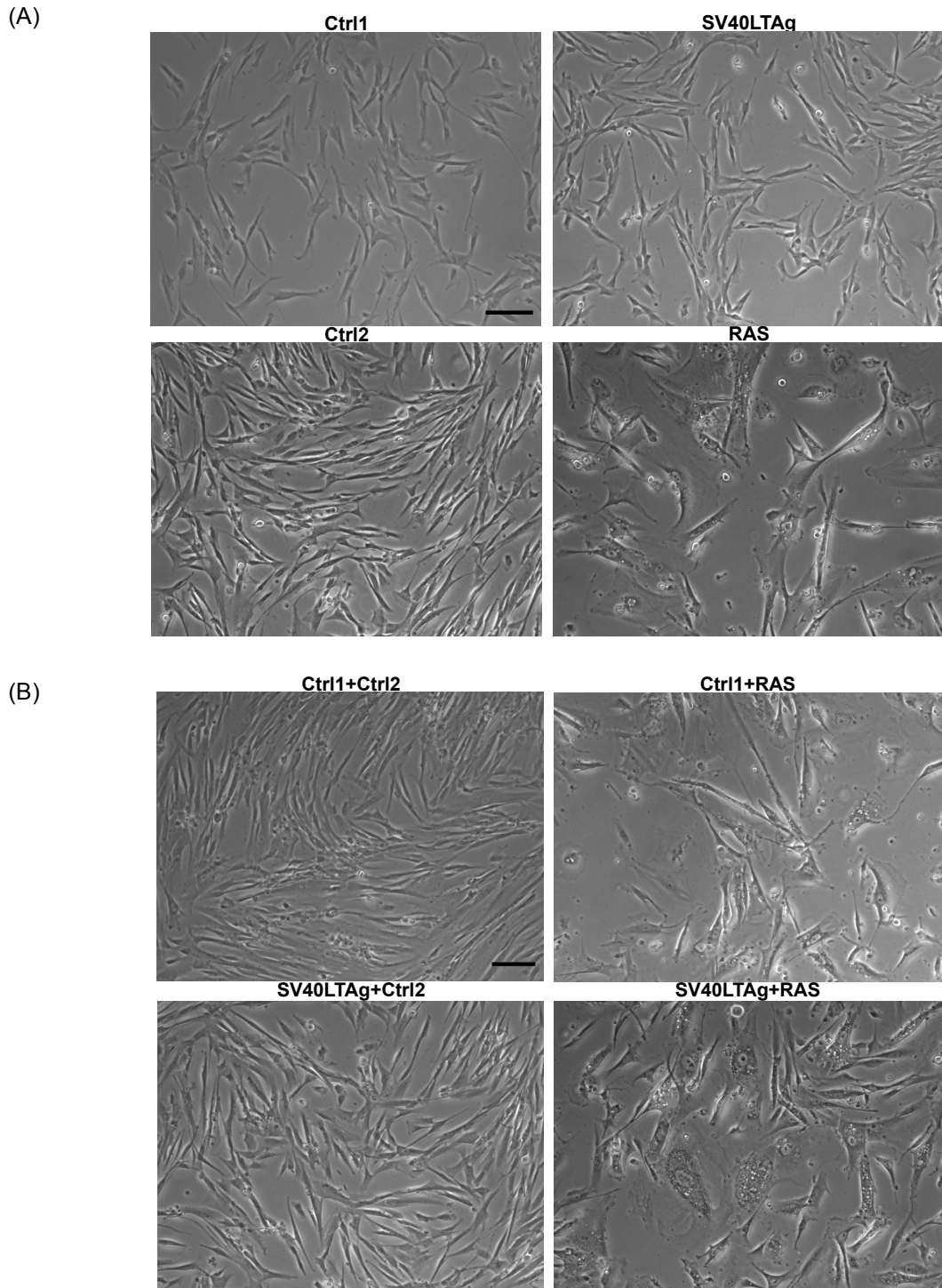


Figure 5.5 Control and SV40LTA<sub>g</sub> transduced cells co-infected with RAS virus.

(A) Bright field images (under 20X objective) were taken of SV40LTA<sub>g</sub> and RAS-infected IMR90 along with their respective controls following drug selection. (B) Further double infections were performed on control and SV40LTA<sub>g</sub> cells with Ctrl2 and RAS virus. Images under 20X objective were collected using bright field microscopy 9 days after puromycin selection.

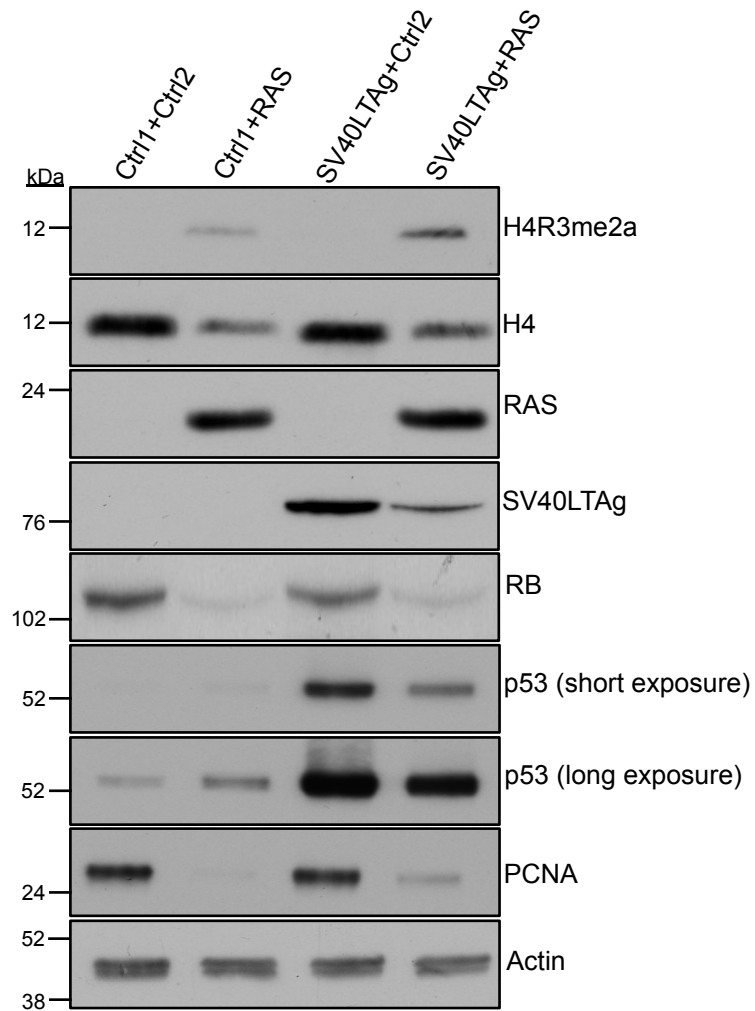


Figure 5.6 Increase in H4R3me2a in OIS is not inhibited by expression of SV40LTAg. Double infections were performed on Ctrl1 and SV40LTAg cells with Ctrl2 and RAS virus. Whole cell lysates were harvested from these cells along with the former for separation by SDS-PAGE electrophoresis at 90-120V using 4-12% gradient gel and Western blotted for a panel of different markers of proliferation (PCNA) and senescence (RB, p53), along with H4R3me2a.

SV40LTA<sub>g</sub> was not sufficiently expressed for the cells to bypass senescence. In order to provide a more quantitative analysis, whole cell lysates were harvested from the cells at the same time as the images were taken. Protein lysate was fractionated using SDS-PAGE and Western blotted. Results confirmed SV40LTA<sub>g</sub> expression along with RAS (Figure 5.6), when using actin as loading control. Loss of RB, reflecting down regulation in senescent cells [171, 493, 494], was noted not only in RAS-infected senescent cells but also in SV40LTA<sub>g</sub>+RAS cells, suggesting that SV40LTA<sub>g</sub> failed to bypass senescence. Also loss of PCNA, a cell cycle marker and E2F target gene, was noted in SV40LTA<sub>g</sub>+RAS cells similar to that of RAS-only senescent cells. This also suggests that SV40LTA<sub>g</sub> failed to efficiently inactivate pRB. The level of H4R3me2a was increased in RAS-expressing cells ectopically expressing SV40LTA<sub>g</sub> in comparison to cells expressing SV40LTA<sub>g</sub> only. I conclude that expression of SV40LTA<sub>g</sub> did not prevent upregulation of H4R3me2a; unfortunately, because of the apparent failure of SV40LTA<sub>g</sub> to fully inactivate pRB (and p53) I cannot conclude as to whether pRB and p53 are required for upregulation of H4R3me2a.

#### *5.2.4.2 Expression of PRMT1 is elevated in senescent cells*

PRMTs (Protein Arginine Methyl Transferase) comprise a family of proteins that contain nine members in humans, which methylate histones, other nuclear proteins and non-histone proteins on arginine residues [495, 496]. Methylation involves the transfer of a methyl group from SAM (S-adenosylmethionine) to arginine at terminal guanidine nitrogens [487, 497]. Type I enzymes generate mono-methyl arginine (MMA) and asymmetric dimethyl arginine (aDMA) and type II class enzymes catalyze the formation of MMA and symmetric dimethyl arginine (sDMA) [498-500]. Type I enzyme PRMT1 catalyzes deposition of asymmetric methylation on R3 of H4 [501] and accounts for more than 85% of all arginine methylation in human cells [502]. Given that H4R3me2a increases in senescence, it was interesting to ask whether PRMT1 also increases in senescence. Whole cell lysates from both RS and OIS model systems, tested previously for markers of proliferation arrest (Figure 3.2, 3.6), were blotted with the Cell Signaling antibody to PRMT1. Interestingly, PRMT1 showed elevated expression levels in both model systems based on using actin as a

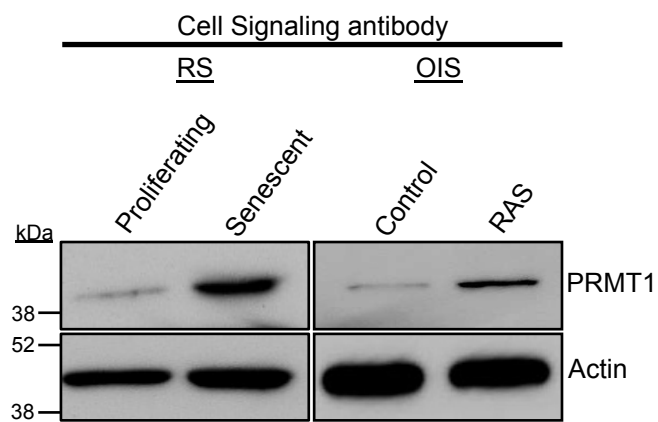


Figure 5.7 Expression of PRMT1 is elevated in senescent cells.

Whole cell lysates were harvested from both models of senescence, RS and OIS. For RS, cells were harvested 2 weeks after the last population doubling. For OIS, cells were harvested 9 days post control and RAS infections and drug selection. Lysates were separated by SDS-PAGE electrophoresis at 90-120V using 12% gel and Western blotted for PRMT1 using actin as loading control.

loading control (Figure 5.7).

To better understand the role of altered PRMT1 and H4R3me2a levels during senescence, and perhaps their effect on cancer, further experiments were performed to KD PRMT1.

#### 5.2.4.3 *Generating IMR90 cells with constitutive KD of PRMT1*

Next, I set out to ask if the increase in PRMT1 is the cause of increase in H4R3me2a in senescence. Thermo Scientific™ TRC Lentiviral™ shRNAs to PRMT1 were purchased. An initial screen of five lentivirus-encoded shRNAs for KD of PRMT1 was performed. HEK-293T cells were used for efficient virus packaging, as described in the Material and Methods (Section 2.2.9). IMR90 cells were infected with different doses of virus delivering the different shRNAs for PRMT1 KD, along with a control virus. Whole cell lysates were harvested three days post puromycin selection and separated by SDS-PAGE. Proteins were Western blotted using a PRMT1 antibody from Abcam. Out of the five short hairpins, shPRMT1(1), shPRMT1(2) and shPRMT1(3) effectively knocked down PRMT1 in comparison to the control as denoted by the arrow mark in Figure 5.8. The antibody also recognized a slightly faster migrating band that remained largely unaffected by the short hairpins. It is to be noted that at the time of this experiment, the PRMT1 antibody from Cell Signaling, used in Figure 5.7, was not available. With the help of the screen, three short hairpins to effectively perform PRMT1 KD studies were identified.

To confirm the identity of the polypeptide labeled as PRMT1 and its requirement for H4R3me2a, this experiment was repeated, but the Western blot was probed with two newly available antibodies to PRMT1. Proliferating IMR90 were infected with a range of viral titres from 1 µl to 16 µl for all three hairpins including the control. PRMT1 KD cells appeared impaired in their cell division compared to control cells in the following order: shPRMT1(3) > shPRMT1(1) > shPRMT1(2). Whole cell lysates were subjected to fractionation and Western blotted (Figure 5.9) using two new antibodies to PRMT1, one obtained from Cell Signaling and the second from Millipore, and an antibody to H4R3me2a. Both of the PRMT1 antibodies confirmed that all 3 shRNAs at least partially knocked down PRMT1 and concurrently suppressed H4R3me2a.

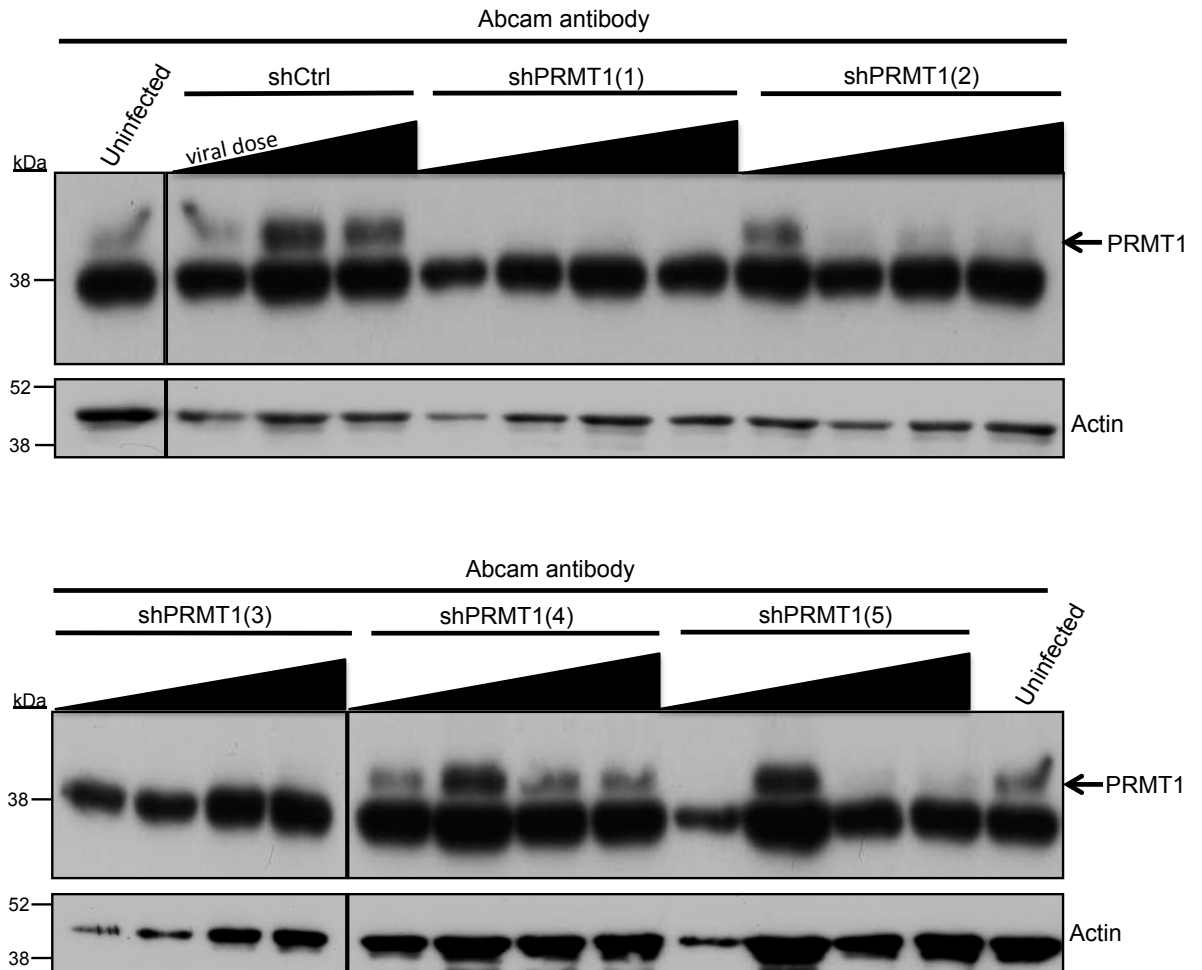


Figure 5.8 Generating IMR90 cells with constitutive KD of the enzyme PRMT1.

IMR90 cells were infected with increasing viral dose of five different short hairpins to PRMT1 along with control. Whole cell lysates were harvested 3 days after drug selection with puromycin, along with uninfected parental cells, and separated by SDS-PAGE electrophoresis at 90-120V using 12% gel and Western blotted for PRMT1. Actin was used as loading control.

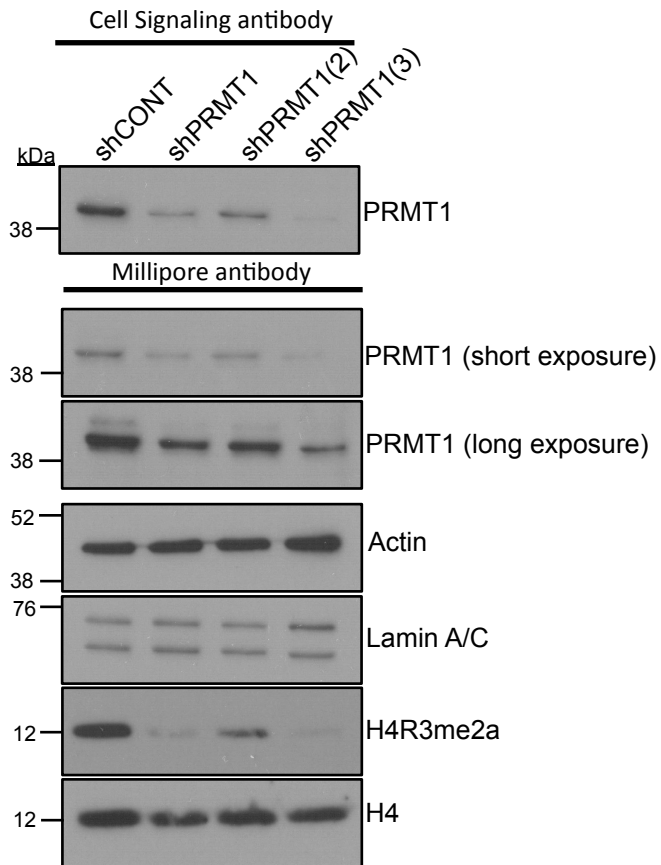


Figure 5.9 Confirmation of PRMT1 KD in biological replicates with new antibodies.

Whole cell lysates from IMR90 infected with shCONT, shPRMT(1), shPRMT1(2), shPRMT1(3) constructs were obtained 4 days after drug selection with puromycin. Lysates were separated by SDS-PAGE and Western blotted for PRMT1 using two different antibodies from Cell Signaling and Millipore. PRMT1 blots were stripped and reprobred with the same membrane. Actin and Lamin A/C were used as loading controls. Lysates were also blotted for H4R3me2a using total H4 as loading control.

#### 5.2.4.4 *PRMT1 is a pre-requisite for increased H4R3me2a in senescent cells*

In order to understand the functional role of PRMT1-mediated H4R3me2a in senescence, it was necessary to establish senescent cells lacking PRMT1. To do this, RAS was overexpressed in PRMT1 KD cells. shCONT, shPRMT1(1) and shPRMT1(3) cells were infected with control (labelled Ctrl2) or RAS virus encoding neomycin resistance. Whole cell lysates were harvested from cells 9 days after RAS infection and protein was subjected to fractionation. Western blotting was performed using the Abcam PRMT1 antibody along with actin as loading control. Also abundance of H4R3me2a was determined (Figure 5.10). Despite overexpression of RAS to induce senescence, PRMT1 KD cells failed to upregulate H4R3me2a in comparison to control cells induced with Ras. This experiment showed that expression of PRMT1 is required for increased H4R3me2a in senescent cells.

To investigate the consequence of PRMT1 KD on RAS-induced senescence, this experiment was repeated with a view to analysing senescence markers. Phenotypic changes were observed following the introduction of RAS into shCONT cells as expected, but this was more pronounced in severity in PRMT1 KD cells, especially in cells containing the shPRMT1(3) construct. The associated KD phenotype was also apparent to a certain degree in shPRMT1(3) cells infected with Ctrl2 virus, suggesting that it is primarily a result of loss of PRMT1. For further analysis, whole cell lysates were harvested 9 days after drug selection and subjected to SDS-PAGE and Western blotting. As expected induction of RAS in shCONT cells showed elevated levels of PRMT1 based on actin as loading control (Figure 5.11). Also as previously noted shPRMT1(3) cells show the highest degree of KD for PRMT1 and shPRMT1(1) and shPRMT1(2) exhibited moderate levels of KD for PRMT1. Expression of activated RAS failed to induce PRMT1 in KD cells in comparison to shCONT cells. As expected, RAS-induced senescence failed to induce H4R3me2a levels in PRMT1 KD cells, especially in shPRMT1(3) cells. These results confirmed that increased PRMT1 is indispensable for induction of H4R3me2a in

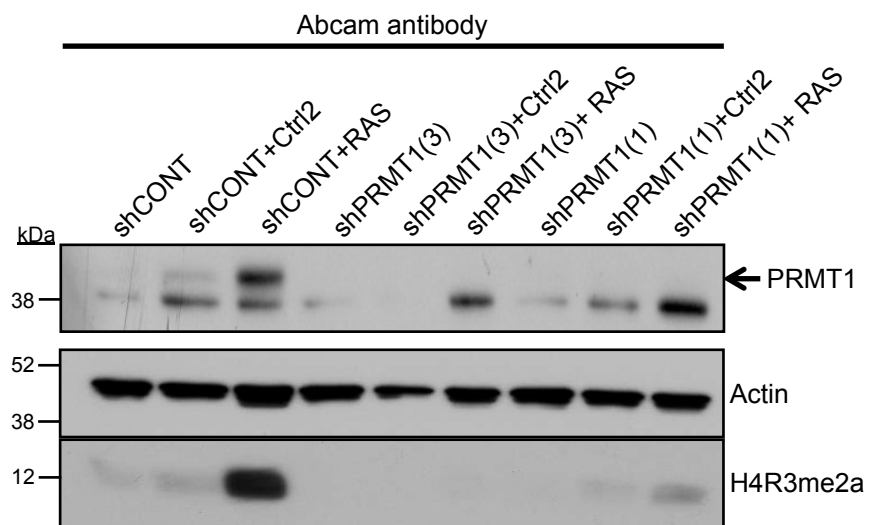


Figure 5.10 Generation of PRMT1 KD cells with activated RAS. Cells containing shCONT, shPRMT1(1), shPRMT1(3) constructs (puromycin resistant) were infected for a second time with control (Ctrl2) or RAS virus encoding neomycin resistance. Whole cell lysates were harvested 9 days post drug selection following infection and separated using SDS-PAGE. Lysates were Western blotted for PRMT1, with actin as the loading control and H4R3me2a.

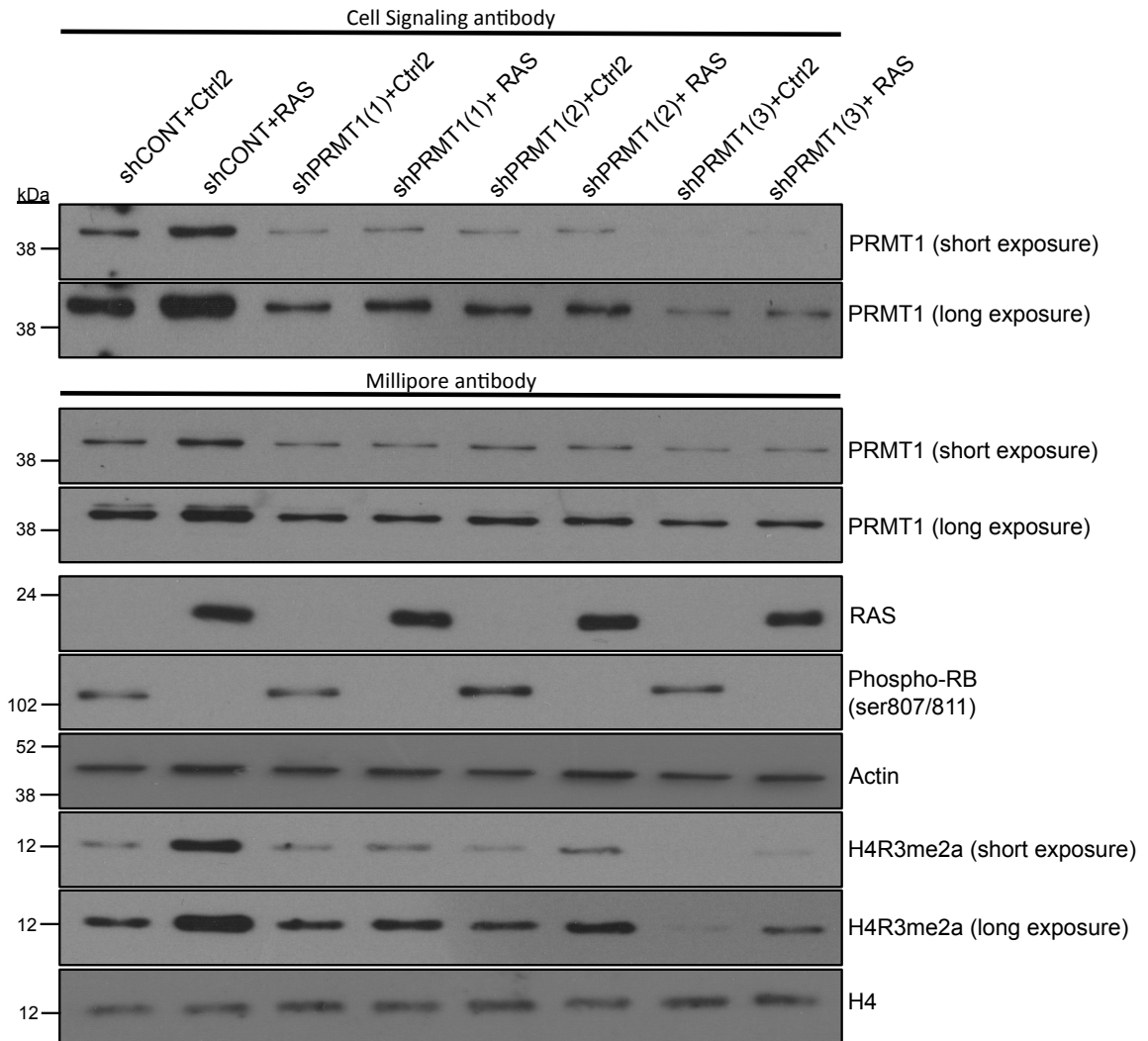


Figure 5.11 PRMT1 is required for induction of H4R3me2a in senescence.

shCONT, shPRMT(1), shPRMT1(2), shPRMT1(3) cells were infected with control (Ctrl2) and RAS virus, followed by drug selected with neomycin. Whole cell lysates were obtained 9 days post infection and separated by SDS-PAGE and Western blotted for the following proteins: PRMT1 (Cell Signaling-antibody 2), PRMT1 (Millipore-antibody 3), RAS and phospho-Rb to serine 807/811. Actin was used as loading control. Lysates were also blotted for H4R3me2a using total H4 as loading control.

cellular senescence. Lysates were also blotted for phosphorylation of pRB at serines 807/811 and were found to have reduced phosphorylation in all RAS-infected senescent cells containing control or PRMT1 hairpins, indicating comparable onset of senescence. Unfortunately, due to toxicity of PRMT1 KD, especially together with activated RAS, I was unable to perform further downstream analysis. Regardless, these results show that PRMT1 is required for induction of H4R3me2a in cellular senescence.

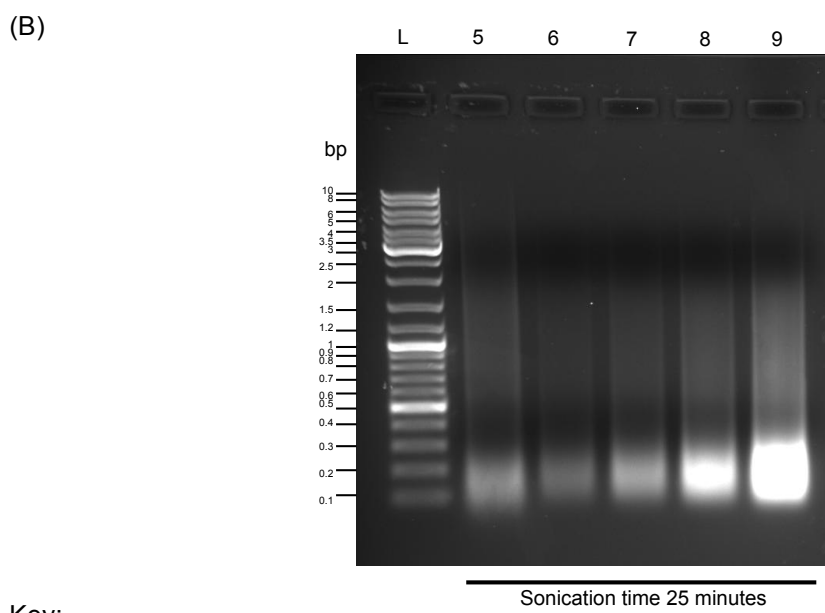
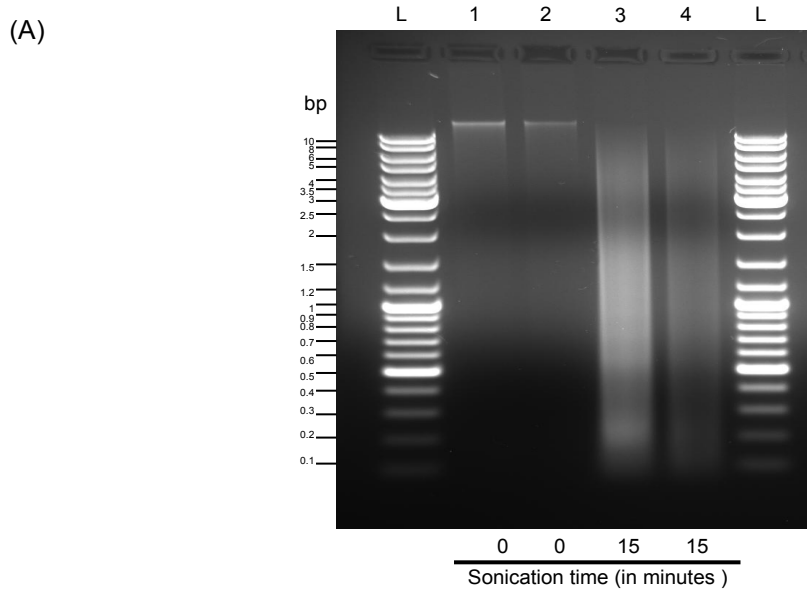
### *5.2.5 Global distribution of H4R3me2a in senescence*

In order to understand how senescence might be regulated by PRMT1 and H4R3me2a, ChIP-sequencing was employed to analyse the global distribution of H4R3me2a in OIS and dividing cells.

#### *5.2.5.1 Optimization of ChIP-seq conditions*

ChIP was originally described in 1988 and comprises four main steps to study protein-DNA interactions [503]. The first step is cross-linking of protein and DNA in cells using a cross-linker, typically formaldehyde. Secondly the DNA-protein complex formed (chromatin) is sheared by sonication. During sonication, high frequency sound waves from the Bioruptor break up the DNA. The third step uses an antibody directed against the protein of interest to co-immunoprecipitate protein-bound DNA complexes. The fourth step reverses the crosslinking of the protein-DNA complexes recovered by IP, and the DNA recovered is analysed to identify sequences bound by the protein in question. ChIP-PCR is essentially chromatin IP DNA preparation followed by real-time PCR analysis.

Alternatively, ChIP-seq differs from ChIP-PCR by analysing DNA sequences by massively parallel sequencing to reliably identify binding sites of the target protein across the genome. The reads generated after library construction are aligned uniquely to the human genome. ChIP-seq reads are analysed according to protocol outlined in Materials and Methods Section 2.2.17. Successful ChIP-seq depends on several optimization steps, including chromatin shearing, antibody validation with appropriate controls, optimized ChIP DNA purification followed by library preparation [504]. Sonication with SDS in buffers improves efficiency of the ChIP by exposing epitopes for efficient antibody binding and perhaps aiding in the sonication itself [504].



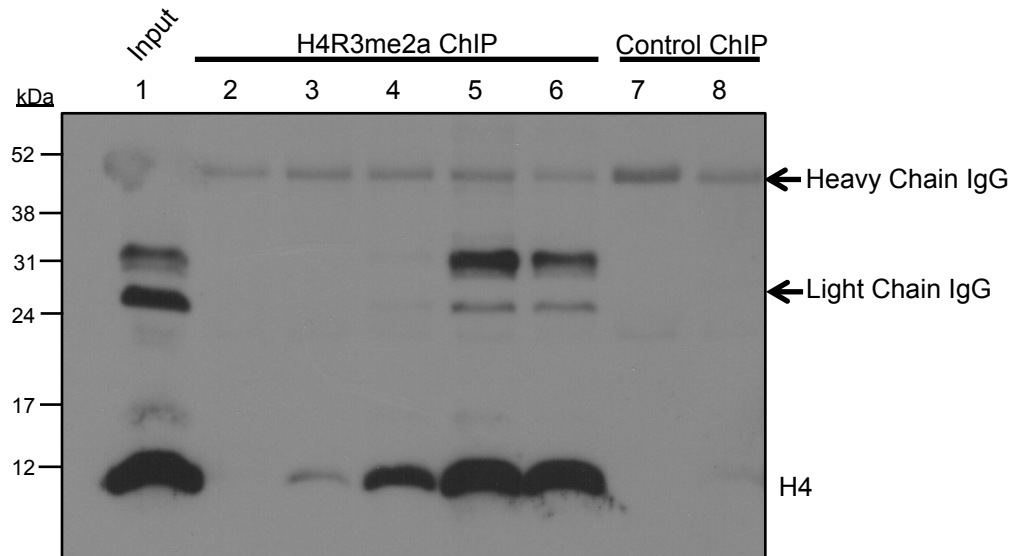
- Key:
- L- Ladder
  - 1- Unsonicated DNA Proliferating (5  $\mu$ l)
  - 2- Unsonicated DNA Senescent (5  $\mu$ l)
  - 3- Sonicated DNA Proliferating (5  $\mu$ l)
  - 4- Sonicated DNA Senescent (5  $\mu$ l)
  - 5- Sonicated DNA Proliferating (5  $\mu$ l)
  - 6- Sonicated DNA Senescent (5  $\mu$ l)
  - 7- Sonicated DNA Senescent (10  $\mu$ l)
  - 8- Sonicated DNA Senescent (15  $\mu$ l)
  - 9- Sonicated DNA Senescent (20  $\mu$ l)

Figure 5.12 Optimization of sonication conditions in proliferating and senescent cells.  
 (A) Chromatin prepared from proliferating and senescent IMR90 cells were sonicated for 15 min and the extent of fragmentation was determined following purification and separation on a 1% TAE agarose gel. (B) Chromatin from proliferating and senescent cells was subjected to a further 10 min (total 25 min) of sonication and resolved on an agarose gel.

However, SDS also can be disruptive in further steps, especially during immunoprecipitation as it hinders antibody-antigen interactions. For ChIP-seq, the optimum DNA size range is between 150 and 300 bp. DNA fragments within this size range are equivalent to mono- and dinucleosome chromatin fragments, which provides high resolution for next generation sequencing platforms.

The first critical step was to optimize sonication conditions for chromatin. Proliferating and senescent IMR90 cells were cross-linked using formaldehyde. Chromatin was prepared by sonication. Unsonicated and sonicated DNA from proliferating and senescent cells were separated on a 1% agarose gel. Figure 5.12.A indicates that although sheared DNA was observed in the sonicated samples (lane 3, 4) in comparison to unsonicated DNA (lane 1, 2), most of the DNA fragments remained large in size (>1kb). Hence, proliferating and senescent chromatin were subjected to a further 10 min sonication. Results showed that after 25 min of sonication the chromatin was sheared to the expected size range of 150-300 bp (Figure 5.12.B). Henceforth, sonication was performed for 25 minutes, as described in Materials and Methods Section 2.2.15.

The next step was to test the performance of the H4R3me2a antibody under routine ChIP conditions. Although the H4R3me2a antibody was tested for its specificity and shown to work for Western blotting, it was essential to confirm IP performance of the antibody under ChIP conditions. ChIP by the H4R3me2a antibody was tested under different stringency conditions, which included three main variables: concentration of SDS in ChIP buffer (diluted after sonication from 1% (w/v) SDS to either 0.25% (w/v) or 0.1% (w/v) SDS), quantity of antibody (2  $\mu$ g, 6  $\mu$ g or 10  $\mu$ g) and inclusion or exclusion of a stringent wash buffer containing 250mM LiCl. Chromatin extracted from senescent cells was subjected to ChIP under these conditions. After washes, ChIP samples were heated in Laemmli sample buffer at 97°C, fractionated by SDS-PAGE and Western blotted using an antibody to total H4 (Figure 5.13). Using 2  $\mu$ g of H4R3me2a antibody with 0.25% (w/v) SDS and LiCl wash did not precipitate any H4 (Figure 5.13, lane 2). Increasing the antibody up to 6  $\mu$ g and excluding the LiCl wash at the same concentration of SDS precipitated H4 moderately (lane 3). Reducing the SDS concentration to 0.1% (w/v) and using 6  $\mu$ g of antibody with the LiCl wash (lane 4), 10  $\mu$ g antibody without LiCl wash (lane 5) or 2  $\mu$ g antibody without the LiCl wash (lane 6) precipitated increasing histone H4, respectively. Using either 2



Key:

- 1) Input chromatin
- 2) 0.25% (w/v) SDS, 2 $\mu$ g H4R3me2a ab, LiCl wash
- 3) 0.25% (w/v) SDS, 6 $\mu$ g H4R3me2a ab, No LiCl wash
- 4) 0.1% (w/v) SDS, 6 $\mu$ g H4R3me2a ab, LiCl wash
- 5) 0.1% (w/v) SDS, 10 $\mu$ g H4R3me2a ab, No LiCl wash
- 6) 0.1% (w/v) SDS, 2 $\mu$ g H4R3me2a ab, No LiCl wash
- 7) 0.1% (w/v) SDS, 10 $\mu$ g Rabbit IgG (M7023) ab, LiCl wash
- 8) 0.25% (w/v) SDS, 6 $\mu$ g Rabbit IgG (M7023) ab, No LiCl wash

Figure 5.13 Optimization of H4R3me2a ChIP conditions.

Sonicated chromatin from senescent cells was subjected to ChIP under varying conditions as per key using H4R3me2a antibody (lanes 2 – 6) and control IgG raised in rabbit, M7023 (lane 7,8). ChIP samples were harvested to make protein lysates, subjected to separation using SDS-PAGE electrophoresis at 90-120V using 4-12% gradient gel and Western blotted using H4 antibody.

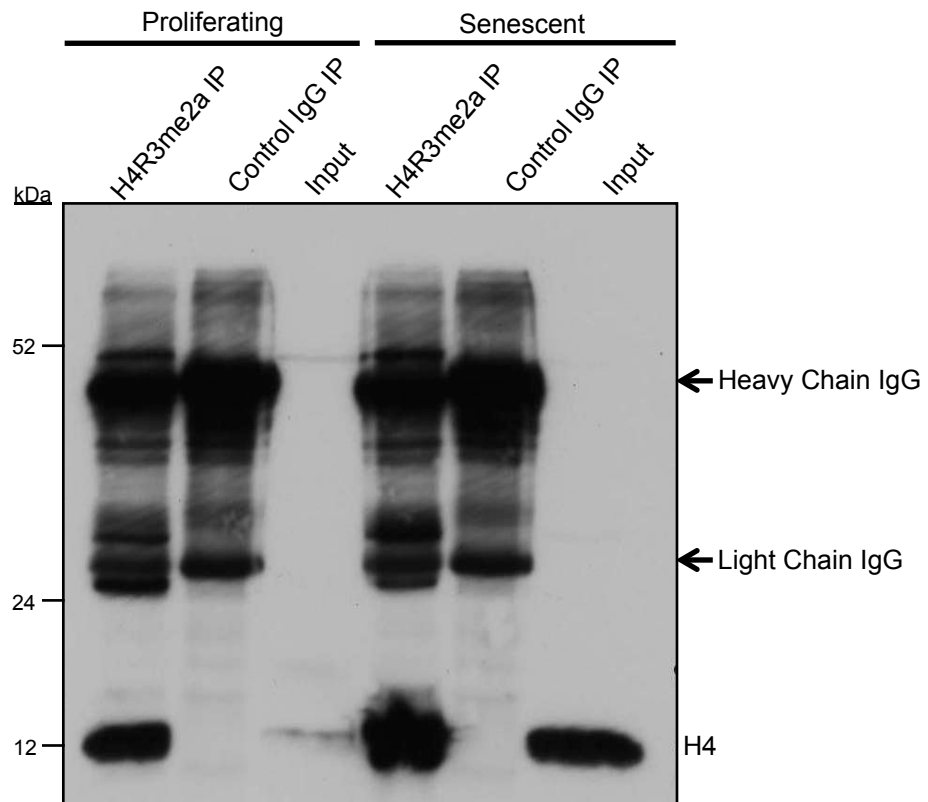


Figure 5.14 H4R3me2a ChIP in proliferating and senescent cells.

Chromatin from proliferating and senescent cells was subjected to ChIP using H4R3me2a antibody and control rabbit IgG (M7023). Along with Input, protein from ChIP samples was subjected to separation using SDS-PAGE and Western blotted using H4 antibody.

µg or 10 µg of H4R3me2a antibody per ChIP without the LiCl wash and 0.1% (w/v) SDS precipitated comparable H4 to the input. Negative control IgG did not precipitate any histone (lane 7, 8). From this, the optimal conditions for H4R3me2a ChIP was determined to employ 2 µg antibody in the presence of 0.1% (w/v) SDS followed by no LiCl wash.

The next step was to perform H4R3me2a ChIP in proliferating and senescent cells and proceed to library preparation for sequencing. Chromatin from both proliferating and senescent cells was subjected to ChIP (in duplicates), using the above-mentioned conditions with H4R3me2a or H4 or control antibody. 500 µg of chromatin prepared from proliferating and senescent cells was subjected to overnight ChIP. One half of the sample was analyzed by Western blot with histone H4 antibody. This confirmed H4R3me2a ChIP, as visualized by H4 blotting in comparison to input (Figure 5.14). The second half of the sample was used for extraction of DNA for sequencing as described in Materials and Methods (Section 2.2.15).

Agilent Bioanalyzer 2100 was used to qualitatively assay ChIP-seq libraries. Figure 5.15 shows resolved libraries. The peaks observed at 15 bp and 1500 bp denote the ladder that was spiked in the samples. The samples ranged from 150 bp - 300 bp in size as required. Also, there is a peak observed at less than 100 bp in all samples. This is non-specific contamination that may be due to the primer-adaptor pairs that were ligated to the DNA during preparation of the ChIP-seq library. The results hence confirmed good quality ChIP DNA libraries for sequencing.

#### *5.2.5.2 ChIP-seq of H4R3me2a in proliferating and senescent cells*

With the support of CRUK Beatson Institute's Molecular Technology Services personnel (William Clark), sequencing was performed. The libraries prepared were hybridized to an Illumina flow cell for cluster generation. The Illumina GAIIx produced a large number of short individual sequence reads. Tony McBryan, a computational biologist in the lab analyzed the raw data. The reads obtained from GAIIx were aligned to the human genome NCBI36/hg18 as outlined in Chapter 2 Materials and Methods (Section 2.2.17). It is to be noted that H4R3me2a ChIP from both proliferating and senescent cells were sequenced in two technical replicates to assess overall similarity and reproducibility of the ChIP experiment, although any

### Electrophoresis File Run Summary

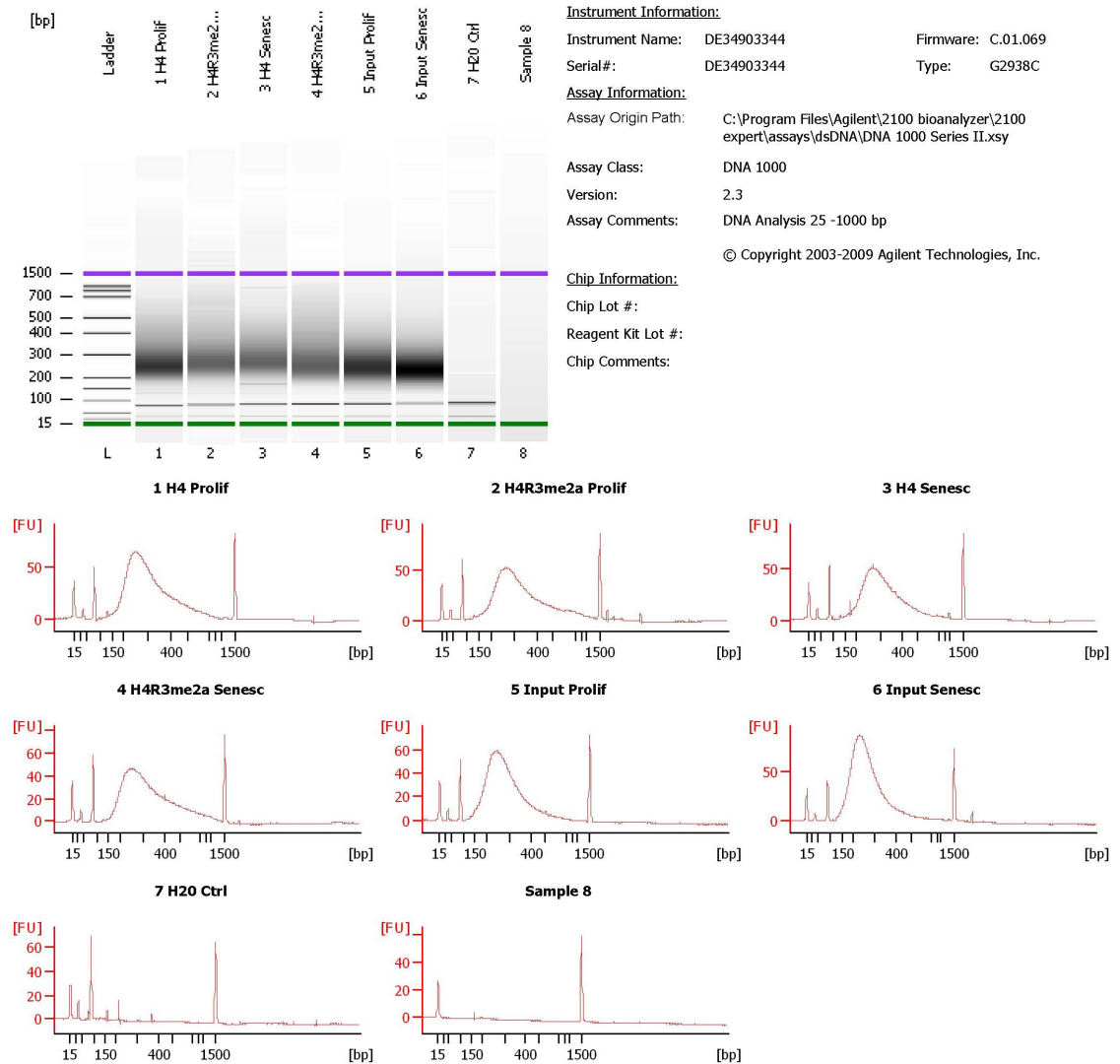


Figure 5.15 Quality control analysis of ChIP libraries using Agilent 2100 Bioanalyzer.

ChIP DNA libraries were qualitatively measured using Agilent Bioanalyzer Software. Samples were loaded along with ladder in the following order: Lane (1) H4 ChIP proliferating, (2) H4Rme2a ChIP proliferating, (3) H4 ChIP senescent, (4) H4R3me2a ChIP senescent, (5) Input proliferating, (6) Input senescent, (7) H2O control. Lane 8 is empty. Electropherograms of DNA indicate shearing between the size range of 150 bp to 300 bp. Green and purple bars represent DNA sizing ladder at 15 bp and 1500 bp, respectively.

No	Sample	Antibody	Total Reads	Aligned Reads	PCR Filtered
1	Proliferating Input	-	35,160,831	28,337,364	18,941,515
2	Proliferating Histone H4 ChIP	Millipore Cat: 05-858	35,306,624	28,373,483	18,856,619
3	Proliferating Histone H4R3me2a ChIP (replicate1)	Active Motif Cat: 39705	31,833,648	25,914,398	16,273,644
4	Proliferating Histone H4R3me2a ChIP (replicate2)	Active Motif Cat: 39705	31,653,073	25,750,374	16,230,747
5	Senescent Input	-	39,227,684	31,772,644	25,333,513
6	Senescent Histone H4 ChIP	Millipore Cat:05-858	33,223,983	26,809,851	16,804,439
7	Senescent Histone H4R3me2a ChIP (replicate1)	Active Motif Cat: 39705	27,000,317	22,211,224	14,638,578
8	Senescent Histone H4R3me2a ChIP (replicate2)	Active Motif Cat: 39705	27,188,411	22,342,177	14,671,734

Table 5.2 Statistical summary of H4R3me2a ChIP-sequencing.

Table represents ChIP-seq reads generated from Illumina GAllx aligned to the human genome NCBI36/hg18.

results need to be independently verified. The total number of reads aligned for proliferating input, H4 and H4R3me2a ChIP ranged between 31,653,073 and 35,306,624 (Table 5.2). The total number of reads aligned for senescent input, H4 and H4R3me2a ChIP ranged between 27,000,317 and 39,227,684. Approximately 20% of reads were lost in both cases after filtering non-unique alignments, likely due to regions such as repetitive elements, telomeres, pericentromeres of the human genome [505]. Further to this, PCR-filtering was applied to remove duplicate reads from the aligned reads. Removing duplicates was performed to mitigate the effects of PCR amplification bias introduced during library construction. The following percentage of reads remained after PCR-filtering uniquely aligned reads, calculated from the total reads present: 53.9% of proliferating input, 53.4% of proliferating H4 ChIP, 51% of proliferating H4R3me2a ChIP, 64.6% of senescent input, 50.5% of senescent H4 ChIP, and 54.1% of senescent H4R3me2a ChIP.

#### *5.2.5.3 H4R3me2a ChIP in proliferating and senescent cells presents technical issues*

To visualize any potential changes in H4R3me2a distribution in senescent cells in comparison to proliferating cells, the mapped reads were visualized on the UCSC genome browser. In Figure 5.16, a segment of Chr 22 between 36,417,502 – 37,626,195 bp was visualized to compare aligned reads between proliferating and senescent cells for control H4 ChIP, H4R3me2a (in duplicates) ChIP and input. Y-axis represented total reads and the bottom track RefSeq genes. Unfortunately side-by-side inspection of selected genomic loci in the H4R3me2a ChIP and total H4 control libraries showed poor enrichment for the histone mark. There was no observable difference in the distribution of H4R3me2a between proliferating and senescent cells. The distribution pattern of H4R3me2a in both proliferating and senescent cells is largely comparable to distribution pattern of H4, suggesting that H4R3me2a ChIP resulted largely in the pull-down of total histone H4 itself, and not the intended modification. Unfortunately, this precluded further analysis of this dataset.

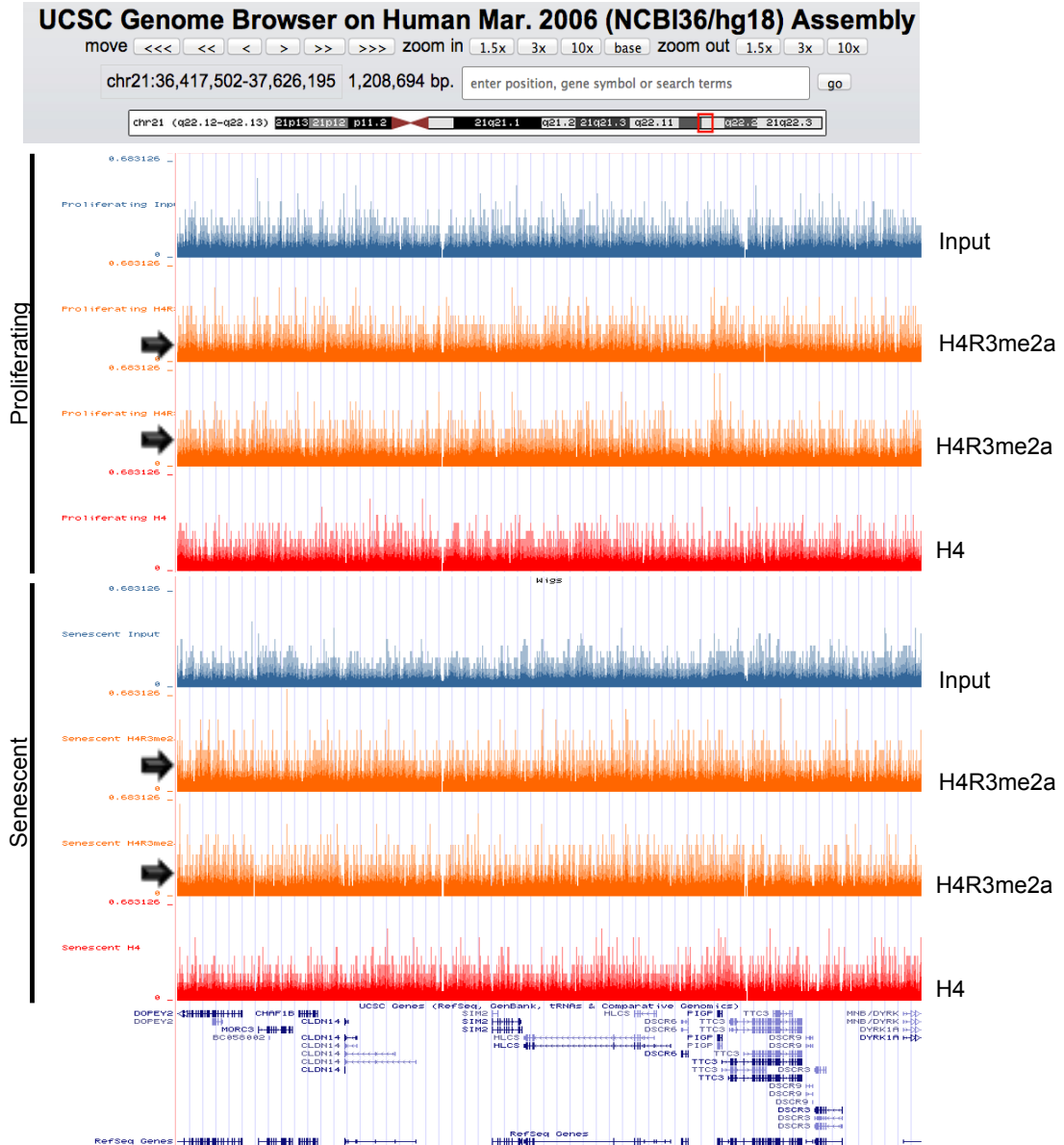


Figure 5.16 Distribution of H4Rme2a on a region of Chr22 as viewed on UCSC genome browser. Aligned reads from proliferating and senescent cells along with input were compared for H4Rme2a ChIP (in duplicates) and H4 ChIP. Y-axis represents total number of reads present. The bottom track represents list of RefSeq genes within the highlighted region of Chr22.

### 5.3 Discussion

Arginine methylation has attracted a lot of interest in the recent years owing to its role in various cellular processes. In particular H4R3me2a deposited by PRMT1 is associated with active transcription in mammals [489, 501]. From the histone modifications screen, H4R3me2a was identified to have elevated levels during RS. Owing to its importance, I set out to characterize the mark during senescence.

Before setting up a broad range of experiments, H4R3me2a antibody from Active Motif was found to show substantial preference for the intended histone modification. Also a second antibody from Suming Huang's lab in Florida indisputably confirmed the increase of histone mark in senescence. Also, a time course performed using ER:RAS cells showed increase in H4R3me2a from day 4 of 4OHT induction with progressive increase leading up to senescence. This suggests that altered H4R3me2a may play a role in aiding effective establishment of senescence in these cells.

To elucidate mechanisms involved in regulation of the mark in OIS, SV40LTA<sub>g</sub> was overexpressed in IMR90 to disrupt p53 and pRB. Induction of senescence was then achieved by infecting SV40LTA<sub>g</sub> cells with RAS virus. Despite overexpression of SV40LTA<sub>g</sub>, RAS induction still resulted in increased H4R3me2a. Also additional analysis by Western blotting and bright field microscopy showed features characteristic to senescence in SV40LTA<sub>g</sub>+RAS cells suggesting that SV40LTA<sub>g</sub> was not sufficiently expressed to bypass senescence. Due to the technical caveat associated with the experiment, results indicated that overexpression of SV40LTA<sub>g</sub> did not alter elevated levels of H4R3me2a in senescence. But in order to determine if p53/pRB effector pathways are required for increased histone mark in IMR90, an alternative approach to disrupting p53 and pRB is essential. For example, to disrupt p53, cells can be transduced with a dominant-negative p53 mutant construct (p53<sup>175H</sup>) as described in [37] and to disrupt pRB, a short hairpin to p16 could be employed [387]. Alternatively, direct KD of the concerned proteins using lentivirus encoding short hairpins can be used. Also, it is questionable if critical shortening of the telomere length in cells under long-term passaging plays a role in the regulation of this mark. To do this long-term passaging of cells lacking H4R3me2a could be performed to test if they affect life-span of cells. Alternatively hTERT can be

introduced into cells to bypass shortening of telomeres. Ultimately, the mechanism by which PRMT1 mediates H4R3me2a in senescence needs to be defined.

The next step was to ask if PRMT1 was altered during senescence. It was interesting to note that PRMT1 level was also increased in RS and OIS as the histone mark. Curiously, another study reported that PRMT1 and asymmetric arginine dimethylated proteins were decreased in expression in WI-38 fibroblasts during replicative and H<sub>2</sub>O<sub>2</sub>-induced senescence [506]. The differences may be broadly based on an inherent cell to cell variations between IMR90 and WI-38 fibroblasts. Also the quoted study did not determine levels of H4R3me2a in senescence with a specific antibody to the mark, and lacked any substantial evidence for decreased PRMT1 as suggested with supporting experiments that could include loss or gain of function studies. Hence, the finding is disputed by my observations. The level of PRMT1 is shown to be elevated in different types of cancer in comparison to non-cancerous counterparts, and PRMT1 is suggested to have dis-regulated activity [507]. Perhaps increased PRMT1 in senescence may be an essential step or a functional requirement for cells to bypass senescence and progress to cancer.

To determine the regulation and function of PRMT1-mediated H4R3me2a in senescence, an effective *in vitro* tool was required. Although different types of inhibitors were available against PRMT1, they lacked specificity and inhibited all methyl transferases using SAM as a methyl donor, thereby including the entire PRMT enzymatic family and also some lysine methyltransferases [508-510]. Compounds such as AMI-I and AML-408 were discovered to be more specific over lysine methyltransferase, yet lack specificity for PRMT1 [508, 511]. More recently, modified peptides were shown to have inhibitor properties for PRMT1 but cross-reacted with other PRMTs, especially PRMT6 [512, 513]. Given the lack of a specific inhibitor, PRMT1 KD cells were established as a means of creating a good model system. Cells with high, moderate and low levels of PRMT1 KD were produced. Attempts to induce senescence in PRMT1 KD proved to be technically challenging and limiting for downstream assays as the cells exhibited enhanced toxicity. Previous studies using mouse cells lacking PRMT1 showed a range of defects including cell cycle delays, checkpoint activation defects following DNA damage, enhanced chromosome instability, polyploidy and impaired DNA repair mechanism [514]. Despite achieving double infections at a high titre, loss of PRMT1 resulted in a toxic phenotype in

IMR90. This suggested that toxicity was due to inherent KD of enzyme and not due to off-target effects known to occur with short hairpins and/or viral infections [515-517]. PRMT1 KD cells appeared to be dividing much slower than its control counterparts and exhibited altered morphology. Nevertheless, results from two biological replicates effectively confirmed that PRMT1 is required for marked increase in H4R3me2a during senescence.

Since KD of PRMT1 reduced the abundance of the histone mark, I set out to ask whether overexpression of the enzyme would cause an increase in H4R3me2a. Interestingly, overexpression of the enzyme lead to decrease in global levels of H4R3me2a rather than the expected increase (data not shown). This effect may be due to a dominant negative "squenching" effect of the ectopically expressed PRMT1 subunit on the multi-subunit endogenous holo-enzyme. PRMT1, predominantly a nuclear protein exists in large complexes sized 300 – 400 kDa [518, 519]. To overcome the presumed squenching effect observed on high-level ectopic expression of PRMT1, the enzyme may be ectopically expressed at lower levels of expression. An alternative would be to achieve conditional overexpression of the enzyme by using a tetracycline-inducible system that can be established using T-Rex System from Invitrogen as described elsewhere [520].

Also, it is to be emphasized that modulating arginine methylation levels and modulating expression of the enzyme PRMT1 itself might have a host of other effects on cell. Both *in vivo* and *in vitro* works have demonstrated that PRMT1-mediated H4R3me2a facilitates p300-mediated histone H4 acetylation leading to transcriptional activation of nuclear receptor activator [489, 501]. An and colleagues demonstrated cross talk between histone and non-histone proteins by proving that p53 recruits PRMT1, p300 and PRMT4 in order to activate transcription in a step-wise manner. Initially, during this cascade of activation, PRMT1 mediates deposition of H4R3me2a following which the mark initiates acetylase activity of p300 towards histone H4 K5, K8 and K12 residues [521]. Additionally, loss of PRMT1 resulting in a global loss of H4R3me2a was shown to affect levels of other histone modifications, such as H4K5ac, H4K8ac and H4K12ac by reduction at the chicken  $\beta$ -globin locus [488]. Hence, given the interplay between PRMT1 and its substrate H4R3me2a with other histone and non-histone proteins, it is essential to state that the KD approaches should be subjected to careful interpretation.

Also it is unclear whether any specific demethylase exist for H4R3me2a. JMJD6 (Jumonji domain-containing 6) was found to demethylate H4R3me2 and also H3R2me2 [522]. However, this finding was disputed two years later by a study demonstrating that JMJD6 is in fact lysine hydroxylase and not a demethylase [523]. Although existence of a particular demethylase for H4R3me2a remains unproven, reports have demonstrated that histone deimination antagonizes arginine methylation [321]. PADI4 (Peptidyl Arginine Deiminase 4) mediates reversal of H4R3me2a. Interestingly, a significance for PADI4-mediated protein citrullination is implied in the p53-signaling pathway [524]. p53 functions as a transactivator of PADI4 and KD of PADI4 and p53 decreased levels of citrullination [524]. Also, DNA damage is an inducer of citrullination [525] and reports suggest a role for PADI4 during chromatin remodeling, carcinogenesis and autoimmune diseases [525-528]. However, any potential role for citrullination in senescence has not been elucidated. Perhaps it would be interesting to ask if H4 citrullination plays a role in regulating H4R3me2a during senescence and how this might impinge on senescence associated effects.

Having tested *in vitro* tools to modulate levels of PRMT1 with this study, our lab, has now also obtained a mouse model to study the function of PRMT1 in senescence *in vivo*. Using the Cre/*loxP* recombination system, Yu et al., first reported the generation of a *PRMT1* conditional allele (*PRMT1<sup>FL</sup>*) that consists of exons 4 and 5 flanked by *loxP* sites. Cre recombinase-mediated deletion of the “floxed” region facilitates removal of part of the methyltransferase domain, including the S-adenosyl-L-methionine-binding site, creating a frameshift, thereby resulting in a functionally null *PRMT1* allele [514]. Deregulation of PRMTs and mechanisms downstream of arginine methylation leading to diseases, such as cancer, are extensively studied [529]. Hence, uncovering the role of PRMT1 during senescence *in vivo* may have significant implications for cancer.

To further substantiate the study, an attempt to understand the distribution of H4R3me2a in senescence was made using ChIP-sequencing. Unfortunately, the results indicated that there was no observable difference in the distribution of H4R3me2a between proliferating and senescent cells due to limitations arising from the only available antibody to the histone mark. Although the antibody was extensively tested for its ability to immunoprecipitate under stringent conditions, the ability to specifically pull-down H4R3me2a appears to have failed in this case. Even

though an antibody may perform well in ChIP, some proteins and DNA fragments tend to be pulled down non-specifically. It is important to iterate that like any technology, ChIP-seq also suffers from its own artefacts and bias. It is promising to note that a second antibody to H4R3me2a has become recently available from Abcam under cat no ab129231 which might prove to be additionally supportive for future experiments involving ChIP. Whilst ChIP-seq is a very promising technique, it would be difficult to map distribution of the histone mark without availability of a reliable ChIP-grade antibody and substantial optimization of ChIP conditions.

## **6. H4K16Ac IN CELLULAR SENESENCE**

## 6 H4K16Ac IN CELLULAR SENESCENCE

---

### 6.1 Introduction

Histone acetylation is one of the most widely studied modifications and is known to be involved in a wide variety of mechanisms in higher eukaryotes [530-532]. It influences chromatin organization in several ways [533, 534], and acts as a binding domain for recruiting chromatin remodellers to exert specific chromatin related functions [535, 536]. In this regard, H4K16ac plays a particularly important role in the evolutionary conservation of chromatin compaction [537]. Positively charged H4K16 [538] forms salt bridges with acidic patches of histone H2A and H2B, thereby contributing to the formation of higher order compaction of chromatin by repeated folding *in vitro* [539-541]. Hence acetylation of K16 on H4 is known to control chromatin structure and protein interactions. H4K16ac recruits specific bromo-domain containing proteins to facilitate gene transcription [542]. In line with the above-mentioned attributes of H4K16ac, it is associated with 'open' chromatin facilitating gene transcription (euchromatin) and unacetylated H4K16 is generally associated with silenced chromatin (heterochromatin) [543, 544]. Given the apparent dramatic change in chromatin reorganization and compaction observed in senescence (Chapter 1, section 1.7) and the already known implications of H4K16ac in chromatin folding and compaction, it was interesting to probe the participation of this particular mark in the context of senescence and its associated effects.

Crucially it is to be noted that H4K16ac is implicated in both ageing and cancer [401, 545, 546]. Reduced H4K16ac was reported in cell senescence [545, 547]. David Nelson, a former graduate student in the lab, also noticed a moderate decrease of H4K16ac in senescent cells in comparison to proliferating cells by Western blotting (data not shown). Despite these reports, it still remains unclear how H4K16ac might modulate senescence. With this chapter I set out to understand if alteration in H4K16ac during senescence has any major epigenetic underpinnings and also to understand how this may be relevant to senescence associated processes such as ageing and cancer.

## 6.2 Genomic distribution of H4K16ac in senescence.

Given the potential significance of H4K16ac in senescence, David Nelson decided to map the localization of this mark across the genome of senescent cells using ChIP-sequencing technology. Chromatin extracted from proliferating and senescent cells was subject to stringent ChIP conditions using two different antibodies to H4K16ac that have been previously tested to work for the intended application. H4K16ac ChIP was carried out along with an internal control i.e., total histone H4 ChIP. Input material and ChIP DNA extracted from proliferating and senescent cells were subjected to qualitative analysis and library preparation. William Clark of the Beatson Molecular Technology Services performed single-read sequencing of the DNA libraries using Illumina GAIIx. Downstream analyses of ChIP-seq data were performed by Tony McBryan and John Cole, computational biologists in the lab.

### *6.2.1 H4K16ac is enriched at gene-rich regions and co-relates to gene expression*

Uniquely aligned reads from the H4K16ac ChIP were visualized using the UCSC genome browser. Input DNA, H4 ChIP and H4K16ac ChIP (in duplicate using two different antibodies, labelled ab1 (Millipore), ab2 (Abcam)) for both proliferating and senescent cells were loaded on the UCSC browser (Figure 6.1). The y-axis represents H4K16ac enrichment as 'peaks' for individual ChIP samples and input DNA. The specific region of the genome, in this case Chr 1, visualized on the browser was represented at the top as a snapshot view. A separate track representing genes from RefSeq was also included at the bottom. Remarkable enrichment of the mark was observed specifically at gene rich regions. Further analysis revealed that H4K16ac peaks are found around the TSS (Transcription Start Site) of genes in senescence, but to a much lesser extent in proliferating cells. Moreover, H4K16ac is markedly enriched at promoters of genes that have high and medium levels of expression in senescent cells, but almost absent at genes with low levels of expression (Figure 6.2). This suggests that H4K16ac enrichment at gene promoters in senescent cells may have a functional role in senescence via regulation of gene expression. With these observations made by colleagues in the lab. I set out to further define the role of H4K16ac in cellular senescence and understand why significant



### H4K16ac distribution in senescent IMR90

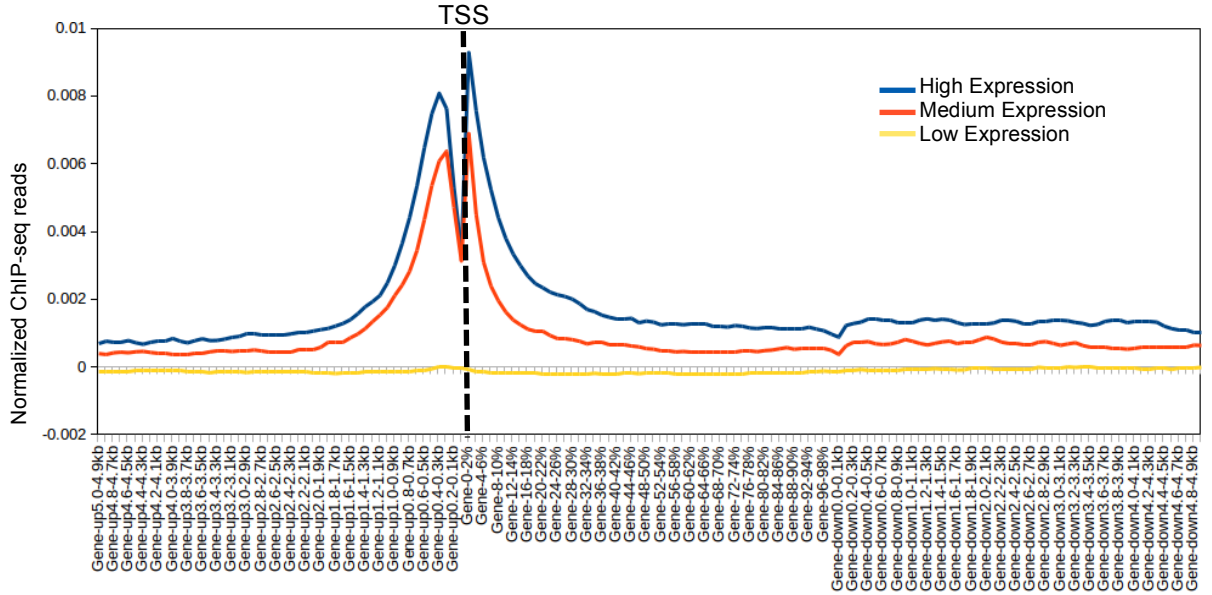


Figure 6.2 H4K16ac distribution relates to gene expression in senescence.

Gene expression in senescence compared to the distribution of H4K16ac in senescent IMR90 with the x-axis representing the position along the gene with TSS (black dotted line), gene body, upstream and downstream of gene. The y-axis represents the normalized ChIP-seq reads. The y-axis is the difference between the number of ChIP-seq reads in the K16ac ChIP (normalised by the number of total reads) and the number of ChIP-seq reads in the matched H4 control (normalised to number of total reads). The x-axis represents the aggregate of top 1000 genes with high (blue), medium (red) and low (yellow) expression. (Data courtesy: David Nelson, Taranjit Rai, Tony McBryan, John Cole)

accumulation of the mark was observed at promoters of expressed genes in senescent cells.

## 6.3 Results

### *6.3.1 Validation of antibody specificity*

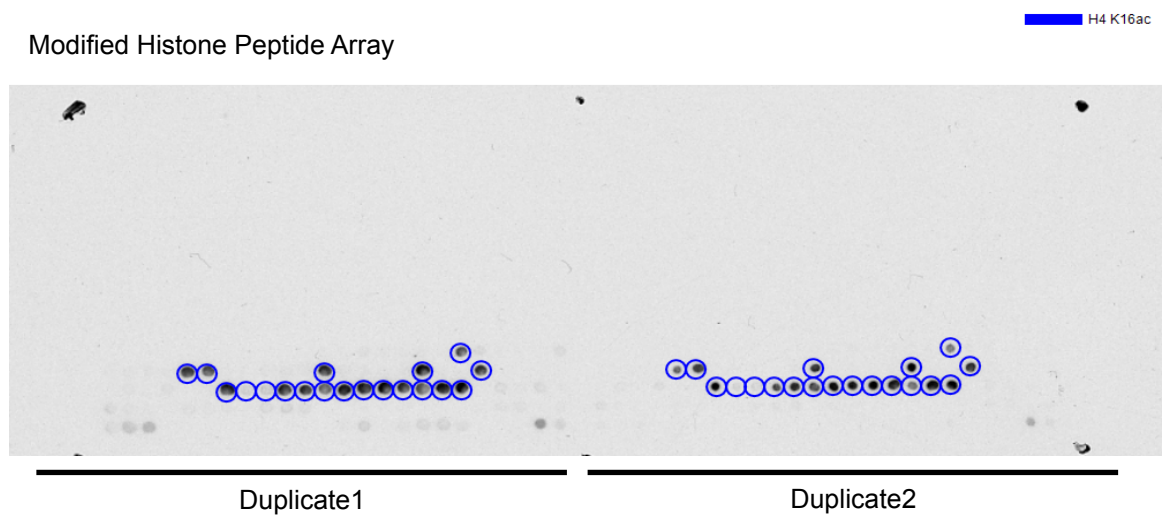
At the time that I set out to investigate H4K16ac, I acquired a new aliquot of antibody from Millipore (Cat no: 07-329; Lot 2073125). MODified histone peptide array was used to confirm the specificity of this antibody, according to Chapter 2 Materials and Methods Section 2.2.19. Scanned images of the array revealed spot intensities (Figure 6.3.A) specific for H4K16ac marked in blue. There was some minor cross reactivity with other histone modifications. The results were quantified using Array Analyse Software and graphical analysis (Figure 6.3.B) showed that despite marginal cross-reactivity with other modifications, such as H4K12ac, H4K20ac, the antibody was highly specific for H4K16ac.

### *6.3.2 Independent confirmation of H4K16ac enrichment in senescence by real time quantitative PCR*

Firstly, I set out to confirm some of the peaks identified by ChIP-seq by conventional ChIP-PCR. ChIPs were performed using the Millipore antibody to H4K16ac in proliferating and replicative senescent cells along with a negative control IgG. Conditions for cell crosslinking, lysis and chromatin sonication and ChIP were previously optimized by David Nelson: 7µg antibody (H4K16ac antibody or Rabbit IgG), 0.1% (w/v) SDS and a LiCl wash. Following the ChIP reaction, DNA was extracted following the standard protocol in Chapter 2 Materials and Methods Section 2.2.15.

PCR primers were designed to specific regions of H4K16ac enrichment and non-enrichment in senescence, based on “DiffBind” analysis across different regions of the genome. Multiple primers pairs were tested in SYBR Green-based real-time quantitative PCR. Primer pairs that failed to produce a single specific product were not used for subsequent experiments. Results (Figure 6.4) obtained from the ChIP-

(A)



(B)

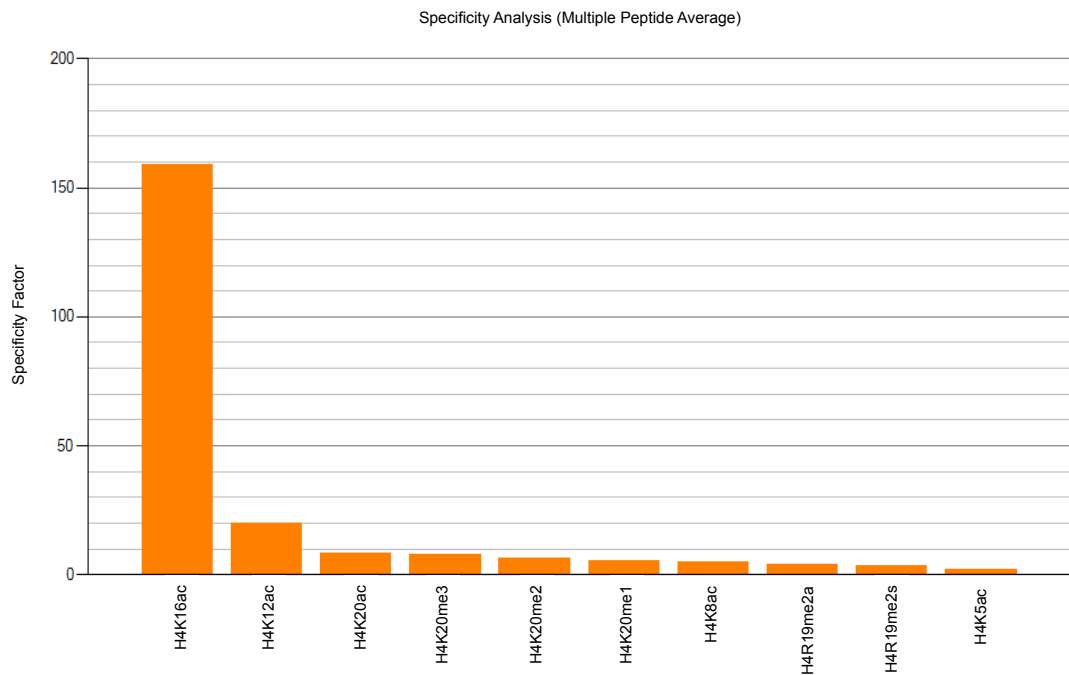


Figure 6.3 Specificity of H4K16ac antibody confirmed using MODified Peptide Array Analysis. The H4K16ac antibody was evaluated using Active Motif's Peptide Array. (A) ECL images of the array represented in duplicates. Blue circles represent antibody reactivity to H4K16ac. (B) Based on the array, the specificity factor was calculated for the antibody using the Array Analyse Software. The specificity factor was calculated from the average intensity of all spots containing the mark divided by the average intensity of all spots not containing the mark.

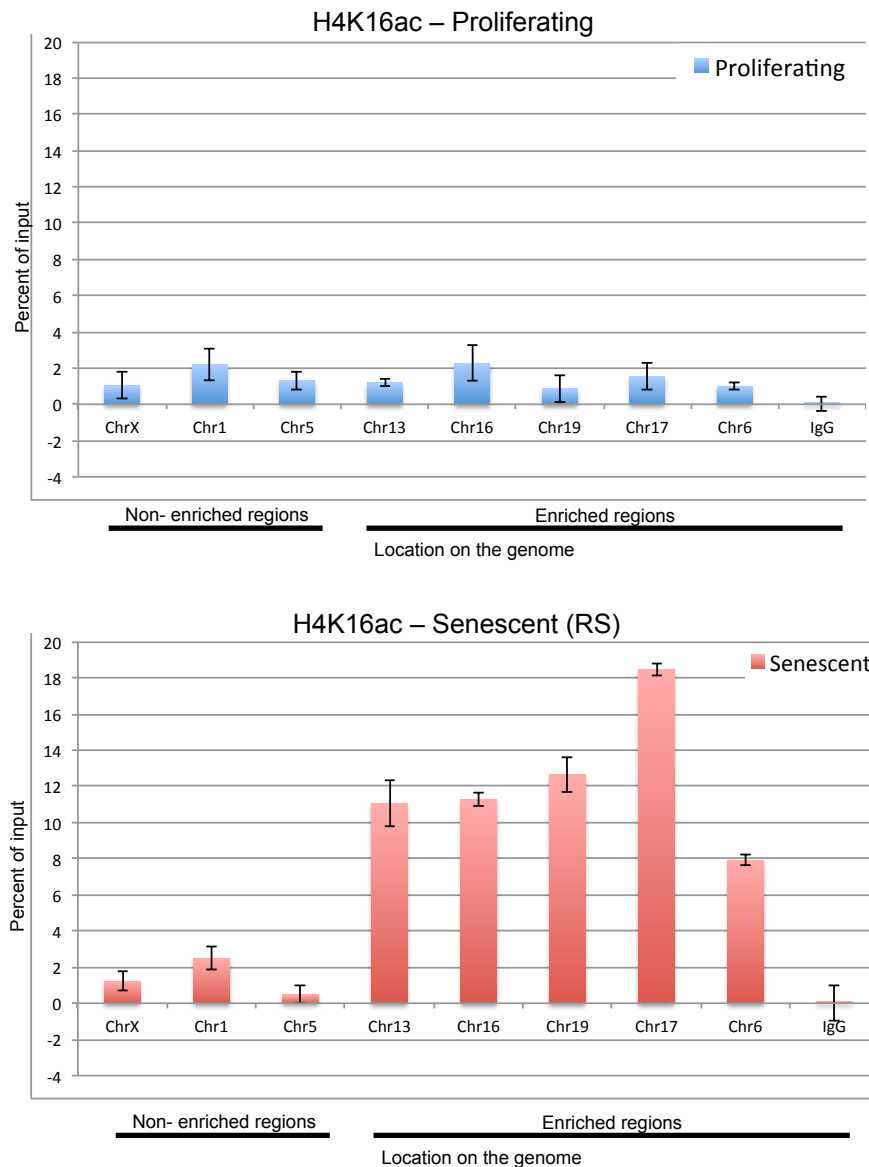


Figure 6.4 ChIP-PCR analysis of H4K16ac distribution.

H4K16ac ChIP in proliferating (blue) and senescent cells (red) followed by real-time SYBR green quantitative PCR was carried out using primer sets corresponding to different regions of the genome along with control IgG ChIP. Chr X, Chr1 and Chr5 represent regions of no enrichment for H4K16ac in senescence by ChIP-seq. Chr13, Chr16, Chr19, Chr17 and Chr6 represent regions of specific enrichment for H4K16ac in senescence, by ChIP-seq. The IgG control was performed on a region from Chr 17. Error bars represent PCR technical replicates, from a single biological replicate.

PCR were plotted as a bar graph. ChrX, Chr1 and Chr5 correspond to regions of non-enrichment for H4K16ac in both proliferating and senescent cells. Chr13, Chr16, Chr19, Chr17 and Chr6 correspond to regions of specific enrichment for H4K16ac in senescent cells, as deduced from ChIP-Seq. Enrichment of H4K16ac was observed at Chr13, Chr16, Chr19, Chr17 and Chr6 sites in senescent cells and not proliferating cells. Regions of non-enrichment of H4K16ac remained unenriched in proliferating and senescent cells. These results confirm the ChIP-seq data by an alternative ChIP-PCR approach.

### *6.3.3 Using IR-induced senescence to study specific enrichment of H4K16ac*

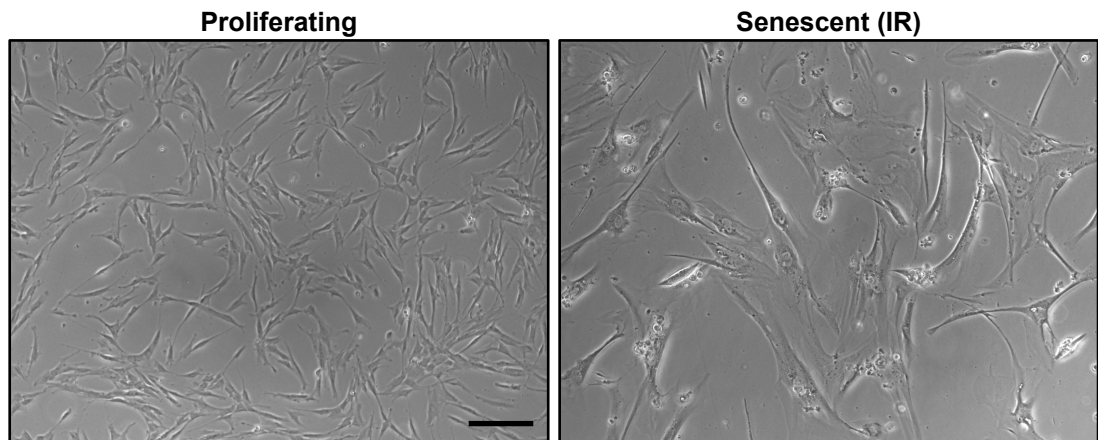
Characterization of IR-induced senescence as a model to study H4K16ac enrichment at gene promoters was performed. Given that replicative senescence would be extremely time consuming and labour intensive for use as a model system to study specific enrichment of H4K16ac, use of another efficient model of senescence i.e., DNA-Damage induced senescence using X-ray irradiation, was implemented.

Proliferating IMR90s were seeded at low density, approximately 20% confluency per 10 cm dish and irradiated with a dose of 20 Gy for induction of senescence. Bright field microscopy images after 10 days revealed marked morphological differences between cells treated without and with IR (Figure 6.5.A). IR-induced senescent cells acquired a more flattened enlarged phenotype in comparison to proliferating cells. Whole cell lysates were prepared and fractionated by SDS-PAGE and Western blotted for markers of proliferation arrest. IR-treated cells showed features of senescence, such as decreased phosphorylation of pRB at serines 807/811 and decreased histone content, thereby denoting establishment of growth arrest. Actin was used a loading control. Hence, a third model of senescence, IR-induced senescence, was successfully established in the lab for further use.

#### *6.3.3.1 Real-time quantitative PCR confirms relative enrichment of H4K16ac IR-induced model of senescence*

Once induction of senescence was established using IR, the next step was to perform H4K16ac ChIP to test whether this modification is enriched at specific sites, similar to

(A)



(B)

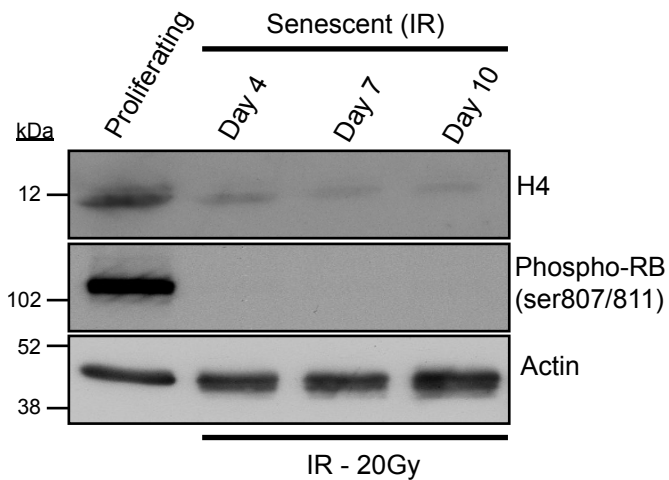


Figure 6.5 Establishment of IR-Induced Senescent cells.

Proliferating IMR90 cells were seeded at low density and exposed to 20 Gy irradiation or left untreated.

(A) Light microscopy images were taken (under 20X objective) of proliferating and IR-induced senescent cells 10 days after irradiation. (B) Whole cell lysates were harvested from proliferating cells on day 10 and from irradiated cells on day 4, day 7 and day 10 post-irradiation. Whole cell lysates were Western blotted for makers of cell cycle arrest. Actin was used as loading control.

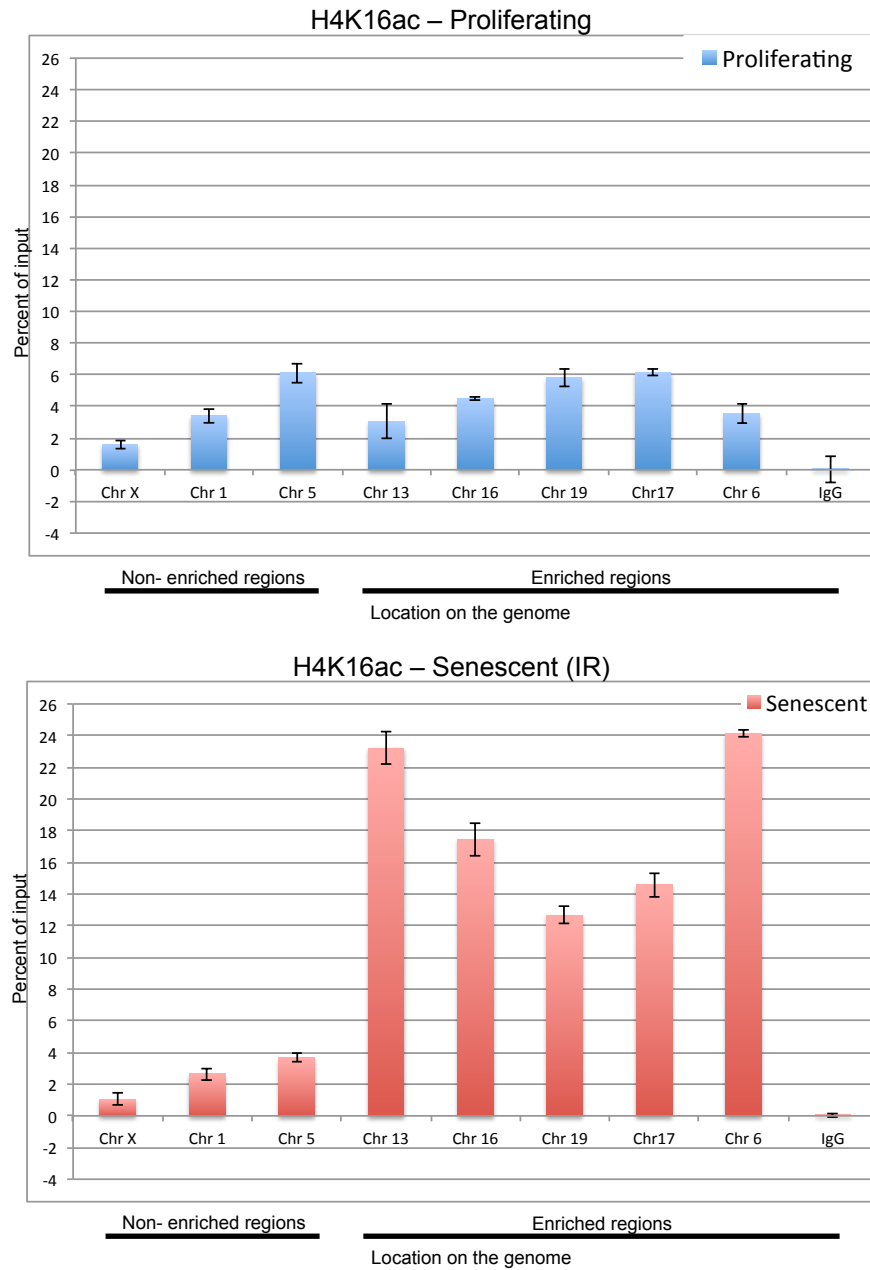


Figure 6.6 ChIP PCR confirms relative enrichment of H4K16ac in the IR-induced model of senescence. H4K16ac ChIP of chromatin from proliferating (blue) and senescent cells (red) followed by real-time SYBR green quantitative PCR was performed on different regions of the genome, along with control IgG ChIP. Chr X, Chr1 and Chr5 represent regions of no enrichment for H4K16ac in senescence, based on ChIP-seq. Chr13, Chr16, Chr19, Chr17 and Chr6 represent regions of specific enrichment for H4K16ac in senescence. IgG control performed on region from Chr 17. Error bars represent PCR technical replicates, from a single biological replicate.

the replicative senescence model. H4K16ac ChIPs and negative control ChIPs were performed using in proliferating and IR-induced senescent cells, as described for RS cells. ChIP DNA was analyzed by real-time quantitative PCR, at the same regions as in Figure 6.4. Results showed that IR-induced senescent cells recapitulated the result observed previously in replicative senescence, showing specific enrichment of H4K16ac at specific regions across the genome. Other regions, such as ChrX, Chr1 and Chr5, did not show any enrichment for H4K16ac. Hence, these findings supported the use of IR to study the specific role of H4K16ac enrichment at gene promoters during senescence.

#### *6.3.4 In vitro approaches to deplete H4K16ac in senescent cells*

To characterize the role of H4K16ac in senescence, I set out to establish tools for the effective suppression of the mark *in vitro*. As discussed in Chapter 1 Introduction, several key events and important players, such as writers (for example, HATs) and erasers (for example, HDACs), are involved in control of histone modifications [486, 548]. With this in mind, I set out to target some key players involved in the modulation of H4K16ac [549, 550].

#### *6.3.5 Knocking down the acetyl transferase hMOF*

A HAT for H4K16ac was originally described in *Drosophila* as dMOF (Drosophila Males Absent On The First) belonging to the MYST family of proteins [551, 552]. Acetylation of H4K16 by dMOF was associated with dosage compensation of the male X chromosome by facilitating transcriptional upregulation [553-555]. The human ortholog is termed hMOF [556]. Under *in vitro* conditions, hMOF has acetyltransferase activity towards H4, H3 and H2A [556]. Following this striking observation of evolutionary conservation from *Drosophila* to humans, Taipale et al., demonstrated that knocking down hMOF lead to a global decrease in H4K16ac in HeLa cells with other acetylation marks left unaffected [549]. With this in mind, the next step was to KD hMOF in IMR90 cells to decrease the levels of H4K16ac at promoters in senescent cells.

#### 6.3.5.1 *Validation of hMOF antibodies using siRNA approaches*

Before attempting to KD hMOF in IMR90, I set out to confirm our ability to detect hMOF by Western blot. To do this, I used siRNA KD to confirm identity of polypeptides recognized by hMOF antibodies. SMARTpool ON-TARGETplus hMOF siRNA was obtained from Thermo Scientific. IMR90 cells were seeded 24 hours prior to transfection and transfected as outlined in Chapter 2, Materials and Methods Section 2.2.8. Control siRNA, hMOF siRNA transfected cells along with mock treated cells were harvested for protein at three different time points: 24 hrs, 48 hrs and 72 hrs. Whole cell lysates were fractionated using SDS-PAGE, transferred onto PVDF membrane and blotted for hMOF using two different antibodies (Figure 6.7). Results showed that the anti-hMOF Rabbit antibody from Bethyl Laboratories clearly identified a polypeptide of the correct MW that was knocked down by siRNA, at all three time points. A second antibody to hMOF from Abcam did not detect a polypeptide knocked down by siRNA, except for a moderate decrease at the 72 hr time point. Also, the polypeptide recognized by this antibody migrated at slightly higher molecular weight. I conclude that anti-hMOF Rabbit antibody from Bethyl Laboratories detects endogenous hMOF by Western blot. Accordingly, only hMOF rabbit antibody from Bethyl Laboratories was used for subsequent experiments.

#### 6.3.5.2 *shRNA KD of hMOF*

Having validated at least one anti-hMOF antibody for Western blot, I set out to establish stable hMOF KD in IMR90. Concentrated lentiviruses encoding five different short hairpins to hMOF were prepared. The viral dose was determined for optimal KD of hMOF in proliferating IMR90. Five different short hairpins including a non-targeting control (luciferase) were tested at doses ranging from 2 $\mu$ l, 4 $\mu$ l, 8 $\mu$ l and 16 $\mu$ l. Whole cell lysates were harvested and fractionated by SDS-PAGE and Western blotted for hMOF. Figure 6.8.A shows that sh3 knocks down hMOF well in comparison to the other short hairpins. Moreover, sh3 cells exhibited loss of H4K16ac in comparison to control cells. Total histone H3 was used as loading control. I conclude that stable KD of hMOF in IMR90 was achieved using sh3 construct.

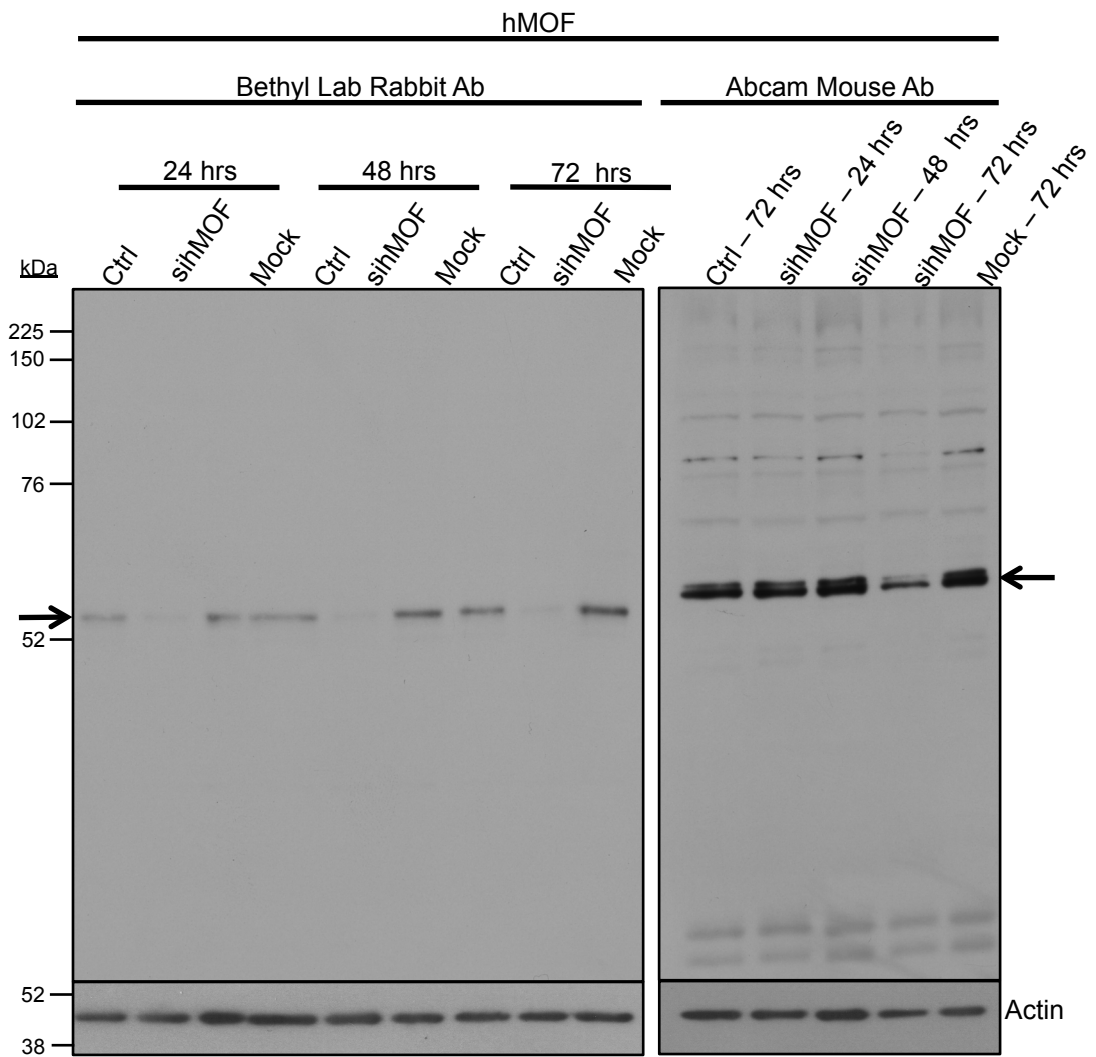
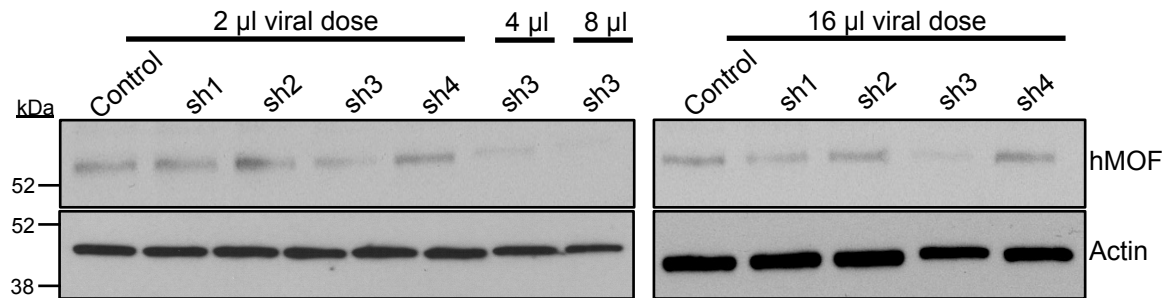


Figure 6.7 Characterization of hMOF antibodies using siRNAs.

Proliferating IMR90s were transiently transfected with a siRNA to KD hMOF. Whole cell lysates were harvested at 24, 48 and 72 hours post transfection. 20  $\mu$ g protein per sample was loaded on to a large SDS-PAGE for fractionation and Western blotted for hMOF using antibodies from Bethyl Laboratories and Abcam. Actin was used as loading control. Arrow indicates potential hMOF polypeptides.

(A)



(B)

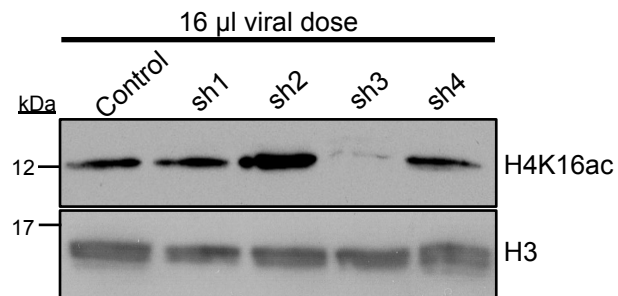


Figure 6.8 Establishment of stable hMOF KD in IMR90s resulting in loss of H4K16a.

Proliferating IMR90s were infected with a range (2  $\mu$ l, 4  $\mu$ l, 8  $\mu$ l and 16  $\mu$ l) of lentivirus encoding short hairpins to KD hMOF along with control hairpin. Whole cell lysates were harvested 3 days after drug selection with puromycin. (A) 20  $\mu$ g protein per sample was loaded on to SDS-PAGE for fractionation and Western blotted for hMOF. Actin was used as loading control. (B) Lysates from cells infected with the highest dose of virus (16  $\mu$ l) were blotted for H4K16ac using H3 as a loading control.

Despite this encouraging result, it was technically challenging to proceed further due to inherent toxicity associated with loss of hMOF, including slower proliferation in comparison to control cells. Defects due to loss of hMOF were previously reported in a study using HeLa cells [549]. Consequently, other *in vitro* tools to decrease levels of H4K16ac were explored in subsequent experiments.

### *6.3.6 Overexpression of the deacetylase, SIRT1*

Overexpression of the deacetylase SIRT1 was considered to deplete H4K16ac during senescence. Of the seven sirtuins in humans, SIRT1 is the most similar to yeast Sir2, often referred to as an NAD<sup>+</sup>-dependent protein deacetylase, although also classified as a prototypic class III Histone Deacetylase (HDAC) [557-560]. SIRT1 deacetylates histone proteins, such as H1, H3 and H4, and also non-histone proteins such as p53, FOXO, Ku70, p300, pRB, E2F1, NF- $\kappa$ B, p73 and PGC-1 $\alpha$  [561, 562]. SIRT1 deacetylates H4K16 and H3K9 and mediates formation of heterochromatin along with deacetylating H1K26 [550]. Also, association of SIRT1 together with LSD1 promotes deacetylation of H4K16 and H3K4 demethylation resulting in gene repression [563].

Given the strong evidence for SIRT1-mediated deacetylation of H4K16ac, I set out to overexpress SIRT1 in cells. Retroviral plasmids encoding SIRT1 and dominant negative mutant SIRT1-H363Y were obtained from Addgene (Courtesy: Bob Weinberg Lab). Proliferating IMR90s were infected with viruses encoding SIRT1 WT, SIRT1-H363Y mutant or empty vector control. Effective establishment of SIRT1 WT and mutant cells was confirmed by Western blotting (data not shown).

#### *6.3.6.1 Confirmation of impaired deacetylase activity in SIRT1-H363Y cells using Etoposide*

Before proceeding further, it was essential to confirm intact activity of SIRT1 WT cells in comparison to the dominant negative mutant SIRT-H363Y. SIRT1 deacetylates p53 at lysine 382 [564] resulting in antagonization of p53-dependent transcriptional activation and also specific inhibition of p53-dependent apoptosis in response to oxidative stress and DNA damage [565, 566]. Hence SIRT1-H363Y cells ought to be impaired in their ability to inactivate p53 by deacetylation at lysine 382. Hence, in

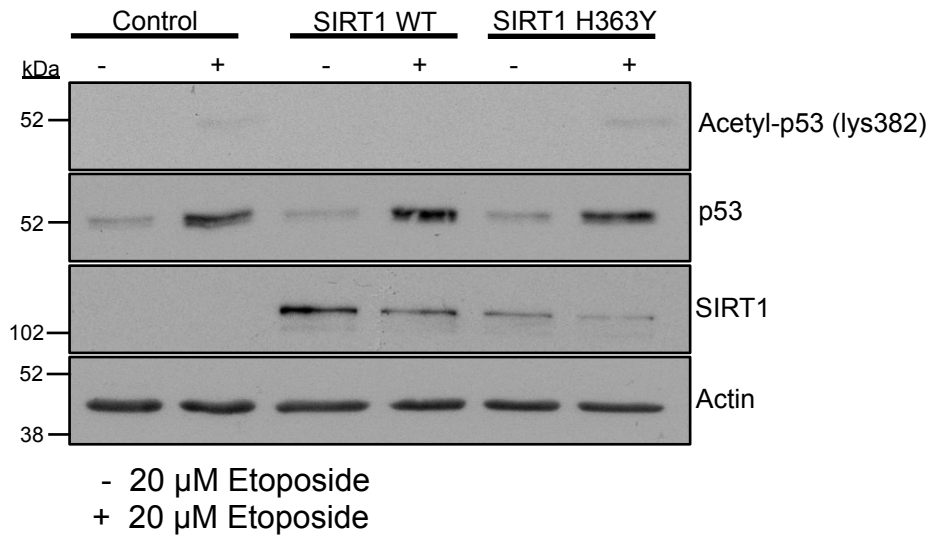


Figure 6.9 Etoposide treatment of SIRT1 WT and SIRT1-H363Y mutant cells demonstrating impaired deacetylase activity of mutant cells.

Proliferating IMR90s overexpressing SIRT1 WT and the catalytically impaired variant SIRT1-H363Y along with control cells were treated with 20 μM etoposide for 24 hours, following which whole cell lysates were harvested from untreated and treated samples. 20 μg protein per sample was loaded on to SDS-PAGE for fractionation and Western blotted using SIRT1, p53 and Acetyl-p53 (lys382). Actin was used as loading control.

order to distinguish between WT and mutant activity, cells were presented with a genotoxic stress. Control, SIRT1 WT and SIRT1-H363Y cells were treated with 20  $\mu$ M Etoposide for 24 hrs. Whole cell lysates were harvested from both treated and untreated populations from all three cell types. Lysates were separated using SDS-PAGE and Western blotted for SIRT1, Acetyl-p53 (lys382) and p53 with actin as loading control (Figure 6.9). Results showed that cells in the presence of a DNA-damaging agent such as etoposide showed increased amount of acetylated p53 at lysine 382 only in control and SIRT1 H636Y cells and not SIRT1 WT cells. Upon etoposide treatment, increased p53 levels were also observed, as expected [567]. Hence, the activity of SIRT1 WT cells was duly reaffirmed with this experiment before proceeding further.

#### 6.3.6.2 *Generating IR-induced senescent SIRT1 cells*

Next, senescence was induced in control and SIRT1 WT cells by irradiation. Both untreated and treated cells were maintained for a period of 10 days in culture and bright microscopy images taken showed morphological changes with enlarged, flattened shape in control and SIRT1 WT cells induced to senescence (Figure 6.10.A) in comparison to proliferating counterparts. For further assay, whole cell lysates harvested from all the four cell types were fractionated using SDS-PAGE and Western blotted for markers of senescence. As expected loss of phosphorylation of RB at serines 807/811 and lamin B1 was observed only in IR-induced senescent cells in comparison to proliferating cells control and SIRT1 WT cells (Figure 6.10.B) based on using actin as loading control. Also overexpression of SIRT1 was duly noted only in SIRT WT cells, thereby confirming establishment of senescent SIRT1 mode system.

Although assays confirmed (Figure 6.11) overexpression of SIRT1, overall levels of H4K16ac did not greatly decrease in SIRT1 overexpressing cells in comparison to control cells. Despite SIRT1 being a known deacetylase for H4K16ac, it is possible that SIRT1 deacetylase activity may be gene specific and localized. Hence it might be an interesting tool to study distinct enrichment and distribution of H4K16ac in the context of senescence. Due to time constraints, further experimental assays could not be set up with the senescent SIRT1 model system and prospective

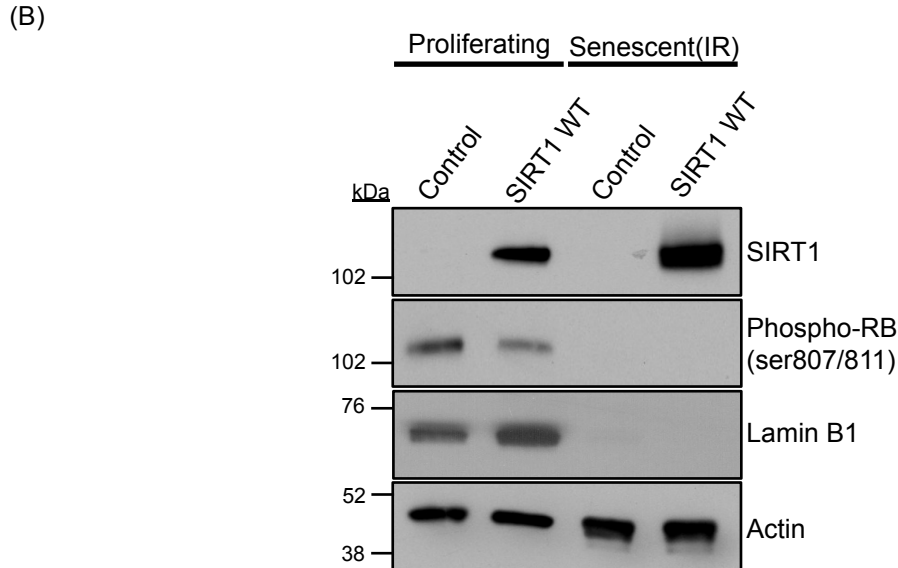
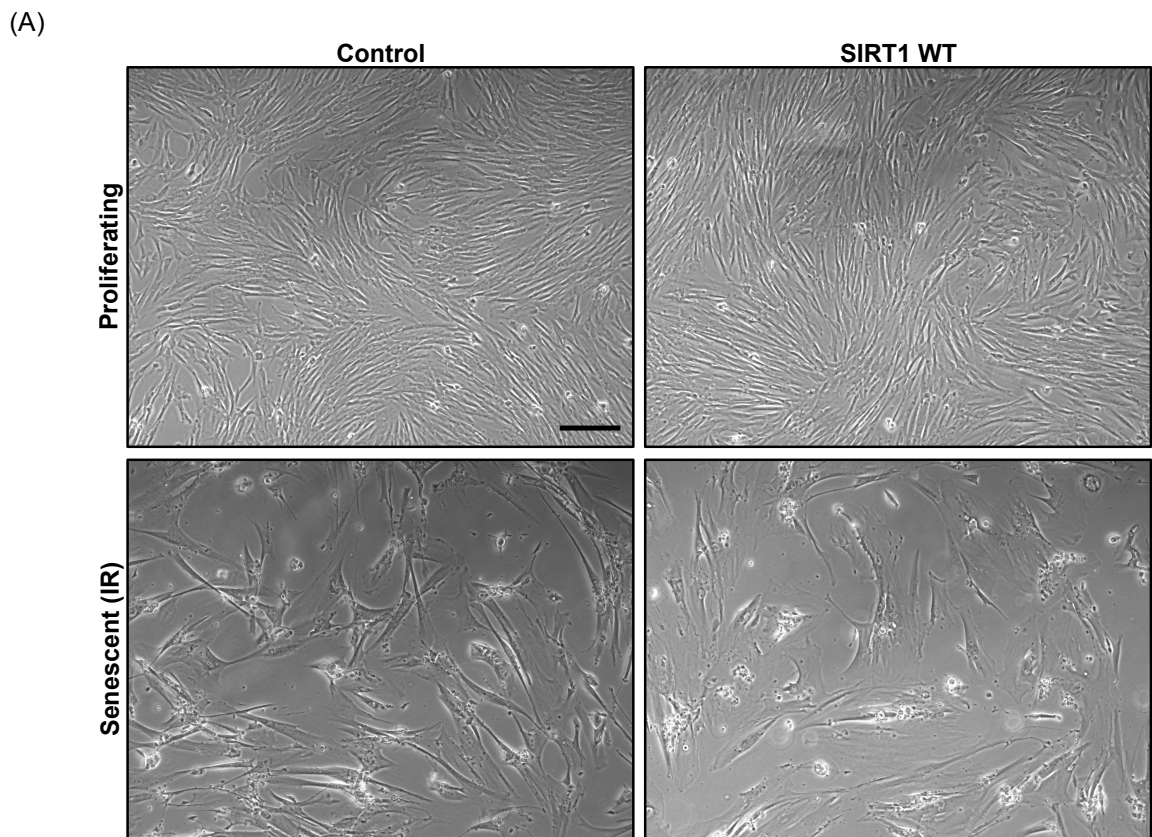


Figure 6.10 Induction of senescence in SIRT1 WT cells.

Control and SIRT1 WT cells were seeded at low density and exposed to 20 Gy irradiation or left untreated. (A) Light microscopy images were taken of proliferating and IR-induced senescent cells 10 days after exposure under 20X objective. (B) Whole cell lysates were harvested from proliferating cells and irradiated cells on day 10. 20 µg protein per sample was loaded on to SDS-PAGE for fractionation and Western blotted for makers of senescence. Actin was used as loading control and SIRT1 overexpression was also assessed.

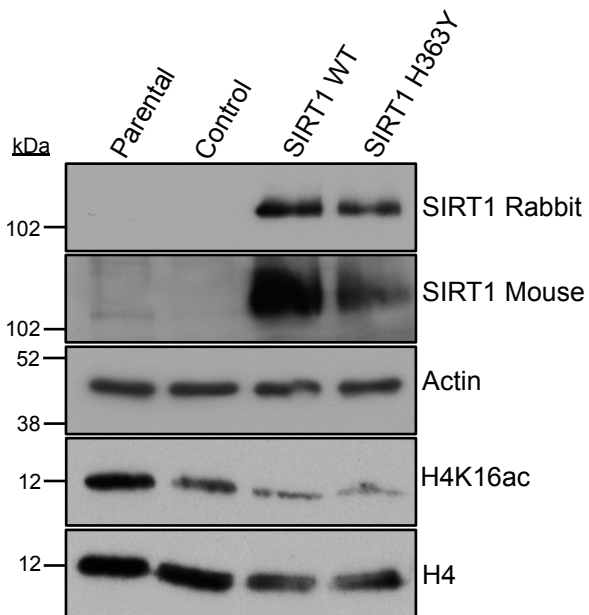


Figure 6.11 SIRT1 overexpression in proliferating cells.

Whole cell lysates were harvested from proliferating cells overexpressing SIRT1 WT, SIRT1-H363Y mutant along with control infected and uninfected parental cells. 20  $\mu$ g protein per sample was loaded on to SDS-PAGE for fractionation and Western blotted using SIRT1 rabbit and mouse antibodies. Actin was used as loading control.

experiments with these cells will be discussed later in subsequent sections.

### *6.3.7 Establishment of H4K16R and H4K16Q mutant cells*

#### *6.3.7.1 Site-specific mutagenesis to create H4K16R and H4K16Q retroviral constructs*

As an alternative approach, I set out to investigate the role of H4K16ac in senescence more directly by using cells expressing histones bearing substitutions at K16 to arginine or glutamine.

Retrovirus plasmids encoding HA-tagged histone H4K16R (lysine to arginine) or H4K16Q (lysine to glutamine) or wild type H4 were generated by site-directed mutagenesis [568, 569] (Figure 6.12A). H4K16R and H4K16Q mimics unacetylated and acetylated states of H4K16, respectively [401, 570]. Several clones for each of the desired plasmids (pBABE-puro-HA-H4WT, pBABE-puro-HA-H4K16R, pBABE-puro-HA-H4K16Q) were picked, expanded and sequenced in the Beatson Molecular Technology Services. Sequencing results revealed correct introduction of base pair substitutions to generate H4K16R (AAG->CGG) and H4K16Q (AAG->CAG) mutants as analysed by the 4Peaks Software (Figure 6.12.B).

#### *6.3.7.2 Overexpression of H4K16 mutants in proliferating cells*

For expression of the WT and histone mutants in IMR90, retroviral production was performed as described in Chapter 2 Materials and Methods Section 2.2.9. Following infection, cells were drug selected and whole cell lysates were harvested from control (empty vector), HA-H4WT, HA-H4K16R and HA-H4K16Q cells. Lysates were fractionated using SDS-PAGE and Western blotted with antibody to HA tag. Results confirmed overexpression of the intended protein, as observed by expression of HA-H4 only in H4WT and mutant cells, compared to control (Figure 6.13). Lysates were also analyzed for expression of H4K16ac, which showed that overall levels of the histone mark did not alter in HA-H4K16R cells, albeit some marginal decrease in HA-H4K16Q cells in comparison to control and HA-H4WT cells. Although a striking loss of H4K16ac was not observed in mutant cells, specific localized effect of the substitutions made at K16, if any, can only be analysed using an advanced

(A)

**Homo sapiens histone cluster 4, H4 (HIST4H4), mRNA**

NCBI Reference Sequence: NM\_175054.2

GCCACCA**ATG**GCCTACCCCTACGACGTGCCGACTACGCCTCCCTCTCTGGGCGAGGTAAAGGTG  
GCAAGGGGCTGGGTAAGGGAGGCGCC**AAG**CGCCACCGGAAGGTGCTGCGGGACAATATCCAAG  
GCATTACAAAGCCGGCGATTTCGCCGTCTGCCCGACGTGGGGCGTCAAGCGCATTCTGGTCT  
CATCTACGAGGAGACCCGGGGAGTCCTCAAAGTCTTCTGGAGAACGTGATCCGTGACGCGGTG  
ACTTACACGGAGCACGCCAAGCGCAAGACCGTCACGGCCATGGATGTGGTGTACGCGCTGAAAC  
GCCAGGGTTCGCACCCCTTTATGTTTCGGCGGT**TGA**

(B)

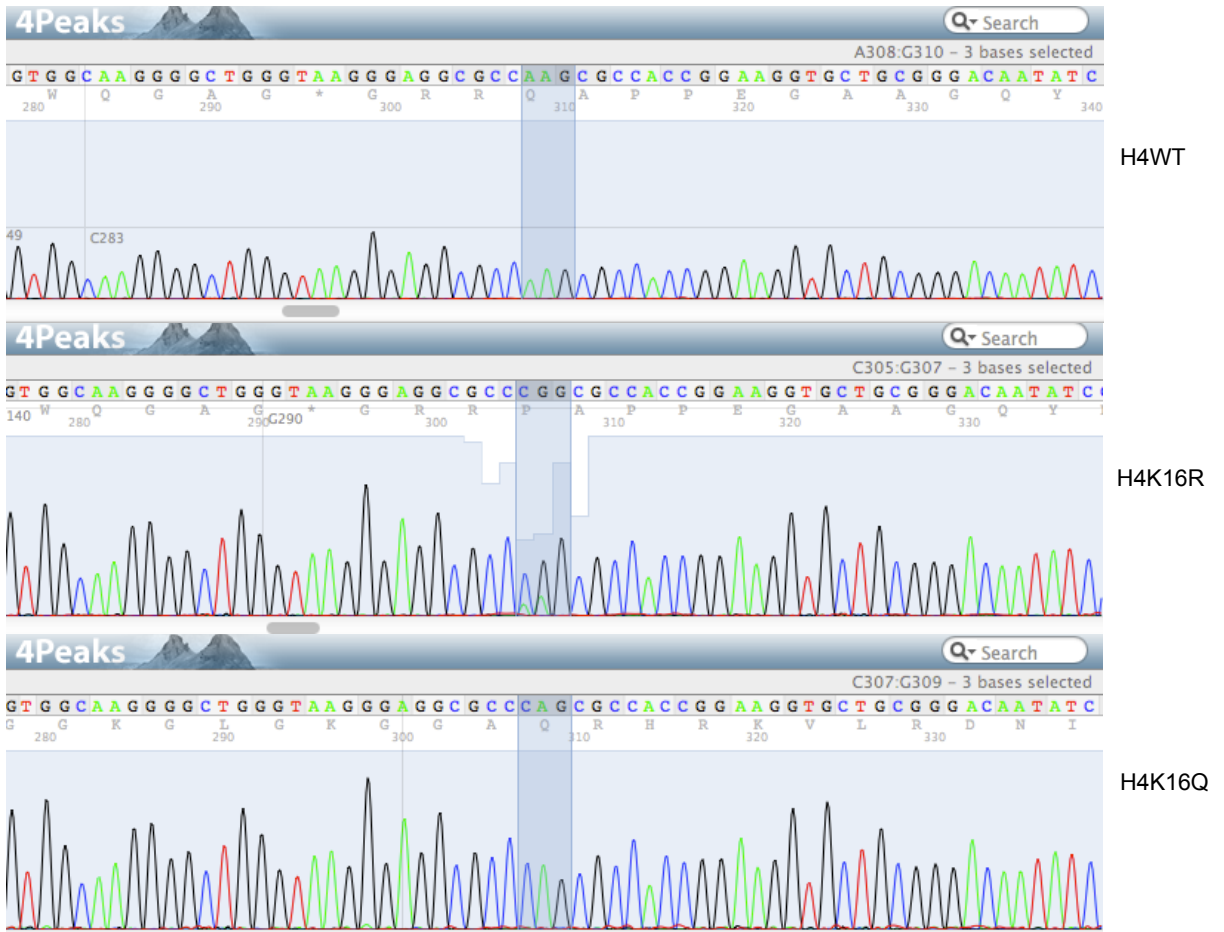


Figure 6.12 DNA sequencing confirms creation of histone H4K16 mutants.

(A) Sequence information obtained for human histone H4 from NCBI (National Centre for Biotechnology Information). The start codon (ATG) and stop codon (TGA) are highlighted in blue and red, respectively. Codon AAG encoding a lysine in the WT sequence where subsequent mutations were generated is highlighted in pink. (B) Analysis of DNA sequencing chromatograms by 4Peaks Software from HA-H4WT, HA-H4K16R, HA-H4K16Q retroviral constructs. Appropriate base pair substitutions were confirmed as highlighted with H4K16R containing AAG-> CGG substitution and H4K16Q containing AAG->CAG substitution.

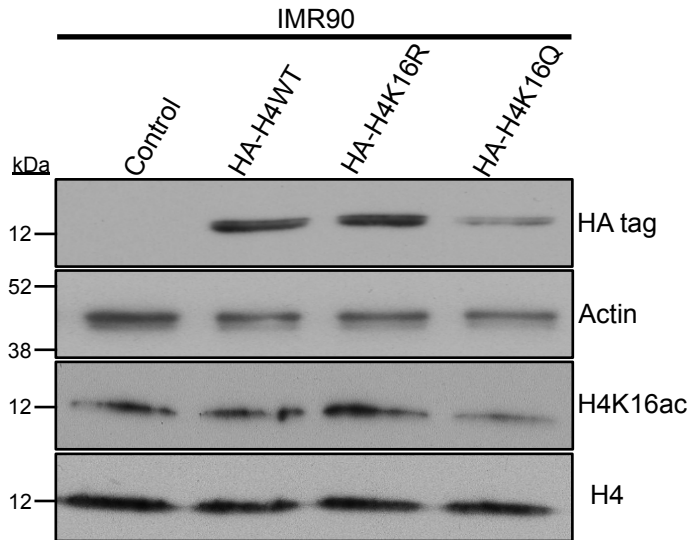


Figure 6.13 Establishment of histone mutant cells.

Proliferating IMR90 were infected with control, HA-H4WT, HA-H4K16R, HA-H4K16Q retroviral constructs. After infection, cells were drug selected with puromycin. Whole cell lysates were then harvested and 20  $\mu$ g protein per sample was loaded on to SDS-PAGE for fractionation and Western blotted for HA tag. Actin was used as loading control. Also expression of H4K16ac was assessed using H4 as loading control.

technology such as ChIP. Also it is reasonable to propose that any effect of mutants will be observed at TSS, as this is where chromatin is most dynamic. Based on this, I conclude effective establishment of histone mutant cells to investigate role of H4K16ac.

#### *6.3.7.3 Induction of senescence in H4WT and H4K16R cells using IR*

The next step was to induce senescence in H4WT and mutant cells that were established to understand the functional role of H4K16ac. For simplicity, proliferating HA-H4WT and HA-H4K16R cells were irradiated with 20Gy to induce senescence. Proliferating (untreated) and IR-treated HA-H4WT and HA-H4K16R cells were harvested 10 days after exposure. Whole cell lysates were harvested from cells and separated using SDS-PAGE. Western blot analysis of extracts confirmed that both proliferating and senescent HA-H4WT, HA-H4K16R mutant cells express the HA tag (Figure 6.14). Also, markers of proliferation arrest such as decreased cyclin A and phosphorylation of pRB at serines 807/811 were observed only in the IR-induced population based on using actin as a loading control. Hence, establishment of senescence using IR treatment was confirmed in HA-H4K16R and HA-H4WT cells for subsequent use.

#### *6.3.7.4 Loss of H4K16ac enrichment observed in H4K16R mutants*

Once senescence was established, chromatin was extracted from proliferating and senescent HA-H4WT and HA-H4K16R mutant cells. H4K16ac and negative control IgG ChIP were performed using the same conditions as before (Section 6.3.2). ChIP DNA extracted was analysed using SYBR green real-time quantitative PCR across the regions mentioned in Figure 6.6. Results indicated that regions with no specific enrichment for H4K16ac, namely ChrX, Chr1 and Chr5, did not show any substantial enrichment for the mark in proliferating and senescent WT and mutant cells (Figure 6.15). Regions of specific enrichment for H4K16ac showed increase in enrichment after IR, as expected in HA-H4WT cells. In comparison to senescent HA-H4WT cells, HA-H4K16R mutant cells exhibited decreased enrichment of H4K16ac across 3 out of 5 regions of senescence-specific enrichment of H4K16ac based on ChIP-seq. These results convincingly suggest that H4K16R mutants may be used to dissect functional

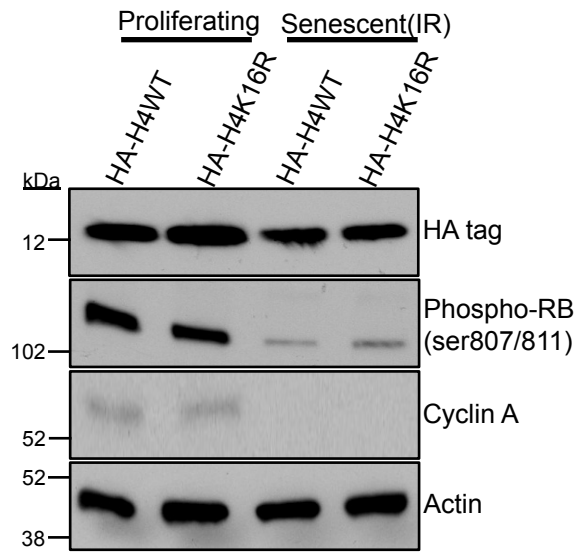


Figure 6.14 Induction of senescence in histone mutant cells.

Proliferating HA-H4WT and HA-H4K16R cells were seeded at low density and exposed to 20 Gy irradiation or left untreated. Whole cell lysates were harvested on day 10 and from untreated and irradiated cells. 20  $\mu$ g protein per sample was loaded on to SDS-PAGE for fractionation and Western blotted for makers of cell cycle arrest, senescence and HA tag. Actin was used as loading control.

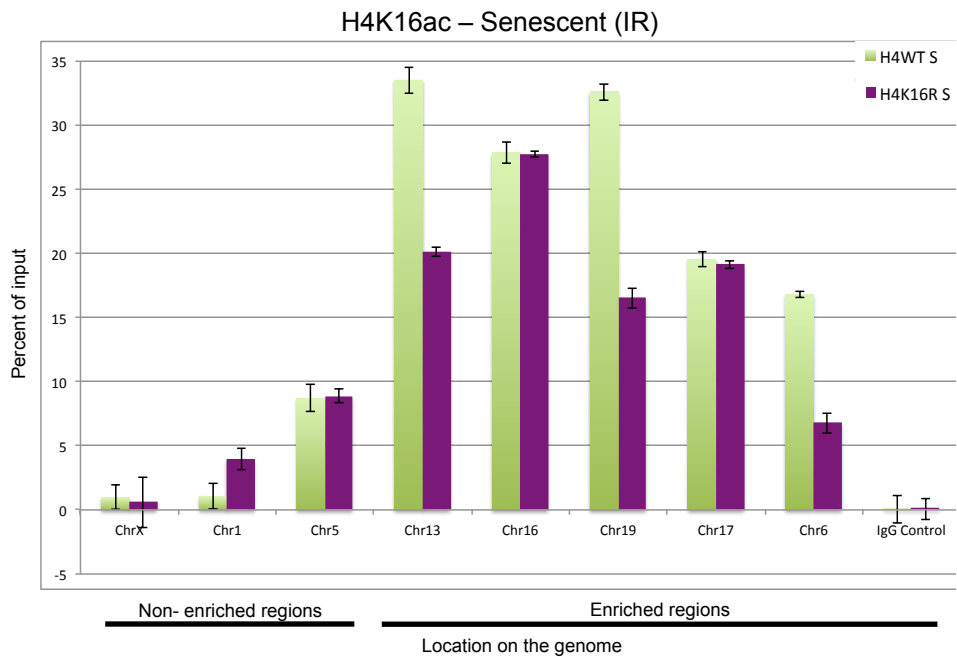
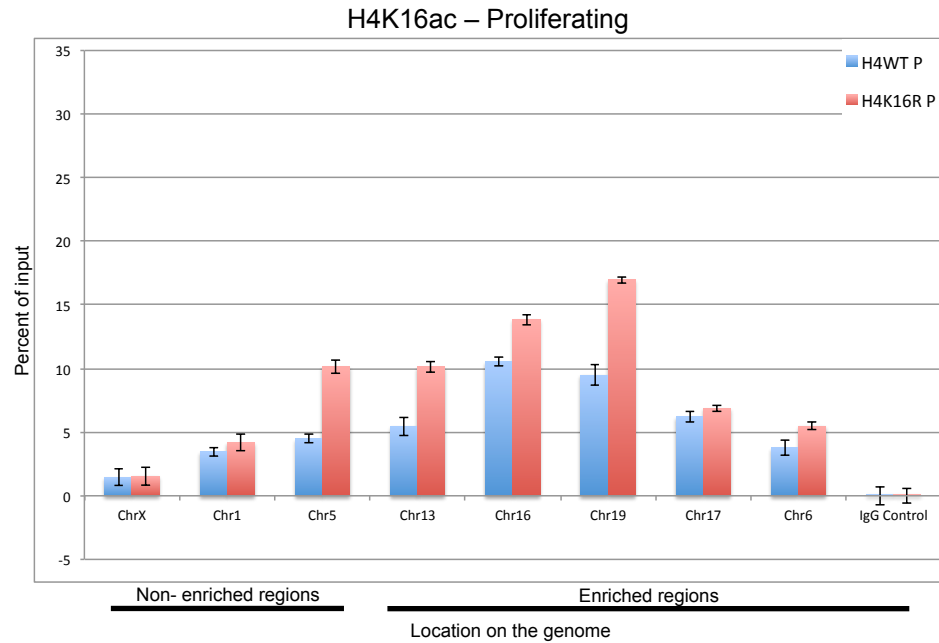


Figure 6.15 Depletion in H4K16ac levels observed in HA-H4K16R-expressing senescent cells. H4K16ac ChIP in proliferating HA-H4WT (blue) and HA-H4K16R (red) and senescent HA-H4WT (green) and HA-H4K16R (purple) cells was performed followed by real-time SYBR green quantitative PCR using primer sets corresponding to different regions of the genome with control IgG ChIP. Chr X, Chr1 and Chr5 represent regions of no enrichment for H4K16ac in senescence, based on ChIP-seq. Chr13, Chr16, Chr19, Chr17 and Chr6 represent regions of specific enrichment for H4K16ac in senescence. IgG control performed on region from Chr 17. Error bars represent PCR technical replicates, from a single biological replicate.

role of acetylation at H4K16 in senescence, albeit effect of substitution was restricted to specific locations.

### **6.3.8 *KD of HIRA***

The HUCA complex, comprising HIRA chaperone complex (HIRA, UBN1, CABIN1) along with ASF1a, incorporates histone variant H3.3 into chromatin in a DNA replication-independent manner [278, 380, 571, 572]. In senescent cells, HIRA mediated H3.3 deposition occurs at gene promoters (Rai et al., In preparation), similar to H4K16ac accumulation at gene promoters. Based on these two independent observations in the lab, it was tempting to speculate that HUCA might be required for deposition of H4K16ac at promoters. In order to test the hypothesis, senescent cells lacking HIRA were established.

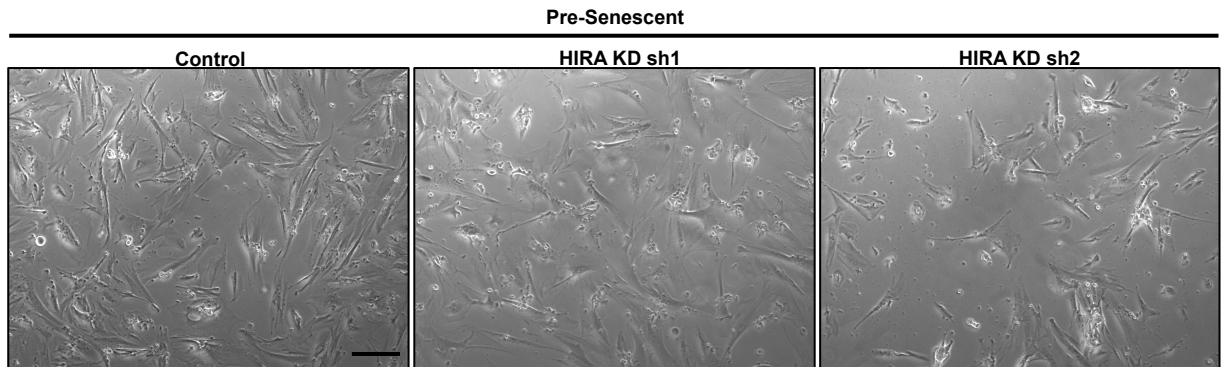
#### **6.3.8.1 *KD of HIRA in pre-senescent cells***

Prior to testing if HIRA is essential for the deposition of H4K16ac at promoters by ChIP, the global level of H4K16ac was assessed in cells lacking HIRA. Pre-senescent IMR90 were infected with lentivirus containing short hairpins to luciferase and HIRA (viruses prepared by Claire Brock in the lab). For HIRA KD, two different short hairpins, hereafter termed sh1 and sh2, were used. Infected cells were drug selected, passaged and bright field microscopy images were used to detect early signs of senescence with enlarged, flattened morphology in control (shluciferase), HIRA sh1 and HIRA sh2 cells (Figure 6.16.A). Also whole cell lysates were harvested from cells and subjected to SDS-PAGE fractionation and Western blotted for HIRA. Figure 6.16.B confirmed HIRA KD in sh1 and sh2 cells in comparison to using, actin as loading control.

#### **6.3.8.2 *Establishing senescent cells lacking HIRA via long-term passaging***

Upon confirmation of HIRA KD, control (shluciferase), HIRA sh1 and sh2 cells were passaged for several weeks until the last population doubling to establish senescence. Cells were assayed for SA  $\beta$ -Gal activity following standard protocol outlined in Chapter 2 Materials and Methods Section 2.2.21. Figure 6.17 confirmed

(A)



(B)

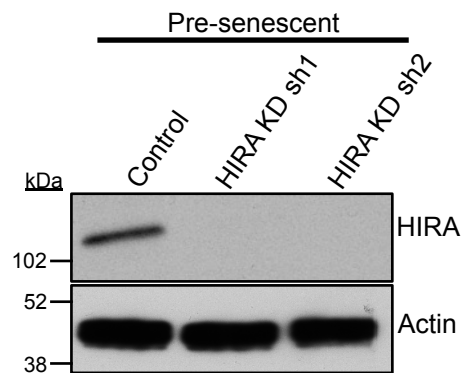


Figure 6.16 KD of HIRA in pre-senescent cells.

IMR90 cells at PD 62 were infected with lentivirus encoding shRNA to luciferase and two different short hairpins to KD HIRA. After drug selection of infected cells (A) light microscopy images of control (shluciferase), HIRA KD sh1, HIRA KD sh2 cells approaching senescence were taken under 20X objective. (B) Whole cell lysates were harvested and 20  $\mu$ g protein per sample was loaded on to SDS-PAGE for fractionation and Western blotted for HIRA. Actin was used as loading control.

senescence in comparison to proliferating cells. Further to this, cells were also assayed using fluorescence microscopy in the green channel along with nuclear DNA staining termed Hoescht. Figure 6.18 further confirmed growth arrest since control (shluciferase) and HIRA sh1 and sh2 cells showed less than 3% EdU incorporation, as opposed to over 80% positive cells in proliferating cells. This was quantified on a bar graph based on visualization of EdU staining. Thus, senescent cells lacking HIRA were successfully established.

#### *6.3.8.3 Decreased H4K16ac in senescent cells lacking HIRA*

To test the effect of HIRA KD on total H4K16ac abundance, whole cell lysates were prepared from senescent control (shluciferase), HIRA sh1 and sh2 cells. Lysates were fractionated using SDS-PAGE and Western blotted for HIRA and H4K16ac. Results confirmed decreased levels of the histone mark in HIRA KD cells in comparison to shluciferase (Figure 6.19), based on total H4 as a loading control.

#### *6.3.8.4 HIRA maybe required for enrichment of H4K16ac at gene promoters in senescent cells*

The next step was to perform ChIP for H4K16ac in senescent cells lacking HIRA and test whether HIRA is required for enrichment of the histone mark at promoters. Chromatin extracted from senescent shluciferase, HIRA sh1 and sh2 cells were subjected to ChIP. H4K16ac and IgG ChIP DNA extracted from the three cell types were analysed using SYBR green real-time quantitative PCR. Regions of non-enrichment (ChrX, Chr1) and regions of enrichment for H4K16ac (Chr13, Chr19, Chr17) were analysed (Figure 6.20.A). In addition to testing various regions across the genome based on H4K16ac ChIP-seq only, a new primer pair was picked to a different region on Chr17 (called region 2, Figure 6.20.B). This was based on HIRA, H3.3 and H4K16ac overlapping regions at the TSS of gene promoters in senescent cells. H4K16ac enrichment and non-enrichment observed at specific regions in senescent shluciferase cells were in concordance with results obtained in replicative senescence (Figure 6.6). Likewise in HIRA sh1 and sh2 cells, ChrX and Chr1 regions remained negative for H4K16ac enrichment. However Chr13 did not show any marked decrease in H4K16ac levels in sh1 and sh2 cells when compared to

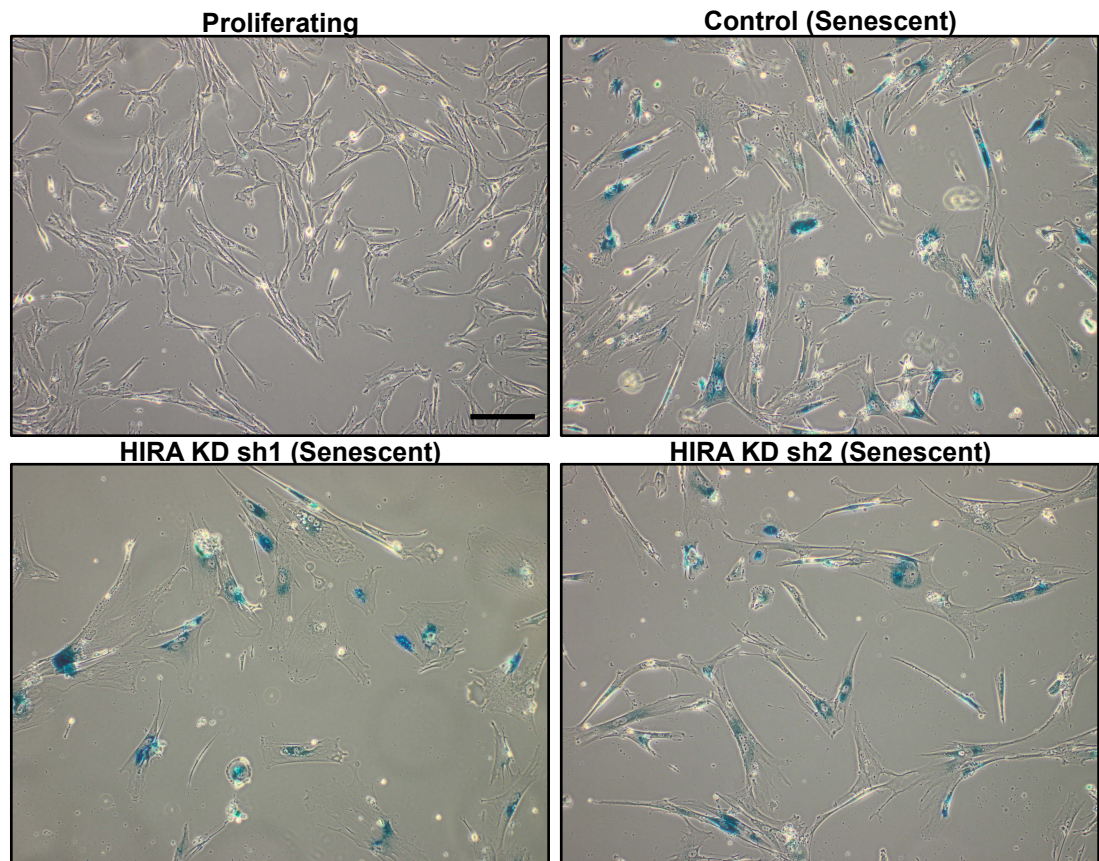


Figure 6.17 Senescent cells lacking HIRA exhibit SA  $\beta$ -Gal staining.

Senescent cells containing shluciferase (control - 97.8% SA  $\beta$ -Gal+) and lacking HIRA (sh1 - 98% SA  $\beta$ -Gal+ and sh2 - 96.7% SA  $\beta$ -Gal+) were stained along with proliferating cells (5.2% SA  $\beta$ -Gal+) overnight at 37°C for their SA  $\beta$ -Gal activity following standard protocol. Light microscopy images were taken under 20X objective along with proliferating IMR90 cells, used as a negative control.

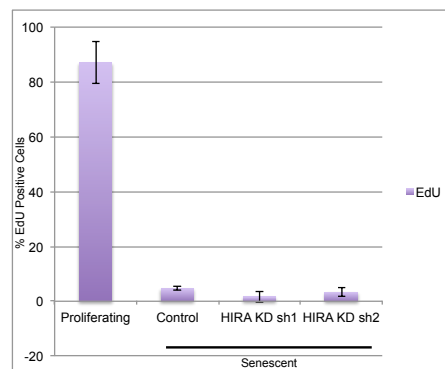
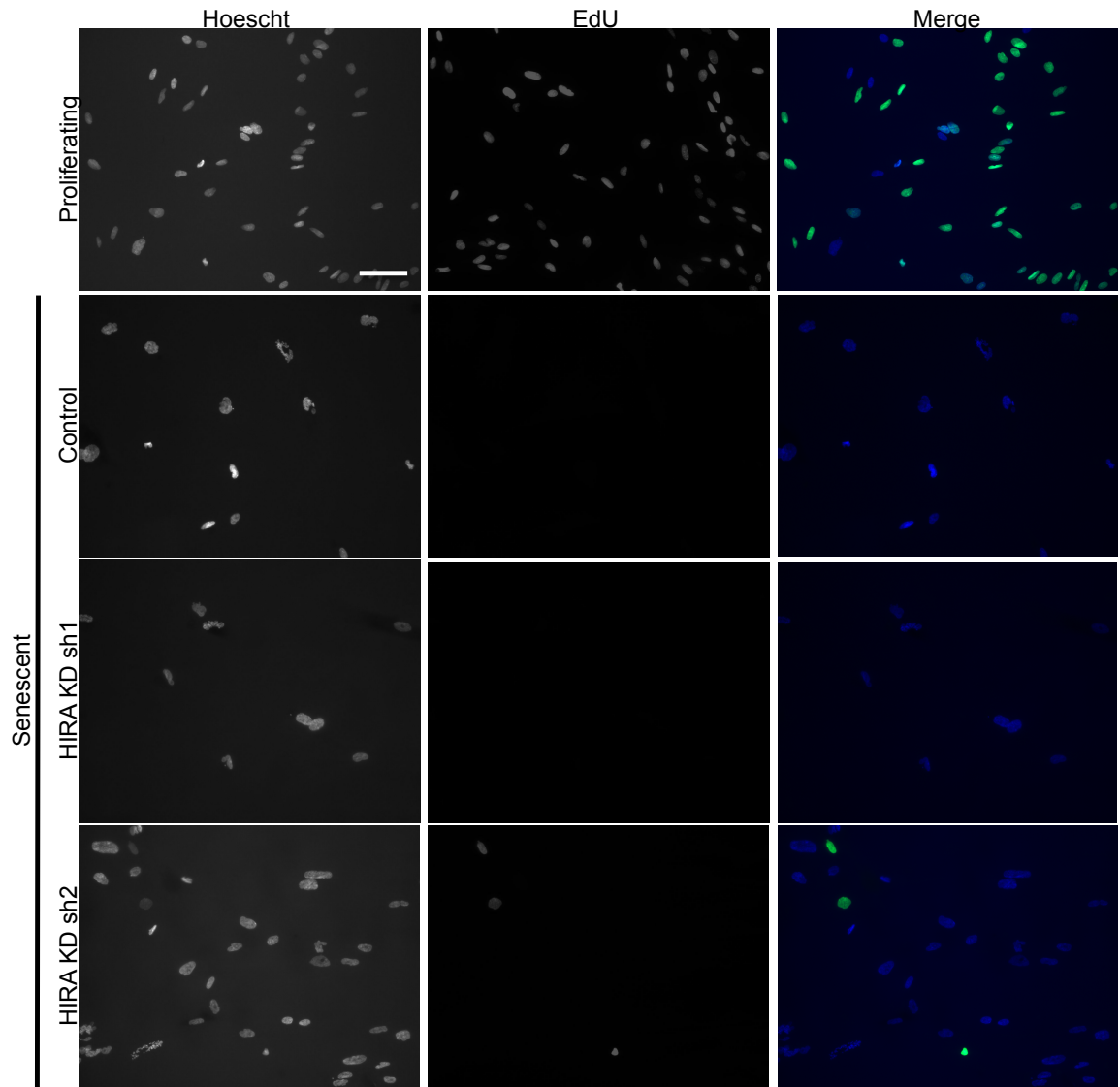


Figure 6.18 Confirmation of growth arrest in senescent cells lacking HIRA.

Proliferating IMR90 and senescent cells containing shluciferase (control) and sh1, sh2 for HIRA KD were assayed for cell proliferation using EdU assay. (A) Stained cells were visualized in the green channel, along with DAPI (blue). All images were taken at the same exposure. (B) Staining was quantified on a bar graph with error bars representing technical replicates.

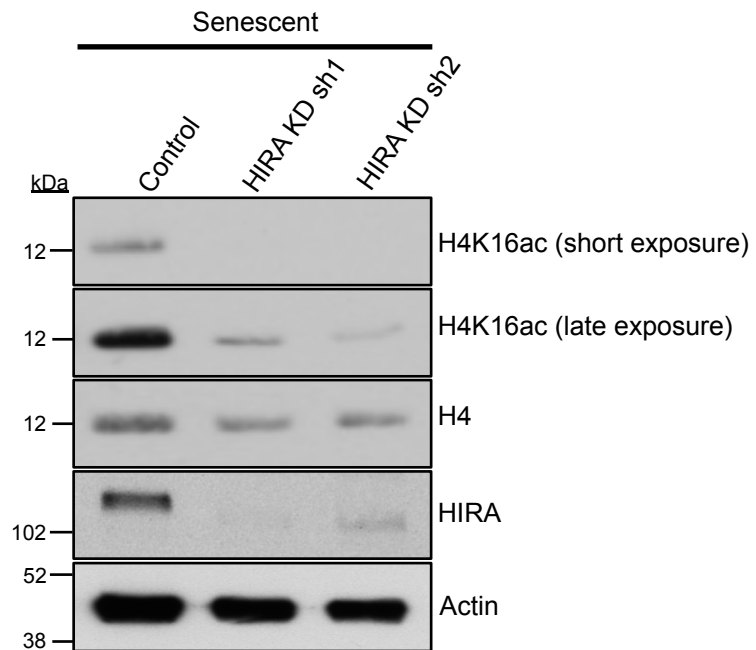
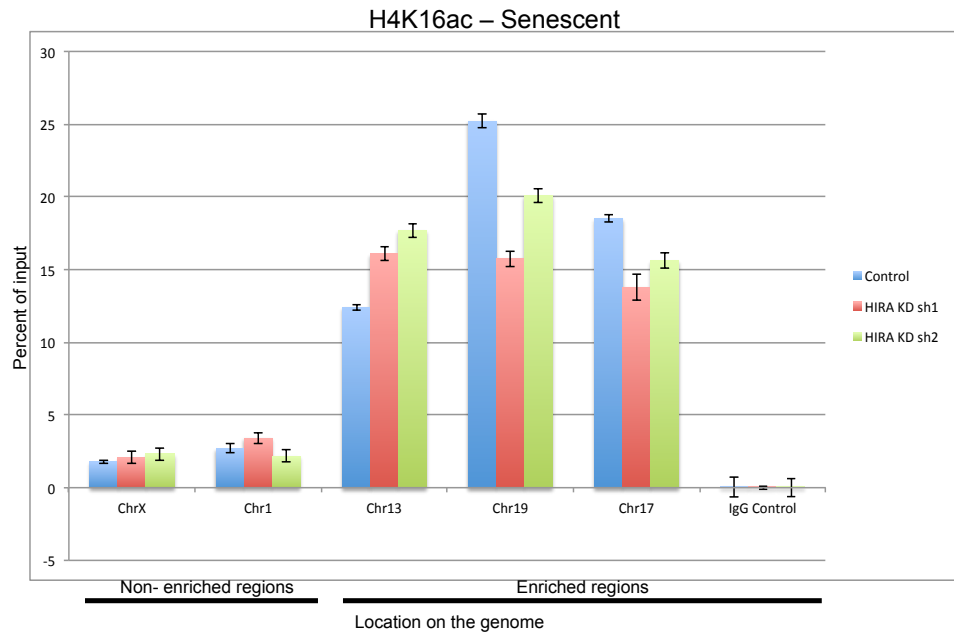


Figure 6.19 Senescent cells lacking HIRA show decreased total H4K16ac.

Whole cell lysates were harvested from control (shluciferase), HIRA KD sh1 and sh2 cells after senescence establishment. 20  $\mu$ g protein per sample was loaded on to SDS-PAGE for fractionation and Western blotted for levels of H4K16ac with H4 as loading control. Lysates were also blotted for HIRA with actin as loading control.

(A)



(B)

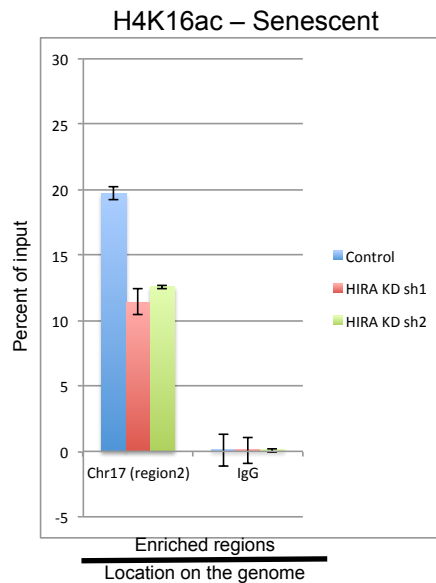


Figure 6.20 Depletion of H4K16ac at regions of the genome observed in senescent cells lacking HIRA. (A) H4K16ac ChIP in senescent control (shLuciferase cells) (in blue), senescent HIRA sh1 (in red) and HIRA sh2 cells (in green) followed by real-time SYBR green quantitative PCR was carried out using primer sets corresponding to different regions of the genome along with control IgG ChIP (Chr17). Chr X and Chr1 represent regions of no enrichment for H4K16ac in senescence, based on ChIP-seq. Chr13, Chr19 and Chr17 represent regions of specific enrichment for H4K16ac in senescence. IgG control performed on a region from Chr 17 (B) ChIP-PCR performed at a different region on Chr 17 termed region 2. Error bars represent PCR technical replicates, from a single biological replicate.

shluciferase. If anything, a marginal increase in H4K16ac enrichment was observed. Whereas Chr19, Chr17, Chr17 region2 showed observably less accumulation of H4K16ac in comparison to shluciferase. It was noticeable that loss of H4K16ac at these regions were more pronounced in HIRA sh1 cells in comparison to sh2 cells. This is in line with efficiency of HIRA KD observed in these cells in comparison to shluciferase (Figure 6.19) where higher levels of KD was observed in sh1 by Western blotting. This novel observation may imply that HIRA may be required for deposition of H4K16ac at specific regions across the genome in senescent cells. Additional studies are required to confirm or refute and/or optimize this.

#### 6.4 Discussion

Deposition of an acetyl group at H4K16 is a key event in regulating chromatin structure [534-537]. Decreased H4K16ac has been reported in cellular senescence [545, 547] and given its importance associated with disease states such as cancer and ageing [401, 545, 546] it was important to understand how this particular mark is regulated during senescence.

David Nelson carried out genome-wide ChIP-sequencing of H4K16ac in replicative senescence to understand how this mark was distributed. Results were analysed by Tony McBryan and John Cole. H4K16ac showed striking enrichment across regions such as the TSS of gene promoters, gene bodies, and CpG islands of the senescent genome. 17,977 domains of differentially enriched regions of H4K16ac were identified in senescent cells compared to proliferating cells. Also enrichment of the histone mark correlated with gene expression in senescent cells, with the mark being significantly enriched at those genes showing high to medium levels of expression during senescence and no specific enrichment at genes with low levels of expression. Hence, key findings revealed that H4K16ac accumulated at gene promoters of senescent cells, despite observations that global levels of H4K16ac decreased during senescence.

Why H4K16ac accumulates at specific promoter regions in senescence despite overall depletion is unclear. Loss of H4K16ac was demonstrated in a multi-stage mouse model of skin carcinogenesis [573]. During the course of tumorigenesis loss of H4K16ac was reported at hypomethylated DNA repetitive sequences. Perhaps

H4K16ac is also lost at repetitive regions in senescence, but gained at promoters. Hence, I set out to establish *in vitro* tools to deplete H4K16ac and further elucidate the role of H4K16ac in senescence and its specific accumulation at gene promoters.

Prior to setting up experiments, ChIP-seq results needed to be confirmed. Results from H4K16ac ChIP reaffirmed original ChIP-seq observation, by showing striking enrichment of H4K16ac in senescent cells across different regions (Chr13, Chr16, Chr19, Chr17 and Chr6). Also, regions of non-enrichment of H4K16ac (ChrX, Chr1 and Chr5) did not show any increase in the mark. Hence, independent experimental validation of the ChIP-seq result by quantitative PCR indicated that identification of H4K16ac enrichment at specific regions across the genome during senescence was accurate and likely to be functionally relevant.

Also, a second model of senescence, i.e., DNA-damage induced senescence, was tested in IMR90s to induce senescence to the same extent as replicative senescence. Successful establishment of IR-induced senescent cells in the lab was confirmed by growth arrest, visualization of morphological changes and also appearance of markers of senescence by Western blotting assays. Hence, this proved to be a more time-effective model for the establishment of senescence, as opposed to several months of serial passaging to attain RS.

Before performing further experiments, it was important to test if accumulation of H4K16ac at specific regions across the genome could be observed in IR-induced model of senescence. Chromatin extracted from proliferating and IR-induced senescent cells were subjected to H4K16ac ChIP PCR to test regions of specific enrichment and non-enrichment of H4K16ac as observed previously in the replicative senescence model. An increase in the histone mark was noted across regions of enrichment (Chr13, Chr16, Chr19, Chr17 and Chr6) in IR-induced senescent cells and no increase in the mark was noted in regions of non-enrichment for H4K16ac (ChrX, Chr1 and Chr5). These observations demonstrate that enrichment of H4K16ac in replicative senescent cells could be remarkably reproduced in a second model of senescence.

To understand the function of H4K16ac at promoters, the next step was to deplete the mark in senescent cells. To do this, KD approaches were directed towards a well-known HAT for H4K16ac, hMOF [556]. Studies showed the KD of hMOF resulted in global loss of H4K16ac [549, 574] in proliferating cells.

To establish stable KD of hMOF in senescent cells, a library of short hairpins from Open Biosystems was screened. Only one short hairpin was identified to have efficient KD of hMOF and cells lacking hMOF showed a stressed phenotype in comparison to control cells or cells with no KD for hMOF. A previous study in HeLa cells reported that loss of hMOF resulted in defects in the nuclear structure of cells. Also the study pointed out that cells lacking hMOF showed compromised cell proliferation, possibly due to the inability of those cells to efficiently repair DNA double strand breaks [549]. Unfortunately, owing to inherent toxicity observed due to loss of hMOF in IMR90, devising further experiments with these cells and also establishing senescence in the same would prove to be extremely challenging. Hence, due to technical issues associated with hMOF loss and also due to the availability of only one validated antibody to visualize hMOF, other *in vitro* tools to deplete H4K16ac were explored.

SIRT1 was reported to deacetylate H4 at K16ac [550, 561-563]. Overexpression of SIRT1 was employed in IMR90 cells to decrease H4K16ac. Western blotting assay confirmed overexpression of SIRT1 WT and H363Y mutant in IMR90s. Prior to establishment of senescent SIRT1 cells, activity of SIRT1 WT was compared against SIRT1-H363Y mutant cells in the presence of genotoxic insult using etoposide. Upon treatment of cells with 20  $\mu$ M etoposide, only SIRT WT (not SIRT1 mutant) showed reduced acetylation of p53 at lysine 382. Control and SIRT WT cells were induced to enter senescence using IR. Overall levels of H4K16ac remained unaffected by Western blotting after overexpression of the deacetylase. With a previous study pointing out that modulation of SIRT1 to alter levels of H4K16ac is possibly gene-specific [575], it is feasible to speculate that this may lead to a decrease in H4K16ac only at specific locations in senescent cells. Any changes of H4K16ac distribution in these cells can only be assayed using ChIP. An alternative approach would be to use the deacetylase SIRT2 that has been shown to be effective at global deacetylation of H4K16ac during mitosis [575].

Depletion of H4K16ac in IMR90s was also possible with the help of mutant cells. Dang et al., originally described H4K16 mutant cells [401] in yeast studies. With the help of site-directed mutagenesis, HA-tagged H4WT, H4K16R and H4K16Q mutant cells were established. Although the cells were engineered to overexpress high levels of the mutant histone, global levels of H4K16ac appeared to be largely

unaffected or unaltered in mutant cells in comparison to H4WT or control cells. This may be because levels of overexpression were not sufficient to displace naturally occurring histones, given that they are one of the most abundant proteins in cells. Nevertheless, with the histone mutant cells, loss of H4K16ac could be effective at specific locations of the genome as some sites turnover more rapidly than the surrounding regions. To test this, a site-specific technique such as ChIP-PCR was necessary.

The next step was to create senescent cells overexpressing H4K16 mutations. For simplification, H4WT and H4K16R cells were treated with IR and maintained in culture for over 10 days. Whole cell lysates tested positive for markers of proliferation arrest. Cells were harvested to perform H4K16ac ChIP and negative control IgG ChIP. Proliferating cells showed a marginal increase of H4K16ac at Chr19 in H4K16R cells. This may be down to disruption of the normal stoichiometry of histones in cells by overexpression of H4K16R. H4WT cells retained specific enrichment and non-enrichment for H4K16ac at specific regions across the genome. However levels of H4K16ac enrichment were remarkably lower in H4K16R mutant cells at regions Chr13, Chr19, and Chr6 in comparison to WT cells. Chr16 and Chr17 did not show an apparent decrease and this may be explained by the fact that turnover rates at some sites may be slower in comparison to surrounding sites. Nevertheless preliminary results using senescent H4K16R mutants appear encouraging with depletion of the histone mark at specific regions across the genome known to have H4K16ac accumulation during senescence.

Lastly, an indirect approach to deplete H4K16ac was used. The idea that HIRA might be responsible for H4K16ac accumulation observed at the TSS of gene promoters in senescent cells was hypothesized after observations from ChIP-seq experiments demonstrating HIRA mediated H3.3 deposition and H4K16ac at the same regions (Rai et al., In preparation). Overlapping results from HIRA/H3.3 ChIP-seq and H4K16ac ChIP-seq demonstrated a striking H3.3 enrichment flanking H4K16ac peaks. The hypothesis was also supported by initial observations made by Taranjit Rai and Claire Brock (and repeated by me) that the total level of H4K16ac is reduced in senescent cells lacking HIRA, and this phenomenon is exclusive to H4K16ac in comparison to other well-known histone modifications, such as H3K27me3, H4K20me3. Encouraged by these striking observations, I set out to

establish senescent cells lacking HIRA. Pre-senescent cells were infected with short hairpins encoding shluciferase and HIRA. Establishment of senescence in HIRA sh1, sh2 and shluciferase cells was confirmed using SA  $\beta$ -Gal and EdU staining.

Senescent cells lacking HIRA were then harvested for H4K16ac and IgG ChIP. Regions of non-enrichment, namely ChrX and Chr1, remained negative for H4K16ac enrichment in shluciferase, HIRA sh1 and sh2 cells. Regions of specific enrichment, Chr13, Chr19 and Chr17 showed marked increase in H4K16ac in senescent shluciferase cells. Remarkably, these regions showed reduced levels of H4K16ac in HIRA KD sh1 and sh2 cells, with the exception of Chr13. In line with levels of HIRA KD, sh1 cells showed a greater decrease in H4K16ac enrichment than sh2 cells.

However, not all regions showed depletion of the histone mark in senescent cells lacking HIRA. Chr13, if anything, showed a marginal increase in enrichment of H4K16ac in HIRA KD cells. At this point it is important to emphasize that regions assayed using ChIP PCR were based on differential binding analysis for H4K16ac using ChIP-seq and correspond to various regions across the genome. Significant enrichment of HIRA mediated H3.3 peaks colocalized with H4K16ac enrichment was observed specifically at TSS of expressed gene promoters. This may imply that HIRA KD may affect H4K16ac distribution more specifically at those regions. Hence, a new primer pair was synthesized to a different region on Chr17, named region2, and decreased H4K16ac enrichment was observed in HIRA KD cells. This might mean that HIRA's deposition of H3.3 at gene promoters and also enrichment of H4K16ac at the same regions might be involved in a dynamic process of regulating chromatin structure and gene expression. These novel observations remain to be tested again in a controlled manner using biological repetitions. Also, more regions, in specific TSS of those genes that are highly expressed in senescent cells remain to be tested, as high expression of the genes may indicate more dynamic turnover of H4K16ac at the promoters.

To summarize, it is extremely important to further characterize and perform functional dissection of H4K16ac in senescence using the *in vitro* tools established through this project.

## **7. DISCUSSION AND FUTURE PERSPECTIVES**

## 7 DISCUSSION AND FUTURE PERSPECTIVES

---

Cellular senescence was originally described as a state of permanent cell cycle arrest arising from limited proliferative capacity of human diploid fibroblasts [1]. It is now apparent that senescence is a more widespread phenomenon than previously appreciated. A number of markers, such as SA  $\beta$ -gal activity, characterize senescent cells. In addition, senescent cells show changes in their chromatin structure, of which SAHF has been intensely studied [13]. Various roles are attributed to SAHF in senescence, including maintenance of senescence arrest via modulation of gene expression and restraining DNA damage [176]. How specific histone modifications impact on key aspects of chromatin regulation and therefore senescence remains to be elucidated. Also, given the fact that senescence contributes to various pathological and physiological processes of ageing and cancer [9], it is important to increase the current understanding of chromatin-mediated regulation of senescence.

To this end, I set out to perform large scale profiling of various histone modifications in senescence. Through this screen, I identified novel histone modifications, such as H3K56me, H3K9 pan-me, H3CS.1, H4R3me2a, H2BK16ac, that increase in abundance at the onset of senescence. H3CS.1 and H4R3me2a were chosen for subsequent study. Apart from these two modifications, the role of H4K16ac in senescence was also probed, owing to its association with senescence and also due to its importance in senescence-associated processes, such as cancer and ageing.

### 7.1 H3CS.1 and senescence

To our knowledge, this is the first study to report an increase in Cathepsin L and H3CS.1 during cellular senescence and demonstrate its potential significance. Strikingly, H3CS.1 was localized largely to the cytoplasmic compartment of senescent cells. This work contributed towards publication of a paper in the Journal of Cell Biology (Ivanov, Pawlikowski, Manoharan et al., 2013 [482]). Accumulation of H3CS.1 was antagonized in senescence by bafilomycin A treatment which inhibits autophagic/lysosomal machinery. Autophagy and senescence are closely related, at least in oncogene-induced senescence [111]. Although bafilomycin A treatment

restricted accumulation of H3CS.1 in senescent cells, it did not abrogate the development of senescence [482]. This led us to hypothesize that Cathepsin L mediated H3CS.1 cytoplasmic accumulation in senescent cells is a result of autophagic/lysosomal processing of histones in senescence and this potentially contributes to 'mass' clearing of histones in senescent cells.

The Tyler and Karlseder groups first reported a direct relationship between loss of core histone H3 and H4 and ageing [173, 174]. DNA damage is proposed to be the driving force of loss of histones in human fibroblasts [174]. Remarkably, Tyler and colleagues demonstrated extension of lifespan in yeast by increasing histone levels [173]. Recently the group reported a decrease in nucleosome occupancy by 50% across the whole genome during replicative ageing [576]. Also, the relative abundance of histone variants also plays a crucial role during ageing. During metazoan ageing, loss of canonical histones H3.1 and H3.2 and increase in replication-independent variant H3.3 occurs [276, 577, 578]. Duncan et al., demonstrated that variant H3.2 is preferably cleaved over H3.3 during ESC differentiation [474]. Such controlled proteolysis of nuclear proteins can play a crucial role during transcriptional regulation and other cell processes. For example, during granulocyte differentiation, transcriptional replication or transcription was facilitated via H2A-specific proteolysis [579]. In *Chlamydia trachomatis*, histone H1-specific proteolytic activity contributes to chromatin decondensation [580]. Also, cultured mammalian cells infected with causative virus for the foot and mouth disease (FMDV) demonstrated proteolytic cleavage of H3 by the enzyme FMDV 3C protease and this was suggested to play a role in restricting host cell transcription [581]. A shorter form of histone H3 was also reported in yeast [582].

In 2009, Kouzarides and colleagues presented a biological function for H3 tail clipping [483]. They reported, in yeast, H3 tail clipping facilitates localized clearing of repressive signals to promote gene expression. Selective clipping of H3 tails carrying repressive marks, such as H3R2me2, occurred to enable gene activation, and somehow tails were protected from clipping when presenting active marks, such as H3K4me3. Interestingly, the authors also linked H3 tail clipping to nucleosome eviction. Hence, it is plausible to suggest that H3CS.1 marks nucleosomes for eviction prior to gene induction.

In this manner, H3CS.1 increase during the transition from proliferation to senescence may have consequences for transcription control during senescence establishment. To test its importance in the same, constructs harboring mutations in the H3 cleavage site (between amino acids 21 and 27) could be introduced into human cells. Following this, mutant cells can be tested for any impairment of gene induction during senescence. In both yeast and mice, amino acid 21 appears to be the primary site of H3 clipping [474, 483]. A crucial role for Cathepsin L in epigenetic regulation of gene expression has already been suggested from cells lacking Cathepsin L [583]. In mouse, H3 cleavage by Cathepsin L inhibits binding of PcG protein CBX7 to methylated H3K27, facilitating derepression of genes in ESC during differentiation [474]. In line with this, it would be interesting to map the distribution of H3CS.1 to identify potential cross talk with other well-known chromatin signatures in senescence. Other possibilities of addressing a potential role for H3CS.1 in transcriptional control can be addressed using chemical inhibition of Cathepsin L [584-586] or siRNA mediated KD of Cathepsin L. Alternatively, stable reduction in H3CS.1 could be achieved using shRNA mediated KD of Cathepsin L.

It also remains to be formally determined whether Cathepsin L is the enzyme responsible for the increase in H3CS.1 during senescence. This can be tested with the proposed Cathepsin L inhibitor experiments (discussed above). It is also possible that there are other enzymes with the capacity to clip H3. In the human genome, Cathepsin V bears close sequence similarity to Cathepsin L and both proteases are suspected to be a result of gene duplication, owing to their proximity to one another on chromosome 9 [587]. In support of overlapping functions, transgenic experiments in mice demonstrated that human Cathepsin V rescues the skin phenotype of Cathepsin L knock out mice [588], characterized by periodic hair loss and epidermal hyperplasia [589, 590]. Given that Cathepsin V does not occur in the mouse genome, the authors performed rescue experiments using a transgenic mouse line expressing human Cathepsin V under the control of human keratin 14 promoter [588]. These Cathepsin V inducible mice provided evidence for a role of Cathepsin V in maintenance of epidermis and hair follicles, similar to Cathepsin L. This leads me to ask whether Cathepsin V and Cathepsin L have similar substrate specificity in senescent cells. Functional redundancy between the two enzymes may exist to effectively control H3CS.1 during senescence. Along with inhibitor experiments,

Cathepsin L knock-out mice will be a useful tool to address requirement of the enzyme in regulation of H3CS.1 during senescence.

Cathepsin L affects other processes such as apoptosis, angiogenesis, invasion and metastasis [591]. Increased Cathepsin L is proven in multiple malignancies, such as colon, gastric, breast, lung, gliomas, head and neck carcinomas and melanomas [592-594]. For example, Cathepsin L was proposed as a biomarker in ovarian cancer, as the serum level of Cathepsin L was markedly higher in patients with ovarian malignant tumors than in benign tumors and healthy controls. Expression of Cathepsin L was also significantly higher in malignant tumor tissues in comparison to benign or normal ovarian tissues [595]. Cathepsin L is also implicated in the sequestration of chemotherapeutic drugs, thereby dampening toxicity on target cells [596-598]. Therefore, efforts are now being diverted to target Cathepsin L in specific anti-cancer therapies to improve drug efficiency [591]. Understanding the role of Cathepsin L and its substrate H3CS.1 in senescent cells may potentially uncover an unprecedented role in cancer.

In summary, future studies aimed at addressing the function and regulation H3CS.1 in senescence might reinforce the relevance of loss of histones from senescent cells. Perhaps this might have significant implications on senescence-mediated functional decline observed with age.

## 7.2 H4R3me2a and senescence

This project demonstrated for the first time that H4R3me2a, an active histone mark, was increased during RS and OIS, accompanied by increase in the methyltransferase, PRMT1. KD experiments of the enzyme proved that PRMT1 was essential for the increase in H4R3me2a during senescence. H4R3me2a is associated with transcriptional activation. The level of methylation on H4R3 predicts the risk of prostate cancer, as the level of the mark positively correlates with tumor grade. Also, aberrant expression and altered regulation of PRMT1 is implicated in cancer [599]. Although PRMT1-mediated arginine methylation is linked to cancer via its role in processes, such as proliferation, transformation and anti-apoptotic properties, the field still lacks an understanding of the precise role in these contexts [600]. Given the link between senescence and cancer, understanding the relative importance of

PRMT1 mediated H4R3me2a during senescence is essential. Key findings from this project, along with current knowledge, leads us to anticipate a role for PRMT1-mediated H4R3me2a in senescence-associated tumor suppression via chromatin regulation.

In line with this, to the understand function and regulation of H4R3me2a during senescence multiple strategies can be employed. Emerging evidence now suggests that H4R3me2a levels can be altered by other mechanisms, such as deimination to convert arginine methylation to citrulline [601-603]. DDR signalling plays an important role in inducing and maintaining senescence and it has also been shown to be an inducer of deamination [524]. Also, cross talk between arginine methylation and citrullination has implications in downstream chromatin events [604]. It will be interesting to test if the increase in PRMT1-mediated H4R3me2a in senescent cells leads to an increase in citrullination, or whether citrullination, whose primary function is to turn off gene expression, is counteracted selectively in senescence by over production of H4R3me2a. To test this, levels of citrullinated H4 and PADI4 (the enzyme responsible for conversion of arginine methylation to citrulline) needs to be analysed during senescence. Additionally, KD or overexpression approaches might help identify any concerted efforts between H4R3me2a and citrullination during senescence.

PRMT1 KD cells generated as part of this study will be useful to study PRMT1 and H4R3me2a function. The next step will be to perform comprehensive expression profiling of senescent cells lacking PRMT1 by microarray or RNA-seq approach to identify and quantify any changes in gene expression. Also, a mouse model of PRMT1 knock out is being generated in the lab, to undertake comprehensive evaluation of PRMT1/H4R3me2a in senescence *in vivo*. We propose to cross PRMT1 conditional knock out mice to a well-established intestinal model, *Braf<sup>+/LSL-V600E</sup>*, *AhcreER<sup>T+o</sup>* mice, in which senescence ensues through upregulation of p16, but eventually inactivation of this tumor suppressor leads to tumorigenesis [605]. This will not only help deduce the function of PRMT1 and H4R3me2a in senescence but also establish its importance in senescence-associated tumor suppression.

Attempts to decipher regulation of PRMT1-mediated arginine methylation lead to the discovery of TDRD3 as an effector of H4R3me2a [606]. TDRD3 also binds to H3R17me2a deposited by CARM1 and ChIP-seq analysis revealed enrichment of

TDRD3 at TSS of highly transcribed genes. Interestingly, in breast cancer patients increased TDRD3 is linked to poor prognosis, thereby underscoring the importance of H4R3me2a and/or H3R17me2a and cancer. Future experiments will be aimed at identify novel binding partners of H4R3me2a during senescence using pull down approaches. For this purpose, H4R3me2a synthetic peptides have now been obtained. With the help of Proteomics facility in the Beatson Institute, future efforts will address the identification of protein-protein interactions using H4R3me2a affinity pull down experiments. Any novel binding partners identified will become an invaluable tool in understanding the functional and regulatory role of PRMT1 mediated H4R3me2a during senescence.

One of the major challenges in this field has been to understand the cross talk between single or multiple modifications to mediate specific outcomes. In this regard, cross talk between H4R3me2a and other histones during senescence is poorly-defined. Under *in vitro* and *in vivo* conditions, deposition of H4R3me2a by PRMT1 contributes to p300-mediated histone H4 acetylation, resulting in nuclear receptor transcriptional activation [607, 608]. In fact, a stepwise transcriptional activation occurs following p53-mediated recruitment of PRMT1, p300 and PRMT4 [609]. Initially during this cascade, H4R3me2a is deposited which then facilitates p300-mediated acetylation at residues K5, K8 and K12. Also, using an erythroid cell line, it was demonstrated that arginine methylation at H4R3 by PRMT1 appeared to be essential for maintenance of *in vivo* histone modifications, specifically 'active' chromatin marks [610]. In this manner, how single or combinatorial effects of H4R3me2a impact the senescence programme remains to be elucidated. In an effort to map the distribution of H4R3me2a and probe into its interactions, an attempt to ChIP H4R3me2a was made in senescent cells. Due to technical limitations, it was not possible to map the location of H4R3me2a and uncover potential functional or regulatory cross talk of the mark. Testing the validity of a newly available antibody to H4R3me2a from Abcam and its efficiency in ChIP applications will be a good starting point. It is important to acquire a reliable antibody to recognize H4R3me2a in its native chromatin-associated form. Inconsistency in the specificity of commercially available ChIP-grade antibodies has become a growing problem. Hence, to perform comprehensive mapping and analysis of H4R3me2a sites during senescence, it is

worthwhile considering the generation of a monoclonal antibody against H4R3me2a to negate cross-reactivity during ChIP.

The implications of PRMT1 in cancer are diverse. PRMT1 is either overexpressed and/or aberrantly spliced in lung, colon, breast, prostate and bladder cancer and leukaemia [600]. The enzyme has histone and non-histone substrates, and apart from H4R3, primary substrates of PRMT1 are MRE11 [611], 53BP1 (DNA repair proteins) [612] and SAM68 [613]. Hence, perturbations to PRMT1 are known to result in DNA damage accumulation. Additionally, PRMT1 is also linked to the maintenance of telomere length and stability [614]. TRF2, a component of the shelterin complex protecting telomeres, is a known substrate of PRMT1. It is well known that disruption of the DDR pathway and telomere maintenance have significant implications in carcinogenesis. PRMT1 is also implicated in the regulation of leukaemia development through cooperation with SAM68 [613].

To summarize, future efforts will be aimed at discovering a novel role for PRMT1-mediated H4R3me2a during senescence and proposed experiments might also shed light on the role of PRMT and H4R3me2a in cancer.

### 7.3 H4K16ac and senescence

Unlike most histone modifications, H4K16ac plays a central role during chromatin remodelling by influencing functional interactions between the chromatin fibre and histones, thereby regulating chromatin folding and transcription. Moreover global loss of H4K16ac is demonstrated in various human cancer cell lines and primary tumors and is a well-known prognostic signature to predict survival in different cancers [615]. Interestingly, H4K16ac regulates cellular lifespan in yeast [401]. Given its potential significance in chromatin regulation, cancer and ageing, David Nelson performed H4K16ac ChIP-sequencing in RS. ChIP-seq revealed that H4K16ac is significantly enriched at promoter regions in senescence. Overlapping evidence from RNA-seq profiling of senescent cells performed by Taranjit Rai showed that H4K16ac enrichment occurs at TSS of gene promoters that are highly expressed in senescence. In addition, HIRA's deposition of H3.3 at gene promoters in senescent cells shows a striking colocalization with H4K16ac (Rai et al., In preparation). This led us to hypothesize that HIRA is required for deposition of H4K16ac at gene promoters

and therefore regulates dynamic chromatin structure and gene expression during cellular senescence.

In this work, I reaffirmed the ChIP-seq results using ChIP-PCR in RS. H4K16ac ChIP PCR showed that knocking down HIRA in senescent cells resulted in decreased H4K16ac at specific regions that accumulate the mark during senescence. Strikingly, using ChIP-PCR in senescent HIRA KD cells, loss of H4K16ac was observed at a specific gene highly expressed during senescence, containing overlapping features of HIRA-mediated H3.3 deposition and H4K16ac during RS. This further supports the original hypothesis of a role for HIRA-mediated deposition of H3.3 and H4K16ac accumulation to regulate gene expression and higher order chromatin structure during senescence. Experiments are ongoing to test a specific link between HIRA and H4K16ac accumulation in senescence (Rai et al., In preparation), and a novel mouse model of conditional HIRA knock out is being employed to test functional significance and its potential impact on tumorigenesis.

I tested other *in vitro* tools to functionally characterize H4K16ac. I demonstrated H4K16ac accumulation in an IR-induced model system of senescence. Significantly, loss of H4K16ac enrichment was noted at specific regions in senescent H4K16R mutant cells in comparison to senescent H4WT cells. This model system is now available for future experiments to study H4K16ac regulation and function. Also of note is the establishment of H4K16Q cells during this study. Perhaps future experiments can be addressed to analyse effect of the histone mutants in regulating life span in human cells.

Recent reports show that H4K16ac plays an important role in DDR and DSB repair. Pandita and colleagues demonstrated that decreased levels of hMOF, the major HAT for H4K16ac, led to decreased H4K16ac and defective NHEJ (Non-Homologous End-Joining) and HR (Homologous Recombination) [616]. Also using a conditional *Mof* knockout mouse, global loss of H4K16ac led to massive chromosomal aberration, severe G2/M arrest and defects during IR-induced DDR [617]. Furthermore, loss of H4K16ac was associated with premature senescence in *Zmpste*-deficient mice [618]. Deficiency of the lamin-A processing enzyme *Zmpste* in these mice recapitulates premature ageing phenotype of HGPS (Hutchinson Gilford Progeria Syndrome). The mice demonstrated genomic instability and early cellular senescence due to defective recruitment of DNA damage proteins at the site of

damage. This delay was associated with decreased association of hMOF and H4K16 hypoacetylation. Such profound demonstrations of the role of H4K16ac during key cellular processes, such as DNA repair and also ageing and cancer, undoubtedly warrant further investigation of the mark during senescence.

Overall, the discussion above suggests that H4K16ac may have critical function in transcriptional regulation via chromatin modulation during cellular senescence.

The primary focus of this project was to understand how senescence is regulated by its chromatin structure. Certainly, work from this project has brought us a step closer to the goal, albeit with leading questions. The findings presented here implicate H3CS.1, H4R3me2a and H4K16ac in control of cellular senescence. Based on the 'histone code' hypothesis [548], I would like to propose the possibility of H3CS.1, H4R3me2a and H4K16ac acting in direct or indirect combination to exert their influence on chromatin regulation during senescence. Apart from the aforementioned future objectives in the sections above, attempts to decipher potential cross-talk between these modifications will leave a remarkable impact on our basic understanding of senescence and may possibly strengthen its links to ageing and cancer.

## 8 REFERENCES

---

- [1] L. Hayflick and P. S. Moorhead, "The serial cultivation of human diploid cell strains," *Exp Cell Res*, vol. 25, pp. 585-621, Dec 1961.
- [2] L. Hayflick, "The Limited in Vitro Lifetime of Human Diploid Cell Strains," *Exp Cell Res*, vol. 37, pp. 614-36, Mar 1965.
- [3] J. W. Shay and W. E. Wright, "Hayflick, his limit, and cellular ageing," *Nat Rev Mol Cell Biol*, vol. 1, pp. 72-6, Oct 2000.
- [4] J. Campisi, J. K. Andersen, P. Kapahi, and S. Melov, "Cellular senescence: a link between cancer and age-related degenerative disease?," *Semin Cancer Biol*, vol. 21, pp. 354-9, Dec 2011.
- [5] N. Ohtani, A. Takahashi, D. J. Mann, and E. Hara, "Cellular senescence: a double-edged sword in the fight against cancer," *Exp Dermatol*, vol. 21 Suppl 1, pp. 1-4, Jul 2012.
- [6] J. Campisi, "Aging and cancer: the double-edged sword of replicative senescence," *J Am Geriatr Soc*, vol. 45, pp. 482-8, Apr 1997.
- [7] R. Sager, "Senescence as a mode of tumor suppression," *Environ Health Perspect*, vol. 93, pp. 59-62, Jun 1991.
- [8] J. Campisi, "Cellular senescence as a tumor-suppressor mechanism," *Trends Cell Biol*, vol. 11, pp. S27-31, Nov 2001.
- [9] J. Campisi, "Senescent cells, tumor suppression, and organismal aging: good citizens, bad neighbors," *Cell*, vol. 120, pp. 513-22, Feb 25 2005.
- [10] M. Braig and C. A. Schmitt, "Oncogene-induced senescence: putting the brakes on tumor development," *Cancer Res*, vol. 66, pp. 2881-4, Mar 15 2006.
- [11] P. D. Adams, "Remodeling of chromatin structure in senescent cells and its potential impact on tumor suppression and aging," *Gene*, vol. 397, pp. 84-93, Aug 1 2007.
- [12] A. Krtolica, S. Parrinello, S. Lockett, P. Y. Desprez, and J. Campisi, "Senescent fibroblasts promote epithelial cell growth and tumorigenesis: a link between cancer and aging," *Proc Natl Acad Sci U S A*, vol. 98, pp. 12072-7, Oct 9 2001.
- [13] F. Rodier and J. Campisi, "Four faces of cellular senescence," *J Cell Biol*, vol. 192, pp. 547-56, Feb 21 2011.
- [14] J. Campisi, S. H. Kim, C. S. Lim, and M. Rubio, "Cellular senescence, cancer and aging: the telomere connection," *Exp Gerontol*, vol. 36, pp. 1619-37, Nov 2001.
- [15] J. Campisi, "Cancer, aging and cellular senescence," *In Vivo*, vol. 14, pp. 183-8, Jan-Feb 2000.
- [16] C. E. Finch, *Longevity, senescence, and the genome*: University of Chicago Press, 1994.
- [17] C. B. Harley, A. B. Futcher, and C. W. Greider, "Telomeres shorten during ageing of human fibroblasts," 1990.
- [18] N. D. Hastie, M. Dempster, M. G. Dunlop, A. M. Thompson, D. K. Green, and R. C. Allshire, "Telomere reduction in human colorectal carcinoma and with ageing," *Nature*, vol. 346, pp. 866-868, 1990.
- [19] A. M. Olovnikov, "A theory of marginotomy: the incomplete copying of template margin in enzymic synthesis of polynucleotides and biological significance of the phenomenon," *Journal of Theoretical Biology*, vol. 41, pp. 181-190, 1973.

- [20] R. K. Moyzis, J. M. Buckingham, L. S. Cram, M. Dani, L. L. Deaven, M. D. Jones, J. Meyne, R. L. Ratliff, and J. R. Wu, "A highly conserved repetitive DNA sequence, (TTAGGG)<sub>n</sub>, present at the telomeres of human chromosomes," *Proc Natl Acad Sci U S A*, vol. 85, pp. 6622-6, Sep 1988.
- [21] R. C. Allshire, M. Dempster, and N. D. Hastie, "Human telomeres contain at least three types of G-rich repeat distributed non-randomly," *Nucleic Acids Res*, vol. 17, pp. 4611-27, Jun 26 1989.
- [22] E. H. Blackburn, "The molecular structure of centromeres and telomeres," *Annu Rev Biochem*, vol. 53, pp. 163-94, 1984.
- [23] A. G. Bodnar, M. Ouellette, M. Frolkis, S. E. Holt, C. P. Chiu, G. B. Morin, C. B. Harley, J. W. Shay, S. Lichtsteiner, and W. E. Wright, "Extension of life-span by introduction of telomerase into normal human cells," *Science*, vol. 279, pp. 349-52, Jan 16 1998.
- [24] G.-L. Yu and E. H. Blackburn, "Developmentally programmed healing of chromosomes by telomerase in *Tetrahymena*," *Cell*, vol. 67, pp. 823-832, 1991.
- [25] W. E. Wright and J. W. Shay, "Telomere positional effects and the regulation of cellular senescence," *Trends in Genetics*, vol. 8, pp. 193-197, 1992.
- [26] F. d'Adda di Fagagna, P. M. Reaper, L. Clay-Farrace, H. Fiegler, P. Carr, T. Von Zglinicki, G. Saretzki, N. P. Carter, and S. P. Jackson, "A DNA damage checkpoint response in telomere-initiated senescence," *Nature*, vol. 426, pp. 194-8, Nov 13 2003.
- [27] U. Herbig, W. A. Jobling, B. P. Chen, D. J. Chen, and J. M. Sedivy, "Telomere shortening triggers senescence of human cells through a pathway involving ATM, p53, and p21(CIP1), but not p16(INK4a)," *Mol Cell*, vol. 14, pp. 501-13, May 21 2004.
- [28] A. Satyanarayana, R. A. Greenberg, S. Schaezlein, J. Buer, K. Masutomi, W. C. Hahn, S. Zimmermann, U. Martens, M. P. Manns, and K. L. Rudolph, "Mitogen stimulation cooperates with telomere shortening to activate DNA damage responses and senescence signaling," *Mol Cell Biol*, vol. 24, pp. 5459-74, Jun 2004.
- [29] I. Ben-Porath and R. A. Weinberg, "When cells get stressed: an integrative view of cellular senescence," *J Clin Invest*, vol. 113, pp. 8-13, Jan 2004.
- [30] T. von Zglinicki, G. Saretzki, W. Docke, and C. Lotze, "Mild hyperoxia shortens telomeres and inhibits proliferation of fibroblasts: a model for senescence?," *Exp Cell Res*, vol. 220, pp. 186-93, Sep 1995.
- [31] S. Parrinello, E. Samper, A. Krtolica, J. Goldstein, S. Melov, and J. Campisi, "Oxygen sensitivity severely limits the replicative lifespan of murine fibroblasts," *Nature cell biology*, vol. 5, pp. 741-747, 2003.
- [32] L. Packer and K. Fuehr, "Low oxygen concentration extends the lifespan of cultured human diploid cells," 1977.
- [33] T. P. Devasagayam, J. C. Tilak, K. K. Bloor, K. S. Sane, S. S. Ghaskadbi, and R. D. Lele, "Free radicals and antioxidants in human health: current status and future prospects," *J Assoc Physicians India*, vol. 52, pp. 794-804, Oct 2004.
- [34] W. Droge, "Free radicals in the physiological control of cell function," *Physiol Rev*, vol. 82, pp. 47-95, Jan 2002.
- [35] Q. Chen, J. Bartholomew, J. Campisi, M. Acosta, J. Reagan, and B. Ames, "Molecular analysis of H<sub>2</sub>O<sub>2</sub>-induced senescent-like growth arrest in normal

- human fibroblasts: p53 and Rb control G1 arrest but not cell replication," *Biochem. J.*, vol. 332, pp. 43-50, 1998.
- [36] T. Finkel, "Oxidant signals and oxidative stress," *Current opinion in cell biology*, vol. 15, pp. 247-254, 2003.
- [37] M. Serrano, A. W. Lin, M. E. McCurrach, D. Beach, and S. W. Lowe, "Oncogenic ras provokes premature cell senescence associated with accumulation of p53 and p16INK4a," *Cell*, vol. 88, pp. 593-602, Mar 7 1997.
- [38] S. W. Lowe, H. E. Ruley, T. Jacks, and D. E. Housman, "p53-dependent apoptosis modulates the cytotoxicity of anticancer agents," *Cell*, vol. 74, pp. 957-67, Sep 24 1993.
- [39] C. Michaloglou, L. C. Vredeveld, M. S. Soengas, C. Denoyelle, T. Kuilman, C. M. van der Horst, D. M. Majoor, J. W. Shay, W. J. Mooi, and D. S. Peeper, "BRAFE600-associated senescence-like cell cycle arrest of human naevi," *Nature*, vol. 436, pp. 720-4, Aug 4 2005.
- [40] V. Gray-Schopfer, C. Wellbrock, and R. Marais, "Melanoma biology and new targeted therapy," *Nature*, vol. 445, pp. 851-7, Feb 22 2007.
- [41] P. M. Pollock and P. S. Meltzer, "A genome-based strategy uncovers frequent BRAF mutations in melanoma," *Cancer Cell*, vol. 2, pp. 5-7, Jul 2002.
- [42] V. C. Gray-Schopfer, M. Karasarides, R. Hayward, and R. Marais, "Tumor necrosis factor-alpha blocks apoptosis in melanoma cells when BRAF signaling is inhibited," *Cancer Res*, vol. 67, pp. 122-9, Jan 1 2007.
- [43] P. M. Pollock, U. L. Harper, K. S. Hansen, L. M. Yudt, M. Stark, C. M. Robbins, T. Y. Moses, G. Hostetter, U. Wagner, J. Kakareka, G. Salem, T. Pohida, P. Heenan, P. Duray, O. Kallioniemi, N. K. Hayward, J. M. Trent, and P. S. Meltzer, "High frequency of BRAF mutations in nevi," *Nat Genet*, vol. 33, pp. 19-20, Jan 2003.
- [44] R. Di Micco, M. Fumagalli, A. Cicalese, S. Piccinin, P. Gasparini, C. Luise, C. Schurra, M. Garre, P. G. Nuciforo, A. Bensimon, R. Maestro, P. G. Pelicci, and F. d'Adda di Fagagna, "Oncogene-induced senescence is a DNA damage response triggered by DNA hyper-replication," *Nature*, vol. 444, pp. 638-42, Nov 30 2006.
- [45] R. H. te Poele, A. L. Okorokov, L. Jardine, J. Cummings, and S. P. Joel, "DNA damage is able to induce senescence in tumor cells in vitro and in vivo," *Cancer Res*, vol. 62, pp. 1876-83, Mar 15 2002.
- [46] C. J. Sherr, "Tumor surveillance via the ARF-p53 pathway," *Genes Dev*, vol. 12, pp. 2984-91, Oct 1 1998.
- [47] C. J. Sherr and R. A. DePinho, "Cellular senescence: mitotic clock or culture shock?," *Cell*, vol. 102, pp. 407-10, Aug 18 2000.
- [48] R. D. Ramirez, C. P. Morales, B. S. Herbert, J. M. Rohde, C. Passons, J. W. Shay, and W. E. Wright, "Putative telomere-independent mechanisms of replicative aging reflect inadequate growth conditions," *Genes Dev*, vol. 15, pp. 398-403, Feb 15 2001.
- [49] S. Drayton and G. Peters, "Immortalisation and transformation revisited," *Curr Opin Genet Dev*, vol. 12, pp. 98-104, Feb 2002.
- [50] G. P. Dimri, X. Lee, G. Basile, M. Acosta, G. Scott, C. Roskelley, E. E. Medrano, M. Linskens, I. Rubelj, O. Pereira-Smith, and et al., "A biomarker that identifies senescent human cells in culture and in aging skin in vivo," *Proc Natl Acad Sci U S A*, vol. 92, pp. 9363-7, Sep 26 1995.

- [51] W. E. Wright and J. W. Shay, "Historical claims and current interpretations of replicative aging," *Nat Biotechnol*, vol. 20, pp. 682-8, Jul 2002.
- [52] X. Wang, S. C. Wong, J. Pan, S. W. Tsao, K. H. Fung, D. L. Kwong, J. S. Sham, and J. M. Nicholls, "Evidence of cisplatin-induced senescent-like growth arrest in nasopharyngeal carcinoma cells," *Cancer Res*, vol. 58, pp. 5019-22, Nov 15 1998.
- [53] B. D. Chang, E. V. Broude, M. Dokmanovic, H. Zhu, A. Ruth, Y. Xuan, E. S. Kandel, E. Lausch, K. Christov, and I. B. Roninson, "A senescence-like phenotype distinguishes tumor cells that undergo terminal proliferation arrest after exposure to anticancer agents," *Cancer Res*, vol. 59, pp. 3761-7, Aug 1 1999.
- [54] E. Michishita, K. Nakabayashi, T. Suzuki, S. C. Kaul, H. Ogino, M. Fujii, Y. Mitsui, and D. Ayusawa, "5-Bromodeoxyuridine induces senescence-like phenomena in mammalian cells regardless of cell type or species," *J Biochem*, vol. 126, pp. 1052-9, Dec 1999.
- [55] T. Suzuki, S. Minagawa, E. Michishita, H. Ogino, M. Fujii, Y. Mitsui, and D. Ayusawa, "Induction of senescence-associated genes by 5-bromodeoxyuridine in HeLa cells," *Exp Gerontol*, vol. 36, pp. 465-74, Mar 2001.
- [56] L. W. Elmore, C. W. Rehder, X. Di, P. A. McChesney, C. K. Jackson-Cook, D. A. Gewirtz, and S. E. Holt, "Adriamycin-induced senescence in breast tumor cells involves functional p53 and telomere dysfunction," *J Biol Chem*, vol. 277, pp. 35509-15, Sep 20 2002.
- [57] Z. Han, W. Wei, S. Dunaway, J. W. Darnowski, P. Calabresi, J. Sedivy, E. A. Hendrickson, K. V. Balan, P. Pantazis, and J. H. Wyche, "Role of p21 in apoptosis and senescence of human colon cancer cells treated with camptothecin," *J Biol Chem*, vol. 277, pp. 17154-60, May 10 2002.
- [58] R. Haq, J. D. Brenton, M. Takahashi, D. Finan, A. Finkielstein, S. Damaraju, R. Rottapel, and B. Zanke, "Constitutive p38HOG mitogen-activated protein kinase activation induces permanent cell cycle arrest and senescence," *Cancer Res*, vol. 62, pp. 5076-82, Sep 1 2002.
- [59] B. D. Chang, M. E. Swift, M. Shen, J. Fang, E. V. Broude, and I. B. Roninson, "Molecular determinants of terminal growth arrest induced in tumor cells by a chemotherapeutic agent," *Proc Natl Acad Sci U S A*, vol. 99, pp. 389-94, Jan 8 2002.
- [60] Y. Katakura, E. Nakata, T. Miura, and S. Shirahata, "Transforming growth factor beta triggers two independent-senescence programs in cancer cells," *Biochem Biophys Res Commun*, vol. 255, pp. 110-5, Feb 5 1999.
- [61] K. T. Christov, A. L. Shilkaitis, E. S. Kim, V. E. Steele, and R. A. Lubet, "Chemopreventive agents induce a senescence-like phenotype in rat mammary tumours," *Eur J Cancer*, vol. 39, pp. 230-9, Jan 2003.
- [62] L. J. Wainwright, A. Lasorella, and A. Iavarone, "Distinct mechanisms of cell cycle arrest control the decision between differentiation and senescence in human neuroblastoma cells," *Proc Natl Acad Sci U S A*, vol. 98, pp. 9396-400, Jul 31 2001.
- [63] Y. Terao, J. Nishida, S. Horiuchi, F. Rong, Y. Ueoka, T. Matsuda, H. Kato, Y. Furugen, K. Yoshida, K. Kato, and N. Wake, "Sodium butyrate induces growth arrest and senescence-like phenotypes in gynecologic cancer cells," *Int J Cancer*, vol. 94, pp. 257-67, Oct 15 2001.

- [64] V. V. Ogryzko, T. H. Hirai, V. R. Russanova, D. A. Barbie, and B. H. Howard, "Human fibroblast commitment to a senescence-like state in response to histone deacetylase inhibitors is cell cycle dependent," *Mol Cell Biol*, vol. 16, pp. 5210-8, Sep 1996.
- [65] J. Munro, N. I. Barr, H. Ireland, V. Morrison, and E. K. Parkinson, "Histone deacetylase inhibitors induce a senescence-like state in human cells by a p16-dependent mechanism that is independent of a mitotic clock," *Exp Cell Res*, vol. 295, pp. 525-38, May 1 2004.
- [66] J. Campisi and F. d'Adda di Fagagna, "Cellular senescence: when bad things happen to good cells," *Nat Rev Mol Cell Biol*, vol. 8, pp. 729-40, Sep 2007.
- [67] H. Yasaei, E. Gilham, J. C. Pickles, T. P. Roberts, M. O'Donovan, and R. F. Newbold, "Carcinogen-specific mutational and epigenetic alterations in INK4A, INK4B and p53 tumour-suppressor genes drive induced senescence bypass in normal diploid mammalian cells," *Oncogene*, vol. 32, pp. 171-9, Jan 10 2013.
- [68] C. J. Sherr and F. McCormick, "The RB and p53 pathways in cancer," *Cancer Cell*, vol. 2, pp. 103-12, Aug 2002.
- [69] J. P. Brown, W. Wei, and J. M. Sedivy, "Bypass of senescence after disruption of p21CIP1/WAF1 gene in normal diploid human fibroblasts," *Science*, vol. 277, pp. 831-4, Aug 8 1997.
- [70] U. Herbig, W. Wei, A. Dutriaux, W. A. Jobling, and J. M. Sedivy, "Real-time imaging of transcriptional activation in live cells reveals rapid up-regulation of the cyclin-dependent kinase inhibitor gene CDKN1A in replicative cellular senescence," *Aging Cell*, vol. 2, pp. 295-304, Dec 2003.
- [71] V. Dulic, L. F. Drullinger, E. Lees, S. I. Reed, and G. H. Stein, "Altered regulation of G1 cyclins in senescent human diploid fibroblasts: accumulation of inactive cyclin E-Cdk2 and cyclin D1-Cdk2 complexes," *Proc Natl Acad Sci U S A*, vol. 90, pp. 11034-8, Dec 1 1993.
- [72] X. D. Wang, E. Lapi, A. Sullivan, I. Ratnayaka, R. Goldin, R. Hay, and X. Lu, "SUMO-modified nuclear cyclin D1 bypasses Ras-induced senescence," *Cell Death Differ*, vol. 18, pp. 304-14, Feb 2011.
- [73] F. Lanigan, J. G. Geraghty, and A. P. Bracken, "Transcriptional regulation of cellular senescence," *Oncogene*, vol. 30, pp. 2901-11, Jun 30 2011.
- [74] J. Brugarolas, C. Chandrasekaran, J. I. Gordon, D. Beach, T. Jacks, and G. J. Hannon, "Radiation-induced cell cycle arrest compromised by p21 deficiency," *Nature*, vol. 377, pp. 552-7, Oct 12 1995.
- [75] B. B. McConnell, M. Starborg, S. Brookes, and G. Peters, "Inhibitors of cyclin-dependent kinases induce features of replicative senescence in early passage human diploid fibroblasts," *Curr Biol*, vol. 8, pp. 351-4, Mar 12 1998.
- [76] B. D. Chang, K. Watanabe, E. V. Broude, J. Fang, J. C. Poole, T. V. Kalinichenko, and I. B. Roninson, "Effects of p21Waf1/Cip1/Sdi1 on cellular gene expression: implications for carcinogenesis, senescence, and age-related diseases," *Proc Natl Acad Sci U S A*, vol. 97, pp. 4291-6, Apr 11 2000.
- [77] J. Krishnamurthy, C. Torrice, M. R. Ramsey, G. I. Kovalev, K. Al-Regaiey, L. Su, and N. E. Sharpless, "Ink4a/Arf expression is a biomarker of aging," *J Clin Invest*, vol. 114, pp. 1299-307, Nov 2004.
- [78] V. Gire, P. Roux, D. Wynford-Thomas, J. M. Brondello, and V. Dulic, "DNA damage checkpoint kinase Chk2 triggers replicative senescence," *EMBO J*, vol. 23, pp. 2554-63, Jul 7 2004.

- [79] J. Won, M. Kim, N. Kim, J. H. Ahn, W. G. Lee, S. S. Kim, K. Y. Chang, Y. W. Yi, and T. K. Kim, "Small molecule-based reversible reprogramming of cellular lifespan," *Nat Chem Biol*, vol. 2, pp. 369-74, Jul 2006.
- [80] O. Aksoy, A. Chicas, T. Zeng, Z. Zhao, M. McCurrach, X. Wang, and S. W. Lowe, "The atypical E2F family member E2F7 couples the p53 and RB pathways during cellular senescence," *Genes Dev*, vol. 26, pp. 1546-57, Jul 15 2012.
- [81] L. A. Carvajal, P. J. Hamard, C. Tonnessen, and J. J. Manfredi, "E2F7, a novel target, is up-regulated by p53 and mediates DNA damage-dependent transcriptional repression," *Genes Dev*, vol. 26, pp. 1533-45, Jul 15 2012.
- [82] D. E. Harrison, R. Strong, Z. D. Sharp, J. F. Nelson, C. M. Astle, K. Flurkey, N. L. Nadon, J. E. Wilkinson, K. Frenkel, C. S. Carter, M. Pahor, M. A. Javors, E. Fernandez, and R. A. Miller, "Rapamycin fed late in life extends lifespan in genetically heterogeneous mice," *Nature*, vol. 460, pp. 392-5, Jul 16 2009.
- [83] R. W. Powers, 3rd, M. Kaerberlein, S. D. Caldwell, B. K. Kennedy, and S. Fields, "Extension of chronological life span in yeast by decreased TOR pathway signaling," *Genes Dev*, vol. 20, pp. 174-84, Jan 15 2006.
- [84] K. H. Vousden and C. Prives, "Blinded by the Light: The Growing Complexity of p53," *Cell*, vol. 137, pp. 413-31, May 1 2009.
- [85] J. J. Jacobs and T. de Lange, "Significant role for p16INK4a in p53-independent telomere-directed senescence," *Curr Biol*, vol. 14, pp. 2302-8, Dec 29 2004.
- [86] G. H. Stein, L. F. Drullinger, A. Soulard, and V. Dulic, "Differential roles for cyclin-dependent kinase inhibitors p21 and p16 in the mechanisms of senescence and differentiation in human fibroblasts," *Mol Cell Biol*, vol. 19, pp. 2109-17, Mar 1999.
- [87] J. W. Shay, W. E. Wright, and H. Werbin, "Defining the molecular mechanisms of human cell immortalization," *Biochim Biophys Acta*, vol. 1072, pp. 1-7, Apr 16 1991.
- [88] B. D. Rowland, S. G. Denisov, S. Douma, H. G. Stunnenberg, R. Bernards, and D. S. Peeper, "E2F transcriptional repressor complexes are critical downstream targets of p19(ARF)/p53-induced proliferative arrest," *Cancer Cell*, vol. 2, pp. 55-65, Jul 2002.
- [89] M. Harvey, A. T. Sands, R. S. Weiss, M. E. Hegi, R. W. Wiseman, P. Pantazis, B. C. Giovanella, M. A. Tainsky, A. Bradley, and L. A. Donehower, "In vitro growth characteristics of embryo fibroblasts isolated from p53-deficient mice," *Oncogene*, vol. 8, pp. 2457-67, Sep 1993.
- [90] A. Smogorzewska and T. de Lange, "Different telomere damage signaling pathways in human and mouse cells," *EMBO J*, vol. 21, pp. 4338-48, Aug 15 2002.
- [91] N. Ohtani, Z. Zebedee, T. J. Huot, J. A. Stinson, M. Sugimoto, Y. Ohashi, A. D. Sharrocks, G. Peters, and E. Hara, "Opposing effects of Ets and Id proteins on p16INK4a expression during cellular senescence," *Nature*, vol. 409, pp. 1067-70, Feb 22 2001.
- [92] A. P. Bracken, D. Kleine-Kohlbrecher, N. Dietrich, D. Pasini, G. Gargiulo, C. Beekman, K. Theilgaard-Mönch, S. Minucci, B. T. Porse, and J.-C. Marine, "The Polycomb group proteins bind throughout the INK4A-ARF locus and are disassociated in senescent cells," *Genes & development*, vol. 21, pp. 525-530, 2007.

- [93] S. W. Lowe and C. J. Sherr, "Tumor suppression by *Ink4a*–*Arf*: progress and puzzles," *Current opinion in genetics & development*, vol. 13, pp. 77-83, 2003.
- [94] R. Cao and Y. Zhang, "The functions of E (Z)/EZH2-mediated methylation of lysine 27 in histone H3," *Current opinion in genetics & development*, vol. 14, pp. 155-164, 2004.
- [95] D. V. Bulavin, C. Phillips, B. Nannenga, O. Timofeev, L. A. Donehower, C. W. Anderson, E. Appella, and A. J. Fornace, "Inactivation of the Wip1 phosphatase inhibits mammary tumorigenesis through p38 MAPK-mediated activation of the p16<sup>Ink4a</sup>-p19<sup>Arf</sup> pathway," *Nature genetics*, vol. 36, pp. 343-350, 2004.
- [96] F. d. A. di Fagagna, "Living on a break: cellular senescence as a DNA-damage response," *Nature Reviews Cancer*, vol. 8, pp. 512-522, 2008.
- [97] Y. Shiloh, "The ATM-mediated DNA-damage response: taking shape," *Trends Biochem Sci*, vol. 31, pp. 402-10, Jul 2006.
- [98] R. C. Taylor, S. P. Cullen, and S. J. Martin, "Apoptosis: controlled demolition at the cellular level," *Nat Rev Mol Cell Biol*, vol. 9, pp. 231-41, Mar 2008.
- [99] J. Karlseder, D. Broccoli, Y. Dai, S. Hardy, and T. de Lange, "p53- and ATM-dependent apoptosis induced by telomeres lacking TRF2," *Science*, vol. 283, pp. 1321-5, Feb 26 1999.
- [100] J. Rouse and S. P. Jackson, "Interfaces between the detection, signaling, and repair of DNA damage," *Science*, vol. 297, pp. 547-51, Jul 26 2002.
- [101] Y. Deng, S. S. Chan, and S. Chang, "Telomere dysfunction and tumour suppression: the senescence connection," *Nature Reviews Cancer*, vol. 8, pp. 450-458, 2008.
- [102] J. Bartkova, N. Rezaei, M. Liontos, P. Karakaidos, D. Kletsas, N. Issaeva, L. V. Vassiliou, E. Kolettas, K. Niforou, V. C. Zoumpourlis, M. Takaoka, H. Nakagawa, F. Tort, K. Fugger, F. Johansson, M. Sehested, C. L. Andersen, L. Dyrskjot, T. Orntoft, J. Lukas, C. Kittas, T. Helleday, T. D. Halazonetis, J. Bartek, and V. G. Gorgoulis, "Oncogene-induced senescence is part of the tumorigenesis barrier imposed by DNA damage checkpoints," *Nature*, vol. 444, pp. 633-7, Nov 30 2006.
- [103] M. Debidda, D. A. Williams, and Y. Zheng, "Rac1 GTPase regulates cell genomic stability and senescence," *J Biol Chem*, vol. 281, pp. 38519-28, Dec 15 2006.
- [104] M. Xu, Q. Yu, R. Subrahmanyam, M. J. Difilippantonio, T. Ried, and J. M. Sen, "Beta-catenin expression results in p53-independent DNA damage and oncogene-induced senescence in prelymphomagenic thymocytes in vivo," *Mol Cell Biol*, vol. 28, pp. 1713-23, Mar 2008.
- [105] C. Gorrini, M. Squatrito, C. Luise, N. Syed, D. Perna, L. Wark, F. Martinato, D. Sardella, A. Verrecchia, S. Bennett, S. Confalonieri, M. Cesaroni, F. Marchesi, M. Gasco, E. Scanziani, M. Capra, S. Mai, P. Nuciforo, T. Crook, J. Lough, and B. Amati, "Tip60 is a haplo-insufficient tumour suppressor required for an oncogene-induced DNA damage response," *Nature*, vol. 448, pp. 1063-7, Aug 30 2007.
- [106] O. Moiseeva, F. A. Mallette, U. K. Mukhopadhyay, A. Moores, and G. Ferbeyre, "DNA damage signaling and p53-dependent senescence after prolonged beta-interferon stimulation," *Mol Biol Cell*, vol. 17, pp. 1583-92, Apr 2006.

- [107] F. A. Mallette, M. F. Gaumont-Leclerc, and G. Ferbeyre, "The DNA damage signaling pathway is a critical mediator of oncogene-induced senescence," *Genes Dev*, vol. 21, pp. 43-8, Jan 1 2007.
- [108] C. Grandori, K. J. Wu, P. Fernandez, C. Ngouenet, J. Grim, B. E. Clurman, M. J. Moser, J. Oshima, D. W. Russell, K. Swisshelm, S. Frank, B. Amati, R. Dalla-Favera, and R. J. Monnat, Jr., "Werner syndrome protein limits MYC-induced cellular senescence," *Genes Dev*, vol. 17, pp. 1569-74, Jul 1 2003.
- [109] R. Di Micco, M. Fumagalli, and F. d'Adda di Fagagna, "Breaking news: high-speed race ends in arrest--how oncogenes induce senescence," *Trends Cell Biol*, vol. 17, pp. 529-36, Nov 2007.
- [110] T. Von Zglinicki, "Replicative senescence and the art of counting," *Exp Gerontol*, vol. 38, pp. 1259-64, Nov-Dec 2003.
- [111] A. R. Young, M. Narita, M. Ferreira, K. Kirschner, M. Sadaie, J. F. Darot, S. Tavaré, S. Arakawa, S. Shimizu, F. M. Watt, and M. Narita, "Autophagy mediates the mitotic senescence transition," *Genes Dev*, vol. 23, pp. 798-803, Apr 1 2009.
- [112] D. Glick, S. Barth, and K. F. Macleod, "Autophagy: cellular and molecular mechanisms," *J Pathol*, vol. 221, pp. 3-12, May 2010.
- [113] D. A. Gewirtz, "Autophagy and senescence: a partnership in search of definition," *Autophagy*, vol. 9, pp. 808-12, May 2013.
- [114] M. Narita, A. R. Young, and M. Narita, "Autophagy facilitates oncogene-induced senescence," *Autophagy*, vol. 5, pp. 1046-7, Oct 2009.
- [115] M. Collado, J. Gil, A. Efeyan, C. Guerra, A. J. Schuhmacher, M. Barradas, A. Benguria, A. Zaballos, J. M. Flores, M. Barbacid, D. Beach, and M. Serrano, "Tumour biology: senescence in premalignant tumours," *Nature*, vol. 436, p. 642, Aug 4 2005.
- [116] M. Gamerding, P. Hajjeva, A. M. Kaya, U. Wolfrum, F. U. Hartl, and C. Behl, "Protein quality control during aging involves recruitment of the macroautophagy pathway by BAG3," *EMBO J*, vol. 28, pp. 889-901, Apr 8 2009.
- [117] R. W. Goehe, X. Di, K. Sharma, M. L. Bristol, S. C. Henderson, K. Valerie, F. Rodier, A. R. Davalos, and D. A. Gewirtz, "The autophagy-senescence connection in chemotherapy: must tumor cells (self) eat before they sleep?," *J Pharmacol Exp Ther*, vol. 343, pp. 763-78, Dec 2012.
- [118] K. Singh, S. Matsuyama, J. A. Drazba, and A. Almasan, "Autophagy-dependent senescence in response to DNA damage and chronic apoptotic stress," *Autophagy*, vol. 8, pp. 236-51, Feb 1 2012.
- [119] S. Patschan, J. Chen, A. Polotskaia, N. Mendeleev, J. Cheng, D. Patschan, and M. S. Goligorsky, "Lipid mediators of autophagy in stress-induced premature senescence of endothelial cells," *Am J Physiol Heart Circ Physiol*, vol. 294, pp. H1119-29, Mar 2008.
- [120] G. Mosieniak, M. Adamowicz, O. Alster, H. Jaskowiak, A. A. Szczepankiewicz, G. M. Wilczynski, I. A. Ciechomska, and E. Sikora, "Curcumin induces permanent growth arrest of human colon cancer cells: link between senescence and autophagy," *Mech Ageing Dev*, vol. 133, pp. 444-55, Jun 2012.
- [121] N. Maddodi, W. Huang, T. Havighurst, K. Kim, B. J. Longley, and V. Setaluri, "Induction of autophagy and inhibition of melanoma growth in vitro and in vivo

- by hyperactivation of oncogenic BRAF," *J Invest Dermatol*, vol. 130, pp. 1657-67, Jun 2010.
- [122] C. Capparelli, B. Chiavarina, D. Whitaker-Menezes, T. G. Pestell, R. G. Pestell, J. Hult, S. Ando, A. Howell, U. E. Martinez-Outschoorn, F. Sotgia, and M. P. Lisanti, "CDK inhibitors (p16/p19/p21) induce senescence and autophagy in cancer-associated fibroblasts, "fueling" tumor growth via paracrine interactions, without an increase in neo-angiogenesis," *Cell Cycle*, vol. 11, pp. 3599-610, Oct 1 2012.
- [123] H. T. Kang, K. B. Lee, S. Y. Kim, H. R. Choi, and S. C. Park, "Autophagy impairment induces premature senescence in primary human fibroblasts," *PLoS One*, vol. 6, p. e23367, 2011.
- [124] Y. Wang, X. D. Wang, E. Lapi, A. Sullivan, W. Jia, Y. W. He, I. Ratnayaka, S. Zhong, R. D. Goldin, C. G. Goemans, A. M. Tolkovsky, and X. Lu, "Autophagic activity dictates the cellular response to oncogenic RAS," *Proc Natl Acad Sci U S A*, vol. 109, pp. 13325-30, Aug 14 2012.
- [125] A. R. Young and M. Narita, "Connecting autophagy to senescence in pathophysiology," *Curr Opin Cell Biol*, vol. 22, pp. 234-40, Apr 2010.
- [126] C. M. Beausejour, A. Krtolica, F. Galimi, M. Narita, S. W. Lowe, P. Yaswen, and J. Campisi, "Reversal of human cellular senescence: roles of the p53 and p16 pathways," *EMBO J*, vol. 22, pp. 4212-22, Aug 15 2003.
- [127] D. N. Shelton, E. Chang, P. S. Whittier, D. Choi, and W. D. Funk, "Microarray analysis of replicative senescence," *Curr Biol*, vol. 9, pp. 939-45, Sep 9 1999.
- [128] T. Kuilman, C. Michaloglou, L. C. Vredeveld, S. Douma, R. van Doorn, C. J. Desmet, L. A. Aarden, W. J. Mooi, and D. S. Peeper, "Oncogene-induced senescence relayed by an interleukin-dependent inflammatory network," *Cell*, vol. 133, pp. 1019-31, Jun 13 2008.
- [129] J. P. Coppe, C. K. Patil, F. Rodier, Y. Sun, D. P. Munoz, J. Goldstein, P. S. Nelson, P. Y. Desprez, and J. Campisi, "Senescence-associated secretory phenotypes reveal cell-nonautonomous functions of oncogenic RAS and the p53 tumor suppressor," *PLoS Biol*, vol. 6, pp. 2853-68, Dec 2 2008.
- [130] Z. Novakova, S. Hubackova, M. Kosar, L. Janderova-Rossmislova, J. Dobrovolna, P. Vasicova, M. Vancurova, Z. Horejsi, P. Hozak, J. Bartek, and Z. Hodny, "Cytokine expression and signaling in drug-induced cellular senescence," *Oncogene*, vol. 29, pp. 273-84, Jan 14 2010.
- [131] F. Rodier, J. P. Coppe, C. K. Patil, W. A. Hoeijmakers, D. P. Munoz, S. R. Raza, A. Freund, E. Campeau, A. R. Davalos, and J. Campisi, "Persistent DNA damage signalling triggers senescence-associated inflammatory cytokine secretion," *Nat Cell Biol*, vol. 11, pp. 973-9, Aug 2009.
- [132] E. Pazolli, E. Alspach, A. Milczarek, J. Prior, D. Piwnica-Worms, and S. A. Stewart, "Chromatin remodeling underlies the senescence-associated secretory phenotype of tumor stromal fibroblasts that supports cancer progression," *Cancer Res*, vol. 72, pp. 2251-61, May 1 2012.
- [133] J. P. Coppe, C. K. Patil, F. Rodier, A. Krtolica, C. M. Beausejour, S. Parrinello, J. G. Hodgson, K. Chin, P. Y. Desprez, and J. Campisi, "A human-like senescence-associated secretory phenotype is conserved in mouse cells dependent on physiological oxygen," *PLoS One*, vol. 5, p. e9188, 2010.
- [134] C. Bavik, I. Coleman, J. P. Dean, B. Knudsen, S. Plymate, and P. S. Nelson, "The gene expression program of prostate fibroblast senescence modulates

- neoplastic epithelial cell proliferation through paracrine mechanisms," *Cancer Res*, vol. 66, pp. 794-802, Jan 15 2006.
- [135] J. C. Acosta, A. O'Loughlen, A. Banito, M. V. Guijarro, A. Augert, S. Raguz, M. Fumagalli, M. Da Costa, C. Brown, N. Popov, Y. Takatsu, J. Melamed, F. d'Adda di Fagagna, D. Bernard, E. Hernando, and J. Gil, "Chemokine signaling via the CXCR2 receptor reinforces senescence," *Cell*, vol. 133, pp. 1006-18, Jun 13 2008.
- [136] B. Hampel, K. Fortschegger, S. Ressler, M. W. Chang, H. Unterluggauer, A. Breitwieser, W. Sommergruber, B. Fitzky, G. Lepperdinger, P. Jansen-Durr, R. Voglauer, and J. Grillari, "Increased expression of extracellular proteins as a hallmark of human endothelial cell in vitro senescence," *Exp Gerontol*, vol. 41, pp. 474-81, May 2006.
- [137] M. K. Kang, A. Kameta, K. H. Shin, M. A. Baluda, H. R. Kim, and N. H. Park, "Senescence-associated genes in normal human oral keratinocytes," *Exp Cell Res*, vol. 287, pp. 272-81, Jul 15 2003.
- [138] N. Wajapeyee, R. W. Serra, X. Zhu, M. Mahalingam, and M. R. Green, "Oncogenic BRAF induces senescence and apoptosis through pathways mediated by the secreted protein IGFBP7," *Cell*, vol. 132, pp. 363-74, Feb 8 2008.
- [139] M. Fumagalli and F. d. A. di Fagagna, "SASPense and DDRama in cancer and ageing," *Nature cell biology*, vol. 11, pp. 921-923, 2009.
- [140] J. P. Coppe, F. Rodier, C. K. Patil, A. Freund, P. Y. Desprez, and J. Campisi, "Tumor suppressor and aging biomarker p16(INK4a) induces cellular senescence without the associated inflammatory secretory phenotype," *J Biol Chem*, vol. 286, pp. 36396-403, Oct 21 2011.
- [141] U. Herbig, M. Ferreira, L. Condel, D. Carey, and J. M. Sedivy, "Cellular senescence in aging primates," *Science*, vol. 311, p. 1257, Mar 3 2006.
- [142] F. Rodier, D. P. Munoz, R. Teachenor, V. Chu, O. Le, D. Bhaumik, J. P. Coppe, E. Campeau, C. M. Beausejour, S. H. Kim, A. R. Davalos, and J. Campisi, "DNA-SCARS: distinct nuclear structures that sustain damage-induced senescence growth arrest and inflammatory cytokine secretion," *J Cell Sci*, vol. 124, pp. 68-81, Jan 1 2011.
- [143] A. Freund, C. K. Patil, and J. Campisi, "p38MAPK is a novel DNA damage response-independent regulator of the senescence-associated secretory phenotype," *EMBO J*, vol. 30, pp. 1536-48, Apr 20 2011.
- [144] E. Wang, "Senescent human fibroblasts resist programmed cell death, and failure to suppress bcl2 is involved," *Cancer research*, vol. 55, pp. 2284-2292, 1995.
- [145] E.-J. Yeo, Y.-C. Hwang, C.-M. Kang, H. E. Choy, and S. C. Park, "Reduction of UV-induced cell death in the human senescent fibroblasts," *Molecules and cells*, vol. 10, pp. 415-422, 2000.
- [146] A. Seluanov, V. Gorbunova, A. Falcovitz, A. Sigal, M. Milyavsky, I. Zurer, G. Shohat, N. Goldfinger, and V. Rotter, "Change of the death pathway in senescent human fibroblasts in response to DNA damage is caused by an inability to stabilize p53," *Molecular and cellular biology*, vol. 21, pp. 1552-1564, 2001.
- [147] D. Kanduc, A. Mittelman, R. Serpico, E. Sinigaglia, A. A. Sinha, C. Natale, R. Santacroce, M. G. Di Corcia, A. Lucchese, and L. Dini, "Cell death: apoptosis

- versus necrosis (review)," *International journal of oncology*, vol. 21, pp. 165-170, 2002.
- [148] W. Chen, J. Kang, J. Xia, B. Yang, B. Chen, W. Sun, X. Song, W. Xiang, X. Wang, and F. Wang, "p53-related apoptosis resistance and tumor suppression activity in UVB-induced premature senescent human skin fibroblasts," *International journal of molecular medicine*, vol. 21, p. 645, 2008.
- [149] A. Burlacu, "Regulation of apoptosis by Bcl - 2 family proteins," *Journal of cellular and molecular medicine*, vol. 7, pp. 249-257, 2003.
- [150] P. J. Rochette and D. E. Brash, "Progressive apoptosis resistance prior to senescence and control by the anti-apoptotic protein BCL-xL," *Mechanisms of ageing and development*, vol. 129, pp. 207-214, 2008.
- [151] Y. Huang, M. J. Corbley, Z. Tang, L. Yang, Y. Peng, Z. Y. Zhang, and T. J. Tong, "Down - regulation of p21WAF1 promotes apoptosis in senescent human fibroblasts: Involvement of retinoblastoma protein phosphorylation and delay of cellular aging," *Journal of cellular physiology*, vol. 201, pp. 483-491, 2004.
- [152] C. Denoyelle, G. Abou-Rjaily, V. Bezrookove, M. Verhaegen, T. M. Johnson, D. R. Fullen, J. N. Pointer, S. B. Gruber, L. D. Su, M. A. Nikiforov, R. J. Kaufman, B. C. Bastian, and M. S. Soengas, "Anti-oncogenic role of the endoplasmic reticulum differentially activated by mutations in the MAPK pathway," *Nat Cell Biol*, vol. 8, pp. 1053-63, Oct 2006.
- [153] Q. Chen and B. N. Ames, "Senescence-like growth arrest induced by hydrogen peroxide in human diploid fibroblast F65 cells," *Proc Natl Acad Sci U S A*, vol. 91, pp. 4130-4, May 10 1994.
- [154] Q. M. Chen, K. R. Prowse, V. C. Tu, S. Purdom, and M. H. Linskens, "Uncoupling the senescent phenotype from telomere shortening in hydrogen peroxide-treated fibroblasts," *Exp Cell Res*, vol. 265, pp. 294-303, May 1 2001.
- [155] H. M. Chan, M. Narita, S. W. Lowe, and D. M. Livingston, "The p400 E1A-associated protein is a novel component of the p53 --> p21 senescence pathway," *Genes Dev*, vol. 19, pp. 196-201, Jan 15 2005.
- [156] B. Y. Lee, J. A. Han, J. S. Im, A. Morrone, K. Johung, E. C. Goodwin, W. J. Kleijer, D. DiMaio, and E. S. Hwang, "Senescence-associated beta-galactosidase is lysosomal beta-galactosidase," *Ageing Cell*, vol. 5, pp. 187-95, Apr 2006.
- [157] Y. E. Yegorov, S. S. Akimov, R. Hass, A. V. Zelenin, and I. A. Prudovsky, "Endogenous beta-galactosidase activity in continuously nonproliferating cells," *Exp Cell Res*, vol. 243, pp. 207-11, Aug 25 1998.
- [158] D. R. Krishna, B. Sperker, P. Fritz, and U. Klotz, "Does pH 6 beta-galactosidase activity indicate cell senescence?," *Mech Ageing Dev*, vol. 109, pp. 113-23, Aug 30 1999.
- [159] D. J. Kurz, S. Decary, Y. Hong, and J. D. Erusalimsky, "Senescence-associated (beta)-galactosidase reflects an increase in lysosomal mass during replicative ageing of human endothelial cells," *J Cell Sci*, vol. 113 ( Pt 20), pp. 3613-22, Oct 2000.
- [160] G. Untergasser, R. Gander, H. Rumpold, E. Heinrich, E. Plas, and P. Berger, "TGF-beta cytokines increase senescence-associated beta-galactosidase activity in human prostate basal cells by supporting differentiation processes, but not cellular senescence," *Exp Gerontol*, vol. 38, pp. 1179-88, Oct 2003.

- [161] P. J. Coates, "Markers of senescence?," *J Pathol*, vol. 196, pp. 371-3, Apr 2002.
- [162] V. J. Cristofalo, "SA beta Gal staining: biomarker or delusion," *Exp Gerontol*, vol. 40, pp. 836-8, Oct 2005.
- [163] N. C. Yang and M. L. Hu, "The limitations and validities of senescence associated-beta-galactosidase activity as an aging marker for human foreskin fibroblast Hs68 cells," *Exp Gerontol*, vol. 40, pp. 813-9, Oct 2005.
- [164] J. Severino, R. G. Allen, S. Balin, A. Balin, and V. J. Cristofalo, "Is beta-galactosidase staining a marker of senescence in vitro and in vivo?," *Exp Cell Res*, vol. 257, pp. 162-71, May 25 2000.
- [165] S. I. Rattan, K. D. Keeler, J. H. Buchanan, and R. Holliday, "Autofluorescence as an index of ageing in human fibroblasts in culture," *Biosci Rep*, vol. 2, pp. 561-7, Aug 1982.
- [166] T. von Zglinicki, E. Nilsson, W. D. Docke, and U. T. Brunk, "Lipofuscin accumulation and ageing of fibroblasts," *Gerontology*, vol. 41 Suppl 2, pp. 95-108, 1995.
- [167] G. P. Dimri, A. Testori, M. Acosta, and J. Campisi, "Replicative senescence, aging and growth-regulatory transcription factors," *Biol Signals*, vol. 5, pp. 154-62, May-Jun 1996.
- [168] N. Ohtani, K. Yamakoshi, A. Takahashi, and E. Hara, "The p16INK4a-RB pathway: molecular link between cellular senescence and tumor suppression," *J Med Invest*, vol. 51, pp. 146-53, Aug 2004.
- [169] A. W. Lin, M. Barradas, J. C. Stone, L. van Aelst, M. Serrano, and S. W. Lowe, "Premature senescence involving p53 and p16 is activated in response to constitutive MEK/MAPK mitogenic signaling," *Genes Dev*, vol. 12, pp. 3008-19, Oct 1 1998.
- [170] P. Atadja, H. Wong, I. Garkavtsev, C. Veillette, and K. Riabowol, "Increased activity of p53 in senescing fibroblasts," *Proc Natl Acad Sci U S A*, vol. 92, pp. 8348-52, Aug 29 1995.
- [171] G. H. Stein, M. Beeson, and L. Gordon, "Failure to phosphorylate the retinoblastoma gene product in senescent human fibroblasts," *Science*, vol. 249, pp. 666-9, Aug 10 1990.
- [172] A. Freund, R. M. Laberge, M. Demaria, and J. Campisi, "Lamin B1 loss is a senescence-associated biomarker," *Mol Biol Cell*, vol. 23, pp. 2066-75, Jun 2012.
- [173] J. Feser, D. Truong, C. Das, J. J. Carson, J. Kieft, T. Harkness, and J. K. Tyler, "Elevated histone expression promotes life span extension," *Mol Cell*, vol. 39, pp. 724-35, Sep 10 2010.
- [174] R. J. O'Sullivan, S. Kubicek, S. L. Schreiber, and J. Karlseder, "Reduced histone biosynthesis and chromatin changes arising from a damage signal at telomeres," *Nat Struct Mol Biol*, vol. 17, pp. 1218-25, Oct 2010.
- [175] T. Shimi, V. Butin-Israeli, S. A. Adam, R. B. Hamanaka, A. E. Goldman, C. A. Lucas, D. K. Shumaker, S. T. Kosak, N. S. Chandel, and R. D. Goldman, "The role of nuclear lamin B1 in cell proliferation and senescence," *Genes Dev*, vol. 25, pp. 2579-93, Dec 15 2011.
- [176] M. Narita, S. Nunez, E. Heard, M. Narita, A. W. Lin, S. A. Hearn, D. L. Spector, G. J. Hannon, and S. W. Lowe, "Rb-mediated heterochromatin formation and silencing of E2F target genes during cellular senescence," *Cell*, vol. 113, pp. 703-16, Jun 13 2003.

- [177] M. Kosar, J. Bartkova, S. Hubackova, Z. Hodny, J. Lukas, and J. Bartek, "Senescence-associated heterochromatin foci are dispensable for cellular senescence, occur in a cell type- and insult-dependent manner and follow expression of p16(ink4a)," *Cell Cycle*, vol. 10, pp. 457-68, Feb 1 2011.
- [178] R. Zhang, M. V. Poustovoitov, X. Ye, H. A. Santos, W. Chen, S. M. Daganzo, J. P. Erzberger, I. G. Serebriiskii, A. A. Canutescu, R. L. Dunbrack, J. R. Pehrson, J. M. Berger, P. D. Kaufman, and P. D. Adams, "Formation of MacroH2A-containing senescence-associated heterochromatin foci and senescence driven by ASF1a and HIRA," *Dev Cell*, vol. 8, pp. 19-30, Jan 2005.
- [179] F. Rodier, J. Campisi, and D. Bhaumik, "Two faces of p53: aging and tumor suppression," *Nucleic Acids Res*, vol. 35, pp. 7475-84, 2007.
- [180] Z. Chen, L. C. Trotman, D. Shaffer, H. K. Lin, Z. A. Dotan, M. Niki, J. A. Koutcher, H. I. Scher, T. Ludwig, W. Gerald, C. Cordon-Cardo, and P. P. Pandolfi, "Crucial role of p53-dependent cellular senescence in suppression of Pten-deficient tumorigenesis," *Nature*, vol. 436, pp. 725-30, Aug 4 2005.
- [181] A. Prieur and D. S. Peeper, "Cellular senescence in vivo: a barrier to tumorigenesis," *Curr Opin Cell Biol*, vol. 20, pp. 150-5, Apr 2008.
- [182] S. K. Chao, S. B. Horwitz, and H. M. McDaid, "Insights into 4E-BP1 and p53 mediated regulation of accelerated cell senescence," *Oncotarget*, vol. 2, pp. 89-98, Jan-Feb 2011.
- [183] V. G. Gorgoulis and T. D. Halazonetis, "Oncogene-induced senescence: the bright and dark side of the response," *Curr Opin Cell Biol*, vol. 22, pp. 816-27, Dec 2010.
- [184] M. Braig, S. Lee, C. Loddenkemper, C. Rudolph, A. H. Peters, B. Schlegelberger, H. Stein, B. Dorken, T. Jenuwein, and C. A. Schmitt, "Oncogene-induced senescence as an initial barrier in lymphoma development," *Nature*, vol. 436, pp. 660-5, Aug 4 2005.
- [185] S. Courtois-Cox, S. M. Genter Williams, E. E. Reczek, B. W. Johnson, L. T. McGillicuddy, C. M. Johannessen, P. E. Hollstein, M. MacCollin, and K. Cichowski, "A negative feedback signaling network underlies oncogene-induced senescence," *Cancer Cell*, vol. 10, pp. 459-72, Dec 2006.
- [186] P. D. Da Forno, J. H. Pringle, A. Fletcher, M. Bamford, L. Su, L. Potter, and G. Saldanha, "BRAF, NRAS and HRAS mutations in spitzoid tumours and their possible pathogenetic significance," *Br J Dermatol*, vol. 161, pp. 364-72, Aug 2009.
- [187] A. L. Ross, M. I. Sanchez, and J. M. Grichnik, "Molecular nevogenesis," *Dermatol Res Pract*, vol. 2011, p. 463184, 2011.
- [188] J. Bauer, J. A. Curtin, D. Pinkel, and B. C. Bastian, "Congenital melanocytic nevi frequently harbor NRAS mutations but no BRAF mutations," *J Invest Dermatol*, vol. 127, pp. 179-82, Jan 2007.
- [189] J. A. Curtin, J. Fridlyand, T. Kageshita, H. N. Patel, K. J. Busam, H. Kutzner, K. H. Cho, S. Aiba, E. B. Brocker, P. E. LeBoit, D. Pinkel, and B. C. Bastian, "Distinct sets of genetic alterations in melanoma," *N Engl J Med*, vol. 353, pp. 2135-47, Nov 17 2005.
- [190] J. L. Maldonado, J. Fridlyand, H. Patel, A. N. Jain, K. Busam, T. Kageshita, T. Ono, D. G. Albertson, D. Pinkel, and B. C. Bastian, "Determinants of BRAF mutations in primary melanomas," *J Natl Cancer Inst*, vol. 95, pp. 1878-90, Dec 17 2003.

- [191] D. Dankort, E. Filenova, M. Collado, M. Serrano, K. Jones, and M. McMahon, "A new mouse model to explore the initiation, progression, and therapy of BRAFV600E-induced lung tumors," *Genes Dev*, vol. 21, pp. 379-84, Feb 15 2007.
- [192] L. Ha, T. Ichikawa, M. Anver, R. Dickins, S. Lowe, N. E. Sharpless, P. Krimpenfort, R. A. Depinho, D. C. Bennett, E. V. Sviderskaya, and G. Merlino, "ARF functions as a melanoma tumor suppressor by inducing p53-independent senescence," *Proc Natl Acad Sci U S A*, vol. 104, pp. 10968-73, Jun 26 2007.
- [193] C. J. Sarkisian, B. A. Keister, D. B. Stairs, R. B. Boxer, S. E. Moody, and L. A. Chodosh, "Dose-dependent oncogene-induced senescence in vivo and its evasion during mammary tumorigenesis," *Nat Cell Biol*, vol. 9, pp. 493-505, May 2007.
- [194] P. Sun, N. Yoshizuka, L. New, B. A. Moser, Y. Li, R. Liao, C. Xie, J. Chen, Q. Deng, M. Yamout, M. Q. Dong, C. G. Frangou, J. R. Yates, 3rd, P. E. Wright, and J. Han, "PRAK is essential for ras-induced senescence and tumor suppression," *Cell*, vol. 128, pp. 295-308, Jan 26 2007.
- [195] A. Ventura, D. G. Kirsch, M. E. McLaughlin, D. A. Tuveson, J. Grimm, L. Lintault, J. Newman, E. E. Reczek, R. Weissleder, and T. Jacks, "Restoration of p53 function leads to tumour regression in vivo," *Nature*, vol. 445, pp. 661-5, Feb 8 2007.
- [196] W. Xue, L. Zender, C. Miething, R. A. Dickins, E. Hernando, V. Krizhanovsky, C. Cordon-Cardo, and S. W. Lowe, "Senescence and tumour clearance is triggered by p53 restoration in murine liver carcinomas," *Nature*, vol. 445, pp. 656-60, Feb 8 2007.
- [197] W. Cosme-Blanco, M. F. Shen, A. J. Lazar, S. Pathak, G. Lozano, A. S. Multani, and S. Chang, "Telomere dysfunction suppresses spontaneous tumorigenesis in vivo by initiating p53-dependent cellular senescence," *EMBO Rep*, vol. 8, pp. 497-503, May 2007.
- [198] D. M. Feldser and C. W. Greider, "Short telomeres limit tumor progression in vivo by inducing senescence," *Cancer Cell*, vol. 11, pp. 461-9, May 2007.
- [199] C. Nardella, J. G. Clohessy, A. Alimonti, and P. P. Pandolfi, "Pro-senescence therapy for cancer treatment," *Nat Rev Cancer*, vol. 11, pp. 503-11, Jul 2011.
- [200] T. W. Kang, T. Yevsa, N. Woller, L. Hoenicke, T. Wuestefeld, D. Dauch, A. Hohmeyer, M. Gereke, R. Rudalska, A. Potapova, M. Iken, M. Vucur, S. Weiss, M. Heikenwalder, S. Khan, J. Gil, D. Bruder, M. Manns, P. Schirmacher, F. Tacke, M. Ott, T. Luedde, T. Longerich, S. Kubicka, and L. Zender, "Senescence surveillance of pre-malignant hepatocytes limits liver cancer development," *Nature*, vol. 479, pp. 547-51, Nov 24 2011.
- [201] Y. Chien, C. Scuoppo, X. Wang, X. Fang, B. Balgley, J. E. Bolden, P. Premrurit, W. Luo, A. Chicas, C. S. Lee, S. C. Kogan, and S. W. Lowe, "Control of the senescence-associated secretory phenotype by NF-kappaB promotes senescence and enhances chemosensitivity," *Genes Dev*, vol. 25, pp. 2125-36, Oct 15 2011.
- [202] V. Krizhanovsky, M. Yon, R. A. Dickins, S. Hearn, J. Simon, C. Miething, H. Yee, L. Zender, and S. W. Lowe, "Senescence of activated stellate cells limits liver fibrosis," *Cell*, vol. 134, pp. 657-67, Aug 22 2008.
- [203] A. Ben-Baruch, "Inflammation-associated immune suppression in cancer: the roles played by cytokines, chemokines and additional mediators," *Semin Cancer Biol*, vol. 16, pp. 38-52, Feb 2006.

- [204] J. P. Coppe, P. Y. Desprez, A. Krtolica, and J. Campisi, "The senescence-associated secretory phenotype: the dark side of tumor suppression," *Annu Rev Pathol*, vol. 5, pp. 99-118, 2010.
- [205] M. P. Purdue, "Re: Determinants of BRAF mutations in primary melanomas," *J Natl Cancer Inst*, vol. 97, pp. 401-2; author reply 402, Mar 2 2005.
- [206] R. M. Kortlever, P. J. Higgins, and R. Bernards, "Plasminogen activator inhibitor-1 is a critical downstream target of p53 in the induction of replicative senescence," *Nat Cell Biol*, vol. 8, pp. 877-84, Aug 2006.
- [207] G. Yang, D. G. Rosen, Z. Zhang, R. C. Bast, Jr., G. B. Mills, J. A. Colacino, I. Mercado-Uribe, and J. Liu, "The chemokine growth-regulated oncogene 1 (Gro-1) links RAS signaling to the senescence of stromal fibroblasts and ovarian tumorigenesis," *Proc Natl Acad Sci U S A*, vol. 103, pp. 16472-7, Oct 31 2006.
- [208] R. Binet, D. Ythier, A. I. Robles, M. Collado, D. Larrieu, C. Fonti, E. Brambilla, C. Brambilla, M. Serrano, C. C. Harris, and R. Pedeux, "WNT16B is a new marker of cellular senescence that regulates p53 activity and the phosphoinositide 3-kinase/AKT pathway," *Cancer Res*, vol. 69, pp. 9183-91, Dec 15 2009.
- [209] C. A. Schmitt, "Cellular senescence and cancer treatment," *Biochim Biophys Acta*, vol. 1775, pp. 5-20, Jan 2007.
- [210] J. W. Shay and I. B. Roninson, "Hallmarks of senescence in carcinogenesis and cancer therapy," *Oncogene*, vol. 23, pp. 2919-33, Apr 12 2004.
- [211] M. Collado and M. Serrano, "Senescence in tumours: evidence from mice and humans," *Nat Rev Cancer*, vol. 10, pp. 51-7, Jan 2010.
- [212] G. D. Mulder and J. S. Vande Berg, "Cellular senescence and matrix metalloproteinase activity in chronic wounds. Relevance to debridement and new technologies," *J Am Podiatr Med Assoc*, vol. 92, pp. 34-7, Jan 2002.
- [213] T. Mustoe, "Understanding chronic wounds: a unifying hypothesis on their pathogenesis and implications for therapy," *Am J Surg*, vol. 187, pp. 65S-70S, May 2004.
- [214] J. S. Vande Berg and M. C. Robson, "Arresting cell cycles and the effect on wound healing," *Surg Clin North Am*, vol. 83, pp. 509-20, Jun 2003.
- [215] M. V. Mendez, A. Stanley, H. Y. Park, K. Shon, T. Phillips, and J. O. Menzoian, "Fibroblasts cultured from venous ulcers display cellular characteristics of senescence," *J Vasc Surg*, vol. 28, pp. 876-83, Nov 1998.
- [216] J. S. Vande Berg, M. A. Rose, P. L. Haywood-Reid, R. Rudolph, W. G. Payne, and M. C. Robson, "Cultured pressure ulcer fibroblasts show replicative senescence with elevated production of plasmin, plasminogen activator inhibitor-1, and transforming growth factor-beta1," *Wound Repair Regen*, vol. 13, pp. 76-83, Jan-Feb 2005.
- [217] M. V. Mendez, J. D. Raffetto, T. Phillips, J. O. Menzoian, and H. Y. Park, "The proliferative capacity of neonatal skin fibroblasts is reduced after exposure to venous ulcer wound fluid: A potential mechanism for senescence in venous ulcers," *J Vasc Surg*, vol. 30, pp. 734-43, Oct 1999.
- [218] D. Bernard, K. Gosselin, D. Monte, C. Vercamer, F. Bouali, A. Pourtier, B. Vandebunder, and C. Abbadie, "Involvement of Rel/nuclear factor-kappaB transcription factors in keratinocyte senescence," *Cancer Res*, vol. 64, pp. 472-81, Jan 15 2004.

- [219] B. M. Min, J. E. Oh, and C. M. Choi, "Retinoic acid delays keratinocyte senescence by suppression of betaig-h3 and p16 expression and induction of telomerase activity," *Int J Mol Med*, vol. 13, pp. 25-31, Jan 2004.
- [220] E. Chang, J. Yang, U. Nagavarapu, and G. S. Herron, "Aging and survival of cutaneous microvasculature," *J Invest Dermatol*, vol. 118, pp. 752-8, May 2002.
- [221] D. Kipling, "Telomeres, replicative senescence and human ageing," *Maturitas*, vol. 38, pp. 25-37; discussion 37-8, Feb 28 2001.
- [222] D. Telgenhoff and B. Shroot, "Cellular senescence mechanisms in chronic wound healing," *Cell Death Differ*, vol. 12, pp. 695-8, Jul 2005.
- [223] J. I. Jun and L. F. Lau, "The matricellular protein CCN1 induces fibroblast senescence and restricts fibrosis in cutaneous wound healing," *Nat Cell Biol*, vol. 12, pp. 676-85, Jul 2010.
- [224] P. D. Adams, "Healing and hurting: molecular mechanisms, functions, and pathologies of cellular senescence," *Mol Cell*, vol. 36, pp. 2-14, Oct 9 2009.
- [225] D. Munoz-Espin, M. Canamero, A. Maraver, G. Gomez-Lopez, J. Contreras, S. Murillo-Cuesta, A. Rodriguez-Baeza, I. Varela-Nieto, J. Ruberte, M. Collado, and M. Serrano, "Programmed cell senescence during mammalian embryonic development," *Cell*, vol. 155, pp. 1104-18, Nov 21 2013.
- [226] M. Storer, A. Mas, A. Robert-Moreno, M. Pecoraro, M. C. Ortells, V. Di Giacomo, R. Yosef, N. Pilpel, V. Krizhanovsky, J. Sharpe, and W. M. Keyes, "Senescence is a developmental mechanism that contributes to embryonic growth and patterning," *Cell*, vol. 155, pp. 1119-30, Nov 21 2013.
- [227] V. Nacher, A. Carretero, M. Navarro, C. Armengol, C. Llombart, A. Rodriguez, I. Herrero-Fresneda, E. Ayuso, and J. Ruberte, "The quail mesonephros: a new model for renal senescence?," *J Vasc Res*, vol. 43, pp. 581-6, 2006.
- [228] J. C. Jeyapalan, M. Ferreira, J. M. Sedivy, and U. Herbig, "Accumulation of senescent cells in mitotic tissue of aging primates," *Mech Ageing Dev*, vol. 128, pp. 36-44, Jan 2007.
- [229] J. D. Erusalimsky and D. J. Kurz, "Cellular senescence in vivo: its relevance in ageing and cardiovascular disease," *Exp Gerontol*, vol. 40, pp. 634-42, Aug-Sep 2005.
- [230] C. Wang, D. Jurk, M. Maddick, G. Nelson, C. Martin-Ruiz, and T. von Zglinicki, "DNA damage response and cellular senescence in tissues of aging mice," *Aging Cell*, vol. 8, pp. 311-23, Jun 2009.
- [231] G. Ding, N. Franki, A. A. Kapasi, K. Reddy, N. Gibbons, and P. C. Singhal, "Tubular cell senescence and expression of TGF-beta1 and p21(WAF1/CIP1) in tubulointerstitial fibrosis of aging rats," *Exp Mol Pathol*, vol. 70, pp. 43-53, Feb 2001.
- [232] J. S. Price, J. G. Waters, C. Darrach, C. Pennington, D. R. Edwards, S. T. Donell, and I. M. Clark, "The role of chondrocyte senescence in osteoarthritis," *Aging Cell*, vol. 1, pp. 57-65, Oct 2002.
- [233] S. Roberts, E. H. Evans, D. Kletsas, D. C. Jaffray, and S. M. Eisenstein, "Senescence in human intervertebral discs," *Eur Spine J*, vol. 15 Suppl 3, pp. S312-6, Aug 2006.
- [234] A. Stanley and T. Osler, "Senescence and the healing rates of venous ulcers," *J Vasc Surg*, vol. 33, pp. 1206-11, Jun 2001.
- [235] W. R. Jeck, A. P. Siebold, and N. E. Sharpless, "Review: a meta - analysis of GWAS and age - associated diseases," *Aging cell*, vol. 11, pp. 727-731, 2012.

- [236] W. M. Keyes, Y. Wu, H. Vogel, X. Guo, S. W. Lowe, and A. A. Mills, "p63 deficiency activates a program of cellular senescence and leads to accelerated aging," *Genes Dev*, vol. 19, pp. 1986-99, Sep 1 2005.
- [237] D. J. Baker, C. Perez-Terzic, F. Jin, K. S. Pitel, N. J. Niederlander, K. Jeganathan, S. Yamada, S. Reyes, L. Rowe, H. J. Hiddinga, N. L. Eberhardt, A. Terzic, and J. M. van Deursen, "Opposing roles for p16Ink4a and p19Arf in senescence and ageing caused by BubR1 insufficiency," *Nat Cell Biol*, vol. 10, pp. 825-36, Jul 2008.
- [238] I. Varela, J. Cadinanos, A. M. Pendas, A. Gutierrez-Fernandez, A. R. Folgueras, L. M. Sanchez, Z. Zhou, F. J. Rodriguez, C. L. Stewart, J. A. Vega, K. Tryggvason, J. M. Freije, and C. Lopez-Otin, "Accelerated ageing in mice deficient in Zmpste24 protease is linked to p53 signalling activation," *Nature*, vol. 437, pp. 564-8, Sep 22 2005.
- [239] J. N. Min, R. A. Whaley, N. E. Sharpless, P. Lockyer, A. L. Portbury, and C. Patterson, "CHIP deficiency decreases longevity, with accelerated aging phenotypes accompanied by altered protein quality control," *Mol Cell Biol*, vol. 28, pp. 4018-25, Jun 2008.
- [240] M. Kuro-o, Y. Matsumura, H. Aizawa, H. Kawaguchi, T. Suga, T. Utsugi, Y. Ohyama, M. Kurabayashi, T. Kaname, E. Kume, H. Iwasaki, A. Iida, T. Shirakida, S. Nishikawa, R. Nagai, and Y. I. Nabeshima, "Mutation of the mouse klotho gene leads to a syndrome resembling ageing," *Nature*, vol. 390, pp. 45-51, Nov 6 1997.
- [241] H. Liu, M. M. Fergusson, R. M. Castilho, J. Liu, L. Cao, J. Chen, D. Malide, Rovira, II, D. Schimel, C. J. Kuo, J. S. Gutkind, P. M. Hwang, and T. Finkel, "Augmented Wnt signaling in a mammalian model of accelerated aging," *Science*, vol. 317, pp. 803-6, Aug 10 2007.
- [242] D. Drummond-Barbosa, "Stem cells, their niches and the systemic environment: an aging network," *Genetics*, vol. 180, pp. 1787-1797, 2008.
- [243] A. Freund, A. V. Orjalo, P. Y. Desprez, and J. Campisi, "Inflammatory networks during cellular senescence: causes and consequences," *Trends Mol Med*, vol. 16, pp. 238-46, May 2010.
- [244] H. Y. Chung, M. Cesari, S. Anton, E. Marzetti, S. Giovannini, A. Y. Seo, C. Carter, B. P. Yu, and C. Leeuwenburgh, "Molecular inflammation: underpinnings of aging and age-related diseases," *Ageing Res Rev*, vol. 8, pp. 18-30, Jan 2009.
- [245] C. Franceschi, M. Capri, D. Monti, S. Giunta, F. Olivieri, F. Sevini, M. P. Panourgia, L. Invidia, L. Celani, M. Scurti, E. Cevenini, G. C. Castellani, and S. Salvioli, "Inflammaging and anti-inflammaging: a systemic perspective on aging and longevity emerged from studies in humans," *Mech Ageing Dev*, vol. 128, pp. 92-105, Jan 2007.
- [246] S. I. Grivennikov, F. R. Greten, and M. Karin, "Immunity, inflammation, and cancer," *Cell*, vol. 140, pp. 883-99, Mar 19 2010.
- [247] A. R. Young and M. Narita, "SASP reflects senescence," *EMBO Rep*, vol. 10, pp. 228-30, Mar 2009.
- [248] D. Liu and P. J. Hornsby, "Senescent human fibroblasts increase the early growth of xenograft tumors via matrix metalloproteinase secretion," *Cancer Res*, vol. 67, pp. 3117-26, Apr 1 2007.

- [249] J. N. Bartholomew, D. Volonte, and F. Galbiati, "Caveolin-1 regulates the antagonistic pleiotropic properties of cellular senescence through a novel Mdm2/p53-mediated pathway," *Cancer Res*, vol. 69, pp. 2878-86, Apr 1 2009.
- [250] J. Campisi, "Cancer and ageing: rival demons?," *Nat Rev Cancer*, vol. 3, pp. 339-49, May 2003.
- [251] L. Balducci and W. B. Ershler, "Cancer and ageing: a nexus at several levels," *Nat Rev Cancer*, vol. 5, pp. 655-62, Aug 2005.
- [252] L. M. Figueiredo, G. A. Cross, and C. J. Janzen, "Epigenetic regulation in African trypanosomes: a new kid on the block," *Nature Reviews Microbiology*, vol. 7, pp. 504-513, 2009.
- [253] K. van Holde, "Springer-Verlag; New York: 1989," ed: Chromatin.
- [254] G. Arents, R. W. Burlingame, B.-C. Wang, W. E. Love, and E. N. Moudrianakis, "The nucleosomal core histone octamer at 3.1 Å resolution: a tripartite protein assembly and a left-handed superhelix," *Proceedings of the National Academy of Sciences*, vol. 88, pp. 10148-10152, 1991.
- [255] K. Luger, A. W. Mäder, R. K. Richmond, D. F. Sargent, and T. J. Richmond, "Crystal structure of the nucleosome core particle at 2.8 Å resolution," *Nature*, vol. 389, pp. 251-260, 1997.
- [256] T. H. Eickbush and E. N. Moudrianakis, "The histone core complex: an octamer assembled by two sets of protein-protein interactions," *Biochemistry*, vol. 17, pp. 4955-4964, 1978.
- [257] V. Karantza, A. D. Baxevanis, E. Freire, and E. N. Moudrianakis, "Thermodynamic studies of the core histones: ionic strength and pH dependence of H2A-H2B dimer stability," *Biochemistry*, vol. 34, pp. 5988-5996, 1995.
- [258] V. Karantza, E. Freire, and E. N. Moudrianakis, "Thermodynamic studies of the core histones: pH and ionic strength effects on the stability of the (H3-H4)/(H3-H4) 2 system," *Biochemistry*, vol. 35, pp. 2037-2046, 1996.
- [259] R. D. Kornberg, "Chromatin structure: a repeating unit of histones and DNA," *Science*, vol. 184, pp. 868-71, May 24 1974.
- [260] K. Shibahara and B. Stillman, "Replication-dependent marking of DNA by PCNA facilitates CAF-1-coupled inheritance of chromatin," *Cell*, vol. 96, pp. 575-85, Feb 19 1999.
- [261] K. L. Yap and M.-M. Zhou, "Structure and function of protein modules in chromatin biology," in *Chromatin Dynamics in Cellular Function*, ed: Springer, 2006, pp. 1-23.
- [262] E. Li, "Chromatin modification and epigenetic reprogramming in mammalian development," *Nat Rev Genet*, vol. 3, pp. 662-73, Sep 2002.
- [263] S. I. Grewal and S. Jia, "Heterochromatin revisited," *Nat Rev Genet*, vol. 8, pp. 35-46, Jan 2007.
- [264] A. Wolffe, *Chromatin: structure and function*: Access Online via Elsevier, 1998.
- [265] K. Sarma and D. Reinberg, "Histone variants meet their match," *Nat Rev Mol Cell Biol*, vol. 6, pp. 139-49, Feb 2005.
- [266] H. S. Malik and S. Henikoff, "Phylogenomics of the nucleosome," *Nat Struct Biol*, vol. 10, pp. 882-91, Nov 2003.
- [267] S. Henikoff and K. Ahmad, "Assembly of variant histones into chromatin," *Annu. Rev. Cell Dev. Biol.*, vol. 21, pp. 133-153, 2005.
- [268] D. K. Palmer, K. O'Day, H. Trong, H. Charbonneau, and R. L. Margolis, "Purification of the centromere-specific protein CENP-A and demonstration that

- it is a distinctive histone," *Proceedings of the National Academy of Sciences*, vol. 88, pp. 3734-3738, 1991.
- [269] D. K. Palmer, K. O'Day, M. H. Wener, B. S. Andrews, and R. L. Margolis, "A 17-kD centromere protein (CENP-A) copurifies with nucleosome core particles and with histones," *The Journal of cell biology*, vol. 104, pp. 805-815, 1987.
- [270] M. D. Blower and G. H. Karpen, "The role of *Drosophila* CID in kinetochore formation, cell-cycle progression and heterochromatin interactions," *Nat Cell Biol*, vol. 3, pp. 730-9, Aug 2001.
- [271] B. J. Buchwitz, K. Ahmad, L. L. Moore, M. B. Roth, and S. Henikoff, "Cell division: a histone-H3-like protein in *C. elegans*," *Nature*, vol. 401, pp. 547-548, 1999.
- [272] E. V. Howman, K. J. Fowler, A. J. Newson, S. Redward, A. C. MacDonald, P. Kalitsis, and K. A. Choo, "Early disruption of centromeric chromatin organization in centromere protein A (Cenpa) null mice," *Proceedings of the National Academy of Sciences*, vol. 97, pp. 1148-1153, 2000.
- [273] S. Stoler, K. C. Keith, K. E. Curnick, and M. Fitzgerald-Hayes, "A mutation in CSE4, an essential gene encoding a novel chromatin-associated protein in yeast, causes chromosome nondisjunction and cell cycle arrest at mitosis," *Genes & development*, vol. 9, pp. 573-586, 1995.
- [274] L. Yu and M. A. Gorovsky, "Constitutive expression, not a particular primary sequence, is the important feature of the H3 replacement variant hv2 in *Tetrahymena thermophila*," *Molecular and cellular biology*, vol. 17, pp. 6303-6310, 1997.
- [275] M. K. Urban and A. Zweidler, "Changes in nucleosomal core histone variants during chicken development and maturation," *Dev Biol*, vol. 95, pp. 421-8, Feb 1983.
- [276] B. Pina and P. Suaud, "Changes in histones H2A and H3 variant composition in differentiating and mature rat brain cortical neurons," *Developmental biology*, vol. 123, pp. 51-58, 1987.
- [277] M. Hendzel and J. Davie, "Nucleosomal histones of transcriptionally active/competent chromatin preferentially exchange with newly synthesized histones in quiescent chicken erythrocytes," *Biochem. J*, vol. 271, pp. 67-73, 1990.
- [278] H. Tagami, D. Ray-Gallet, G. Almouzni, and Y. Nakatani, "Histone H3.1 and H3.3 complexes mediate nucleosome assembly pathways dependent or independent of DNA synthesis," *Cell*, vol. 116, pp. 51-61, Jan 9 2004.
- [279] K. Ahmad and S. Henikoff, "The histone variant H3. 3 marks active chromatin by replication-independent nucleosome assembly," *Molecular cell*, vol. 9, pp. 1191-1200, 2002.
- [280] A. D. Goldberg, L. A. Banaszynski, K.-M. Noh, P. W. Lewis, S. J. Elsaesser, S. Stadler, S. Dewell, M. Law, X. Guo, and X. Li, "Distinct factors control histone variant H3. 3 localization at specific genomic regions," *Cell*, vol. 140, pp. 678-691, 2010.
- [281] J. Ausio and D. W. Abbott, "The many tales of a tail: carboxyl-terminal tail heterogeneity specializes histone H2A variants for defined chromatin function," *Biochemistry*, vol. 41, pp. 5945-9, May 14 2002.
- [282] C. Redon, D. Pilch, E. Rogakou, O. Sedelnikova, K. Newrock, and W. Bonner, "Histone H2A variants H2AX and H2AZ," *Curr Opin Genet Dev*, vol. 12, pp. 162-9, Apr 2002.

- [283] O. Fernandez-Capetillo, A. Lee, M. Nussenzweig, and A. Nussenzweig, "H2AX: the histone guardian of the genome," *DNA Repair (Amst)*, vol. 3, pp. 959-67, Aug-Sep 2004.
- [284] R. Faast, V. Thonglairoam, T. C. Schulz, J. Beall, J. R. Wells, H. Taylor, K. Matthaei, P. D. Rathjen, D. J. Tremethick, and I. Lyons, "Histone variant H2A.Z is required for early mammalian development," *Current Biology*, vol. 11, pp. 1183-1187, 2001.
- [285] D. Rangasamy, I. Greaves, and D. J. Tremethick, "RNA interference demonstrates a novel role for H2A.Z in chromosome segregation," *Nat Struct Mol Biol*, vol. 11, pp. 650-5, Jul 2004.
- [286] A. Celeste, S. Petersen, P. J. Romanienko, O. Fernandez-Capetillo, H. T. Chen, O. A. Sedelnikova, B. Reina-San-Martin, V. Coppola, E. Meffre, M. J. Difilippantonio, C. Redon, D. R. Pilch, A. Olaru, M. Eckhaus, R. D. Camerini-Otero, L. Tessarollo, F. Livak, K. Manova, W. M. Bonner, M. C. Nussenzweig, and A. Nussenzweig, "Genomic instability in mice lacking histone H2AX," *Science*, vol. 296, pp. 922-7, May 3 2002.
- [287] A. Celeste, O. Fernandez-Capetillo, M. J. Kruhlak, D. R. Pilch, D. W. Staudt, A. Lee, R. F. Bonner, W. M. Bonner, and A. Nussenzweig, "Histone H2AX phosphorylation is dispensable for the initial recognition of DNA breaks," *Nature cell biology*, vol. 5, pp. 675-679, 2003.
- [288] O. Fernandez-Capetillo, S. K. Mahadevaiah, A. Celeste, P. J. Romanienko, R. D. Camerini-Otero, W. M. Bonner, K. Manova, P. Burgoyne, and A. Nussenzweig, "H2AX is required for chromatin remodeling and inactivation of sex chromosomes in male mouse meiosis," *Developmental cell*, vol. 4, pp. 497-508, 2003.
- [289] E. P. Rogakou, D. R. Pilch, A. H. Orr, V. S. Ivanova, and W. M. Bonner, "DNA double-stranded breaks induce histone H2AX phosphorylation on serine 139," *J Biol Chem*, vol. 273, pp. 5858-68, Mar 6 1998.
- [290] J. R. Pehrson and V. A. Fried, "MacroH2A, a core histone containing a large nonhistone region," *Science*, vol. 257, pp. 1398-400, Sep 4 1992.
- [291] C. Costanzi and J. R. Pehrson, "Histone macroH2A1 is concentrated in the inactive X chromosome of female mammals," *Nature*, vol. 393, pp. 599-601, 1998.
- [292] T.-C. TSENG, S.-H. CHEN, Y.-P. P. HSU, and T. K. TANG, "Protein kinase profile of sperm and eggs: cloning and characterization of two novel testis-specific protein kinases (AIE1, AIE2) related to yeast and fly chromosome segregation regulators," *DNA and cell biology*, vol. 17, pp. 823-833, 1998.
- [293] D. Angelov, A. Molla, P.-Y. Perche, F. Hans, J. Côté, S. Khochbin, P. Bouvet, and S. Dimitrov, "The histone variant macroH2A interferes with transcription factor binding and SWI/SNF nucleosome remodeling," *Molecular cell*, vol. 11, pp. 1033-1041, 2003.
- [294] B. P. Chadwick, C. M. Valley, and H. F. Willard, "Histone variant macroH2A contains two distinct macrochromatin domains capable of directing macroH2A to the inactive X chromosome," *Nucleic acids research*, vol. 29, pp. 2699-2705, 2001.
- [295] T. Gautier, D. W. Abbott, A. Molla, A. Verdell, J. Ausio, and S. Dimitrov, "Histone variant H2ABbd confers lower stability to the nucleosome," *EMBO reports*, vol. 5, pp. 715-720, 2004.

- [296] A. O. Zalensky, J. S. Siino, A. A. Gineitis, I. A. Zalenskaya, N. V. Tomilin, P. Yau, and E. M. Bradbury, "Human testis/sperm-specific histone H2B (hTSH2B). Molecular cloning and characterization," *J Biol Chem*, vol. 277, pp. 43474-80, Nov 8 2002.
- [297] Y. S. Niino, T. Irie, M. Takaishi, T. Hosono, N.-h. Huh, T. Tachikawa, and T. Kuroki, "PKC  $\theta$  II, a new isoform of protein kinase C specifically expressed in the seminiferous tubules of mouse testis," *Journal of Biological Chemistry*, vol. 276, pp. 36711-36717, 2001.
- [298] T. Kouzarides, "Chromatin modifications and their function," *Cell*, vol. 128, pp. 693-705, 2007.
- [299] M. J. Hendzel, M. A. Lever, E. Crawford, and J. P. Th'ng, "The C-terminal domain is the primary determinant of histone H1 binding to chromatin in vivo," *Journal of Biological Chemistry*, vol. 279, pp. 20028-20034, 2004.
- [300] D. A. Fantz, W. R. Hatfield, G. Horvath, M. K. Kistler, and W. S. Kistler, "Mice with a targeted disruption of the H1t gene are fertile and undergo normal changes in structural chromosomal proteins during spermiogenesis," *Biology of reproduction*, vol. 64, pp. 425-431, 2001.
- [301] I. Martianov, S. Brancorsini, R. Catena, A. Gansmuller, N. Kotaja, M. Parvinen, P. Sassone-Corsi, and I. Davidson, "Polar nuclear localization of H1T2, a histone H1 variant, required for spermatid elongation and DNA condensation during spermiogenesis," *Proceedings of the National Academy of Sciences of the United States of America*, vol. 102, pp. 2808-2813, 2005.
- [302] S. Kimmins and P. Sassone-Corsi, "Chromatin remodelling and epigenetic features of germ cells," *Nature*, vol. 434, pp. 583-9, Mar 31 2005.
- [303] A. Akhmanova, K. Miedema, and W. Hennig, "Identification and characterization of the Drosophila histone H4 replacement gene," *FEBS Lett*, vol. 388, pp. 219-22, Jun 17 1996.
- [304] D. E. Sterner and S. L. Berger, "Acetylation of histones and transcription-related factors," *Microbiology and Molecular Biology Reviews*, vol. 64, pp. 435-459, 2000.
- [305] Y. Zhang and D. Reinberg, "Transcription regulation by histone methylation: interplay between different covalent modifications of the core histone tails," *Genes & development*, vol. 15, pp. 2343-2360, 2001.
- [306] A. Shilatifard, "Chromatin modifications by methylation and ubiquitination: implications in the regulation of gene expression," *Annu. Rev. Biochem.*, vol. 75, pp. 243-269, 2006.
- [307] S. J. Nowak and V. G. Corces, "Phosphorylation of histone H3: a balancing act between chromosome condensation and transcriptional activation," *TRENDS in Genetics*, vol. 20, pp. 214-220, 2004.
- [308] G. L. Cuthbert, S. Daujat, A. W. Snowden, H. Erdjument-Bromage, T. Hagiwara, M. Yamada, R. Schneider, P. D. Gregory, P. Tempst, and A. J. Bannister, "Histone deimination antagonizes arginine methylation," *Cell*, vol. 118, pp. 545-553, 2004.
- [309] P. O. Hassa, S. S. Haenni, M. Elser, and M. O. Hottiger, "Nuclear ADP-ribosylation reactions in mammalian cells: where are we today and where are we going?," *Microbiology and Molecular Biology Reviews*, vol. 70, pp. 789-829, 2006.
- [310] D. Nathan, K. Ingvarsdottir, D. E. Sterner, G. R. Bylebyl, M. Dokmanovic, J. A. Dorsey, K. A. Whelan, M. Krsmanovic, W. S. Lane, and P. B. Meluh, "Histone

- sumoylation is a negative regulator in *Saccharomyces cerevisiae* and shows dynamic interplay with positive-acting histone modifications," *Genes & development*, vol. 20, pp. 966-976, 2006.
- [311] C. J. Nelson, H. Santos-Rosa, and T. Kouzarides, "Proline isomerization of histone H3 regulates lysine methylation and gene expression," *Cell*, vol. 126, pp. 905-916, 2006.
- [312] A. U. Khan and S. Krishnamurthy, "Histone modifications as key regulators of transcription," *Front Biosci*, vol. 10, pp. 866-872, 2005.
- [313] A. Eberharter and P. B. Becker, "Histone acetylation: a switch between repressive and permissive chromatin," *EMBO reports*, vol. 3, pp. 224-229, 2002.
- [314] S. L. Berger, "Histone modifications in transcriptional regulation," *Current opinion in genetics & development*, vol. 12, pp. 142-148, 2002.
- [315] T. Kouzarides, "Histone methylation in transcriptional control," *Current opinion in genetics & development*, vol. 12, pp. 198-209, 2002.
- [316] S. L. Berger, "The complex language of chromatin regulation during transcription," *Nature*, vol. 447, pp. 407-12, May 24 2007.
- [317] C. Chen, T. J. Nott, J. Jin, and T. Pawson, "Deciphering arginine methylation: Tudor tells the tale," *Nature Reviews Molecular Cell Biology*, vol. 12, pp. 629-642, 2011.
- [318] S. R. Bhaumik, E. Smith, and A. Shilatifard, "Covalent modifications of histones during development and disease pathogenesis," *Nature structural & molecular biology*, vol. 14, pp. 1008-1016, 2007.
- [319] D. Y. Lee, C. Teyssier, B. D. Strahl, and M. R. Stallcup, "Role of protein methylation in regulation of transcription," *Endocr Rev*, vol. 26, pp. 147-70, Apr 2005.
- [320] R. Métivier, G. Penot, M. R. Hübner, G. Reid, H. Brand, M. Koš, and F. Gannon, "Estrogen receptor- $\alpha$  directs ordered, cyclical, and combinatorial recruitment of cofactors on a natural target promoter," *Cell*, vol. 115, pp. 751-763, 2003.
- [321] G. L. Cuthbert, S. Daujat, A. W. Snowden, H. Erdjument-Bromage, T. Hagiwara, M. Yamada, R. Schneider, P. D. Gregory, P. Tempst, A. J. Bannister, and T. Kouzarides, "Histone deimination antagonizes arginine methylation," *Cell*, vol. 118, pp. 545-53, Sep 3 2004.
- [322] H. Wang, L. Wang, H. Erdjument-Bromage, M. Vidal, P. Tempst, R. S. Jones, and Y. Zhang, "Role of histone H2A ubiquitination in Polycomb silencing," *Nature*, vol. 431, pp. 873-8, Oct 14 2004.
- [323] J. Han, H. Zhou, B. Horazdovsky, K. Zhang, R. M. Xu, and Z. Zhang, "Rtt109 acetylates histone H3 lysine 56 and functions in DNA replication," *Science*, vol. 315, pp. 653-5, Feb 2 2007.
- [324] M. D. Shahbazian and M. Grunstein, "Functions of site-specific histone acetylation and deacetylation," *Annu. Rev. Biochem.*, vol. 76, pp. 75-100, 2007.
- [325] P. A. Marks, T. Miller, and V. M. Richon, "Histone deacetylases," *Curr Opin Pharmacol*, vol. 3, pp. 344-51, Aug 2003.
- [326] J. Berger and A. Bird, "Role of MBD2 in gene regulation and tumorigenesis," *Biochem Soc Trans*, vol. 33, pp. 1537-40, Dec 2005.

- [327] C. Dhalluin, J. E. Carlson, L. Zeng, C. He, A. K. Aggarwal, and M. M. Zhou, "Structure and ligand of a histone acetyltransferase bromodomain," *Nature*, vol. 399, pp. 491-6, Jun 3 1999.
- [328] R. H. Jacobson, A. G. Ladurner, D. S. King, and R. Tjian, "Structure and function of a human TAFII250 double bromodomain module," *Science*, vol. 288, pp. 1422-5, May 26 2000.
- [329] L. Zeng and M. M. Zhou, "Bromodomain: an acetyl-lysine binding domain," *FEBS Lett*, vol. 513, pp. 124-8, Feb 20 2002.
- [330] M. Lachner, D. O'Carroll, S. Rea, K. Mechtler, and T. Jenuwein, "Methylation of histone H3 lysine 9 creates a binding site for HP1 proteins," *Nature*, vol. 410, pp. 116-20, Mar 1 2001.
- [331] A. J. Bannister, P. Zegerman, J. F. Partridge, E. A. Miska, J. O. Thomas, R. C. Allshire, and T. Kouzarides, "Selective recognition of methylated lysine 9 on histone H3 by the HP1 chromo domain," *Nature*, vol. 410, pp. 120-4, Mar 1 2001.
- [332] C. A. Musselman and T. G. Kutateladze, "Handpicking epigenetic marks with PHD fingers," *Nucleic Acids Res*, vol. 39, pp. 9061-71, Nov 2011.
- [333] A. J. Ruthenburg, C. D. Allis, and J. Wysocka, "Methylation of lysine 4 on histone H3: intricacy of writing and reading a single epigenetic mark," *Mol Cell*, vol. 25, pp. 15-30, Jan 12 2007.
- [334] D. K. Morrison, "The 14-3-3 proteins: integrators of diverse signaling cues that impact cell fate and cancer development," *Trends in cell biology*, vol. 19, pp. 16-23, 2009.
- [335] U. Schindler, H. Beckmann, and A. R. Cashmore, "HAT3. 1, a novel Arabidopsis homeodomain protein containing a conserved cysteine - rich region," *The Plant Journal*, vol. 4, pp. 137-150, 1993.
- [336] R. Sanchez and M. M. Zhou, "The role of human bromodomains in chromatin biology and gene transcription," *Curr Opin Drug Discov Devel*, vol. 12, pp. 659-65, Sep 2009.
- [337] D. J. Owen, P. Ornaghi, J.-C. Yang, N. Lowe, P. R. Evans, P. Ballario, D. Neuhaus, P. Filetici, and A. A. Travers, "The structural basis for the recognition of acetylated histone H4 by the bromodomain of histone acetyltransferase gcn5p," *The EMBO journal*, vol. 19, pp. 6141-6149, 2000.
- [338] G. A. Josling, S. A. Selvarajah, M. Petter, and M. F. Duffy, "The Role of Bromodomain Proteins in Regulating Gene Expression," *Genes*, vol. 3, pp. 320-343, 2012.
- [339] A. J. Ruthenburg, H. Li, T. A. Milne, S. Dewell, R. K. McGinty, M. Yuen, B. Ueberheide, Y. Dou, T. W. Muir, and D. J. Patel, "Recognition of a mononucleosomal histone modification pattern by BPTF via multivalent interactions," *Cell*, vol. 145, pp. 692-706, 2011.
- [340] J. Morinière, S. Rousseaux, U. Steuerwald, M. Soler-López, S. Curtet, A.-L. Vitte, J. Govin, J. Gaucher, K. Sadoul, and D. J. Hart, "Cooperative binding of two acetylation marks on a histone tail by a single bromodomain," *Nature*, vol. 461, pp. 664-668, 2009.
- [341] J. E. Delmore, G. C. Issa, M. E. Lemieux, P. B. Rahl, J. Shi, H. M. Jacobs, E. Kastiris, T. Gilpatrick, R. M. Paranal, and J. Qi, "BET bromodomain inhibition as a therapeutic strategy to target c-Myc," *Cell*, vol. 146, pp. 904-917, 2011.

- [342] G. C. Yuan, Y. J. Liu, M. F. Dion, M. D. Slack, L. F. Wu, S. J. Altschuler, and O. J. Rando, "Genome-scale identification of nucleosome positions in *S. cerevisiae*," *Science*, vol. 309, pp. 626-30, Jul 22 2005.
- [343] D. E. Schones, K. Cui, S. Cuddapah, T. Y. Roh, A. Barski, Z. Wang, G. Wei, and K. Zhao, "Dynamic regulation of nucleosome positioning in the human genome," *Cell*, vol. 132, pp. 887-98, Mar 7 2008.
- [344] A. Valouev, S. M. Johnson, S. D. Boyd, C. L. Smith, A. Z. Fire, and A. Sidow, "Determinants of nucleosome organization in primary human cells," *Nature*, vol. 474, pp. 516-20, Jun 23 2011.
- [345] F. H. Lam, D. J. Steger, and E. K. O'Shea, "Chromatin decouples promoter threshold from dynamic range," *Nature*, vol. 453, pp. 246-50, May 8 2008.
- [346] S. Shivaswamy, A. Bhinge, Y. Zhao, S. Jones, M. Hirst, and V. R. Iyer, "Dynamic remodeling of individual nucleosomes across a eukaryotic genome in response to transcriptional perturbation," *PLoS Biol*, vol. 6, p. e65, Mar 18 2008.
- [347] T. Raveh-Sadka, M. Levo, U. Shabi, B. Shany, L. Keren, M. Lotan-Pompan, D. Zeevi, E. Sharon, A. Weinberger, and E. Segal, "Manipulating nucleosome disfavoring sequences allows fine-tune regulation of gene expression in yeast," *Nat Genet*, vol. 44, pp. 743-50, Jul 2012.
- [348] B. E. Bernstein, C. L. Liu, E. L. Humphrey, E. O. Perlstein, and S. L. Schreiber, "Global nucleosome occupancy in yeast," *Genome Biol*, vol. 5, p. R62, 2004.
- [349] F. Ozsolak, J. S. Song, X. S. Liu, and D. E. Fisher, "High-throughput mapping of the chromatin structure of human promoters," *Nat Biotechnol*, vol. 25, pp. 244-8, Feb 2007.
- [350] H. Reinke and W. Hörz, "Histones Are First Hyperacetylated and Then Lose Contact with the Activated *PHO5* Promoter," *Molecular cell*, vol. 11, pp. 1599-1607, 2003.
- [351] H. Boeger, J. Griesenbeck, J. S. Strattan, and R. D. Kornberg, "Nucleosomes unfold completely at a transcriptionally active promoter," *Molecular cell*, vol. 11, pp. 1587-1598, 2003.
- [352] S. Lomvardas and D. Thanos, "Modifying gene expression programs by altering core promoter chromatin architecture," *Cell*, vol. 110, pp. 261-271, 2002.
- [353] J. L. Gutierrez, M. Chandy, M. J. Carrozza, and J. L. Workman, "Activation domains drive nucleosome eviction by SWI/SNF," *The EMBO journal*, vol. 26, pp. 730-740, 2007.
- [354] T. Owen-Hughes, R. Utley, J. Cote, C. Peterson, and J. Workman, "Persistent site-specific remodeling of a nucleosome array by transient action of the SWI/SNF complex," *Science*, vol. 273, pp. 513-516, 1996.
- [355] M. A. Schwabish and K. Struhl, "The Swi/Snf complex is important for histone eviction during transcriptional activation and RNA polymerase II elongation in vivo," *Molecular and cellular biology*, vol. 27, pp. 6987-6995, 2007.
- [356] M. S. Kobor, S. Venkatasubrahmanyam, M. D. Meneghini, J. W. Gin, J. L. Jennings, A. J. Link, H. D. Madhani, and J. Rine, "A protein complex containing the conserved Swi2/Snf2-related ATPase Swr1p deposits histone variant H2A. Z into euchromatin," *PLoS biology*, vol. 2, p. e131, 2004.
- [357] A. Thakar, P. Gupta, T. Ishibashi, R. Finn, B. Silva-Moreno, S. Uchiyama, K. Fukui, M. Tomschik, J. Ausio, and J. Zlatanova, "H2A. Z and H3. 3 histone

- variants affect nucleosome structure: biochemical and biophysical studies," *Biochemistry*, vol. 48, pp. 10852-10857, 2009.
- [358] F. Collins, E. Lander, J. Rogers, R. Waterston, and I. Conso, "Finishing the euchromatic sequence of the human genome," *Nature*, vol. 431, pp. 931-945, 2004.
- [359] R. P. Alexander, G. Fang, J. Rozowsky, M. Snyder, and M. B. Gerstein, "Annotating non-coding regions of the genome," *Nat Rev Genet*, vol. 11, pp. 559-71, Aug 2010.
- [360] K. Sandberg, W. K. Samson, and H. Ji, "Decoding Noncoding RNA Da Vinci Redux?," *Circulation research*, vol. 113, pp. 240-241, 2013.
- [361] M. Esteller, "Non-coding RNAs in human disease," *Nature Reviews Genetics*, vol. 12, pp. 861-874, 2011.
- [362] M. Boehm and F. Slack, "A developmental timing microRNA and its target regulate life span in *C. elegans*," *Science*, vol. 310, pp. 1954-1957, 2005.
- [363] O. C. Maes, H. Sarojini, and E. Wang, "Stepwise up - regulation of microRNA expression levels from replicating to reversible and irreversible growth arrest states in WI - 38 human fibroblasts," *Journal of cellular physiology*, vol. 221, pp. 109-119, 2009.
- [364] T. Ito, S. Yagi, and M. Yamakuchi, "MicroRNA-34a regulation of endothelial senescence," *Biochemical and biophysical research communications*, vol. 398, pp. 735-740, 2010.
- [365] X. Li, A. Khanna, N. Li, and E. Wang, "Circulatory miR-34a as an RNA-based, noninvasive biomarker for brain aging," *Aging (Albany NY)*, vol. 3, p. 985, 2011.
- [366] N. Li, S. Muthusamy, R. Liang, H. Sarojini, and E. Wang, "Increased expression of miR-34a and miR-93 in rat liver during aging, and their impact on the expression of Mgst1 and Sirt1," *Mechanisms of ageing and development*, vol. 132, pp. 75-85, 2011.
- [367] M. G. Overhoff, J. C. Garbe, J. Koh, M. R. Stampfer, D. H. Beach, and C. L. Bishop, "Cellular senescence mediated by p16INK4A-coupled miRNA pathways," *Nucleic acids research*, p. gkt1096, 2013.
- [368] M. Benhamed, U. Herbig, T. Ye, A. Dejean, and O. Bischof, "Senescence is an endogenous trigger for microRNA-directed transcriptional gene silencing in human cells," *Nature Cell Biology*, vol. 14, pp. 266-275, 2012.
- [369] R. Ohsawa, J.-H. Seol, and J. K. Tyler, "At the intersection of non-coding transcription, DNA repair, chromatin structure, and cellular senescence," *Frontiers in genetics*, vol. 4, 2013.
- [370] J. L. Rinn, M. Kertesz, J. K. Wang, S. L. Squazzo, X. Xu, S. A. Brugmann, L. H. Goodnough, J. A. Helms, P. J. Farnham, and E. Segal, "Functional Demarcation of Active and Silent Chromatin Domains in Human HOX Loci by Noncoding RNAs," *Cell*, vol. 129, pp. 1311-1323, 2007.
- [371] A. Fatica and I. Bozzoni, "Long non-coding RNAs: new players in cell differentiation and development," *Nature Reviews Genetics*, 2013.
- [372] T. R. Mercer, M. E. Dinger, and J. S. Mattick, "Long non-coding RNAs: insights into functions," *Nature Reviews Genetics*, vol. 10, pp. 155-159, 2009.
- [373] M. Narita, M. Narita, V. Krizhanovsky, S. Nuñez, A. Chicas, S. A. Hearn, M. P. Myers, and S. W. Lowe, "A novel role for high-mobility group a proteins in cellular senescence and heterochromatin formation," *Cell*, vol. 126, pp. 503-514, 2006.

- [374] M. Narita, S. Nuñez, E. Heard, M. Narita, A. W. Lin, S. A. Hearn, D. L. Spector, G. J. Hannon, and S. W. Lowe, "Rb-mediated heterochromatin formation and silencing of E2F target genes during cellular senescence," *Cell*, vol. 113, pp. 703-716, 2003.
- [375] R. Zhang, M. V. Poustovoitov, X. Ye, H. A. Santos, W. Chen, S. M. Daganzo, J. P. Erzberger, I. G. Serebriiskii, A. A. Canutescu, and R. L. Dunbrack, "Formation of MacroH2A-containing senescence-associated heterochromatin foci and senescence driven by ASF1a and HIRA," *Developmental cell*, vol. 8, pp. 19-30, 2005.
- [376] H. M. Chan, M. Narita, S. W. Lowe, and D. M. Livingston, "The p400 E1A-associated protein is a novel component of the p53 → p21 senescence pathway," *Genes & development*, vol. 19, pp. 196-201, 2005.
- [377] M. Collado, J. Gil, A. Efeyan, C. Guerra, A. J. Schuhmacher, M. Barradas, A. Benguría, A. Zaballos, J. M. Flores, and M. Barbacid, "Tumour biology: senescence in premalignant tumours," *Nature*, vol. 436, pp. 642-642, 2005.
- [378] E. L. Denchi, C. Attwooll, D. Pasini, and K. Helin, "Deregulated E2F activity induces hyperplasia and senescence-like features in the mouse pituitary gland," *Molecular and cellular biology*, vol. 25, pp. 2660-2672, 2005.
- [379] B. Loppin, E. Bonnefoy, C. Anselme, A. Laurençon, T. L. Karr, and P. Couble, "The histone H3. 3 chaperone HIRA is essential for chromatin assembly in the male pronucleus," *Nature*, vol. 437, pp. 1386-1390, 2005.
- [380] D. Ray-Gallet, J.-P. Quivy, C. Scamps, E. M.-D. Martini, M. Lipinski, and G. Almouzni, "HIRA is critical for a nucleosome assembly pathway independent of DNA synthesis," *Molecular cell*, vol. 9, pp. 1091-1100, 2002.
- [381] H. Tagami, D. Ray-Gallet, G. Almouzni, and Y. Nakatani, "Histone H3. 1 and H3. 3 complexes mediate nucleosome assembly pathways dependent or independent of DNA synthesis," *Cell*, vol. 116, pp. 51-61, 2004.
- [382] L. H. Wong, J. D. McGhie, M. Sim, M. A. Anderson, S. Ahn, R. D. Hannan, A. J. George, K. A. Morgan, J. R. Mann, and K. A. Choo, "ATRX interacts with H3. 3 in maintaining telomere structural integrity in pluripotent embryonic stem cells," *Genome research*, vol. 20, pp. 351-360, 2010.
- [383] L. H. Wong, H. Ren, E. Williams, J. McGhie, S. Ahn, M. Sim, A. Tam, E. Earle, M. A. Anderson, and J. Mann, "Histone H3. 3 incorporation provides a unique and functionally essential telomeric chromatin in embryonic stem cells," *Genome research*, vol. 19, pp. 404-414, 2009.
- [384] A. Corpet, T. Olbrich, M. Gwerder, D. Fink, and M. Stucki, "Dynamics of histone H3. 3 deposition in proliferating and senescent cells reveals a DAXX-dependent targeting to PML-NBs important for pericentromeric heterochromatin organization," *Cell Cycle*, vol. 13, pp. 0--1, 2013.
- [385] R. Funayama, M. Saito, H. Tanobe, and F. Ishikawa, "Loss of linker histone H1 in cellular senescence," *The Journal of cell biology*, vol. 175, pp. 869-880, 2006.
- [386] R. Zhang, W. Chen, and P. D. Adams, "Molecular dissection of formation of senescence-associated heterochromatin foci," *Mol Cell Biol*, vol. 27, pp. 2343-58, Mar 2007.
- [387] X. Ye, B. Zerlanko, R. Zhang, N. Somaiah, M. Lipinski, P. Salomoni, and P. D. Adams, "Definition of pRB- and p53-dependent and -independent steps in HIRA/ASF1a-mediated formation of senescence-associated heterochromatin foci," *Mol Cell Biol*, vol. 27, pp. 2452-65, Apr 2007.

- [388] R. Scully and D. M. Livingston, "In search of the tumour-suppressor functions of BRCA1 and BRCA2," *Nature*, vol. 408, pp. 429-432, 2000.
- [389] K. Gudmundsdottir and A. Ashworth, "The roles of BRCA1 and BRCA2 and associated proteins in the maintenance of genomic stability," *Oncogene*, vol. 25, pp. 5864-5874, 2006.
- [390] Z. Tu, K. M. Aird, B. G. Bitler, J. P. Nicodemus, N. Beeharry, B. Xia, T. J. Yen, and R. Zhang, "Oncogenic RAS regulates BRIP1 expression to induce dissociation of BRCA1 from chromatin, inhibit DNA repair, and promote senescence," *Developmental cell*, vol. 21, pp. 1077-1091, 2011.
- [391] D. A. Bochar, L. Wang, H. Beniya, A. Kinev, Y. Xue, W. S. Lane, W. Wang, F. Kashanchi, and R. Shiekhattar, "BRCA1 is associated with a human SWI/SNF-related complex: linking chromatin remodeling to breast cancer," *Cell*, vol. 102, pp. 257-265, 2000.
- [392] J. L. Dunaief, B. E. Strober, S. Guha, P. A. Khavari, K. Ålin, J. Luban, M. Begemann, G. R. Crabtree, and S. P. Goff, "The retinoblastoma protein and BRG1 form a complex and cooperate to induce cell cycle arrest," *Cell*, vol. 79, pp. 119-130, 1994.
- [393] M. A. Napolitano, M. Cipollaro, A. Cascino, M. A. Melone, A. Giordano, and U. Galderisi, "Brg1 chromatin remodeling factor is involved in cell growth arrest, apoptosis and senescence of rat mesenchymal stem cells," *Journal of cell science*, vol. 120, pp. 2904-2911, 2007.
- [394] Z. Tu, X. Zhuang, Y.-G. Yao, and R. Zhang, "BRG1 Is Required for Formation of Senescence-Associated Heterochromatin Foci Induced by Oncogenic RAS or BRCA1 Loss," *Molecular and cellular biology*, vol. 33, pp. 1819-1829, 2013.
- [395] R. Di Micco, G. Sulli, M. Dobрева, M. Lontos, O. A. Botrugno, G. Gargiulo, R. dal Zuffo, V. Matti, G. d'Ario, and E. Montani, "Interplay between oncogene-induced DNA damage response and heterochromatin in senescence and cancer," *Nature cell biology*, vol. 13, pp. 292-302, 2011.
- [396] A. L. Kennedy, J. P. Morton, I. Manoharan, D. M. Nelson, N. B. Jamieson, J. S. Pawlikowski, T. McBryan, B. Doyle, C. McKay, and K. A. Oien, "Activation of the PIK3CA/AKT pathway suppresses senescence induced by an activated RAS oncogene to promote tumorigenesis," *Molecular cell*, vol. 42, pp. 36-49, 2011.
- [397] M. Kosar, J. Bartkova, S. Hubackova, Z. Hodny, J. Lukas, and J. Bartek, "Senescence-associated heterochromatin foci are dispensable for cellular senescence, occur in a cell type- and insult-dependent manner and follow expression of p16<sup>ink4a</sup>," *Cell Cycle*, vol. 10, pp. 457-468, 2011.
- [398] A. L. Kennedy, T. McBryan, G. H. Enders, F. B. Johnson, R. Zhang, and P. D. Adams, "Senescent mouse cells fail to overtly regulate the HIRA histone chaperone and do not form robust Senescence Associated Heterochromatin Foci," *Cell division*, vol. 5, p. 16, 2010.
- [399] K. Plath, J. Fang, S. K. Mlynarczyk-Evans, R. Cao, K. A. Worringer, H. Wang, C. Cecile, A. P. Otte, B. Panning, and Y. Zhang, "Role of histone H3 lysine 27 methylation in X inactivation," *Science*, vol. 300, pp. 131-135, 2003.
- [400] R. J. O'Sullivan, S. Kubicek, S. L. Schreiber, and J. Karlseder, "Reduced histone biosynthesis and chromatin changes arising from a damage signal at telomeres," *Nature structural & molecular biology*, vol. 17, pp. 1218-1225, 2010.

- [401] W. Dang, K. K. Steffen, R. Perry, J. A. Dorsey, F. B. Johnson, A. Shilatifard, M. Kaeberlein, B. K. Kennedy, and S. L. Berger, "Histone H4 lysine 16 acetylation regulates cellular lifespan," *Nature*, vol. 459, pp. 802-7, Jun 11 2009.
- [402] R. K. Mortimer and J. R. Johnston, "Life span of individual yeast cells," 1959.
- [403] K. Lee, Z. Z. Lau, C. Meredith, and J. H. Park, "Decrease of p400 ATPase complex and loss of H2A. Z within the p21 promoter occur in senescent IMR-90 human fibroblasts," *Mechanisms of ageing and development*, 2012.
- [404] Y. Cai, J. Jin, L. Florens, S. K. Swanson, T. Kusch, B. Li, J. L. Workman, M. P. Washburn, R. C. Conaway, and J. W. Conaway, "The mammalian YL1 protein is a shared subunit of the TRRAP/TIP60 histone acetyltransferase and SRCAP complexes," *Journal of Biological Chemistry*, vol. 280, pp. 13665-13670, 2005.
- [405] J. H. Park, X.-J. Sun, and R. G. Roeder, "The SANT domain of p400 ATPase represses acetyltransferase activity and coactivator function of TIP60 in basal p21 gene expression," *Molecular and cellular biology*, vol. 30, pp. 2750-2761, 2010.
- [406] D. D. Ruhl, J. Jin, Y. Cai, S. Swanson, L. Florens, M. P. Washburn, R. C. Conaway, J. W. Conaway, and J. C. Chrivia, "Purification of a human SRCAP complex that remodels chromatin by incorporating the histone variant H2A. Z into nucleosomes," *Biochemistry*, vol. 45, pp. 5671-5677, 2006.
- [407] P. Y. Lu, N. Levesque, and M. S. Kobor, "NuA4 and SWR1-C: two chromatin-modifying complexes with overlapping functions and components This paper is one of a selection of papers published in this Special Issue, entitled 30th Annual International Asilomar Chromatin and Chromosomes Conference, and has undergone the Journal's usual peer review process," *Biochemistry and Cell Biology*, vol. 87, pp. 799-815, 2009.
- [408] N. Gévry, H. M. Chan, L. Laflamme, D. M. Livingston, and L. Gaudreau, "p21 transcription is regulated by differential localization of histone H2A. Z," *Genes & development*, vol. 21, pp. 1869-1881, 2007.
- [409] J. M. Sedivy, G. Banumathy, and P. D. Adams, "Aging by epigenetics—A consequence of chromatin damage?," *Experimental cell research*, vol. 314, pp. 1909-1917, 2008.
- [410] J. Feser and J. Tyler, "Chromatin structure as a mediator of aging," *FEBS letters*, vol. 585, pp. 2041-2048, 2011.
- [411] E. I. Campos and D. Reinberg, "Histones: annotating chromatin," *Annual review of genetics*, vol. 43, pp. 559-599, 2009.
- [412] J.-i. Nakayama, J. C. Rice, B. D. Strahl, C. D. Allis, and S. I. Grewal, "Role of histone H3 lysine 9 methylation in epigenetic control of heterochromatin assembly," *Science*, vol. 292, pp. 110-113, 2001.
- [413] T. Chandra, K. Kirschner, J.-Y. Thuret, B. D. Pope, T. Ryba, S. Newman, K. Ahmed, S. A. Samarajiwa, R. Salama, and T. Carroll, "Independence of repressive histone marks and chromatin compaction during senescent heterochromatic layer formation," *Molecular cell*, 2012.
- [414] A. Chicas, A. Kapoor, X. Wang, O. Aksoy, A. G. Everitts, M. Q. Zhang, B. A. Garcia, E. Bernstein, and S. W. Lowe, "H3K4 demethylation by Jarid1a and Jarid1b contributes to retinoblastoma-mediated gene silencing during cellular senescence," *Proceedings of the National Academy of Sciences*, vol. 109, pp. 8971-8976, 2012.
- [415] M. Barradas, E. Anderton, J. C. Acosta, S. Li, A. Banito, M. Rodriguez-Niedenführ, G. Maertens, M. Banck, M.-M. Zhou, and M. J. Walsh, "Histone

- demethylase JMJD3 contributes to epigenetic control of INK4a/ARF by oncogenic RAS," *Genes & development*, vol. 23, pp. 1177-1182, 2009.
- [416] B. Liu, Z. Wang, L. Zhang, S. Ghosh, H. Zheng, and Z. Zhou, "Depleting the methyltransferase Suv39h1 improves DNA repair and extends lifespan in a progeria mouse model," *Nature communications*, vol. 4, p. 1868, 2013.
- [417] A. M. Pendás, Z. Zhou, J. Cadiñanos, J. M. Freije, J. Wang, K. Hultenby, A. Astudillo, A. Wernerson, F. Rodríguez, and K. Tryggvason, "Defective prelamin A processing and muscular and adipocyte alterations in Zmpste24 metalloproteinase-deficient mice," *Nature genetics*, vol. 31, pp. 94-99, 2002.
- [418] P. P. Shah, G. Donahue, G. L. Otte, B. C. Capell, D. M. Nelson, K. Cao, V. Aggarwala, H. A. Cruickshanks, T. S. Rai, T. McBryan, B. D. Gregory, P. D. Adams, and S. L. Berger, "Lamin B1 depletion in senescent cells triggers large-scale changes in gene expression and the chromatin landscape," *Genes Dev*, vol. 27, pp. 1787-99, Aug 15 2013.
- [419] U. K. Laemmli, "Cleavage of structural proteins during the assembly of the head of bacteriophage T4," *Nature*, vol. 227, pp. 680-5, Aug 15 1970.
- [420] E. Soriano, J. A. Del Rio, F. J. Martinez-Guijarro, I. Ferrer, and C. Lopez, "Immunocytochemical detection of 5'-bromodeoxyuridine in fluoro-gold-labeled neurons: a simple technique to combine retrograde axonal tracing and neurogenetic characterization of neurons," *J Histochem Cytochem*, vol. 39, pp. 1565-70, Nov 1991.
- [421] S. Shibui, T. Hoshino, M. Vanderlaan, and J. W. Gray, "Double labeling with iodo- and bromodeoxyuridine for cell kinetics studies," *J Histochem Cytochem*, vol. 37, pp. 1007-11, Jul 1989.
- [422] A. Salic and T. J. Mitchison, "A chemical method for fast and sensitive detection of DNA synthesis in vivo," *Proc Natl Acad Sci U S A*, vol. 105, pp. 2415-20, Feb 19 2008.
- [423] R. Breinbauer and M. Kohn, "Azide-alkyne coupling: a powerful reaction for bioconjugate chemistry," *ChemBiochem*, vol. 4, pp. 1147-9, Nov 7 2003.
- [424] Q. Wang, T. R. Chan, R. Hilgraf, V. V. Fokin, K. B. Sharpless, and M. G. Finn, "Bioconjugation by copper(I)-catalyzed azide-alkyne [3 + 2] cycloaddition," *J Am Chem Soc*, vol. 125, pp. 3192-3, Mar 19 2003.
- [425] V. V. Rostovtsev, L. G. Green, V. V. Fokin, and K. B. Sharpless, "A stepwise Huisgen cycloaddition process: copper(I)-catalyzed regioselective "ligation" of azides and terminal alkynes," *Angew Chem Int Ed Engl*, vol. 41, pp. 2596-9, Jul 15 2002.
- [426] H. C. Kolb, M. G. Finn, and K. B. Sharpless, "Click Chemistry: Diverse Chemical Function from a Few Good Reactions," *Angew Chem Int Ed Engl*, vol. 40, pp. 2004-2021, Jun 1 2001.
- [427] U. Herbig and J. M. Sedivy, "Regulation of growth arrest in senescence: telomere damage is not the end of the story," *Mech Ageing Dev*, vol. 127, pp. 16-24, Jan 2006.
- [428] M. Collado, M. A. Blasco, and M. Serrano, "Cellular senescence in cancer and aging," *Cell*, vol. 130, pp. 223-233, 2007.
- [429] T. S. Rai and P. D. Adams, "Lessons from senescence: Chromatin maintenance in non-proliferating cells," *Biochim Biophys Acta*, vol. 1819, pp. 322-31, Mar 2012.
- [430] A. J. Bannister and T. Kouzarides, "Regulation of chromatin by histone modifications," *Cell research*, vol. 21, pp. 381-395, 2011.

- [431] B. Charlesworth, "Evolution of senescence: Alzheimer's disease and evolution," *Current Biology*, vol. 6, pp. 20-22, 1996.
- [432] B.-D. Chang, K. Watanabe, E. V. Broude, J. Fang, J. C. Poole, T. V. Kalinichenko, and I. B. Roninson, "Effects of p21Waf1/Cip1/Sdi1 on cellular gene expression: implications for carcinogenesis, senescence, and age-related diseases," *Proceedings of the National Academy of Sciences*, vol. 97, pp. 4291-4296, 2000.
- [433] J. Campisi, S.-h. Kim, C.-S. Lim, and M. Rubio, "Cellular senescence, cancer and aging: the telomere connection," *Experimental gerontology*, vol. 36, pp. 1619-1637, 2001.
- [434] J. Campisi, "Cancer, aging and cellular senescence," *In vivo (Athens, Greece)*, vol. 14, pp. 183-188, 1999.
- [435] M. Narita, M. Narita, V. Krizhanovsky, S. Nunez, A. Chicas, S. A. Hearn, M. P. Myers, and S. W. Lowe, "A novel role for high-mobility group a proteins in cellular senescence and heterochromatin formation," *Cell*, vol. 126, pp. 503-14, Aug 11 2006.
- [436] M. Yoshida, M. Kijima, M. Akita, and T. Beppu, "Potent and specific inhibition of mammalian histone deacetylase both in vivo and in vitro by trichostatin A," *Journal of Biological Chemistry*, vol. 265, pp. 17174-17179, 1990.
- [437] C. Henderson, M. Mizzau, G. Paroni, R. Maestro, C. Schneider, and C. Brancolini, "Role of caspases, Bid, and p53 in the apoptotic response triggered by histone deacetylase inhibitors trichostatin-A (TSA) and suberoylanilide hydroxamic acid (SAHA)," *Journal of Biological Chemistry*, vol. 278, pp. 12579-12589, 2003.
- [438] M. Dokmanovic and P. A. Marks, "Prospects: histone deacetylase inhibitors," *Journal of cellular biochemistry*, vol. 96, pp. 293-304, 2005.
- [439] O. Moradei, C. R. Maroun, I. Paquin, and A. Vaisburg, "Histone deacetylase inhibitors: latest developments, trends and prospects," *Current Medicinal Chemistry-Anti-Cancer Agents*, vol. 5, pp. 529-560, 2005.
- [440] M. Riggs, R. Whittaker, J. Neumann, and V. Ingram, "n-Butyrate causes histone modification in HeLa and Friend erythroleukaemia cells," 1977.
- [441] L. S. Cousens, D. Gallwitz, and B. M. Alberts, "Different accessibilities in chromatin to histone acetylase," *J. Biol. Chem*, vol. 254, pp. 1716-1723, 1979.
- [442] R. T. Simpson, "Structure of chromatin containing extensively acetylated H3 and H4," *Cell*, vol. 13, pp. 691-699, 1978.
- [443] E. P. M. Candido, R. Reeves, and J. R. Davie, "Sodium butyrate inhibits histone deacetylation in cultured cells," *Cell*, vol. 14, pp. 105-113, 1978.
- [444] L. Sealy and R. Chalkley, "The effect of sodium butyrate on histone modification," *Cell*, vol. 14, pp. 115-121, 1978.
- [445] J. Timson, "Hydroxyurea," *Mutation Research/Reviews in Genetic Toxicology*, vol. 32, pp. 115-131, 1975.
- [446] A. B. Pardee, "A restriction point for control of normal animal cell proliferation," *Proceedings of the National Academy of Sciences*, vol. 71, pp. 1286-1290, 1974.
- [447] P. Weisman - Shomer, A. Kaftory, and M. Fry, "Replicative activity of isolated chromatin from proliferating and quiescent early passage and aging cultured mouse cells," *Journal of cellular physiology*, vol. 101, pp. 219-227, 1979.

- [448] P. J. Hauser, D. Agrawal, M. Flanagan, and W. J. Pledger, "The role of p27kip1 in the in vitro differentiation of murine keratinocytes," *Cell Growth Differ*, vol. 8, pp. 203-11, Feb 1997.
- [449] B. L. Harvat, A. Wang, P. Seth, and A. M. Jetten, "Up-regulation of p27Kip1, p21WAF1/Cip1 and p16Ink4a is associated with, but not sufficient for, induction of squamous differentiation," *J Cell Sci*, vol. 111 ( Pt 9), pp. 1185-96, May 1998.
- [450] H. Norsgaard, B. F. Clark, and S. I. Rattan, "Distinction between differentiation and senescence and the absence of increased apoptosis in human keratinocytes undergoing cellular aging in vitro," *Exp Gerontol*, vol. 31, pp. 563-70, Sep-Oct 1996.
- [451] R. Zhang, W. Chen, and P. D. Adams, "Molecular dissection of formation of senescence-associated heterochromatin foci," *Molecular and cellular biology*, vol. 27, pp. 2343-2358, 2007.
- [452] R. Di Micco, G. Sulli, M. Dobrev, M. Lontos, O. A. Botrugno, G. Gargiulo, R. dal Zuffo, V. Matti, G. d'Ario, E. Montani, C. Mercurio, W. C. Hahn, V. Gorgoulis, S. Minucci, and F. d'Adda di Fagagna, "Interplay between oncogene-induced DNA damage response and heterochromatin in senescence and cancer," *Nat Cell Biol*, vol. 13, pp. 292-302, Mar 2011.
- [453] A. H. Peters, S. Kubicek, K. Mechtler, R. J. O'Sullivan, A. A. Derijck, L. Perez-Burgos, A. Kohlmaier, S. Opravil, M. Tachibana, Y. Shinkai, J. H. Martens, and T. Jenuwein, "Partitioning and plasticity of repressive histone methylation states in mammalian chromatin," *Mol Cell*, vol. 12, pp. 1577-89, Dec 2003.
- [454] Y. Yu, C. Song, Q. Zhang, P. A. DiMaggio, B. A. Garcia, A. York, M. F. Carey, and M. Grunstein, "Histone H3 lysine 56 methylation regulates DNA replication through its interaction with PCNA," *Mol Cell*, vol. 46, pp. 7-17, Apr 13 2012.
- [455] B. Goulet, A. Baruch, N. S. Moon, M. Poirier, L. L. Sansregret, A. Erickson, M. Bogyo, and A. Nepveu, "A cathepsin L isoform that is devoid of a signal peptide localizes to the nucleus in S phase and processes the CDP/Cux transcription factor," *Mol Cell*, vol. 14, pp. 207-19, Apr 23 2004.
- [456] J. L. Vogel and T. M. Kristie, "Site-specific proteolysis of the transcriptional coactivator HCF-1 can regulate its interaction with protein cofactors," *Proceedings of the National Academy of Sciences*, vol. 103, pp. 6817-6822, 2006.
- [457] A. Ciechanover, "Intracellular protein degradation: from a vague idea, through the lysosome and the ubiquitin-proteasome system, and onto human diseases and drug targeting (Nobel lecture)," *Angewandte Chemie International Edition*, vol. 44, pp. 5944-5967, 2005.
- [458] D. R. Green and J. C. Reed, "Mitochondria and apoptosis," *Science-AAAS-Weekly Paper Edition*, vol. 281, pp. 1309-1311, 1998.
- [459] M. Duffy, "Proteases as prognostic markers in cancer," *Clinical Cancer Research*, vol. 2, pp. 613-618, 1996.
- [460] S. Hashmi, C. Britton, J. Liu, D. B. Guiliano, Y. Oksov, and S. Lustigman, "Cathepsin L is essential for embryogenesis and development of *Caenorhabditis elegans*," *Journal of Biological Chemistry*, vol. 277, pp. 3477-3486, 2002.
- [461] J. Stypmann, K. Glaser, W. Roth, D. J. Tobin, I. Petermann, R. Matthias, G. Monnig, W. Haverkamp, G. Breithardt, W. Schmahl, C. Peters, and T. Reinheckel, "Dilated cardiomyopathy in mice deficient for the lysosomal

- cysteine peptidase cathepsin L," *Proc Natl Acad Sci U S A*, vol. 99, pp. 6234-9, Apr 30 2002.
- [462] U. Felbor, B. Kessler, W. Mothes, H. H. Goebel, H. L. Ploegh, R. T. Bronson, and B. R. Olsen, "Neuronal loss and brain atrophy in mice lacking cathepsins B and L," *Proc Natl Acad Sci U S A*, vol. 99, pp. 7883-8, Jun 11 2002.
- [463] F. Benavides, M. F. Starost, M. Flores, I. B. Gimenez-Conti, J. L. Guenet, and C. J. Conti, "Impaired hair follicle morphogenesis and cycling with abnormal epidermal differentiation in nackt mice, a cathepsin L-deficient mutation," *Am J Pathol*, vol. 161, pp. 693-703, Aug 2002.
- [464] D. J. Tobin, K. Foitzik, T. Reinheckel, L. Mecklenburg, V. A. Botchkarev, C. Peters, and R. Paus, "The lysosomal protease cathepsin L is an important regulator of keratinocyte and melanocyte differentiation during hair follicle morphogenesis and cycling," *Am J Pathol*, vol. 160, pp. 1807-21, May 2002.
- [465] H. A. Chapman, R. J. Riese, and G. P. Shi, "Emerging roles for cysteine proteases in human biology," *Annu Rev Physiol*, vol. 59, pp. 63-88, 1997.
- [466] A. J. Barrett, J. F. Woessner, and N. D. Rawlings, *Handbook of proteolytic enzymes* vol. 1: Access Online via Elsevier, 2004.
- [467] P. Gorden, J. L. Carpentier, S. Cohen, and L. Orci, "Epidermal growth factor: morphological demonstration of binding, internalization, and lysosomal association in human fibroblasts," *Proc Natl Acad Sci U S A*, vol. 75, pp. 5025-9, Oct 1978.
- [468] R. C. Pittman, S. R. Green, A. D. Attie, and D. Steinberg, "Radiolabeled sucrose covalently linked to protein. A device for quantifying degradation of plasma proteins catabolized by lysosomal mechanisms," *J Biol Chem*, vol. 254, pp. 6876-9, Aug 10 1979.
- [469] C. de Duve and R. Wattiaux, "Functions of lysosomes," *Annual review of physiology*, vol. 28, pp. 435-492, 1966.
- [470] B. Goulet, L. Sansregret, L. Leduy, M. Bogyo, E. Weber, S. S. Chauhan, and A. Nepveu, "Increased expression and activity of nuclear cathepsin L in cancer cells suggests a novel mechanism of cell transformation," *Mol Cancer Res*, vol. 5, pp. 899-907, Sep 2007.
- [471] S. Ceru, S. Konjar, K. Maher, U. Repnik, I. Krizaj, M. Bencina, M. Renko, A. Nepveu, E. Zerovnik, B. Turk, and N. Kopitar-Jerala, "Stefin B interacts with histones and cathepsin L in the nucleus," *J Biol Chem*, vol. 285, pp. 10078-86, Mar 26 2010.
- [472] S. Sullivan, M. Tosetto, D. Kevans, A. Coss, L. Wang, D. O'Donoghue, J. Hyland, K. Sheahan, H. Mulcahy, and J. O'Sullivan, "Localization of nuclear cathepsin L and its association with disease progression and poor outcome in colorectal cancer," *Int J Cancer*, vol. 125, pp. 54-61, Jul 1 2009.
- [473] A. M. Troy, K. Sheahan, H. E. Mulcahy, M. J. Duffy, J. M. Hyland, and D. P. O'Donoghue, "Expression of Cathepsin B and L antigen and activity is associated with early colorectal cancer progression," *Eur J Cancer*, vol. 40, pp. 1610-6, Jul 2004.
- [474] E. M. Duncan, T. L. Muratore-Schroeder, R. G. Cook, B. A. Garcia, J. Shabanowitz, D. F. Hunt, and C. D. Allis, "Cathepsin L proteolytically processes histone H3 during mouse embryonic stem cell differentiation," *Cell*, vol. 135, pp. 284-94, Oct 17 2008.
- [475] T. A. Egelhofer, A. Minoda, S. Klugman, K. Lee, P. Kolasinska-Zwierz, A. A. Alekseyenko, M.-S. Cheung, D. S. Day, S. Gadel, and A. A. Gorchakov, "An

- assessment of histone-modification antibody quality," *Nature structural & molecular biology*, vol. 18, pp. 91-93, 2011.
- [476] T. D. Littlewood, D. C. Hancock, P. S. Danielian, M. G. Parker, and G. I. Evan, "A modified oestrogen receptor ligand-binding domain as an improved switch for the regulation of heterologous proteins," *Nucleic Acids Res*, vol. 23, pp. 1686-90, May 25 1995.
- [477] J. A. Reuter and P. A. Khavari, "Use of conditionally active ras fusion proteins to study epidermal growth, differentiation, and neoplasia," *Methods in enzymology*, vol. 407, pp. 691-702, 2006.
- [478] K. Brix, "Lysosomal proteases," in *Lysosomes*, ed: Springer, 2005, pp. 50-59.
- [479] G. Lopez-Castejon, J. Theaker, P. Pelegrin, A. D. Clifton, M. Braddock, and A. Surprenant, "P2X(7) receptor-mediated release of cathepsins from macrophages is a cytokine-independent mechanism potentially involved in joint diseases," *J Immunol*, vol. 185, pp. 2611-9, Aug 15 2010.
- [480] A. Wyczalkowska-Tomasik and L. Paczek, "Cathepsin B and L activity in the serum during the human aging process: cathepsin B and L in aging," *Arch Gerontol Geriatr*, vol. 55, pp. 735-8, Nov-Dec 2012.
- [481] S. S. Chauhan, L. J. Goldstein, and M. M. Gottesman, "Expression of cathepsin L in human tumors," *Cancer Res*, vol. 51, pp. 1478-81, Mar 1 1991.
- [482] A. Ivanov, J. Pawlikowski, I. Manoharan, J. van Tuyn, D. M. Nelson, T. S. Rai, P. P. Shah, G. Hewitt, V. I. Korolchuk, J. F. Passos, H. Wu, S. L. Berger, and P. D. Adams, "Lysosome-mediated processing of chromatin in senescence," *J Cell Biol*, vol. 202, pp. 129-43, Jul 8 2013.
- [483] H. Santos-Rosa, A. Kirmizis, C. Nelson, T. Bartke, N. Saksouk, J. Cote, and T. Kouzarides, "Histone H3 tail clipping regulates gene expression," *Nat Struct Mol Biol*, vol. 16, pp. 17-22, Jan 2009.
- [484] G. Schotta, M. Lachner, A. H. Peters, and T. Jenuwein, "The indexing potential of histone lysine methylation," *Novartis Found Symp*, vol. 259, pp. 22-37; discussion 37-47, 163-9, 2004.
- [485] R. J. Sims, 3rd, K. Nishioka, and D. Reinberg, "Histone lysine methylation: a signature for chromatin function," *Trends Genet*, vol. 19, pp. 629-39, Nov 2003.
- [486] T. Jenuwein and C. D. Allis, "Translating the histone code," *Science*, vol. 293, pp. 1074-80, Aug 10 2001.
- [487] M. T. Bedford and S. Richard, "Arginine methylation an emerging regulator of protein function," *Mol Cell*, vol. 18, pp. 263-72, Apr 29 2005.
- [488] S. Huang, M. Litt, and G. Felsenfeld, "Methylation of histone H4 by arginine methyltransferase PRMT1 is essential in vivo for many subsequent histone modifications," *Genes Dev*, vol. 19, pp. 1885-93, Aug 15 2005.
- [489] B. D. Strahl, S. D. Briggs, C. J. Brame, J. A. Caldwell, S. S. Koh, H. Ma, R. G. Cook, J. Shabanowitz, D. F. Hunt, M. R. Stallcup, and C. D. Allis, "Methylation of histone H4 at arginine 3 occurs in vivo and is mediated by the nuclear receptor coactivator PRMT1," *Curr Biol*, vol. 11, pp. 996-1000, Jun 26 2001.
- [490] G. Reid, R. Metivier, C. Y. Lin, S. Denger, D. Ibberson, T. Ivacevic, H. Brand, V. Benes, E. T. Liu, and F. Gannon, "Multiple mechanisms induce transcriptional silencing of a subset of genes, including oestrogen receptor alpha, in response to deacetylase inhibition by valproic acid and trichostatin A," *Oncogene*, vol. 24, pp. 4894-907, Jul 21 2005.
- [491] T. B. van Dijk, N. Gillemans, C. Stein, P. Fanis, J. Demmers, M. van de Corput, J. Essers, F. Grosveld, U. M. Bauer, and S. Philipsen, "Friend of

- Prmt1, a novel chromatin target of protein arginine methyltransferases," *Mol Cell Biol*, vol. 30, pp. 260-72, Jan 2010.
- [492] D. Ahuja, M. T. Saenz-Robles, and J. M. Pipas, "SV40 large T antigen targets multiple cellular pathways to elicit cellular transformation," *Oncogene*, vol. 24, pp. 7729-45, Nov 21 2005.
- [493] J. W. Shay, O. M. Pereira-Smith, and W. E. Wright, "A role for both RB and p53 in the regulation of human cellular senescence," *Exp Cell Res*, vol. 196, pp. 33-9, Sep 1991.
- [494] J. Sage, A. L. Miller, P. A. Perez-Mancera, J. M. Wysocki, and T. Jacks, "Acute mutation of retinoblastoma gene function is sufficient for cell cycle re-entry," *Nature*, vol. 424, pp. 223-8, Jul 10 2003.
- [495] F. M. Boisvert, C. A. Chenard, and S. Richard, "Protein interfaces in signaling regulated by arginine methylation," *Sci STKE*, vol. 2005, p. re2, Feb 15 2005.
- [496] J. R. Cook, J. H. Lee, Z. H. Yang, C. D. Krause, N. Herth, R. Hoffmann, and S. Pestka, "FBXO11/PRMT9, a new protein arginine methyltransferase, symmetrically dimethylates arginine residues," *Biochem Biophys Res Commun*, vol. 342, pp. 472-81, Apr 7 2006.
- [497] A. E. McBride and P. A. Silver, "State of the arg: protein methylation at arginine comes of age," *Cell*, vol. 106, pp. 5-8, Jul 13 2001.
- [498] Y. Igarashi, S. Hakomori, T. Toyokuni, B. Dean, S. Fujita, M. Sugimoto, T. Ogawa, K. El-Ghendy, and E. Racker, "Effect of chemically well-defined sphingosine and its N-methyl derivatives on protein kinase C and src kinase activities," *Biochemistry*, vol. 28, pp. 6796-6800, 1989.
- [499] H. S. Scott, S. E. Antonarakis, M. D. Lalioti, C. Rossier, P. A. Silver, and M. F. Henry, "Identification and characterization of two putative human arginine methyltransferases (HRMT1L1 and HRMT1L2)," *Genomics*, vol. 48, pp. 330-40, Mar 15 1998.
- [500] J. D. Gary and S. Clarke, "RNA and protein interactions modulated by protein arginine methylation," *Prog Nucleic Acid Res Mol Biol*, vol. 61, pp. 65-131, 1998.
- [501] H. Wang, Z. Q. Huang, L. Xia, Q. Feng, H. Erdjument-Bromage, B. D. Strahl, S. D. Briggs, C. D. Allis, J. Wong, P. Tempst, and Y. Zhang, "Methylation of histone H4 at arginine 3 facilitating transcriptional activation by nuclear hormone receptor," *Science*, vol. 293, pp. 853-7, Aug 3 2001.
- [502] J. Tang, P. N. Kao, and H. R. Herschman, "Protein-arginine methyltransferase I, the predominant protein-arginine methyltransferase in cells, interacts with and is regulated by interleukin enhancer-binding factor 3," *J Biol Chem*, vol. 275, pp. 19866-76, Jun 30 2000.
- [503] M. J. Solomon, P. L. Larsen, and A. Varshavsky, "Mapping protein-DNA interactions in vivo with formaldehyde: Evidence that histone H4 is retained on a highly transcribed gene," *Cell*, vol. 53, pp. 937-947, 1988.
- [504] B. L. Kidder, G. Hu, and K. Zhao, "ChIP-Seq: technical considerations for obtaining high-quality data," *Nat Immunol*, vol. 12, pp. 918-22, Oct 2011.
- [505] D. Schmidt, R. Stark, M. D. Wilson, G. D. Brown, and D. T. Odom, "Genome-scale validation of deep-sequencing libraries," *PLoS One*, vol. 3, p. e3713, 2008.
- [506] Y. Lim, E. Lee, J. Lee, S. Oh, and S. Kim, "Down-regulation of asymmetric arginine methylation during replicative and H<sub>2</sub>O<sub>2</sub>-induced premature

- senescence in WI-38 human diploid fibroblasts," *J Biochem*, vol. 144, pp. 523-9, Oct 2008.
- [507] M. Yoshimatsu, G. Toyokawa, S. Hayami, M. Unoki, T. Tsunoda, H. I. Field, J. D. Kelly, D. E. Neal, Y. Maehara, B. A. Ponder, Y. Nakamura, and R. Hamamoto, "Dysregulation of PRMT1 and PRMT6, Type I arginine methyltransferases, is involved in various types of human cancers," *Int J Cancer*, vol. 128, pp. 562-73, Feb 1 2011.
- [508] D. Cheng, N. Yadav, R. W. King, M. S. Swanson, E. J. Weinstein, and M. T. Bedford, "Small molecule regulators of protein arginine methyltransferases," *J Biol Chem*, vol. 279, pp. 23892-9, Jun 4 2004.
- [509] C. D. Krause, Z. H. Yang, Y. S. Kim, J. H. Lee, J. R. Cook, and S. Pestka, "Protein arginine methyltransferases: evolution and assessment of their pharmacological and therapeutic potential," *Pharmacol Ther*, vol. 113, pp. 50-87, Jan 2007.
- [510] H. G. Williams-Ashman, J. Seidenfeld, and P. Galletti, "Trends in the biochemical pharmacology of 5'-deoxy-5'-methylthioadenosine," *Biochemical pharmacology*, vol. 31, pp. 277-288, 1982.
- [511] K. Bonham, S. Hemmers, Y. H. Lim, D. M. Hill, M. G. Finn, and K. A. Mowen, "Effects of a novel arginine methyltransferase inhibitor on T-helper cell cytokine production," *FEBS J*, vol. 277, pp. 2096-108, May 2010.
- [512] T. M. Lakowski, P. t Hart, C. A. Ahern, N. I. Martin, and A. Frankel, "Neta-substituted arginyl peptide inhibitors of protein arginine N-methyltransferases," *ACS Chem Biol*, vol. 5, pp. 1053-63, Nov 19 2010.
- [513] O. Obianyo, C. P. Causey, J. E. Jones, and P. R. Thompson, "Activity-based protein profiling of protein arginine methyltransferase 1," *ACS Chem Biol*, vol. 6, pp. 1127-35, Oct 21 2011.
- [514] Z. Yu, T. Chen, J. Hebert, E. Li, and S. Richard, "A mouse PRMT1 null allele defines an essential role for arginine methylation in genome maintenance and cell proliferation," *Mol Cell Biol*, vol. 29, pp. 2982-96, Jun 2009.
- [515] A. L. Jackson and P. S. Linsley, "Noise amidst the silence: off-target effects of siRNAs?," *Trends Genet*, vol. 20, pp. 521-4, Nov 2004.
- [516] A. L. Jackson, S. R. Bartz, J. Schelter, S. V. Kobayashi, J. Burchard, M. Mao, B. Li, G. Cavet, and P. S. Linsley, "Expression profiling reveals off-target gene regulation by RNAi," *Nat Biotechnol*, vol. 21, pp. 635-7, Jun 2003.
- [517] K. B. Schwarz, "Oxidative stress during viral infection: a review," *Free Radic Biol Med*, vol. 21, pp. 641-9, 1996.
- [518] W. J. Lin, J. D. Gary, M. C. Yang, S. Clarke, and H. R. Herschman, "The mammalian immediate-early TIS21 protein and the leukemia-associated BTG1 protein interact with a protein-arginine N-methyltransferase," *J Biol Chem*, vol. 271, pp. 15034-44, Jun 21 1996.
- [519] J. Tang, J. D. Gary, S. Clarke, and H. R. Herschman, "PRMT 3, a type I protein arginine N-methyltransferase that differs from PRMT1 in its oligomerization, subcellular localization, substrate specificity, and regulation," *Journal of Biological Chemistry*, vol. 273, pp. 16935-16945, 1998.
- [520] S. Koga, S. Kojima, T. Kishimoto, S. Kuwabara, and A. Yamaguchi, "Over-expression of map kinase phosphatase-1 (MKP-1) suppresses neuronal death through regulating JNK signaling in hypoxia/re-oxygenation," *Brain Res*, vol. 1436, pp. 137-46, Feb 3 2012.

- [521] W. An, J. Kim, and R. G. Roeder, "Ordered cooperative functions of PRMT1, p300, and CARM1 in transcriptional activation by p53," *Cell*, vol. 117, pp. 735-48, Jun 11 2004.
- [522] B. Chang, Y. Chen, Y. Zhao, and R. K. Bruick, "JMJD6 is a histone arginine demethylase," *Science*, vol. 318, pp. 444-7, Oct 19 2007.
- [523] C. J. Webby, A. Wolf, N. Gromak, M. Dreger, H. Kramer, B. Kessler, M. L. Nielsen, C. Schmitz, D. S. Butler, J. R. Yates, 3rd, C. M. Delahunty, P. Hahn, A. Lengeling, M. Mann, N. J. Proudfoot, C. J. Schofield, and A. Bottger, "Jmjd6 catalyses lysyl-hydroxylation of U2AF65, a protein associated with RNA splicing," *Science*, vol. 325, pp. 90-3, Jul 3 2009.
- [524] C. Tanikawa, K. Ueda, H. Nakagawa, N. Yoshida, Y. Nakamura, and K. Matsuda, "Regulation of protein Citrullination through p53/PADI4 network in DNA damage response," *Cancer research*, vol. 69, pp. 8761-8769, 2009.
- [525] C. Tanikawa, M. Espinosa, A. Suzuki, K. Masuda, K. Yamamoto, E. Tsuchiya, K. Ueda, Y. Daigo, Y. Nakamura, and K. Matsuda, "Regulation of histone modification and chromatin structure by the p53–PADI4 pathway," *Nature communications*, vol. 3, p. 676, 2012.
- [526] M. A. Christophorou, G. Castelo-Branco, R. P. Halley-Stott, C. S. Oliveira, R. Loos, A. Radziskeuskaya, K. A. Mowen, P. Bertone, J. C. Silva, and M. Zernicka-Goetz, "Citrullination regulates pluripotency and histone H1 binding to chromatin," *Nature*, 2014.
- [527] A. Ishigami and N. Maruyama, "Importance of research on peptidylarginine deiminase and citrullinated proteins in age - related disease," *Geriatrics & gerontology international*, vol. 10, pp. S53-S58, 2010.
- [528] C. Anzilotti, F. Pratesi, C. Tommasi, and P. Migliorini, "Peptidylarginine deiminase 4 and citrullination in health and disease," *Autoimmunity reviews*, vol. 9, pp. 158-160, 2010.
- [529] Y. Yang and M. T. Bedford, "Protein arginine methyltransferases and cancer," *Nat Rev Cancer*, vol. 13, pp. 37-50, Jan 2013.
- [530] M. Vogelauer, J. Wu, N. Suka, and M. Grunstein, "Global histone acetylation and deacetylation in yeast," *Nature*, vol. 408, pp. 495-8, Nov 23 2000.
- [531] A. H. Hassan, K. E. Neely, and J. L. Workman, "Histone acetyltransferase complexes stabilize swi/snf binding to promoter nucleosomes," *Cell*, vol. 104, pp. 817-27, Mar 23 2001.
- [532] Z. Wang, C. Zang, K. Cui, D. E. Schones, A. Barski, W. Peng, and K. Zhao, "Genome-wide mapping of HATs and HDACs reveals distinct functions in active and inactive genes," *Cell*, vol. 138, pp. 1019-31, Sep 4 2009.
- [533] K. Luger and T. J. Richmond, "The histone tails of the nucleosome," *Curr Opin Genet Dev*, vol. 8, pp. 140-6, Apr 1998.
- [534] A. T. Annunziato and J. C. Hansen, "Role of histone acetylation in the assembly and modulation of chromatin structures," *Gene Expr*, vol. 9, pp. 37-61, 2000.
- [535] B. M. Turner, "Histone acetylation and an epigenetic code," *Bioessays*, vol. 22, pp. 836-45, Sep 2000.
- [536] M. D. Shahbazian and M. Grunstein, "Functions of site-specific histone acetylation and deacetylation," *Annu Rev Biochem*, vol. 76, pp. 75-100, 2007.
- [537] A. Vaquero, R. Sternglanz, and D. Reinberg, "NAD<sup>+</sup>-dependent deacetylation of H4 lysine 16 by class III HDACs," *Oncogene*, vol. 26, pp. 5505-20, Aug 13 2007.

- [538] B. Dorigo, T. Schalch, K. Bystricky, and T. J. Richmond, "Chromatin fiber folding: requirement for the histone H4 N-terminal tail," *J Mol Biol*, vol. 327, pp. 85-96, Mar 14 2003.
- [539] B. Dorigo, T. Schalch, A. Kulangara, S. Duda, R. R. Schroeder, and T. J. Richmond, "Nucleosome arrays reveal the two-start organization of the chromatin fiber," *Science*, vol. 306, pp. 1571-3, Nov 26 2004.
- [540] M. Shogren-Knaak, H. Ishii, J. M. Sun, M. J. Pazin, J. R. Davie, and C. L. Peterson, "Histone H4-K16 acetylation controls chromatin structure and protein interactions," *Science*, vol. 311, pp. 844-7, Feb 10 2006.
- [541] P. J. Robinson, W. An, A. Routh, F. Martino, L. Chapman, R. G. Roeder, and D. Rhodes, "30 nm chromatin fibre decompaction requires both H4-K16 acetylation and linker histone eviction," *J Mol Biol*, vol. 381, pp. 816-25, Sep 12 2008.
- [542] A. Zippo, R. Serafini, M. Rocchigiani, S. Pennacchini, A. Krepelova, and S. Oliviero, "Histone crosstalk between H3S10ph and H4K16ac generates a histone code that mediates transcription elongation," *Cell*, vol. 138, pp. 1122-36, Sep 18 2009.
- [543] P. Jeppesen and B. M. Turner, "The inactive X chromosome in female mammals is distinguished by a lack of histone H4 acetylation, a cytogenetic marker for gene expression," *Cell*, vol. 74, pp. 281-9, Jul 30 1993.
- [544] C. Lavery, J. Lucci, and A. Akhtar, "The MSL complex: X chromosome and beyond," *Curr Opin Genet Dev*, vol. 20, pp. 171-8, Apr 2010.
- [545] V. Krishnan, M. Z. Chow, Z. Wang, L. Zhang, B. Liu, X. Liu, and Z. Zhou, "Histone H4 lysine 16 hypoacetylation is associated with defective DNA repair and premature senescence in Zmpste24-deficient mice," *Proc Natl Acad Sci U S A*, vol. 108, pp. 12325-30, Jul 26 2011.
- [546] M. F. Fraga, E. Ballestar, A. Villar-Garea, M. Boix-Chornet, J. Espada, G. Schotta, T. Bonaldi, C. Haydon, S. Roper, K. Petrie, N. G. Iyer, A. Perez-Rosado, E. Calvo, J. A. Lopez, A. Cano, M. J. Calasanz, D. Colomer, M. A. Piris, N. Ahn, A. Imhof, C. Caldas, T. Jenuwein, and M. Esteller, "Loss of acetylation at Lys16 and trimethylation at Lys20 of histone H4 is a common hallmark of human cancer," *Nat Genet*, vol. 37, pp. 391-400, Apr 2005.
- [547] K. Contrepois, J. Y. Thuret, R. Courbeyrette, F. Fenaille, and C. Mann, "Deacetylation of H4-K16Ac and heterochromatin assembly in senescence," *Epigenetics Chromatin*, vol. 5, p. 15, 2012.
- [548] B. D. Strahl and C. D. Allis, "The language of covalent histone modifications," *Nature*, vol. 403, pp. 41-5, Jan 6 2000.
- [549] M. Taipale, S. Rea, K. Richter, A. Vilar, P. Lichter, A. Imhof, and A. Akhtar, "hMOF histone acetyltransferase is required for histone H4 lysine 16 acetylation in mammalian cells," *Mol Cell Biol*, vol. 25, pp. 6798-810, Aug 2005.
- [550] A. Vaquero, M. Scher, D. Lee, H. Erdjument-Bromage, P. Tempst, and D. Reinberg, "Human SirT1 interacts with histone H1 and promotes formation of facultative heterochromatin," *Mol Cell*, vol. 16, pp. 93-105, Oct 8 2004.
- [551] R. T. Utley and J. Cote, "The MYST family of histone acetyltransferases," *Curr Top Microbiol Immunol*, vol. 274, pp. 203-36, 2003.
- [552] S. Y. Roth, J. M. Denu, and C. D. Allis, "Histone acetyltransferases," *Annu Rev Biochem*, vol. 70, pp. 81-120, 2001.

- [553] A. Akhtar and P. B. Becker, "The histone H4 acetyltransferase MOF uses a C2HC zinc finger for substrate recognition," *EMBO Rep*, vol. 2, pp. 113-8, Feb 2001.
- [554] J. R. Bone, J. Lavender, R. Richman, M. J. Palmer, B. M. Turner, and M. I. Kuroda, "Acetylated histone H4 on the male X chromosome is associated with dosage compensation in *Drosophila*," *Genes Dev*, vol. 8, pp. 96-104, Jan 1994.
- [555] E. R. Smith, A. Pannuti, W. Gu, A. Steurnagel, R. G. Cook, C. D. Allis, and J. C. Lucchesi, "The *drosophila* MSL complex acetylates histone H4 at lysine 16, a chromatin modification linked to dosage compensation," *Mol Cell Biol*, vol. 20, pp. 312-8, Jan 2000.
- [556] K. C. Neal, A. Pannuti, E. R. Smith, and J. C. Lucchesi, "A new human member of the MYST family of histone acetyl transferases with high sequence similarity to *Drosophila* MOF," *Biochim Biophys Acta*, vol. 1490, pp. 170-4, Jan 31 2000.
- [557] G. Blander and L. Guarente, "The Sir2 family of protein deacetylases," *Annu Rev Biochem*, vol. 73, pp. 417-35, 2004.
- [558] A. Gupta, T. G. Guerin-Peyrou, G. G. Sharma, C. Park, M. Agarwal, R. K. Ganju, S. Pandita, K. Choi, S. Sukumar, R. K. Pandita, T. Ludwig, and T. K. Pandita, "The mammalian ortholog of *Drosophila* MOF that acetylates histone H4 lysine 16 is essential for embryogenesis and oncogenesis," *Mol Cell Biol*, vol. 28, pp. 397-409, Jan 2008.
- [559] T. Finkel, C. X. Deng, and R. Mostoslavsky, "Recent progress in the biology and physiology of sirtuins," *Nature*, vol. 460, pp. 587-91, Jul 30 2009.
- [560] S. Michan and D. Sinclair, "Sirtuins in mammals: insights into their biological function," *Biochem J*, vol. 404, pp. 1-13, May 15 2007.
- [561] C. L. Brooks and W. Gu, "How does SIRT1 affect metabolism, senescence and cancer?," *Nat Rev Cancer*, vol. 9, pp. 123-8, Feb 2009.
- [562] C. X. Deng, "SIRT1, is it a tumor promoter or tumor suppressor?," *Int J Biol Sci*, vol. 5, pp. 147-52, 2009.
- [563] P. Mulligan, F. Yang, L. Di Stefano, J. Y. Ji, J. Ouyang, J. L. Nishikawa, D. Toiber, M. Kulkarni, Q. Wang, S. H. Najafi-Shoushtari, R. Mostoslavsky, S. P. Gygi, G. Gill, N. J. Dyson, and A. M. Naar, "A SIRT1-LSD1 corepressor complex regulates Notch target gene expression and development," *Mol Cell*, vol. 42, pp. 689-99, Jun 10 2011.
- [564] Y. Zhao, S. Lu, L. Wu, G. Chai, H. Wang, Y. Chen, J. Sun, Y. Yu, W. Zhou, Q. Zheng, M. Wu, G. A. Otterson, and W. G. Zhu, "Acetylation of p53 at lysine 373/382 by the histone deacetylase inhibitor depsipeptide induces expression of p21(Waf1/Cip1)," *Mol Cell Biol*, vol. 26, pp. 2782-90, Apr 2006.
- [565] J. Luo, A. Y. Nikolaev, S. Imai, D. Chen, F. Su, A. Shiloh, L. Guarente, and W. Gu, "Negative control of p53 by Sir2alpha promotes cell survival under stress," *Cell*, vol. 107, pp. 137-48, Oct 19 2001.
- [566] H. Vaziri, S. K. Dessain, E. Ng Eaton, S. I. Imai, R. A. Frye, T. K. Pandita, L. Guarente, and R. A. Weinberg, "hSIR2(SIRT1) functions as an NAD-dependent p53 deacetylase," *Cell*, vol. 107, pp. 149-59, Oct 19 2001.
- [567] H. Lu, Y. Taya, M. Ikeda, and A. J. Levine, "Ultraviolet radiation, but not gamma radiation or etoposide-induced DNA damage, results in the phosphorylation of the murine p53 protein at serine-389," *Proc Natl Acad Sci U S A*, vol. 95, pp. 6399-402, May 26 1998.

- [568] S. Gillam and M. Smith, "[65] Use of *E. coli* polynucleotide phosphorylase for the synthesis of oligodeoxyribonucleotides of defined sequence," *Methods in enzymology*, vol. 65, pp. 687-701, 1980.
- [569] M. J. Zoller and M. Smith, "Oligonucleotide-directed mutagenesis using M13-derived vectors: an efficient and general procedure for the production of point mutations in any fragment of DNA," *Nucleic Acids Research*, vol. 10, pp. 6487-6500, 1982.
- [570] J. Wang, X. Tadeo, H. Hou, P. G. Tu, J. Thompson, J. R. Yates, 3rd, and S. Jia, "Epe1 recruits BET family bromodomain protein Bdf2 to establish heterochromatin boundaries," *Genes Dev*, vol. 27, pp. 1886-902, Sep 1 2013.
- [571] B. Loppin, E. Bonnefoy, C. Anselme, A. Laurencon, T. L. Karr, and P. Couble, "The histone H3.3 chaperone HIRA is essential for chromatin assembly in the male pronucleus," *Nature*, vol. 437, pp. 1386-90, Oct 27 2005.
- [572] N. A. Pchelintsev, T. McBryan, T. S. Rai, J. van Tuyn, D. Ray-Gallet, G. Almouzni, and P. D. Adams, "Placing the HIRA histone chaperone complex in the chromatin landscape," *Cell Rep*, vol. 3, pp. 1012-9, Apr 25 2013.
- [573] M. F. Fraga, E. Ballestar, A. Villar-Garea, M. Boix-Chornet, J. Espada, G. Schotta, T. Bonaldi, C. Haydon, S. Roperio, and K. Petrie, "Loss of acetylation at Lys16 and trimethylation at Lys20 of histone H4 is a common hallmark of human cancer," *Nature genetics*, vol. 37, pp. 391-400, 2005.
- [574] G. G. Sharma, S. So, A. Gupta, R. Kumar, C. Cayrou, N. Avvakumov, U. Bhadra, R. K. Pandita, M. H. Porteus, D. J. Chen, J. Cote, and T. K. Pandita, "MOF and histone H4 acetylation at lysine 16 are critical for DNA damage response and double-strand break repair," *Mol Cell Biol*, vol. 30, pp. 3582-95, Jul 2010.
- [575] A. Vaquero, M. B. Scher, D. H. Lee, A. Sutton, H. L. Cheng, F. W. Alt, L. Serrano, R. Sternglanz, and D. Reinberg, "SirT2 is a histone deacetylase with preference for histone H4 Lys 16 during mitosis," *Genes Dev*, vol. 20, pp. 1256-61, May 15 2006.
- [576] Z. Hu, K. Chen, Z. Xia, M. Chavez, S. Pal, J.-H. Seol, C.-C. Chen, W. Li, and J. K. Tyler, "Nucleosome loss leads to global transcriptional up-regulation and genomic instability during yeast aging," *Genes & Development*, vol. 28, pp. 396-408, 2014.
- [577] E. P. Rogakou and K. E. Sekeri-Pataryas, "Histone variants of H2A and H3 families are regulated during in vitro aging in the same manner as during differentiation," *Experimental gerontology*, vol. 34, pp. 741-754, 1999.
- [578] M. K. Urban and A. Zweidler, "Changes in nucleosomal core histone variants during chicken development and maturation," *Developmental biology*, vol. 95, pp. 421-428, 1983.
- [579] M. C. Elia and E. N. Moudrianakis, "Regulation of H2a-specific proteolysis by the histone H3: H4 tetramer," *Journal of Biological Chemistry*, vol. 263, pp. 9958-9964, 1988.
- [580] R. Kaul, A. Hoang, P. Yau, E. M. Bradbury, and W. M. Wenman, "The chlamydial EUO gene encodes a histone H1-specific protease," *Journal of bacteriology*, vol. 179, pp. 5928-5934, 1997.
- [581] M. Falk, P. Grigera, I. Bergmann, A. Zibert, G. Multhaup, and E. Beck, "Foot-and-mouth disease virus protease 3C induces specific proteolytic cleavage of host cell histone H3," *Journal of virology*, vol. 64, pp. 748-756, 1990.

- [582] A. Bortvin and F. Winston, "Evidence that Spt6p controls chromatin structure by a direct interaction with histones," *Science*, vol. 272, pp. 1473-1476, 1996.
- [583] Y. A. Bulyanko, L. C. Hsing, R. W. Mason, D. J. Tremethick, and S. A. Grigoryev, "Cathepsin L stabilizes the histone modification landscape on the Y chromosome and pericentromeric heterochromatin," *Molecular and cellular biology*, vol. 26, pp. 4172-4184, 2006.
- [584] G. Simmons, D. N. Gosalia, A. J. Rennekamp, J. D. Reeves, S. L. Diamond, and P. Bates, "Inhibitors of cathepsin L prevent severe acute respiratory syndrome coronavirus entry," *Proceedings of the National Academy of Sciences of the United States of America*, vol. 102, pp. 11876-11881, 2005.
- [585] D. R. Sudhan and D. W. Siemann, "Cathepsin L inhibition by the small molecule KGP94 suppresses tumor microenvironment enhanced metastasis associated cell functions of prostate and breast cancer cells," *Clinical & experimental metastasis*, vol. 30, pp. 891-902, 2013.
- [586] A. Kaasik, T. Rikk, A. Piirsoo, T. Zharkovsky, and A. Zharkovsky, "Up - regulation of lysosomal cathepsin L and autophagy during neuronal death induced by reduced serum and potassium," *European Journal of Neuroscience*, vol. 22, pp. 1023-1031, 2005.
- [587] M. A. Adams-Cioaba, J. C. Krupa, C. Xu, J. S. Mort, and J. Min, "Structural basis for the recognition and cleavage of histone H3 by cathepsin L," *Nature communications*, vol. 2, p. 197, 2011.
- [588] S. Hagemann, T. Günther, J. Dennemärker, T. Lohmüller, D. Brömme, R. Schüle, C. Peters, and T. Reinheckel, "The human cysteine protease cathepsin V can compensate for murine cathepsin L in mouse epidermis and hair follicles," *European journal of cell biology*, vol. 83, pp. 775-780, 2004.
- [589] W. ROTH, J. Deussing, V. A. BOTCHKAREV, M. PAULY-EVERS, P. SAFTIG, A. HAFNER, P. SCHMIDT, W. SCHMAHL, J. SCHERER, and I. ANTON-LAMPRECHT, "Cathepsin L deficiency as molecular defect of furless: hyperproliferation of keratinocytes and perturbation of hair follicle cycling," *The FASEB Journal*, vol. 14, pp. 2075-2086, 2000.
- [590] D. J. Tobin, K. Foitzik, T. Reinheckel, L. Mecklenburg, V. A. Botchkarev, C. Peters, and R. Paus, "The lysosomal protease cathepsin L is an important regulator of keratinocyte and melanocyte differentiation during hair follicle morphogenesis and cycling," *The American journal of pathology*, vol. 160, pp. 1807-1821, 2002.
- [591] J. M. Lankelma, D. M. Voorend, T. Barwari, J. Koetsveld, A. H. Van der Spek, A. P. De Porto, G. Van Rooijen, and C. J. Van Noorden, "Cathepsin L, target in cancer treatment?," *Life sciences*, vol. 86, pp. 225-233, 2010.
- [592] V. Gocheva and J. A. Joyce, "Cysteine cathepsins and the cutting edge of cancer invasion," *CELL CYCLE-LANDES BIOSCIENCE-*, vol. 6, p. 60, 2007.
- [593] C. Jedeszko and B. F. Sloane, "Cysteine cathepsins in human cancer," *Biological chemistry*, vol. 385, pp. 1017-1027, 2004.
- [594] J. Kos, B. Stabuc, A. Schweiger, M. Krasovec, N. Cimerman, N. Kopitar-Jerala, and I. Vrhovec, "Cathepsins B, H, and L and their inhibitors stefin A and cystatin C in sera of melanoma patients," *Clinical cancer research*, vol. 3, pp. 1815-1822, 1997.
- [595] W. Zhang, S. Wang, Q. Wang, Z. Yang, Z. Pan, and L. Li, "Overexpression of cysteine cathepsin L is a marker of invasion and metastasis in ovarian cancer," *Oncology reports*, vol. 31, pp. 1334-1342, 2014.

- [596] A. Rebbaa, "Targeting senescence pathways to reverse drug resistance in cancer," *Cancer letters*, vol. 219, pp. 1-13, 2005.
- [597] X. Zheng, P. M. Chou, B. L. Mirkin, and A. Rebbaa, "Senescence-initiated reversal of drug resistance specific role of Cathepsin L," *Cancer research*, vol. 64, pp. 1773-1780, 2004.
- [598] X. Zheng, F. Chu, P. M. Chou, C. Gallati, U. Dier, B. L. Mirkin, S. A. Mousa, and A. Rebbaa, "Cathepsin L inhibition suppresses drug resistance in vitro and in vivo: a putative mechanism," *American Journal of Physiology-Cell Physiology*, vol. 296, pp. C65-C74, 2009.
- [599] D. B. Seligson, S. Horvath, T. Shi, H. Yu, S. Tze, M. Grunstein, and S. K. Kurdistani, "Global histone modification patterns predict risk of prostate cancer recurrence," *Nature*, vol. 435, pp. 1262-1266, 2005.
- [600] Y. Yang and M. T. Bedford, "Protein arginine methyltransferases and cancer," *Nature Reviews Cancer*, vol. 13, pp. 37-50, 2013.
- [601] K. Nakashima, T. Hagiwara, and M. Yamada, "Nuclear localization of peptidylarginine deiminase V and histone deimination in granulocytes," *Journal of Biological Chemistry*, vol. 277, pp. 49562-49568, 2002.
- [602] R. Raijmakers, A. J. Zendman, W. V. Egberts, E. R. Vossenaar, J. Raats, C. Soede-Huijbregts, F. P. Rutjes, P. A. van Veelen, J. W. Drijfhout, and G. J. Pruijn, "Methylation of Arginine Residues Interferes with Citrullination by Peptidylarginine Deiminases in vitro," *Journal of molecular biology*, vol. 367, pp. 1118-1129, 2007.
- [603] P. R. Thompson and W. Fast, "Histone citrullination by protein arginine deiminase: is arginine methylation a green light or a roadblock?," *ACS chemical biology*, vol. 1, pp. 433-441, 2006.
- [604] P. Sharma, S. Azebi, P. England, T. Christensen, A. Møller-Larsen, T. Petersen, E. Batsché, and C. Muchardt, "Citrullination of histone H3 interferes with HP1-mediated transcriptional repression," *PLoS genetics*, vol. 8, p. e1002934, 2012.
- [605] L. A. Carragher, K. R. Snell, S. M. Giblett, V. S. Aldridge, B. Patel, S. J. Cook, D. J. Winton, R. Marais, and C. A. Pritchard, "V600EBraf induces gastrointestinal crypt senescence and promotes tumour progression through enhanced CpG methylation of p16INK4a," *EMBO molecular medicine*, vol. 2, pp. 458-471, 2010.
- [606] Y. Yang, Y. Lu, A. Espejo, J. Wu, W. Xu, S. Liang, and M. T. Bedford, "TDRD3 is an effector molecule for arginine-methylated histone marks," *Molecular cell*, vol. 40, pp. 1016-1023, 2010.
- [607] B. D. Strahl, S. D. Briggs, C. J. Brame, J. A. Caldwell, S. S. Koh, H. Ma, R. G. Cook, J. Shabanowitz, D. F. Hunt, and M. R. Stallcup, "Methylation of histone H4 at arginine 3 occurs in vivo and is mediated by the nuclear receptor coactivator PRMT1," *Current Biology*, vol. 11, pp. 996-1000, 2001.
- [608] H. Wang, Z.-Q. Huang, L. Xia, Q. Feng, H. Erdjument-Bromage, B. D. Strahl, S. D. Briggs, C. D. Allis, J. Wong, and P. Tempst, "Methylation of histone H4 at arginine 3 facilitating transcriptional activation by nuclear hormone receptor," *Science*, vol. 293, pp. 853-857, 2001.
- [609] W. An, J. Kim, and R. G. Roeder, "Ordered cooperative functions of PRMT1, p300, and CARM1 in transcriptional activation by p53," *Cell*, vol. 117, pp. 735-748, 2004.

- [610] S. Huang, M. Litt, and G. Felsenfeld, "Methylation of histone H4 by arginine methyltransferase PRMT1 is essential in vivo for many subsequent histone modifications," *Genes & development*, vol. 19, pp. 1885-1893, 2005.
- [611] Z. Yu, G. Vogel, Y. Coulombe, D. Dubeau, E. Spehalski, J. Hébert, D. O. Ferguson, J. Y. Masson, and S. Richard, "The MRE11 GAR motif regulates DNA double-strand break processing and ATR activation," *Cell research*, vol. 22, pp. 305-320, 2012.
- [612] F.-M. Boisvert, A. Rhie, S. Richard, and A. J. Doherty, "Report The GAR Motif of 53BP1 is Arginine Methylated by PRMT1 and is Necessary for 53BP1 DNA Binding Activity," *Cell Cycle*, vol. 4, pp. 1834-1841, 2005.
- [613] N. Cheung, L. C. Chan, A. Thompson, M. L. Cleary, and C. W. E. So, "Protein arginine-methyltransferase-dependent oncogenesis," *Nature cell biology*, vol. 9, pp. 1208-1215, 2007.
- [614] T. R. Mitchell, K. Glenfield, K. Jeyanthan, and X.-D. Zhu, "Arginine methylation regulates telomere length and stability," *Molecular and cellular biology*, vol. 29, pp. 4918-4934, 2009.
- [615] K. Chiam, C. Ricciardelli, and T. Bianco-Miotto, "Epigenetic biomarkers in prostate cancer: Current and future uses," *Cancer letters*, vol. 342, pp. 248-256, 2014.
- [616] N. Horikoshi, P. Kumar, G. G. Sharma, M. Chen, C. R. Hunt, K. Westover, S. Chowdhury, and T. K. Pandita, "Genome-wide distribution of histone H4 Lysine 16 acetylation sites and their relationship to gene expression," *Genome Integr*, vol. 4, 2013.
- [617] X. Li, C. A. S. Corsa, P. W. Pan, L. Wu, D. Ferguson, X. Yu, J. Min, and Y. Dou, "MOF and H4 K16 acetylation play important roles in DNA damage repair by modulating recruitment of DNA damage repair protein Mdc1," *Molecular and cellular biology*, vol. 30, pp. 5335-5347, 2010.
- [618] V. Krishnan, M. Z. Y. Chow, Z. Wang, L. Zhang, B. Liu, X. Liu, and Z. Zhou, "Histone H4 lysine 16 hypoacetylation is associated with defective DNA repair and premature senescence in Zmpste24-deficient mice," *Proceedings of the National Academy of Sciences*, vol. 108, pp. 12325-12330, 2011.